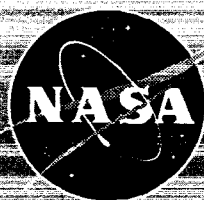


NASA SP-7037 (320)
August 1995

AERONAUTICAL ENGINEERING

A CONTINUING BIBLIOGRAPHY WITH INDEXES



Scientific and Technical
Information Office

The NASA STI Office ... in Profile

Since its founding, NASA has been dedicated to the advancement of aeronautics and space science. The NASA Scientific and Technical Information (STI) Office plays a key part in helping NASA maintain this important role.

The NASA STI Office provides access to the NASA STI Database, the largest collection of aeronautical and space science STI in the world. The Office is also NASA's institutional mechanism for disseminating the results of its research and development activities.

Specialized services that help round out the Office's diverse offerings include creating custom thesauri, translating material to or from 34 foreign languages, building customized databases, organizing and publishing research results ... even providing videos.

For more information about the NASA STI Office, you can:

- **Phone** the NASA Access Help Desk at (301) 621-0390
- **Fax** your question to the NASA Access Help Desk at (301) 621-0134
- **E-mail** your question via the **Internet** to help@sti.nasa.gov
- **Write** to:

NASA Access Help Desk
NASA Center for AeroSpace Information
800 Elkridge Landing Road
Linthicum Heights, MD 21090-2934

NASA SP-7037 (320)
August 1995

AERONAUTICAL ENGINEERING

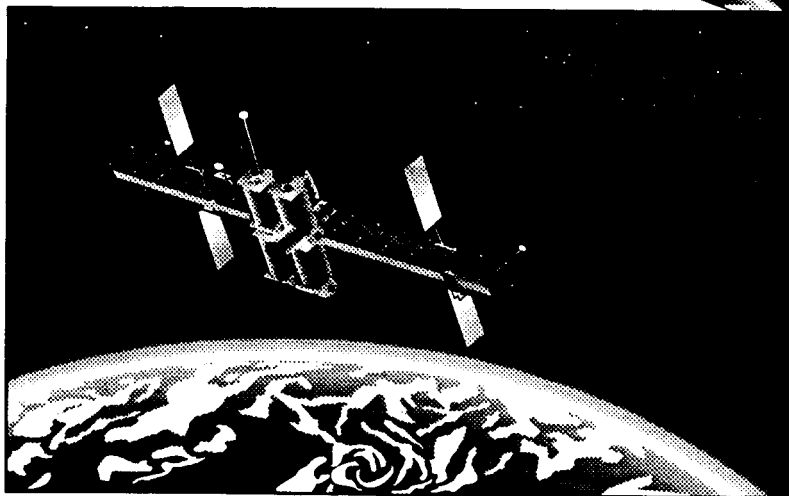
A CONTINUING BIBLIOGRAPHY WITH INDEXES



National Aeronautics and Space Administration
Scientific and Technical Information Office
Washington, DC

1995

The New NASA Video Catalog is Here



Free!

To order your free copy call
the NASA Access Help Desk at
(301) 621-0390 or
fax to (301) 621-0134 or
e-mail to helpdesk@sti.nasa.gov

EXPLORE THE UNIVERSE

This publication was prepared by the NASA Center for AeroSpace Information,
800 Elkridge Landing Road, Linthicum Heights, MD 21090-2934, (301) 621-0390.

INTRODUCTION

This issue of *Aeronautical Engineering — A Continuing Bibliography with Indexes* (NASA SP-7037) lists 193 reports, journal articles, and other documents recently announced in the NASA STI Database.

Accession numbers cited in this issue include:

Scientific and Technical Aerospace Reports (STAR) (N-10000 Series)
Open Literature (A-60000 Series)

N95-24195 — N95-26341
A95-77373 — A95-82073

The coverage includes documents on the engineering and theoretical aspects of design, construction, evaluation, testing, operation, and performance of aircraft (including aircraft engines) and associated components, equipment, and systems. It also includes research and development in aerodynamics, aeronautics, and ground support equipment for aeronautical vehicles.

Each entry in the publication consists of a standard bibliographic citation accompanied, in most cases, by an abstract. The listing of the entries is arranged by the first nine *STAR* specific categories and the remaining *STAR* major categories. This arrangement offers the user the most advantageous breakdown for individual objectives. The citations include the original accession numbers from the respective announcement journals.

Seven indexes—subject, personal author, corporate source, foreign technology, contract number, report number, and accession number—are included.

A cumulative index for 1995 will be published in early 1996.

The NASA CASI price code table, addresses of organizations, and document availability information are located at the back of this issue.



SCAN Goes Electronic!

If you have NASA Mail or if you can access the Internet, you can get biweekly issues of *SCAN* delivered to your desktop absolutely free!

Electronic SCAN takes advantage of computer technology to alert you to the latest aerospace-related, worldwide scientific and technical information that has been published.

No more waiting while the paper copy is printed and mailed to you. You can review *Electronic SCAN* the same day it is released! And you get all 191—or any combination of—subject areas of announcements with abstracts to browse at your leisure. When you locate a publication of interest, you can print the announcement or electronically add it to your publication order list. Start your free access to *Electronic SCAN* today.

Electronic SCAN
Timely
Flexible
Complete
Free!

For instant access via Internet:

<ftp.sti.nasa.gov>
<gopher.sti.nasa.gov>
listserv@sti.nasa.gov

For additional information:

e-mail: help@sti.nasa.gov
scan@sti.nasa.gov

(Enter this address on the "To" line. Leave the subject line blank and send. You will receive an automatic reply with instructions in minutes.)

Phone: (301) 621-0390 Fax: (301) 621-0134

Write: NASA Access Help Desk
NASA STI Office
NASA Center for AeroSpace Information
800 Elkridge Landing Road
Linthicum Heights, MD 21090-2934



National Aeronautics and
Space Administration
Scientific and Technical
Information Office

Home Page: <http://www.sti.nasa.gov/STI-homepage.html>

TABLE OF CONTENTS

Category 01	Aeronautics	327
Category 02	Aerodynamics Includes aerodynamics of bodies, combinations, wings, rotors, and control surfaces; and internal flow in ducts and turbomachinery.	329
Category 03	Air Transportation and Safety Includes passenger and cargo air transport operations; and aircraft accidents.	332
Category 04	Aircraft Communications and Navigation Includes digital and voice communication with aircraft; air navigation systems (satellite and ground based); and air traffic control.	N.A.
Category 05	Aircraft Design, Testing and Performance Includes aircraft simulation technology.	334
Category 06	Aircraft Instrumentation Includes cockpit and cabin display devices; and flight instruments.	336
Category 07	Aircraft Propulsion and Power Includes prime propulsion systems and systems components, e.g., gas turbine engines and compressors; and onboard auxiliary power plants for aircraft.	338
Category 08	Aircraft Stability and Control Includes aircraft handling qualities; piloting; flight controls; and autopilots.	340
Category 09	Research and Support Facilities (Air) Includes airports, hangars and runways; aircraft repair and overhaul facilities; wind tunnels; shock tubes; and aircraft engine test stands.	340
Category 10	Astronautics Includes astronautics (general); astrodynamics; ground support systems and facilities (space); launch vehicles and space vehicles; space transportation; space communications, spacecraft communications, command and tracking; spacecraft design, testing and performance; spacecraft instrumentation; and spacecraft propulsion and power.	341
Category 11	Chemistry and Materials Includes chemistry and materials (general); composite materials; inorganic and physical chemistry; metallic materials; nonmetallic materials; propellants and fuels; and materials processing.	343
Category 12	Engineering Includes engineering (general); communications and radar; electronics and electri- cal engineering; fluid mechanics and heat transfer; instrumentation and photogra- phy; lasers and masers; mechanical engineering; quality assurance and reliability; and structural mechanics.	346

Category 13 Geosciences	351
Includes geosciences (general); earth resources and remote sensing; energy production and conversion; environment pollution; geophysics; meteorology and climatology; and oceanography.	
Category 14 Life Sciences	N.A.
Includes life sciences (general); aerospace medicine; behavioral sciences; man/system technology and life support; and space biology.	
Category 15 Mathematical and Computer Sciences	358
Includes mathematical and computer sciences (general); computer operations and hardware; computer programming and software; computer systems; cybernetics; numerical analysis; statistics and probability; systems analysis; and theoretical mathematics.	
Category 16 Physics	361
Includes physics (general); acoustics; atomic and molecular physics; nuclear and high-energy; optics; plasma physics; solid-state physics; and thermodynamics and statistical physics.	
Category 17 Social Sciences	363
Includes social sciences (general); administration and management; documentation and information science; economics and cost analysis; law, political science, and space policy; and urban technology and transportation.	
Category 18 Space Sciences	363
Includes space sciences (general); astronomy; astrophysics; lunar and planetary exploration; solar physics; and space radiation.	
Category 19 General	N.A.
Subject Index	A-1
Personal Author Index	B-1
Corporate Source Index.....	C-1
Foreign Technology Index.....	D-1
Contract Number Index	E-1
Report Number Index.....	F-1
Accession Number Index	G-1
Appendix	APP-1

TYPICAL REPORT CITATION AND ABSTRACT

NASA SPONSORED

↓ ON MICROFICHE

ACCESSION NUMBER → N95-10318*# Dow Chemical Co., Midland, MI. ← CORPORATE SOURCE
 TITLE → NOVEL MATRIX RESINS FOR COMPOSITES FOR AIRCRAFT
 PRIMARY STRUCTURES, PHASE 1 Final Report, Apr. 1989 -
 Mar. 1992
 AUTHORS → EDMUND P. WOO, P. M. PUCKETT, S. MAYNARD, M. T. BISHOP,
 K. J. BRUZA, J. P. GODSCHALX, AND M. J. MULLINS Aug. 1992 ← PUBLICATION DATE
 164 p
 CONTRACT NUMBERS → (Contracts NAS1-18841; RTOP 510-02-11-02)
 REPORT NUMBERS → (NASA-CR-189657; NAS 1.26:189657) Avail: CASI HC A08/MFA02 ← AVAILABILITY AND
 PRICE CODE

The objective of the contract is the development of matrix resins with improved processability and properties for composites for primarily aircraft structures. To this end, several resins/systems were identified for subsonic and supersonic applications. For subsonic aircraft, a series of epoxy resins suitable for RTM and powder prepreg was shown to give composites with about 40 ksi compressive strength after impact (CAI) and 200 F/wet mechanical performance. For supersonic applications, a thermoplastic toughened cyanate prepreg system has demonstrated excellent resistance to heat aging at 360 F for 4000 hours, 40 ksi CAI and useful mechanical properties at greater than or equal to 310 F. An AB-BCB-maleimide resin was identified as a leading candidate for the HSCT. Composite panels fabricated by RTM show CAI of approximately 50 ksi, 350 F/wet performance and excellent retention of mechanical properties after aging at 400 F for 4000 hours. Author

TYPICAL JOURNAL ARTICLE CITATION AND ABSTRACT

NASA SPONSORED

↓

ACCESSION NUMBER → A95-60192* National Aeronautics and Space Administration. Ames. ← CORPORATE SOURCE
 Research Center, Moffett Field, CA.
 TITLE → AERODYNAMIC INTERACTIONS BETWEEN A ROTOR AND
 WING IN HOVER
 AUTHORS → FORT F. FELKER NASA. Ames Research Center, Moffett Field, ← AUTHOR'S AFFILIATION
 CA, US and JEFFREY S. LIGHT NASA. Ames Research Center,
 Moffett Field, CA, US Journal of the American Helicopter Society ← JOURNAL TITLE
 PUBLICATION DATE → 2 Jun. 1986 p. 53-61
 REPORT NUMBER → (HTN-94-00714) Copyright

An experimental investigation of rotor/wing aerodynamic interactions in hover is described. The investigation consisted of both a large-scale and a small-scale test. A 0.658-scale V-22 rotor and wing was used in the large-scale test. Wing download, wing surface pressure, rotor performance, and rotor downwash data from the large-scale test are presented. A small-scale experiment was conducted to determine how changes in the rotor/wing geometry affected the aerodynamic interactions. These geometry variations included the distance between the rotor and wing, wing incidence angle, wing flap angle, rotor rotation direction, and configurations both with the rotor axis at the tip of the wing (tilt rotor configuration) and with the rotor axis at the center of the wing (compound helicopter configuration). Author (Hemer)

AERONAUTICAL ENGINEERING

A Continuing Bibliography (Suppl. 320)

August 1995

01

AERONAUTICS (GENERAL)

A95-79237

STUDY OF SUBSONIC BASE CAVITY FLOWFIELD STRUCTURE USING PARTICLE IMAGE VELOCIMETRY

MICHAEL J. MOLEZZI Univ of Illinois at Urbana-Champaign, Urbana, IL, United States and CRAIG J. DUTTON AIAA Journal (ISSN 0001-1452) vol. 33, no. 2 February 1995 p. 201-209 refs (BTN-95-EIX95222650781) Copyright

A new particle image velocimetry system has been used to study the near-wake structure of a two-dimensional base in subsonic flow to determine the fluid dynamic mechanisms of observed base drag reduction in the presence of a base cavity. Experiments were done over a range of freestream Mach numbers up to 0.8, including local flowfield velocities over 300 m/s. Effects of the base cavity on the von Karman vortex street wake were found to be related to the expansion and diffusion of vortices near the cavity, although the effects are of small magnitude and no significant change in the vortex formation location or path was observed. The base cavity effects are also less significant at higher freestream velocities due to the formation of vortices further downstream from the base. The base cavity drag reduction was found to be mainly due to the displacement of the base surface to a location upstream of the low-pressure wake vortices, with only a slight modification in the vortex street itself. Author (EI)

A95-81077

DETERMINATION OF PILOTING FEEDBACK STRUCTURES FOR AN ALTITUDE TRACKING TASK

NORIHIRO GOTO Kyushu Univ, Fukuoka, Japan Journal of Guidance, Control, and Dynamics (ISSN 0731-5090) vol. 18, no. 1 January-February 1995 p. 183-185 refs (BTN-95-EIX95242670770) Copyright

The feedback structure employed by the pilot in a system with a choice of feedback structures is determined using an identification method which utilizes an autoregressive scheme and a singular value analysis. The method is applied to an analysis of the computer simulation data of an altitude tracking task. It is shown that the method can make clear judgement on the feedback structure. EI

A95-81092

INTEGRATED DEVELOPMENT OF THE EQUATIONS OF MOTION FOR ELASTIC HYPERSONIC FLIGHT VEHICLES

KARL D. BILIMORIA Arizona State Univ, Tempe, AZ, United States and DAVID K. SCHMIDT Journal of Guidance, Control, and Dynamics (ISSN 0731-5090) vol. 18, no. 1 January-February 1995 p. 73-81 refs (BTN-95-EIX95242670755) Copyright

An integrated, consistent analytical framework for modeling the dynamics of elastic hypersonic flight vehicles has been developed using modal shape functions and in vacuo modal vibration frequencies obtained from structural dynamic analysis. A Lagrangian approach was used to capture the dynamics of rigid-body motion, elastic deformation, fluid flow, rotating machinery, wind, and a

spherical rotating Earth model to account for their mutual interactions. The resulting equations of motion govern the rigid-body and elastic degrees of freedom. The appropriate kinematic equations were developed and presented in a usable form. EI

A95-81099

DIRECT ADAPTIVE AND NEURAL CONTROL OF WING- ROCK MOTION OF SLENDER DELTA WINGS

SAHJENDRA N. SINGH Univ of Nevada, Las Vegas, NV, United States, WOOSON YIM, and WILLIAM R. WELLS Journal of Guidance, Control, and Dynamics (ISSN 0731-5090) vol. 18, no. 1 January-February 1995 p. 25-30 refs (BTN-95-EIX95242670748) Copyright

The question of wing-rock suppression of slender delta wings is considered. Based on a nonlinear model, an adaptive control law for wing-rock control is derived. In this derivation, it is assumed that the aerodynamic parameters in the nonlinear model are not known. The derivation of a control law for wing-rock suppression using neural networks when the dynamics of wing rock are completely unknown is also treated. A radial basis function network is used for synthesizing the controller. An adaptation law is derived for adjusting the parameters of the network. Digital simulation results show that in the closed-loop system wing-rock motion is suppressed using the adaptive and neural controllers. Author (EI)

A95-81101

FUNDAMENTAL MECHANISMS OF AEROELASTIC CONTROL WITH CONTROL SURFACE AND STRAIN ACTUATION

KENNETH B. LAZARUS Massachusetts Inst of Technology, Cambridge, MA, United States, EDWARD F. CRAWLEY, and CHARRISSA Y. LIN Journal of Guidance, Control, and Dynamics (ISSN 0731-5090) vol. 18, no. 1 January-February 1995 p. 10-17 refs (BTN-95-EIX95242670746) Copyright

A typical section analysis is employed to provide an understanding of the fundamental mechanisms and limitations involved in performing aeroelastic control. The effects of both articulated aerodynamic control surfaces and induced strain actuators are included in the model. The ability of these actuators to effect aeroelastic control is studied for each actuator individually as well as in various combinations. The control options available are examined for single-input, single-output (SISO) and multiple-input, multiple-output (MIMO) classical and optimal control laws. A state-cost-vs-control-cost analysis is performed to assess the effectiveness of optimal linear quadratic regulator (LQR) control laws for different actuators and actuator combinations. The cost comparisons show that strain actuation is an effective means of achieving aeroelastic control and a viable alternative to articulated control surface methods. In addition, the advantages of using multiple actuators to avoid limitations associated with single-actuator systems are demonstrated. Author (EI)

N95-24200 Defence Science and Technology Organisation, Melbourne (Australia). Airframes and Engines Div.

AN OVERVIEW OF HEALTH AND USAGE MONITORING SYSTEMS (HUMS) FOR MILITARY HELICOPTERS

KEN F. FRASER Sep. 1994 41 p

ABSTRACTS

01 AERONAUTICS (GENERAL)

(DSTO-TR-0061; AR-008-923) Copyright Avail: Issuing Activity (DSTO Aeronautical nad Maritime Research Lab., GPO Box 4331, Melbourne, Victoria 3001, Australia)

The application of health and usage monitoring systems (HUMS) for military helicopters is lagging that for civil helicopters, but military operators are seriously examining the effectiveness of such systems for their fleets. The material presented in this document is based mainly on the author's recent discussions with researchers, manufacturers and military operators. It outlines some of the important issues which operators face and some initiatives in the area.

Author

N95-24201 Defence Science and Technology Organisation, Melbourne (Australia). Airframes and Engines Div.

HELICOPTER LIFE SUBSTANTIATION: REVIEW OF SOME USA AND UK INITIATIVES

KEN F. FRASER Sep. 1994 26 p

(DSTO-TR-0062; AR-008-924) Copyright Avail: Issuing Activity (DSTO Aeronautical and Maritime Research Lab., GPO Box 4331, Melbourne, Victoria 3001, Australia)

Military operators normally undertake programs to substantiate the fatigue lives of life-limited components in their major helicopter fleets. During recent visits to military helicopter representatives in the USA and the UK, the author discussed the motivation and the technical approach adopted by these operators for helicopter component life substantiation. Issues and programs of particular relevance to the Australian Defense Force are examined in this document.

Author

N95-24295# Federal Aviation Administration, Cambridge, MA.

ESTIMATE OF PROBABILITY OF CRACK DETECTION FROM SERVICE DIFFICULTY REPORT DATA Final Report, Oct. 1992-1993

J. C. BREWER Sep. 1994 53 p Sponsored by Federal Aviation Administration Technical Center, Atlantic City, NJ

(Contract(s)/Grant(s): DOT-FA4H2/A4044)

(PB95-149381; DOT-VNTSC-FAA-94-4; DOT/FAA/CT-94/90) Avail: CASI HC A04/MF A01

The initiation and growth of cracks in a fuselage lap joint were simulated. Stochastic distributions of crack initiation and rivet interference were included. The simulation also contained a simplified crack link-up criterion and the effect of rivet interference on crack growth. Nominal crack growth behavior of large cracks was derived from the simulation results. These calculations implied that large cracks spend most of their lives as multiple small cracks and that the final growth and coalescence occur rapidly. The nominal crack growth histories were applied to 'C-check' crack detection data from the Service Difficulty Report (SDR) database to estimate the sizes of cracks when they were missed during previous inspections. These nondetection events were also estimated by assuming that each detected crack had always been a single crack. The results of each method were appropriately filtered and used to estimate probability of crack detection (POD) using the maximum likelihood technique. The POD estimates obtained from the single crack model are probably conservative, but the underlying assumption of slow crack growth (and therefore more inspection opportunities) might result in unconservative damage tolerance analyses.

NTIS

N95-24465* National Aeronautics and Space Administration, Washington, DC.

AERONAUTICAL ENGINEERING: A CONTINUING BIBLIOGRAPHY WITH INDEXES (SUPPLEMENT 316)

Apr. 1995 146 p

(NASA-SP-7037(316); NAS 1.21:7037(316)) Avail: CASI HC A07

This bibliography lists 413 reports, articles, and other documents introduced into the NASA scientific and technical information system in April 1995. Subject coverage includes: aeronautics; mathematical and computer sciences; chemistry and material sci-

ences; geosciences; design, construction and testing of aircraft and aircraft engines; aircraft components, equipment, and systems; ground support systems; and theoretical and applied aspects of aerodynamics and general fluid dynamics.

Author

N95-25401 Sandia National Labs., Albuquerque, NM. Aging Aircraft NDI Validation Center.

EMERGING NONDESTRUCTIVE INSPECTION FOR AGING AIRCRAFT Final Report

ALLAN BEATTIE, LUTZ DAHLKE, JOHN GIESKE, BRUCE HANSCHKE, GARY PHIPPS, DENNIS ROACH, RICH SHAGAM, and KYLE THOMPSON Oct. 1994 167 p See also N92-33480 Limited Reproducibility: More than 20% of this document may be affected by microfiche quality

(Contract(s)/Grant(s): DTFA03-91-A-00018)

(PB95-143053; DOT/FAA/CT-94/11) Avail: CASI HC A08

The report identifies and describes emerging nondestructive inspection (NDI) methods that can potentially be used to inspect commercial transport and commuter aircraft for structural damage. The nine categories of emerging NDI techniques are acoustic emission, x-ray computed tomography, backscatter radiation, reverse geometry x-ray, advanced electromagnetics (including magneto-optic imaging and advanced eddy current techniques), coherent optics, advanced ultrasonics, and advanced visual and infrared thermography.

NTIS

N95-25607 Science Applications International Corp., Dayton, OH. **VISUAL CONTRAST DETECTION THRESHOLDS FOR AIRCRAFT CONTRAILS Interim Report, Dec. 1993 - Jul. 1994**

JEFFREY A. DOYAL, DAVID P. RAMER, MICHAEL D. STRATTON, and BRADLEY D. PURVIS Jul. 1994 55 p Limited Reproducibility: More than 20% of this document may be affected by microfiche quality

(Contract(s)/Grant(s): F33615-92-D-2293)

(AD-A288618; AL-TR-1994-0116) Avail: Issuing Activity (Defense Technical Information Center (DTIC))

Twenty licensed pilots participated in a laboratory investigation of visual detection thresholds for simulated aircraft contrails. Subjects searched a projection screen for simulated contrails while maintaining a prescribed flight profile on a simple flight simulator. Simulated contrails varied in width from 5 arc min of visual angle to 25 arc min, and varied in length from 2 deg to 10 deg. Subjects performed the detection task in an uncued condition, in which they searched an area measuring 135 deg x 37 deg; and in a cued condition, in which they searched an area measuring 45 deg x 37 deg. Detection thresholds decreased with increasing widths and length, however, thresholds were found to be higher than those demonstrated in previous studies. This difference is attributed to the use of a large visual search area and a secondary task. Cued detection, as described above, led to slightly lower detection thresholds. Psychometric functions were drawn that allow the reader to extrapolate the probability of detection associated with contrails of a given size and contrast.

DTIC

N95-25798* National Aeronautics and Space Administration, Washington, DC.

AERONAUTICAL ENGINEERING: A CONTINUING BIBLIOGRAPHY WITH INDEXES (SUPPLEMENT 317)

May 1995 89 p

(NASA-SP-7037(317); NAS 1.21:7037(317)) Avail: CASI HC A05

This bibliography lists 224 reports, articles, and other documents introduced into the NASA scientific and technical information system in May 1995. Subject coverage includes: design, construction and testing of aircraft and aircraft engines; aircraft components, equipment, and systems; ground support systems; and theoretical and applied aspects of aerodynamics and general fluid dynamics.

Author

AERODYNAMICS

Includes aerodynamics of bodies, combinations, wings, rotors, and control surfaces; and internal flow in ducts and turbomachinery.

A95-79245

HYPERSONIC MODEL TESTING IN A SHOCK TUNNEL

H. OLIVIER Shock Wave Lab, H. GRONIG, and A. LEBOZEC AIAA Journal (ISSN 0001-1452) vol. 33, no. 2 February 1995 p. 262-265 refs

(BTN-95-EIX95222650789) Copyright

A shock tunnel is used to perform test at hypersonic flow conditions including weak real gas effects. Pressure and heat flux distributions are measured around typical reentry configurations. From these data c_p values and Stanton numbers are deduced. For constant Mach and Reynolds number the experimental results achieved indicate a strong influence of the total temperature on the Stanton number distribution. For the results presented this behavior is mainly based on entropy layer and viscous interaction effects. A correlation function which takes into account these effects correlates the Stanton numbers achieved for different flow conditions and in different wind tunnels fairly well.

Author (EI)

A95-79246

PREDICTION OF SUPERSONIC INLET UNSTART CAUSED BY FREESTREAM DISTURBANCES

DAVID W. MAYER Boeing Commercial Airplane Group, Seattle, WA, United States and GERALD C. PAYNTER AIAA Journal (ISSN 0001-1452) vol. 33, no. 2 February 1995 p. 266-275 refs

(BTN-95-EIX95222650790) Copyright

The objective is to report progress toward the development of an Euler analysis procedure for predicting the unstart tolerance of supersonic inlets. As an aid to understanding boundary condition issues, a one-dimensional, linear-analysis procedure was developed and used to analyze inlet unstart behavior. Using these results as a guide, an Euler analysis procedure was extended through the addition of a new bleed boundary condition, a new compressor face boundary condition, and an engine demand model for the simulation of unsteady inlet flows caused by freestream flow disturbances. Five unstart conditions were identified with the Euler analysis of the axisymmetric inlet for both 20- and 90-deg throat bleed configurations. Results show that both increases and decreases in temperature or velocity will unstart the inlet, whereas only pressure decreases will unstart the inlet. It was also found that 90-deg throat bleed improves the unstart tolerance relative to 20-deg throat bleed for freestream pressure decreases, temperature increases, and changes in velocity.

Author (EI)

A95-79247

SIMILARITY RULE FOR JET-TEMPERATURE EFFECTS ON TRANSONIC BASE PRESSURE

KEISUKE ASAI Natl Aerospace Lab, Tokyo, Japan AIAA Journal (ISSN 0001-1452) vol. 33, no. 2 February 1995 p. 276-281 refs

(BTN-95-EIX95222650791) Copyright

On the basis of the similarity rule for jet interaction, a hot jet can be simulated in a cryogenic wind tunnel with a test gas at ambient or moderately elevated temperatures. By using this approach, jet-temperature effects on the base pressure of a cylindrical afterbody model at transonic speeds have been investigated in the 0.1-m transonic cryogenic wind tunnel at the National Aerospace Laboratory. Mixtures of nitrogen and either methane, argon, or helium at varying temperatures were used as a jet gas to determine separate effects of jet temperature, specific heat ratio, and gas constant. It has been found that data obtained for various jet conditions can be correlated very well with two similarity parameters: the plume maximum diameter for the plume shape effect and the jet to freestream mass flux ratio for the jet entrainment effect. To verify this

similarity rule, the same model was tested in an ambient wind tunnel. It was found that an ambient temperature gas having low molecular weight could simulate the jet temperature effects on the transonic base pressure.

Author (EI)

A95-79248

EXPERIMENTAL STUDY OF FLOW SEPARATION ON AN OSCILLATING FLAP AT MACH 2.4

MICHAEL D. COON Univ of California, Berkeley, CA, United States and GARY T. CHAPMAN AIAA Journal (ISSN 0001-1452) vol. 33, no. 2 February 1995 p. 282-288 refs

(BTN-95-EIX95222650792) Copyright

Measurements of unsteady wall pressures have been made in the turbulent boundary layer just upstream of the hinge line of an oscillating flap. The flap, which creates a highly three-dimensional compression corner flowfield, was oscillated in fully attached, crossing incipient separation, and fully separated flow regimes over a range of frequencies. It was found that a substantial lag of the pressure on the flap was produced when oscillating across the point of incipient separation. This occurred at much lower reduced frequencies than for the case of dynamic stall on an airfoil in transonic flow. The dynamic hysteresis was much less in the fully separated case and negligible in the fully attached case.

Author (EI)

A95-80030

UNSTEADY LIFT ON A SWEEPED BLADE TIP

N. PEAKE Univ of Cambridge, Cambridge, United Kingdom Journal of Fluid Mechanics (ISSN 0022-1120) vol. 271 July 25 1994 p. 87-101 refs

(BTN-94-EIX95011441154) Copyright

The paper presents a study on the unsteady lift on a swept blade tip. The solution of a model problem up to the understanding and prediction of noise generation by the interaction between incident vortical disturbances and swept blades is also evaluated. The solution is completed with the use of a Wiener-Hopf technique wherein the usual factorization is carried out with respect to two independent variables separately and closed form expressions for the lift per unit span are derived for both subsonic and supersonic regimes.

EI

N95-24210# Cambridge Univ., Cambridge (England). Dept. of Engineering.

THREE-DIMENSIONAL INTERACTION OF WAKE/BOUNDARY-LAYER AND VORTEX/BOUNDARY-LAYER DATA REPORT

C. P. YEUNG and L. C. SQUIRE 1993 141 p Sponsored by Croucher Foundation of Hong Kong (ISSN 0309-7293)

(CUED/A-AERO/TR-23) Avail: CASI HC A07/MF A02

In an attempt to study the three-dimensional interaction of wake and boundary-layer that commonly occurs on the suction surface of a high-lift multi-element airfoil, an experimental test case has been established, which has a realistic slat/wing flow configuration under infinite swept wing conditions. This enables the effect of the crossflow induced by the wing sweep on the slat wake and the wing boundary-layer interaction process to be investigated. The measurements of the mean velocity and Reynolds stress components are carried out by an orthogonal triple hot-wire system developed by the authors. As well as the wake/boundary-layer interaction experiment, a three-dimensional boundary-layer experiment without the slat has also been conducted. As an extension of the project, the three-dimensional vortex/boundary-layer interaction which also commonly occurs on a high-lift airfoil has been studied. The experimental configuration simulates the trailing vortices generated by two differentially-deflected slats which interact with an otherwise two-dimensional boundary-layer developed on the wing surface under a nominal zero pressure gradient. The mean and turbulent flowfields are measured by the same triple hot-wire system. This report essentially describes the experimental configurations of these three

experiments and documents the triple-wire measurements of the mean and turbulent flowfields of the respective flow. Author

N95-24217* Rockwell International Corp., Huntsville, AL. Space Systems Div.

HIGH FREQUENCY FLOW-STRUCTURAL INTERACTION IN DENSE SUBSONIC FLUIDS

BAW-LIN LIU and J. M. OFARRELL Washington NASA Mar. 1995 216 p

(Contract(s)/Grant(s): NAS8-38187)

(NASA-CR-4652; M-773; NAS 1.26:4652) Avail: CASI HC A10/MF A03

Prediction of the detailed dynamic behavior in rocket propellant feed systems and engines and other such high-energy fluid systems requires precise analysis to assure structural performance. Designs sometimes require placement of bluff bodies in a flow passage. Additionally, there are flexibilities in ducts, liners, and piping systems. A design handbook and interactive data base have been developed for assessing flow/structural interactions to be used as a tool in design and development, to evaluate applicable geometries before problems develop, or to eliminate or minimize problems with existing hardware. This is a compilation of analytical/empirical data and techniques to evaluate detailed dynamic characteristics of both the fluid and structures. These techniques have direct applicability to rocket engine internal flow passages, hot gas drive systems, and vehicle propellant feed systems. Organization of the handbook is by basic geometries for estimating Strouhal numbers, added mass effects, mode shapes for various end constraints, critical onset flow conditions, and possible structural response amplitudes. Emphasis is on dense fluids and high structural loading potential for fatigue at low subsonic flow speeds where high-frequency excitations are possible. Avoidance and corrective measure illustrations are presented together with analytical curve fits for predictions compiled from a comprehensive data base. Author

N95-24308* Sandia National Labs., Albuquerque, NM. VERIFICATION OF COMPUTATIONAL AERODYNAMIC PREDICTIONS FOR COMPLEX HYPERSONIC VEHICLES USING THE INCA(TRADEMARK) CODE

J. L. PAYNE and M. A. WALKER 1995 11 p Presented at the 33rd AIAA Aerospace Sciences Meeting, Reno, NV, 9-12 Jan. 1995

(Contract(s)/Grant(s): DE-AC04-94AL-85000)

(DE95-004757; SAND-94-3190C; CONF-950130-3) Avail: CASI HC A03/MF A01

This paper describes a process of combining two state-of-the-art CFD tools, SPRINT and INCA, in a manner which extends the utility of both codes beyond what is possible from either code alone. The speed and efficiency of the PNS code, SPRING, has been combined with the capability of a Navier-Stokes code to model fully elliptic, viscous separated regions on high performance, high speed flight systems. The coupled SPRINT/INCA capability is applicable for design and evaluation of high speed flight vehicles in the supersonic to hypersonic speed regimes. This paper describes the codes involved, the interface process and a few selected test cases which illustrate the SPRINT/INCA coupling process. Results have shown that the combination of SPRINT and INCA produces correct results and can lead to improved computational analyses for complex, three-dimensional problems. DOE

N95-24379* Overset Methods, Inc., Los Altos, CA. AERODYNAMIC OPTIMIZATION STUDIES ON ADVANCED ARCHITECTURE COMPUTERS Final Report

KALPANA CHAWLA 28 Feb. 1995 31 p Original contains color illustrations

(Contract(s)/Grant(s): NCC2-806)

(NASA-CR-198045; NAS 1.26:198045; OMI-02-93) Avail: CASI HC A03/MF A01; 2 functional color pages

The approach to carrying out multi-discipline aerospace design studies in the future, especially in massively parallel computing environments, comprises of choosing (1) suitable solvers to compute solutions to equations characterizing a discipline, and (2)

efficient optimization methods. In addition, for aerodynamic optimization problems, (3) smart methodologies must be selected to modify the surface shape. In this research effort, a 'direct' optimization method is implemented on the Cray C-90 to improve aerodynamic design. It is coupled with an existing implicit Navier-Stokes solver, OVERFLOW, to compute flow solutions. The optimization method is chosen such that it can accommodate multi-discipline optimization in future computations. In the work, however, only single discipline aerodynamic optimization will be included.

Author

N95-24397* National Aeronautics and Space Administration. Langley Research Center, Hampton, VA.

PERFORMANCE OF AN AERODYNAMIC YAW CONTROLLER MOUNTED ON THE SPACE SHUTTLE ORBITER BODY FLAP AT MACH 10

W. I. SCALLION Feb. 1995 28 p

(Contract(s)/Grant(s): RTOP 242-80-01-01)

(NASA-TM-109179; NAS 1.15:109179) Avail: CASI HC A03/MF A01

A wind-tunnel investigation of the effectiveness of an aerodynamic yaw controller mounted on the lower surface of a shuttle orbiter model body flap was conducted in the Langley 31-Inch Mach 10 Tunnel. The controller consisted of a 60 deg delta fin mounted perpendicular to the body flap lower surface and yawed 30 deg to the free stream direction. The control was tested at angles of attack from 20 deg to 40 deg at zero sideslip for a Reynolds number based on wing mean aerodynamic chord of 0.66×10^6 (exp 6). The aerodynamic and control effectiveness characteristics are presented along with an analysis of the effectiveness of the controller in making a bank maneuver for Mach 18 flight conditions. The controller was effective in yaw and produced a favorable rolling moment. The analysis showed that the controller was as effective as the reaction control system in making the bank maneuver. These results warrant further studies of the aerodynamic/aerothermodynamic characteristics of the control concept for application to future transportation vehicles. Author

N95-24443* Bihrie Applied Research, Inc., Hampton, VA. EXPERIMENTAL STUDY OF THE EFFECTS OF REYNOLDS NUMBER ON HIGH ANGLE OF ATTACK AERODYNAMIC CHARACTERISTICS OF FOREBODIES DURING ROTARY MOTION Final Report

H. PAULEY, J. RALSTON, and E. DICKES Jan. 1995 97 p Original contains color illustrations

(Contract(s)/Grant(s): NAS1-20228; RTOP 505-68-30-01)

(NASA-CR-195033; REPT-94-4; NAS 1.26:195033) Avail: CASI HC A05/MF A02; 32 functional color pages

The National Aeronautics and Space Administration and the Defense Research Agency (United Kingdom) have ongoing experimental research programs in rotary-flow aerodynamics. A cooperative effort between the two agencies is currently underway to collect an extensive database for the development of high angle of attack computational methods to predict the effects of Reynolds number on the forebody flowfield at dynamic conditions, as well as to study the use of low Reynolds number data for the evaluation of high Reynolds number characteristics. Rotary balance experiments, including force and moment and surface pressure measurements, were conducted on circular and rectangular airfoils with hemispherical and ogive noses at the Bedford and Farnborough wind tunnel facilities in the United Kingdom. The bodies were tested at 60 and 90 deg angle of attack for a wide range of Reynolds numbers in order to observe the effects of laminar, transitional, and turbulent flow separation on the forebody characteristics when rolling about the velocity vector. Author

Author

N95-24566* Army Aviation Systems Command, Hampton, VA. EXPLORATORY FLOW VISUALIZATION INVESTIGATION OF MAST-MOUNTED SIGHTS IN PRESENCE OF A ROTOR
TERENCE A. GHEE (Analytical Services and Materials, Inc., Hampton, VA.) and HENRY L. KELLEY Mar. 1995 36 p

(Contract(s)/Grant(s): RTOP 505-59-36-01; RTOP 282-10-01-01)
(NASA-TM-4634; L-17409; NAS 1.15:4634; ATCOM-TR-95-A-001)
Avail: CASI HC A03/MF A01

A flow visualization investigation with a laser light sheet system was conducted on a 27-percent-scale AH-64 attack helicopter model fitted with two mast-mounted sights in the Langley 14- by 22-foot subsonic tunnel. The investigation was conducted to identify aerodynamic phenomena that may have contributed to adverse vibration encountered during full-scale flight of the AH-64D Apache/Longbow helicopter with an asymmetric mast-mounted sight. Symmetric and asymmetric mast-mounted sights oriented at several skew angles were tested at simulated forward and rearward flight speeds of 30 and 45 knots. A laser light sheet system was used to visualize the flow in planes parallel to and perpendicular to the free-stream flow. Analysis of these flow visualization data identified frequencies of flow patterns in the wake shed from the sight, the streamline angle at the sight, and the location where the shed wake crossed the rotor plane. Differences in wake structure were observed between the sight configurations and various skew angles. Analysis of lateral light sheet plane data implied significant vortex structure in the wake of the asymmetric mast-mounted sight in the configuration that produced maximum in-flight vibration. The data showed no significant vortex structure in the wake of the asymmetric and symmetric configurations that produced no increase in in-flight adverse vibration. Author

N95-24998# National Aerospace Lab., Tokyo (Japan). Aircraft Aerodynamics Div.

NUMERICAL AND EXPERIMENTAL STUDY OF DRAG CHARACTERISTICS OF TWO-DIMENSIONAL HLFC AIRFOILS IN HIGH SUBSONIC, HIGH REYNOLDS NUMBER FLOW

YOJI ISHIDA, MASAYOSHI NOGUCHI, MAMORU SATO, and HIROSHI KANDA Jul. 1994 14 p
(ISSN 0389-4010)

(NAL-TR-1244T) Avail: CASI HC A03/MF A01

Hybrid laminar flow control (HLFC) is one of the most promising aircraft drag reduction technologies. However, very few experimental and theoretical studies have been reported. We have investigated both numerically and experimentally the aerodynamic characteristics of an HLFC airfoil and wing at high subsonic, high Reynolds number conditions. In this paper, we report the results of the wind tunnel test on drag characteristics, with and without suction, of two-dimensional HLFC airfoils with porous and slot suction approach under some adverse factors against laminar flow, and a numerical analysis of the wind tunnel data, which is based on the boundary layer calculation with a new transition prediction method allowed for the adverse factors and the Squire-Young drag formula. The HLFC models achieved total drag reduction as high as 20% at realistic flight condition and the numerical methods has given satisfactory predictions. Author

N95-25105# National Aerospace Lab., Tokyo (Japan). Advanced Aircraft Research Group.

LOW SPEED AERODYNAMIC CHARACTERISTICS OF DELTA WINGS WITH VORTEX FLAPS: 60 DEG AND 70 DEG DELTA WINGS

KENICHI RINOIE (Tokyo Univ., Japan.), TOSHIMI FUJITA, AKIHITO IWASAKI, and HIROTOSHI FUJIEDA Jul. 1994 15 p in JAPANESE

(ISSN 0389-4010)

(NAL-TR-1245) Avail: CASI HC A03/MF A01

Low-speed wind tunnel tests have been made on a 70 deg delta wing model with tapered vortex flaps to investigate the effects of the swept-back angle on the performance of vortex flaps. The force, surface pressure measurements, and oil flow visualization tests were made on a 0.5 m span 70 deg delta wing model. The results were compared between 60 deg and 70 deg delta wing models. Flow patterns around the vortex flaps at the optimum lift/drag ratio flap configuration of 70 deg delta wing were found to be different from those of 60 deg delta wing. The maximum lift/drag ratio improvement

for 70 deg delta wing is attained when a separated region is formed over the whole vortex flap surface. Author

N95-25338# National Aeronautics and Space Administration. Langley Research Center, Hampton, VA.

INTERNAL PERFORMANCE CHARACTERISTICS OF THRUST-VECTORED AXISYMMETRIC EJECTOR NOZZLES

MILTON LAMB Mar. 1995 227 p Prepared in cooperation with Pratt and Whitney (the Government Engines and Space Propulsion Div. of the United Technologies)

(Contract(s)/Grant(s): RTOP 505-59-30-04)

(NASA-TM-4610; L-17386; NAS 1.15:4610) Avail: CASI HC A11/MF A03

A series of thrust-vectored axisymmetric ejector nozzles were designed and experimentally tested for internal performance and pumping characteristics at the Langley research center. This study indicated that discontinuities in the performance occurred at low primary nozzle pressure ratios and that these discontinuities were mitigated by decreasing expansion area ratio. The addition of secondary flow increased the performance of the nozzles. The mid-to-high range of secondary flow provided the most overall improvements, and the greatest improvements were seen for the largest ejector area ratio. Thrust vectoring the ejector nozzles caused a reduction in performance and discharge coefficient. With or without secondary flow, the vectored ejector nozzles produced thrust vector angles that were equivalent to or greater than the geometric turning angle. With or without secondary flow, spacing ratio (ejector passage symmetry) had little effect on performance (gross thrust ratio), discharge coefficient, or thrust vector angle. For the unvectored ejectors, a small amount of secondary flow was sufficient to reduce the pressure levels on the shroud to provide cooling, but for the vectored ejector nozzles, a larger amount of secondary air was required to reduce the pressure levels to provide cooling. Author

N95-25649# Defence Research Agency, Farnborough, Hampshire (England).

A THEORETICAL AND EXPERIMENTAL INVESTIGATION OF THE FLOW OVER SUPERSONIC LEADING EDGE WING/BODY CONFIGURATIONS

J. L. FULKER (Defence Research Agency, Bedford, England.), P. R. ASHILL, and A. SHIRES Aug. 1993 42 p Presented at the 1993 European Forum on Recent Developments and Applications in Aeronautical CFD, Bristol, England, 1-3 Sep. 1993 Sponsored by Ministry of Defence Original contains color illustrations (DRA-TM-AERO-PROP-41; DRA/AP/TM9341/1.0) Copyright Avail: CASI HC A03/MF A01

A theoretical and experimental study is described, of the flow over wing-body configurations with a supersonic component of free-stream normal to the leading edge, i.e. with a supersonic leading edge. The theoretical calculations have been performed using a code for solving Euler's equations for complex configurations known as SAUNA. An assessment is made of the predictions of this method, by comparison with the experimental results. Significant reductions in local pressure drag by the use of nose blunting are both predicted and measured over a substantial portion of the wing span. However, it is also shown that nose blunting results in a marked increase in local drag in the region of the wing/body junction. In this region the flow is complex, the bow shock having low local sweep and high strength. It is shown how the CFD method can be used both to identify this problem and to effect a redesign of the wing/body junction, for the blunt-nose configuration, with the aim of realizing the benefits of nose blunting. Significant drag reductions are obtained relative to the untreated configuration, indicating how advanced codes can provide a solution to problems of this kind without resort to further expensive wind-tunnel tests. Author

N95-25761# National Aerospace Lab., Tokyo (Japan). Aircraft Aerodynamics Div.

MEASUREMENTS OF LONGITUDINAL STATIC AERODYNAMIC COEFFICIENTS BY THE CABLE MOUNT SYSTEM

KATSUICHI MUROTA and MASAOKI YANAGIHARA Feb. 1994 22 p In JAPANESE (ISSN 0389-4010) (NAL-TR-1226) Avail: CASI HC A03/MF A01

The longitudinal static aerodynamic coefficients of an NAL spaceplane model were measured in the NAL 6.5 m x 5.5 m low-speed wind tunnel. The model was supported by a pair of cables, one spanned horizontally and the other vertically (cable mount system). The aerodynamic interference of the cable mount system is generally smaller than that of conventional model support systems such as the strut and sting system. This paper outlines the cable mount system, the cable mounted system, the method used to measure the trimmed longitudinal aerodynamic coefficients and the test results.

Author

N95-25762# National Aerospace Lab., Tokyo (Japan). Airframe Div.

FUNDAMENTAL WIND TUNNEL EXPERIMENTS ON LOW-SPEED FLUTTER OF A TIP-FIN CONFIGURATION WING TETSUHIKO UEDA, TOKUO SOTOZAKI, and KAZUO IWASAKI Mar. 1994 23 p In JAPANESE (ISSN 0389-4010)

(NAL-TR-1228) Avail: CASI HC A03/MF A01

Wind tunnel tests were conducted to investigate the fundamental flutter characteristics of a tip-fin configuration wing. Two types of models were tested to provide experimental data for the flutter analysis of non-coplanar wings. One is a normally plain wing and the other has a cant angle of 15 deg at the tip-fin. They were tested in the 2m x 2m low-speed wind tunnel. On the tip-fin wing, mild flutter with limited amplitudes was observed in a certain range of speeds well below the typical violent flutter speed. It was caused by the coupling between wing torsion and the deflection of the rotationally free rudder with mass balance. The effects of mass balance of the rudder located at the tip-fin were also studied to confirm its role in flutter prevention. Modal tests on the models were performed automatically using the Dynamic Displacement Measurement System.

Author

N95-25962*# National Aeronautics and Space Administration. Lewis Research Center, Cleveland, OH.

RECENT IMPROVEMENTS TO AND VALIDATION OF THE ONE DIMENSIONAL NASA WAVE ROTOR MODEL

DANIEL E. PAXSON and JACK WILSON (NYMA, Inc., Cleveland, OH.) May 1995 20 p

(Contract(s)/Grant(s): NAS3-25266; RTOP 505-62-50)

(NASA-TM-106913; E-9621; NAS 1.15:106913) Avail: CASI HC A03/MF A01

A numerical model has been developed at the NASA Lewis Research Center which can predict both the unsteady flow quantities within a wave rotor passage and the steady averaged flows in the ports. The model is based on the assumptions of one-dimensional, unsteady, perfect gas flow. The model assesses not only the dominant wave behavior, but the loss effects of finite passage opening time, leakage from the passage ends, viscosity, and heat transfer to and from the passages. The model operates in the rotor reference frame; however, until recently no account was made for the often significant effect of the rotor circumferential velocity component. The present model accounts for this by modifying the passage boundary conditions, allowing the internal computational scheme to remain the rotor reference frame, while quantities such as inlet duct stagnation properties may be specified in the fixed or absolute reference frame. Accurate modeling of this effect is critical to successful wave rotor analysis and design, particularly in off-design predictions where the flows in the inlet ducts are mismatched with the rotor passages and significant turning may take place (i.e., work is done on the gas). The relative simplicity of the model makes it useful for design and optimization, as well as analysis, of wave rotor cycles for many applications. This report, building on several earlier papers, describes the most recent modifications to the model. These include accounting for the relative/absolute transition at the passage boundaries and refinements to the viscous source term

correlation which resulted from this accounting. Comparison of model predictions with measured data is then presented and discussed.

Author

N95-26075*# National Aeronautics and Space Administration. Lewis Research Center, Cleveland, OH.

A COMBINED GEOMETRIC APPROACH FOR SOLVING THE NAVIER-STOKES EQUATIONS ON DYNAMIC GRIDS

JOHN W. SLATER May 1995 9 p Presented at the Conference on Numerical Methods for Fluid Dynamics, Oxford, England, United Kingdom, 3-6 Apr. 1995; sponsored by the University of Oxford and Reading

(Contract(s)/Grant(s): RTOP 505-62-52)

(NASA-TM-106919; E-9630; NAS 1.15:106919) Avail: CASI HC A02/MF A01

A combined geometric approach for solving the Navier-Stokes equations is presented for the analysis of planar, unsteady flow about mechanisms with components in moderate relative motion. The approach emphasizes the relationships between the geometry model, grid, and flow model for the benefit of the total dynamics problem. One application is the analysis of the restart operation of a variable-geometry, high-speed inlet.

Author

N95-26302*# National Aeronautics and Space Administration. Ames Research Center, Moffett Field, CA.

AERODYNAMICS MODEL FOR A GENERIC ASTOVL LIFT-FAN AIRCRAFT

LOURDES G. BIRCKELBAW, WALTER E. MCNEIL, and DOUGLAS A. WARDWELL Apr. 1995 63 p

(Contract(s)/Grant(s): RTOP 505-68-32)

(NASA-TM-110347; A-950051; NAS 1.15:110347) Avail: CASI HC A04/MF A01

This report describes the aerodynamics model used in a simulation model of an advanced short takeoff and vertical landing (ASTOVL) lift-fan fighter aircraft. The simulation model was developed for use in piloted evaluations of transition and hover flight regimes, so that only low speed (M approximately 0.2) aerodynamics are included in the mathematical model. The aerodynamic model includes the power-off aerodynamic forces and moments and the propulsion system induced aerodynamic effects, including ground effects. The power-off aerodynamics data were generated using the U.S. Air Force Stability and Control Digital DATCOM program and a NASA Ames in-house graphics program called VORVIEW which allows the user to easily analyze arbitrary conceptual aircraft configurations using the VORLAX program. The jet-induced data were generated using the prediction methods of R. E. Kuhn et al., as referenced in this report.

Author

03

AIR TRANSPORTATION AND SAFETY

Includes passenger and cargo air transport operations; and aircraft accidents.

A95-78583

REAL-TIME DECISION AIDING: AIRCRAFT GUIDANCE FOR WIND SHEAR AVOIDANCE

D. ALEXANDER STRATTON Parker Hannifin Corp, Smithtown, NY, United States and ROBERTS STENGEL IEEE Transactions on Aerospace and Electronic Systems (ISSN 0018-9251) vol. 31, no. 1 January 1995 p. 117-124 refs

(BTN-95-EIX95202637575) Copyright

Modern estimation theory and artificial intelligence technology are applied to the Wind Shear Safety Advisor, a conceptual airborne advisory system to help flight crews avoid or survive encounter with hazardous low-altitude wind shear. Numerical and symbolic processes of the system fuse diverse, time-varying data from ground-based and airborne measurements. Simulated wind-shear-encounter scenarios illustrate the need to consider a variety of factors for

optimal decision reliability. The wind-shear-encounter simulations show the potential of the Wind Shear Safety Advisor for effectively integrating the available information, highlighting the benefits of the computational techniques employed. Author (EI)

N95-24206# National Transportation Safety Board, Washington, DC.

AIRCRAFT ACCIDENT REPORT: IMPACT WITH BLAST FENCE UPON LANDING ROLLOUT ACTION AIR CHARTERS FLIGHT 990 PIPER PA-31-350, N990RA, STRATFORD, CONNECTICUT, 27 APRIL 1994

1994 75 p

(PB94-910410; NTSB/AAR-94/08) Avail: CASI HC A04/MF A01

On April 28, 1994, about 2256 eastern daylight time, Action Air Charters flight 990, a Piper PA-31-350 Navajo Chieftain, N990RA, crashed into a blast fence at the departure end of runway 6 after landing at Sikorsky Memorial Airport, Stratford, Connecticut. The flight originated in Atlantic City, New Jersey, and operated on a visual flight rules flight plan. The airplane was operating under Title 14 Code of Federal Regulations Part 135 as a single pilot, on-demand air carrier flight. Following handling touchdown and during rollout, the airplane collided with a blast deflector fence at the departure end of runway 6. The airplane was destroyed by impact forces and postcrash fire. Eight of the nine occupants sustained fatal injuries. One passenger was seriously injured. The National Transportation Safety Board determines that the probable causes of this accident were the failure of the captain to use the available instrument landing system (ILS) glideslope, his failure to execute a go-around when the conditions were not suitable for landing, and his failure to land the airplane on the runway at a point sufficient to allow for a safe stopping distance; the fatalities were caused by the presence of the nonfrangible blast fence and the absence of a safety area at the end of the runway. Safety issues in this report focused on the instrument landing system, runway safety areas, and runway lighting systems. Safety recommendations concerning these issues were made to the Federal Aviation Administration, the Connecticut Department of Transportation, the City of Bridgeport, and the Town of Stratford, Connecticut. Also, as a result of the investigation of this accident, on May 11, 1994, the Safety Board issued Urgent Action Safety Recommendations A-94-111 and A-94-112 to the Federal Aviation Administration concerning aircraft maintenance performed by Harrington Industries, Inc. Author

N95-24384# Civil Aeromedical Inst., Oklahoma City, OK.

DEVELOPMENT OF AN INTERVENTION PROGRAM TO ENCOURAGE SHOULDER HARNESS USE AND AIRCRAFT RETROFIT IN GENERAL AVIATION AIRCRAFT, PHASES 1 AND 2

JAMES F. PARKER, JR. (BioTechnology, Inc., Falls Church, VA.), WILLIAM T. SHEPARD (Federal Aviation Administration, Washington, DC.), WALTER J. GUNN (Arlington Associates, Daytona Beach, FL.), and DIANE G. CHRISTENSEN (BioTechnology, Inc., Falls Church, VA.) Jan. 1995 63 p

(DOT/FAA/AM-95/2) Avail: CASI HC A04/MF A01

This report describes a study of shoulder harness installation and use rates in general aviation aircraft. Observations were made at six geographically separate areas to determine estimates of current installation and use rates. An expert panel was employed to identify important factors that affect installation and use of shoulder harness in general aviation aircraft. Analyses are presented to explain reasons for shoulder harness installation and use rates. An educational program is proposed to influence pilots to install and/or use shoulder harnesses in their general aviation aircraft. Author

N95-24391*# Clemson Univ., SC. Radar Systems Lab. **CHARACTERIZING THE WAKE VORTEX SIGNATURE FOR AN ACTIVE LINE OF SIGHT REMOTE SENSOR M.S. Thesis** Technical Report No. 19

ROBERT MILTON HEIL 5 Aug. 1994 80 p

(Contract(s)/Grant(s): NGT-50975)

(NASA-CR-197697; NAS 1.26:197697; TR-080594-4871F) Avail:

CASI HC A05/MF A01

A recurring phenomenon, described as a wake vortex, develops as an aircraft approaches the runway to land. As the aircraft moves along the runway, each of the wing tips generates a spiraling and expanding cone of air. During the lifetime of this turbulent event, conditions exist over the runway which can be hazardous to following aircraft, particularly when a small aircraft is following a large aircraft. Left to themselves, these twin vortex patterns will converge toward each other near the center of the runway, harmlessly dissipating through interaction with each other or by contact with the ground. Unfortunately, the time necessary to disperse the vortex is often not predictable, and at busy airports can severely impact terminal area productivity. Rudimentary methods of avoidance are in place. Generally, time delays between landing aircraft are based on what is required to protect a small aircraft. Existing ambient wind conditions can complicate the situation. Reliable detection and tracking of a wake vortex hazard is a major technical problem which can significantly impact runway productivity. Landing minimums could be determined on the basis of the actual hazard rather than imposed on the basis of a worst case scenario. This work focuses on using a windfield description of a wake vortex to generate line-of-sight Doppler velocity truth data appropriate to an arbitrarily located active sensor such as a high resolution radar or lidar. The goal is to isolate a range Doppler signature of the vortex phenomenon that can be used to improve detection. Results are presented based on use of a simplified model of a wake vortex pattern. However, it is important to note that the method of analysis can easily be applied to any vortex model used to generate a windfield snapshot. Results involving several scan strategies are shown for a point sensor with a range resolution of 1 to 4 meters. Vortex signatures presented appear to offer potential for detection and tracking. Author

N95-24631# Federal Aviation Administration, Atlantic City, NJ. **BIRD INGESTION INTO LARGE TURBOFAN ENGINES Final Report**

HOWARD BANILOWER and COLIN GOODALL (Pennsylvania State Univ., University Park, PA.) Feb. 1995 139 p

(DOT/FAA/CT-93/14) Avail: CASI HC A07/MF A02

This final report contains findings from a study conducted by the Federal Aviation Administration (FAA) of bird ingestion into certain modern large high bypass turbofan engines. These engines were certified to current FAA standards and are installed in A-300, A-320, B-747, B-757, B-767, DC-10, and MD-11 aircraft in commercial service worldwide. Data pertaining to 644 aircraft ingestion events were collected for the FAA during 1989-1991 by the principal engine manufacturers. Topics addressed in the report include characteristics of ingested birds (numbers, species, and weights), ingestion rates, airports, aircraft parameters (flight phase, altitude, speed, engine position), and ingestion events which pose a potential threat to aircraft safety (multiple-engines or birds, transverse fracture of fan blades, power loss). Using statistical methods, the data are analyzed to determine the influence of flight phase (departure or arrival), bird weight, and bird numbers (single or multiple bird), both separately and in combination, on overall engine damage, fan blade damage, core damage, and other adverse effects on flight. A summary of all pertinent data from each ingestion is included in an appendix. Author

N95-24633*# National Aeronautics and Space Administration. Langley Research Center, Hampton, VA.

AVIATION SYSTEM CAPACITY IMPROVEMENTS THROUGH TECHNOLOGY

W. DON HARVEY Mar. 1995 82 p

(Contract(s)/Grant(s): RTOP 505-69-20-01)

(NASA-TM-109165; NAS 1.15:109165) Avail: CASI HC A05/MF A01

A study was conducted with the primary objective of determining the impact of technology on capacity improvements in the U.S. air transportation system and, consequently, to assess the areas where NASA's expertise and technical contributions would be the most beneficial. The outlook of the study is considered both near-

and long-term (5 to 25 years). The approach was that of actively working with the Massachusetts Institute of Technology (MIT) Flight Transportation Laboratory and included interactions with 'users' outside of both agencies as well as with organizations within. This report includes an overall survey of what are believed to be the causes of the capacity problems, ongoing work with the Federal Aviation Administration (FAA) to alleviate the problems, and identifies improvements in technology that would increase capacity and reduce delays. Author

N95-25341*# Boeing Commercial Airplane Co., Seattle, WA. CONSISTENT APPROACH TO DESCRIBING AIRCRAFT HIRF PROTECTION Final Report

P. R. RIMBEY and D. B. WALEN Mar. 1995 93 p
(Contract(s)/Grant(s): NAS1-19360; RTOP 538-01-13-01)
(NASA-CR-195067) Avail: CASI HC A05/MF A01

The high intensity radiated fields (HIRF) certification process as currently implemented is comprised of an inconsistent combination of factors that tend to emphasize worst case scenarios in assessing commercial airplane certification requirements. By examining these factors which include the process definition, the external HIRF environment, the aircraft coupling and corresponding internal fields, and methods of measuring equipment susceptibilities, activities leading to an approach to appraising airplane vulnerability to HIRF are proposed. This approach utilizes technically based criteria to evaluate the nature of the threat, including the probability of encountering the external HIRF environment. No single test or analytic method comprehensively addresses the full HIRF threat frequency spectrum. Additional tools such as statistical methods must be adopted to arrive at more realistic requirements to reflect commercial aircraft vulnerability to the HIRF threat. Test and analytic data are provided to support the conclusions of this report. This work was performed under NASA contract NAS1-19360, Task 52. Author

N95-25609 Army Engineer Waterways Experiment Station, Vicksburg, MS.

REAL-TIME TESTING AND DEMONSTRATION OF THE US ARMY CORPS OF ENGINEERS' REAL-TIME ON-THE-FLY POSITIONING SYSTEM

SALLY L. FRODGE, BENJAMIN W. REMONDI, DARIUSZ LAPUCHA, and JOHN E. CHANCE Sep. 1994 16 p Limited
Reproducibility: More than 20% of this document may be affected by microfiche quality
(AD-A288624; WES/TN/DRP-4-10) Avail: Issuing Activity (Defense Technical Information Center (DTIC))

This technical note describes the U.S. Army Corps of Engineers' Real-Time On-the-Fly (OTF) positioning system and summarizes the results of testing and demonstrations conducted to date. DTIC

N95-25764# National Aerospace Lab., Tokyo (Japan). Advanced Aircraft Research Group

REENTRY GUIDANCE FOR HYPERSONIC FLIGHT EXPERIMENT (HYFLEX) VEHICLE Report No. 1 HIROKAZU SUZUKI Apr. 1994 19 p In JAPANESE (ISSN 0389-4010)

(NAL-TR-1235) Avail: CASI HC A03/MF A01

This paper describes the design of the reentry guidance for Hypersonic Flight Experiment vehicle (HYFLEX), which is now under development at NAL and NASDA to prepare for its scheduled launch in 1996. First, the mission requirements of this flight experiment are described. Secondly, a reentry guidance based on the drag deceleration and the azimuth angle misalignment correction is suggested and its ability is evaluated. Consequently, the proposed reentry guidance is proved to have sufficient ability to satisfy the mission requirements. Author

AIRCRAFT DESIGN, TESTING AND PERFORMANCE

Includes aircraft simulation technology.

A95-79240

MULTILEVEL DECOMPOSITION PROCEDURE FOR EFFICIENT DESIGN OPTIMIZATION OF HELICOPTER ROTOR BLADES

ADITI CHATTOPADHYAY Arizona State Univ, Tempe, AZ, United States, THOMAS R. MCCARTHY, and NARAYANAN PAGALDIPTI AIAA Journal (ISSN 0001-1452) vol. 33, no. 2 February 1995 p. 223-230 refs

(BTN-95-EIX95222650784) Copyright

This paper addresses a multilevel decomposition procedure for efficient design optimization of helicopter blades, with the coupling of aerodynamics, blade dynamics, aeroelasticity, and structures. The multidisciplinary optimization problem is decomposed into three levels. The rotor is optimized for improved aerodynamic performance at the first level. At the second level, the objective is to improve the dynamic and aeroelastic characteristics of the rotor. A structural optimization is performed at the third level. Interdisciplinary coupling is established through the use of optimal sensitivity derivatives. The Kreisselmeier-Steinhauser function approach is used to formulate the optimization problem when multiple design objectives are involved. A nonlinear programming technique and an approximate analysis procedure are used for optimization. Results obtained show significant improvements in the rotor aerodynamic, dynamic, and structural characteristics, when compared with a reference or baseline rotor. Author (EI)

A95-79249

DYNAMIC STALL CONTROL FOR ADVANCED ROTORCRAFT APPLICATION

YUNG H. YU U.S. Army Aeroflightdynamics Directorate, Moffett Field, CA, United States, SOOGAB LEE, KENNETH W. MCALISTER, CHEE TUNG, and CLIN M. WANG AIAA Journal (ISSN 0001-1452) vol. 33, no. 2 February 1995 p. 289-295 refs
(BTN-95-EIX95222650793) Copyright

Advanced concepts designed to improve the lift, drag, and pitching moment characteristics of rotor blades have been investigated for the purpose of enhancing rotor maneuver capability. The advantages and disadvantages of these concepts have been evaluated using both computational and experimental means. The concepts that were considered in this study included a leading-edge slat, a deformable leading-edge, and upper-surface blowing. The results show the potential of these concepts for substantially improving the performance of a rotor. Author (EI)

A95-81097

ROTORCRAFT HANDLING QUALITIES IN TURBULENCE

R. A. HESS Univ of California, Davis, CA, United States Journal of Guidance, Control, and Dynamics (ISSN 0731-5090) vol. 18, no. 1 January-February 1995 p. 39-45 refs

(BTN-95-EIX95242670750) Copyright

Rotorcraft are often required to perform tasks in environments where atmospheric disturbances can significantly affect performance and vehicle handling qualities. Establishing requirements for rotorcraft handling qualities in turbulence is thus of prime importance, particularly to the military. An analytical study is described that addresses this issue. First, a simplified approach to modeling the aerodynamic effects of turbulence on rotorcraft is presented. A structural pilot model employing a handling-qualities sensitivity function is next used to quantify handling qualities. Next, an hypothesis regarding the manner in which turbulence affects vehicle handling qualities is proposed. Finally, an example of the analytical approach is presented involving the longitudinal hover task of an AH-1G rotorcraft. In addition to the unaugmented vehicle, three levels of stability augmentation are considered, each involving different levels of feedback to achieve their goals. Author (EI)

A95-81098* National Aeronautics and Space Administration. Ames Research Center, Moffett Field, CA.

IDENTIFICATION AND SIMULATION EVALUATION OF A COMBAT HELICOPTER IN HOVER

JEFFERY A. SCHROEDER National Aeronautics and Space Administration. Ames Research Center, Moffett Field, CA, MARK B. TISCHLER, DOUGLAS C. WATSON, and MICHELLE M. ESHOW Journal of Guidance, Control, and Dynamics (ISSN 0731-5090) vol. 18, no. 1 January-February 1995 p. 31-38 refs (BTN-95-EIX95242670749) Copyright

Frequency-domain parameter identification techniques were used to develop a hover mathematical model of the AH-64 Apache helicopter from eight data. The unstable AH-64 bare-airframe characteristics, without a stability augmentation system, were parameterized in the conventional stability-derivative form. To improve the model's vertical response, a simple transfer-function model approximating the effects of dynamic inflow was developed. The model, with and without stability augmentation, was then evaluated by AH-64 pilots in a moving-base simulation. It was the opinion of the pilots that the simulation was a satisfactory representation of the aircraft for the tasks of interest. The principal negative comment was that height control was more difficult in the simulation than in the aircraft. Author (EI)

A95-81974

SR-71 MAY LAUNCH TARGETS FOR MISSILE DEFENSE TESTS

WILLIAM B. SCOTT Aviation Week & Space Technology (ISSN 0005-2175) vol. 140, no. 12 March 21, 1994 p. 56-57 (HTN-95-91872) Copyright

High-speed target vehicles air-launched from a NASA-operated SR-71 Blackbird may give Pentagon officials new options for conducting realistic tests of next-generation theater missile interceptor systems. A preliminary NASA study indicates that one of three SR-71 testbeds the agency operates could carry and launch a Coleman Research HERA Target System mated to a M57A1 Minuteman 1 third-stage booster. In essence, the SR-71 would serve as a relatively inexpensive, reusable first stage of the target vehicle. The SR-71 would carry the HERA/M57A1 target in a protective shroud and launch the vehicle at speeds up to Mach 3.0 for theater missile defense tests. Various scenarios developed under the study are briefly discussed. Hemer

N95-24541# Joint Publications Research Service, Arlington, VA. JPRS REPORT: SCIENCE AND TECHNOLOGY. CENTRAL EURASIA

28 Feb. 1995 41 p Transl. into ENGLISH from various Central Eurasian articles (JPRS-UST-95-011) Avail: CASI HC A03/MF A01

Translated articles cover the following topics: problems of constructing welded aircraft structures; automatic welding of aluminum and titanium alloy structures; fusion welding thin-sheet titanium alloys to corrosion-resistant steels; and reconditioning aircraft parts with laser-fused hard-facing coatings. Author

N95-24582* National Aeronautics and Space Administration. Langley Research Center, Hampton, VA.

A CREW-CENTERED FLIGHT DECK DESIGN PHILOSOPHY FOR HIGH-SPEED CIVIL TRANSPORT (HSCT) AIRCRAFT

MICHAEL T. PALMER, WILLIAM H. ROGERS (Boft, Beranek, and Newman, Inc., Cambridge, MA.), HAYES N. PRESS (Lockheed Engineering and Sciences Co., Hampton, VA.), KARAA. LATORELLA (State Univ. of New York, Buffalo, NY.), and TERENCE S. ABBOTT Jan. 1995 55 p

(Contract(s)/Grant(s): RTOP 537-08-21-01)

(NASA-TM-109171; NAS 1.15:109171) Avail: CASI HC A04/MF A01

Past flight deck design practices used within the U.S. commercial transport aircraft industry have been highly successful in producing safe and efficient aircraft. However, recent advances in automation have changed the way pilots operate aircraft, and these changes make it necessary to reconsider overall flight deck design. The High Speed

Civil Transport (HSCT) mission will likely add new information requirements, such as those for sonic boom management and supersonic/subsonic speed management. Consequently, whether one is concerned with the design of the HSCT, or a next generation subsonic aircraft that will include technological leaps in automated systems, basic issues in human usability of complex systems will be magnified. These concerns must be addressed, in part, with an explicit, written design philosophy focusing on human performance and systems operability in the context of the overall flight crew/flight deck system (i.e., a crew-centered philosophy). This document provides such a philosophy, expressed as a set of guiding design principles, and accompanied by information that will help focus attention on flight crew issues earlier and iteratively within the design process. This document is part 1 of a two-part set. Author

N95-24629* National Aeronautics and Space Administration. Ames Research Center, Moffett Field, CA.

GEOMETRIC ANALYSIS OF WING SECTIONS

I.-CHUNG CHANG, FRANCISCO J. TORRES, and CHEE TUNG (Army Aviation Systems Command, Moffett Field, CA.) Apr. 1995 18 p

(Contract(s)/Grant(s): RTOP 505-10-11)

(NASA-TM-110346; A-950049; NAS 1.15:110346) Avail: CASI HC A03/MF A01

This paper describes a new geometric analysis procedure for wing sections. This procedure is based on the normal mode analysis for continuous functions. A set of special shape functions is introduced to represent the geometry of the wing section. The generators of the NACA 4-digit airfoils were included in this set of shape functions. It is found that the supercritical wing section, Korn airfoil, could be well represented by a set of ten shape functions. Preliminary results showed that the number of parameters to define a wing section could be greatly reduced to about ten. Hence, the present research clearly advances the airfoil design technology by reducing the number of design variables. Author

N95-24630* Brown Univ., Providence, RI. Dept. of Engineering. AERODYNAMIC PARAMETER ESTIMATION VIA FOURIER MODULATING FUNCTION TECHNIQUES

A. E. PEARSON Hampton, VA NASA Apr. 1995 44 p

(Contract(s)/Grant(s): NAG1-1065; RTOP 505-64-52-01)

(NASA-CR-4654; NAS 1.26:4654) Avail: CASI HC A03/MF A01

Parameter estimation algorithms are developed in the frequency domain for systems modeled by input/output ordinary differential equations. The approach is based on Shintrot's method of moment functionals utilizing Fourier based modulating functions. Assuming white measurement noises for linear multivariable system models, an adaptive weighted least squares algorithm is developed which approximates a maximum likelihood estimate and cannot be biased by unknown initial or boundary conditions in the data owing to a special property attending Shintrot-type modulating functions. Application is made to perturbation equation modeling of the longitudinal and lateral dynamics of a high performance aircraft using flight-test data. Comparative studies are included which demonstrate potential advantages of the algorithm relative to some well established techniques for parameter identification. Deterministic least squares extensions of the approach are made to the frequency transfer function identification problem for linear systems and to the parameter identification problem for a class of nonlinear-time-varying differential system models. Author

N95-25334* National Aeronautics and Space Administration. Ames Research Center, Moffett Field, CA.

AERODYNAMIC SHAPE OPTIMIZATION OF WING AND WING-BODY CONFIGURATIONS USING CONTROL THEORY

JAMES REUTHER and ANTONY JAMESON (Princeton Univ., NJ.) Jan. 1995 33 p

(Contract(s)/Grant(s): NAS2-13721)

(NASA-CR-198024; NAS 1.26:198024; RIACS-TR-95-01) Avail: CASI HC A03/MF A01

This paper describes the implementation of optimization tech-

niques based on control theory for wing and wing-body design. In previous studies it was shown that control theory could be used to devise an effective optimization procedure for airfoils and wings in which the shape and the surrounding body-fitted mesh are both generated analytically, and the control is the mapping function. Recently, the method has been implemented for both potential flows and flows governed by the Euler equations using an alternative formulation which employs numerically generated grids, so that it can more easily be extended to treat general configurations. Here results are presented both for the optimization of a swept wing using an analytic mapping, and for the optimization of wing and wing-body configurations using a general mesh. Author

N95-25578 Oklahoma City Air Logistics Center, Tinker AFB, OK.
PROCEEDINGS OF THE 2D USAF AGING AIRCRAFT CONFERENCE

C. I. CHANG 19 May 1994 431 p Conference held in Del City, OK, 17-19 May 1994

(AD-A288217; AFOSR-94-0756TR) Avail: Issuing Activity (Defense Technical Information Center (DTIC))

The Air Force Office of Scientific Research gathered together representatives of universities funded under the University Research Institutes to present results of their Aging Aircraft research conducted over the preceding year. The purpose was to provide a forum for Technical Interchange and provide AFOSR an opportunity for the research community to interact with the applied engineering community and gain insight into the day to day problems experienced on Aging Aircraft. Technical presentations by personnel from HO AFMC/EN Wright Labs, ASC, the five Air Logistics Centers, FAA and NASA were delivered on various topics including corrosion, corrosion fatigue, multi-site damage and advanced non-destructive evaluation methods. Approximately 160 people attended the conference. DTIC

N95-25862# National Aerospace Lab., Tokyo (Japan). Aircraft Development Section.

A QUIET STOL RESEARCH AIRCRAFT DEVELOPMENT PROGRAM

Jan. 1994 35 p In JAPANESE

(ISSN 0389-4010)

(NAL-TR-1223) Avail: CASI HC A03/MF A01

This report presents a general account of a program undertaken by the National Aerospace Laboratory to develop a STOL research aircraft, designated ASKA. ASKA made its first flight on October 28, 1985. Descriptions of the development over the eight years from 1977 to 1985 are included along with descriptions of the aircraft and its systems, and various development tests. ASKA is a modified C-1 medium-sized troop and freight transport, manufactured by Kawasaki Heavy Industries for the Air Self-Defence Force. The airframe was made anew and the two engines of C-1 were replaced with four FJR710/600S fan-jet engines arranged as in upper surface blowing system to provide powered lift for STOL operations. Author

N95-25935 Aeronautical Research Labs., Melbourne (Australia). Airframes and Engines Div.

CONFIGURATION AND OTHER DIFFERENCES BETWEEN BLACK HAWK AND SEAHAWK HELICOPTERS IN MILITARY SERVICE IN THE USA AND AUSTRALIA Abstract Only

R. W. JACKSON Dec. 1993 1 p

(AR-008-386; ARL-GD-43) Avail: Issuing Activity (Aeronautical Research Labs., Melbourne, Australia)

Various versions of Black Hawk and Seahawk helicopters have been produced to match the requirements of different operators. Some of the differences between these versions, particularly those relevant to the dynamic system, are briefly reviewed. Author

N95-26009 Mechanical Engineering Lab., Sakura (Japan). **LONG ENDURANCE STRATOSPHERIC SOLAR POWERED AIRSHIP**

Mar. 1994 71 p In JAPANESE

(PB95-178729) Avail: Issuing Activity (National Technical Informa-

tion Service (NTIS))

This is a report on HALROP (High Altitude Long Range Observational Platform), a solar powered airship entitled 'Long Endurance Stratospheric Solar Powered Airship,' and was published by the New Airship System Study Group of the Japan Industrial Technology Promotion Association. The report covers history of previous research on stratospheric platform; the concept and design specifications of HALROP (a proposed model for 20 km altitude airship); relationship between the altitude and meteorological data; liftoff, descent, and recovery operations; design of high efficiency solar power system; structure and weight balance problems, a feasibility study of antarctic exploration by HALROP; the conceptual design of solar powered transport airship called JS-RESAT which makes use of the jet stream; and the feasibility study of stratospheric power generation. NTIS

N95-26338# General Accounting Office, Washington, DC. National Security and International Affairs Div.

REPORT TO CONGRESSIONAL COMMITTEES. TACTICAL AIRCRAFT: CONCURRENCY IN DEVELOPMENT AND PRODUCTION OF F-22 AIRCRAFT SHOULD BE REDUCED

19 Apr. 1995 33 p

(GAO/NSIAD-95-59; B-259204) Avail: CASI HC A03/MF A01

The concurrency between the development and production phases of the Air Force's F-22 fighter program and the risk associated with that concurrency are assessed. Although the F-22 program involves considerable risk because it embodies important technological advances that are critical to its operational success, the F-22 program exhibits a high degree of concurrency because the program will enter production well before commencement of initial operational testing and evaluation (IOT&E). The Air Force plans to procure 80 F-22s under low-rate initial production (LRIP), or 18 percent of the total planned procurement, at an estimated cost of \$12.4 billion, before completing IOT&E. F-22 production rates in the LRIP phase are planned to accelerate so that 75 percent of the full-production rate, or 36 aircraft a year, will be achieved under the LRIP phase of the program. The planned rate of acceleration, it is believed, exceeds the amount that is needed to successfully complete the LRIP phase of the program and essentially represents a plan to commit to a full-rate production schedule before IOT&E is completed. The need for the F-22, based on analysis, is not urgent. Moreover, engine and stealthiness problems already disclosed by DOD, and the potential for avionics and software problems, underscore the need to demonstrate the weapon system's performance through flight testing before significant commitments are made to production. CASI

06

AIRCRAFT INSTRUMENTATION

Includes cockpit and cabin display devices; and flight instruments.

A95-81096

HIGH-PERFORMANCE, ROBUST, BANK-TO-TURN MISSILE AUTOPILOT DESIGN

CHING-FANG LIN American GNC Corp, Chatsworth, CA, United States, JAMES R. CLOUTIER, and JOHNNY H. EVERS Journal of Guidance, Control, and Dynamics (ISSN 0731-5090) vol. 18, no. 1 January-February 1995 p. 46-53 refs (BTN-95-EIX95242670751) Copyright

Subjects related to a robust multivariable autopilot design are examined. First, a canonical robust control design formulation is introduced and is illustrated by formulating an integrated autopilot design problem. This formulation addresses the considerations of missile command following, model parameter variations, actuator dynamics, flexible dynamics, and parasitic feedback effects. Then, three robust autopilot designs for the HAVE DASH 2 missile system are executed. The controllers are solved using the generalized Hamiltonian approach which unifies a class of robust control designs

in the same framework in terms of the formulation, data structure, and solution algorithm. The simulation shows that the designs achieve good response against significant kinematic and inertia couplings and aerodynamic parameter variations. Author (EI)

N95-24207* National Aeronautics and Space Administration. Lewis Research Center, Cleveland, OH.

THE 1994 FIBER OPTIC SENSORS FOR AEROSPACE TECHNOLOGY (FOSAT) WORKSHOP

ROBERT BAUMBICK, comp., GRIGORY ADAMOVSKY, comp., MEG TUMA, comp., GLENN BEHEIM, comp., and JORGE SOTOMAYOR, comp. Feb. 1995 90p Workshop held in Cleveland OH, 18-20 Oct. 1994

(Contract(s)/Grant(s): RTOP 505-60-00)

(NASA-CP-10166; E-9426; NAS 1.55:10166) Avail: CASI HC A05/MF A01

The NASA Lewis Research Center conducted a workshop on fiber optic technology on October 18-20, 1994. The workshop objective was to discuss the future direction of fiber optics and optical sensor research, especially in the aerospace arena. The workshop was separated into four sections: (1) a Systems Section which dealt specifically with top level overall architectures for the aircraft and engine; (2) a Subsystems Section considered the parts and pieces that made up the subsystems of the overall systems; (3) a Sensor/Actuators section considered the status of research on passive optical sensors and optical powered actuators; and (4) Components Section which addressed the interconnects for the optical systems (e.g., optical connectors, optical fibers, etc.). This report contains the minutes of the discussion on the workshop, both in each section and in the plenary sessions. The slides used by a limited number of presenters are also included as presented. No attempt was made to homogenize this report. The view of most of the attendees was: (1) the government must do a better job of disseminating technical information in a more timely fashion; (2) enough work has been done on the components, and system level architecture definition must dictate what work should be done on components; (3) a Photonics Steering Committee should be formed to coordinate the efforts of government and industry in the photonics area, to make sure that programs complimented each other and that technology transferred from one program was used in other programs to the best advantage of the government and industry.

Author

N95-24624* National Aeronautics and Space Administration. Lewis Research Center, Cleveland, OH.

ASSESSMENT OF AVIONICS TECHNOLOGY IN EUROPEAN AEROSPACE ORGANIZATIONS Final Contractor Report

D. A. MARTINEC (Aeronautical Radio, Inc., Annapolis, MD.), ROBERT BAUMBICK, ELLIS HITT (Battelle Columbus Labs., OH.), CORNELIUS LEONDES (Washington Univ., Bellingham, WA.), MONICA MAYTON (Air Force Systems Command, Wright-Patterson AFB, OH.), JOSEPH SCHWIND (Airline Pilots Association, Denison, TX.), and JOSEPH TRAYBAR (Federal Aviation Administration, Atlantic City, NJ.) 21 Sep. 1992 179 p

(Contract(s)/Grant(s): NAS3-88622)

(NASA-CR-189201; E-9592; NAS 1.26:189201) Avail: CASI HC A09/MF A02

This report provides a summary of the observations and recommendations made by a technical panel formed by the National Aeronautics and Space Administration (NASA). The panel, comprising prominent experts in the avionics field, was tasked to visit various organizations in Europe to assess the level of technology planned for use in manufactured civil avionics in the future. The primary purpose of the study was to assess avionics systems planned for implementation or already employed on civil aircraft and to evaluate future research, development, and engineering (RD&E) programs, address avionics systems and aircraft programs. The ultimate goal is to ensure that the technology addressed by NASA programs is commensurate with the needs of the aerospace industry

at an international level. The panel focused on specific technologies, including guidance and control systems, advanced cockpit displays, sensors and data networks, and fly-by-wire/fly-by-light systems. However, discussions the panel had with the European organizations were not limited to these topics. Author

N95-25005# National Aerospace Lab., Tokyo (Japan). Control Systems Div.

FLIGHT REFERENCE DISPLAY FOR POWERED-LIFT STOL AIRCRAFT

KEIJI TANAKA, KOHEI FUNABIKI, MASARU NAKAMURA, YUSHI TERUI, TOSHIHARU INAGAKI, HIROYASU KAWAHARA, YUKICHI TSUKANO, and TAKATSUGU ONO Oct. 1994 26 p

(ISSN 0389-4010)

(NAL-TR-1251) Avail: CASI HC A03/MF A01

This study deals with a proposed flight reference display for powered-lift STOL aircraft. The display design aims at providing pilots with new control cues for maintaining flight safety during low-speed high-power approach. The display utilizes angle of attack, pitch angle, and airspeed to indicate the flight reference for maintaining the flight safety margins. Piloted simulation using a moving-base flight simulator was conducted to verify the display scheme. The parameters of the display equations were designed on the basis of the flight test achievements of 'ASKA,' the experimental STOL aircraft of the National Aerospace Laboratory. This preliminary evaluation demonstrated that the display can be used for both flight reference tracking and safety margin monitoring, and provided appropriate values of coefficients of the display equations. The succeeding flight evaluation of the proposed flight reference display was conducted after installing the display upon an in-flight simulator, whose motion cues yield ultimate fidelity of flight simulation environment for the display evaluation. As the in-flight simulator, the variable stability and response airplane (VSRA) of the National Aerospace Laboratory was utilized for this experiment. The flight reference display for this flight evaluation was developed by using a color liquid crystal display. The results of the approach flight experiments provided proof of satisfactory performance of the display for pilots to monitor and regulate the safety margins, as well as suggestion for future improvement. Author

N95-26190 Organisatie voor Toegepast Natuurwetenschappelijk Onderzoek, Delft (Netherlands).

PARTIAL CAMERA AUTOMATION IN A SIMULATED UNMANNED AIR VEHICLE Interim Report

J. E. KORTELING and W. VANDERBORG 5 Oct. 1994 29 p Limited Reproducibility: More than 20% of this document may be affected by microfiche quality

(AD-A288786; TNO-TM-1994-B-16; TDCK-94-2179) Avail: Issuing Activity (Defense Technical Information Center (DTIC))

With the rapid development of automatic control techniques a central question is how the division of labor between the human operator and the automaton should be optimally distributed. In this connection, the present study focussed on an intelligent, semi-autonomous, interface for a camera operator of a simulated Unmanned Air Vehicle (UAV). This interface used inherent system knowledge concerning UAV motion in order to assist a camera operator in tracking an object moving through the landscape below. This landscape was sensed by the video camera attached to the UAV-platform and presented to the operator on a monitor display. The semi-automated system compensated for the translations of the UAV relative to the earth. This compensation was accompanied by the appropriate joystick movements ensuring tactile (haptic) feedback of these system interventions. The operator had to superimpose camera movements over these system actions required to track the motion of a target (a driving truck) relative to the terrain. Consequently, the operator remained in the loop; he still had total control of the camera-motion system. In order to investigate the effects of this semi-automation over a broad range of task situations, the tracking task was carried out under two conditions of update frequency of the monitor image and control mode difficulty. DTIC

AIRCRAFT PROPULSION AND POWER

Includes prime propulsion systems and systems components, e.g., gas turbine engines and compressors; and on-board auxiliary power plants for aircraft.

N95-24213*# Auburn Univ., AL. Dept. of Mechanical Engineering. DYNAMIC BEHAVIOR OF A MAGNETIC BEARING SUPPORTED JET ENGINE ROTOR WITH AUXILIARY BEARINGS

ABDOLLAH HOMAIFAR, ed. (North Carolina Agricultural and Technical State Univ., Greensboro, NC.), JOHN C. KELLY, JR., ed. (North Carolina Agricultural and Technical State Univ., Greensboro, NC.), G. T. FLOWERS, H. XIE, and S. C. SINHA Albuquerque, NM 1994 7 p Presented at the First Industry/Academy Symposium on Research for Future Supersonic and Hypersonic Vehicles: Applications, Design, Development and Research, volume 1, Greensboro, NC, 4-6 Dec. 1994 Its TSI Press Series (Contract(s)/Grant(s): NAG3-1507) (NASA-CR-197860; NAS 1.26:197860) Avail: CASI HC A02/MF A01

This paper presents a study of the dynamic behavior of a rotor system supported by auxiliary bearings. The steady-state behavior of a simulation model based upon a production jet engine is explored over a wide range of operating conditions for varying rotor imbalance, support stiffness and damping. Interesting dynamical phenomena, such as chaos, subharmonic responses, and double-valued responses, are presented and discussed. Author

N95-24293 Northern Research and Engineering Corp., Woburn, MA.

SMALL GAS TURBINE COMPONENT EVALUATION STUDY Final Report, Jun. 1990-1992

J. B. KESSELI Jun. 1994 114 p Sponsored by Gas Research Inst. Limited Reproducibility: More than 20% of this document may be affected by microfiche quality (Contract(s)/Grant(s): GRI-5089-291-2077) (PB95-147542; NREC-1762; GRI-94/0350) Avail: CASI HC A06

The low pressure ratio, highly recuperated gas turbine engine is a candidate for future small (under 200 kW) cogeneration systems and other prime-mover applications. Existing gas engine equipment (cogeneration, chillers, pump and compressor-drives) based on spark ignition (Otto cycle) technology has not been successful enough to substantially expand the sale of natural gas. The small gas turbine is being considered for its potential economic advantages that stem from superior reliability (lower maintenance costs), increased shaft-power efficiency, less costly installation, and lower costs associated with meeting future emission standards. In this study and experimental program, the focus was in two areas of critical importance. These are the ability of the engine to meet future California State emission standards, and the cost-effectiveness of the recuperator. A complete engine test was performed based on non-developmental commercial components, including a non-optimum recuperator. NOx emissions were below 5 ppmv at 15% excess oxygen, while carbon monoxide was in the range of 25 ppmv. Engine electrical generation efficiency was 21% with a 71% effective recuperator, proving that the goal of 30 to 33% electrical efficiencies are attainable with an optimally sized recuperator. NTIS

N95-24304*# McDonnell-Douglas Aerospace, Long Beach, CA. ADVANCED SUBSONIC AIRPLANE DESIGN AND ECONOMIC STUDIES Final Report

ROBERT H. LIEBECK, DONALD A. ANDRASTEK, JOHNNY CHAU, RAQUEL GIRVIN, ROGER LYON, BLAINE K. RAWDON, PAUL W. SCOTT, and ROBERT A. WRIGHT Apr. 1995 37 p (Contract(s)/Grant(s): NAS3-25965; RTOP 538-08-11) (NASA-CR-195443; E-9488; NAS 1.26:195443) Avail: CASI HC

A03/MF A01

A study was made to examine the effect of advanced technology engines on the performance of subsonic airplanes and provide a vision of the potential which these advanced engines offered. The year 2005 was selected as the entry-into-service (EIS) date for engine/airframe combination. A set of four airplane classes (passenger and design range combinations) that were envisioned to span the needs for the 2005 EIS period were defined. The airframes for all classes were designed and sized using 2005 EIS advanced technology. Two airplanes were designed and sized for each class: one using current technology (1995) engines to provide a baseline, and one using advanced technology (2005) engines. The resulting engine/airframe combinations were compared and evaluated on the basis on sensitivity to basic engine performance parameters (e.g. SFC and engine weight) as well as DOC+I. The advanced technology engines provided significant reductions in fuel burn, weight, and wing area. Average values were as follows: reduction in fuel burn = 18%, reduction in wing area = 7%, and reduction in TOGW = 9%. Average DOC+I reduction was 3.5% using the pricing model based on payload-range index and 5% using the pricing model based on airframe weight. Noise and emissions were not considered. Author

N95-24390*# National Aeronautics and Space Administration. Lewis Research Center, Cleveland, OH.

CROSSFLOW MIXING OF NONCIRCULAR JETS

D. S. LISCINSKY (United Technologies Corp., East Hartford, CT.), B. TRUE (United Technologies Corp., East Hartford, CT.), and J. D. HOLDEMAN Feb. 1995 13 p Presented at the 33rd Aerospace Sciences Meeting and Exhibit, Reno, NV, 9-12 Jan. 1995; sponsored by AIAA Original contains color illustrations (Contract(s)/Grant(s): NAS3-25954)

(NASA-TM-106865; E-9477; NAS 1.15:106865; AIAA PAPER 95-0732) Avail: CASI HC A03/MF A01; 5 functional color pages

An experimental investigation has been conducted of the isothermal mixing of a turbulent jet injected perpendicular to a uniform crossflow through several different types of sharp-edged orifices. Jet penetration and mixing was studied using planar Mie scattering to measure time-averaged mixture fraction distributions of circular, square, elliptical, and rectangular orifices of equal geometric area injected into a constant velocity crossflow. Hot-wire anemometry was also used to measure streamwise turbulence intensity distributions at several downstream planes. Mixing effectiveness was determined using (1) a spatial unmixedness parameter based on the variance of the mean jet concentration distributions and (2) by direct comparison of the planar distributions of concentration and of turbulence intensity. No significant difference in mixing performance was observed for the six configurations based on comparison of the mean properties. Author

N95-24392*# Iowa State Univ. of Science and Technology, Ames, IA.

STUDY OF COMPRESSIBLE FLOW THROUGH A RECTANGULAR-TO-SEMIANNULAR TRANSITION DUCT Final Report

JEFFRY FOSTER, THEODORE H. OKIISHI, BRUCE J. WENDT (Modern Technologies Corp., Middleburg Heights, OH.), and BRUCE A. REICHERT (Kansas State Univ., Manhattan, KS.) Cleveland, OH NASA Apr. 1995 61 p

(Contract(s)/Grant(s): NAG3-1561) (NASA-CR-4660; E-9582; NAS 1.26:4660) Avail: CASI HC A04/MF A01

Detailed flow field measurements are presented for compressible flow through a diffusing rectangular-to-semiannular transition duct. Comparisons are made with published computational results for flow through the duct. Three-dimensional velocity vectors and total pressures were measured at the exit plane of the diffuser model. The inlet flow was also measured. These measurements are made using calibrated five-hole probes. Surface oil flow visualization and surface static pressure data were also taken. The study was

conducted with an inlet Mach number of 0.786. The diffuser Reynolds based on the inlet centerline velocity and the exit diameter of the diffuser was 3,200,000. Comparison of the measured data with previously published computational results are made. Data demonstrating the ability of vortex generators to reduce flow separation and circumferential distortion is also presented. Author

N95-24561* National Aeronautics and Space Administration, Lewis Research Center, Cleveland, OH.

THE EFFECT OF ALTITUDE CONDITIONS ON THE PARTICLE EMISSIONS OF A J85-GE-5L TURBOJET ENGINE

JUNE ELIZABETH RICKEY Feb. 1995 52 p

(Contract(s)/Grant(s): RTOP 505-62-00)

(NASA-TM-106669; E-9143; NAS 1.15:106669) Avail: CASI HC A04/MF A01

Particles from a J85-GE-5L turbojet engine were measured over a range of engine speeds at simulated altitude conditions ranging from near sea level to 45,000 ft and at flight Mach numbers of 0.5 and 0.8. Samples were collected from the engine by using a specially designed probe positioned several inches behind the exhaust nozzle. A differential mobility particle sizing system was used to determine particle size. Particle data measured at near sea-level conditions were compared with Navy Aircraft Environmental Support Office (AESO) particle data taken from a GE-J85-4A engine at a sea-level static condition. Particle data from the J85 engine were also compared with particle data from a J85 combustor at three different simulated altitudes. Author

N95-24990* National Aerospace Lab., Tokyo (Japan).

EFFECT OF FILM COOLING/REGENERATIVE COOLING ON SCRAMJET ENGINE PERFORMANCES

FUMIEI ONO, TAKESHI KANDA, GORO MASUYA, TOSHIHITO SAITO, and YOSHIO WAKAMATSU Jul. 1994 16 p In JAPANESE (ISSN 0389-4010)

(NAL-TR-1242) Avail: CASI HC A03/MF A01

Film cooling was modeled to allow performance prediction of scramjet engine design. The model was based on experimental results of compressible mixing layers for the vicinity of the injection slot, and on analytical results of the turbulent boundary layer in the region far from the slot. The film cooling model was integrated to a quasi one-dimensional scramjet performance prediction model. In the engine employing a combination of film cooling and regenerative cooling, coolant flow rate of the engine slightly exceeded the stoichiometric flow rate, even at high flight Mach numbers, and had the best specific impulse and system pressure performances. These advantages were achieved by increasing the volume flow rate and decreasing the velocity difference between the main flow and the coolant, both due to an increase in the film coolant temperature. The effective cooling system with a combination of film cooling and regenerative cooling was also advantageous in that excess cooling of the engine wall could be avoided. The combination of film cooling and regenerative cooling was also effective from the viewpoint of the propellant feed system. The turbine exhaust gas was suitable for the coolant of film cooling. Author

N95-25395* Queensland Univ., Saint Lucia (Australia). Dept. of Mechanical Engineering.

THRUST MEASUREMENTS OF A COMPLETE AXISYMMETRIC SCRAMJET IN AN IMPULSE FACILITY

A. PAULL, R. J. STALKER, and D. J. MEE In its Shock Tunnel Studies of Scramjet Phenomena 1993 p 15-18 Jan. 1995 Sponsored in cooperation with NASA. Langley Research Center and the Australian Research Council

Avail: CASI HC A01/MF A02

This paper describes tests which were conducted in the hypersonic impulse facility T4 on a fully integrated axisymmetric scramjet configuration. In these tests the net force on the scramjet vehicle was measured using a deconvolution force balance. This measurement technique and its application to a complex model such as the scramjet are discussed. Results are presented for the scramjet's

aerodynamic drag and the net force on the scramjet when fuel is injected into the combustion chambers. It is shown that a scramjet using a hydrogen-silane fuel produces greater thrust than its aerodynamic drag at flight speeds equivalent to 260 m/s. Author

N95-25396* Queensland Univ., Saint Lucia (Australia). Dept. of Mechanical Engineering.

SCRAMJET THRUST MEASUREMENT IN A SHOCK TUNNEL

A. PAULL, R. J. STALKER, and D. J. MEE In its Shock Tunnel Studies of Scramjet Phenomena 1993 p 19-27 Jan. 1995 Sponsored in cooperation with the Australian Research Council

Avail: CASI HC A02/MF A02

This note reports tests in a shock tunnel in which a fully integrated scramjet configuration produced net thrust. The experiments not only showed that impulse facilities can be used for assessing thrust performance, but also were a demonstration of the application of a new technique to the measurement of thrust on scramjet configurations in shock tunnels. These two developments are of significance because scramjets are expected to operate at speeds well in excess of 2 km/sec, and shock tunnels offer a means of generating high Mach number flows at such speeds. Author

N95-25397* Queensland Univ., Saint Lucia (Australia). Dept. of Mechanical Engineering.

THRUST MEASUREMENT IN A 2-D SCRAMJET NOZZLE

SEAN TUTTLE In its Shock Tunnel Studies of Scramjet Phenomena 1993 p 29-36 Jan. 1995

Avail: CASI HC A02/MF A02

The two-dimensional thrust nozzle presents a challenging problem. The loading is not axisymmetric as in the case of a cone and the internal flow presents some design difficulties. A two-sting system has been chosen to accommodate the internal flow and achieve some symmetry. The situation is complicated by the fact that with the small ramp angle and the internal pressure on the nozzle walls, loading is predominantly transverse. Yet it is the axial thrust which is to be measured (i.e., the tensile waves propagating in the stings). Although bending stress waves travel at most at only 60% of the speed of the axial stress waves, the system needs to be stiffened against bending. The second sting was originally only used to preserve symmetry. However, the pressures on each thrust surface may be quite different at some conditions, so at this stage the signals from both stings are being averaged as a first order approximation of the net thrust. The expected axial thrust from this nozzle is not large so thin stings are required. In addition, the contact area between nozzle and sting needs to be maximized. The result was that it was decided to twist the stings through 90 deg, without distorting their cross-sectional shape, just aft of the nozzle. Finite element analysis showed that this would not significantly alter the propagation of the axial stress wave in the sting, while the rigidity of the system is greatly increased. A Mach 4 contoured nozzle is used in the experiments. The thrust calculated by integrating the static pressure measurements on the thrust surfaces is compared with the deconvolved strain measurement of the net thrust for the cases of air only and hydrogen fuel injected into air at approximately 9 MJ/kg nozzle supply enthalpy. The gain in thrust due to combustion is visible in this result. Derived from text

N95-25936 Aeronautical Research Labs., Melbourne (Australia). Airframes and Engines Div.

ASSESSMENT OF OVERHAUL SURGE MARGIN TESTS APPLIED TO THE T53 ENGINES IN ADF IROQUOIS HELICOPTERS Abstract Only

P. C. W. FRITH Feb. 1994 1 p

(AR-008-389; ARL-TN-48) Avail: Issuing Activity (Aeronautical Research Labs., Melbourne, Australia)

The validity of the test procedures used at overhaul to establish the surge margin of Lycoming T53 engines installed in Australian Defence Force (ADF) Iroquois helicopters has been assessed. Recommendations are made on the use of wave-off tests, on the

08 AIRCRAFT STABILITY AND CONTROL

increased surge margin applied at overhaul to ADF T53 engines and on the implementation of improved inspection criteria at the unit level. Author

08

AIRCRAFT STABILITY AND CONTROL

Includes aircraft handling qualities; piloting; flight controls; and autopilots.

A95-79251

AEROSERVOELASTIC ASPECTS OF WING/CONTROL SURFACE PLANFORM SHAPE OPTIMIZATION

ELI LIVNE Univ of Washington, Seattle, WA, United States and WEI-LIN LI AIAA Journal (ISSN 0001-1452) vol. 33, no. 2 February 1995 p. 302-311 refs (BTN-95-EIX95222650795) Copyright

Equivalent plate structural modeling and doublet point lifting surface unsteady aerodynamics are used to obtain analytic sensitivities of aeroelastic and aeroservoelastic response with respect to wing and control surface planform shape parameters. Rational function approximations for unsteady aerodynamic forces, their shape sensitivities, and the resulting linear time invariant state space models of aeroservoelastic systems and their shape sensitivities are examined. The goal is to develop effective and numerically efficient approximation techniques for wing shape optimization for use with nonlinear programming and approximation concepts as a multidisciplinary optimization strategy. Effects of structural and unsteady aerodynamic modeling errors are studied. Examination of approximation accuracy using alternative approximation techniques (and the resulting move limits) provide insight and experience on the way to realistic wing/control surface shape optimization with active controls and aeroservoelastic constraints. Author (EI)

N95-24260 National Defence Research Establishment, Linköping (Sweden).

INTERFACING A DIGITAL COMPASS TO A REMOTE-CONTROLLED HELICOPTER [INTERFACE MELLAN DIGITAL KOMPASS OCH RADIOSTYRD HELIKOPTER]

C. EKSTROEM Jun. 1994 13 p In SWAHILI (PB95-164927; FOA-C-30768-3.6) Avail: Issuing Activity (National Technical Information Service (NTIS))

One can use a digital compass as a tool to navigate a semiautonomous mini helicopter. This thesis describes how to create an interface between the digital compass (KVH C100) and the controlling servos in the mini helicopter. NTIS

09

RESEARCH AND SUPPORT FACILITIES (AIR)

Includes airports, hangars and runways; aircraft repair and overhaul facilities; wind tunnels; shock tube facilities; and engine test blocks.

A95-81020

SUPERCOOLING IN HYPERSONIC NITROGEN WIND TUNNELS

WAYLAND C. GRIFFITH North Carolina State Univ, Raleigh, NC, United States, WILLIAM J. YANTA, and WILLIAM C. RAGSDALE Journal of Fluid Mechanics (ISSN 0022-1120) vol. 269 June 25 1994 p. 283-299 refs (BTN-94-EIX95011441134) Copyright

Recent experimental observation of supercooling in large hypersonic wind tunnels using pure nitrogen identified a broad range

of nonequilibrium metastable vapor states of the flow in the test cell. To investigate this phenomenon a number of real-gas effects are analyzed and compared with predictions made using the ideal-gas equation of state and equilibrium thermodynamics. The observed limit on the extent of supercooling is found to be at 60% of the temperature difference from the sublimation line to Gibb's absolute limit on phase stability. The mass fraction then condensing is calculated to be 12-14%. Included in the study are virial effects, quantization of rotational and vibrational energy, and the possible role of vibrational relaxation and freezing in supercooling. Results suggest that use of the supercooled region to enlarge the Mach-Reynolds number test envelope may be practical. Data from model tests in supercooled flows support this possibility. Author (EI)

N95-24302* Purdue Univ., West Lafayette, IN. School of Aeronautical and Astronautical Engineering.

SUPERSONIC QUIET-TUNNEL DEVELOPMENT FOR LAMINAR-TURBULENCE TRANSITION RESEARCH Final Report, Feb. 1994 - Feb. 1995

STEVEN P. SCHNEIDER Feb. 1995 172 p

(Contract(s)/Grant(s): NAG1-1607)

(NASA-CR-198040; NAS 1.26:198040) Avail: CASI HC A08/MF A02

This grant supported research into quiet-flow supersonic wind-tunnels, between February 1994 and February 1995. Quiet-flow nozzles operate with laminar nozzle-wall boundary layers, in order to provide low-disturbance flow for studies of laminar-turbulent transition under conditions comparable to flight. Major accomplishments include: (1) development of the Purdue Quiet-Flow Ludwig Tube, (2) computational evaluation of the square nozzle concept for quiet-flow nozzles, and (3) measurement of the presence of early transition on the flat sidewalls of the NASA LaRC Mach 3.5 supersonic low-disturbance tunnel. Since items (1) and (2) are described in the final report for companion grant NAG1-1133, only item (3) is described here. A thesis addressing the development of square nozzles for high-speed, low-disturbance wind tunnels is included as an appendix. Author (revised)

N95-24388* North Carolina State Univ., Raleigh, NC.

DEVELOPMENT OF A MODEL PROTECTION AND DYNAMIC RESPONSE MONITORING SYSTEM FOR THE NATIONAL TRANSONIC FACILITY

CLARENCE P. YOUNG, JR., S. BALAKRISHNA (Vigyan Research Associates, Inc., Hampton, VA.), and W. ALLEN KILGORE (Calspan Corp., Hampton, VA.) Feb. 1995 30 p Prepared in cooperation with ViGYAN, Inc. and Calspan Corp.

(Contract(s)/Grant(s): NCC1-141; RTOP 505-59-85-01)

(NASA-CR-195041; NAS 1.26:195041) Avail: CASI HC A03/MF A01

A state-of-the-art, computerized model protection and dynamic response monitoring system has been developed for the NASA Langley Research Center National Transonic Facility (NTF). This report describes the development of the model protection and shutdown system (MPSS). A technical description of the system is given along with discussions on operation and capabilities of the system. Applications of the system to vibration problems are presented to demonstrate the system capabilities, typical applications, versatility, and investment research return derived from the system to date. The system was custom designed for the NTF but can be used at other facilities or for other dynamic measurement/diagnostic applications. Potential commercial uses of the system are described. System capability has been demonstrated for forced response testing and for characterizing and quantifying bias errors for onboard inertial model attitude measurement devices. The system is installed in the NTF control room and has been used successfully for monitoring, recording and analyzing the dynamic response of several model systems tested in the NTF. Author

N95-24424 Baker (Wilfred) Engineering, Inc., San Antonio, TX. **QUANTITY-DISTANCE REQUIREMENTS FOR EARTH-BERME**

MARK G. WHITNEY and KATHY H. SPIVEY Jun. 1993 52 p Limited Reproducibility: More than 20% of this document may be affected by microfiche quality

(Contract(s)/Grant(s): F08635-91-C-0189) (AD-A279692; WBE-228-001; AFCESA/ESL-TR-92-25) Avail: CASI HC A04

The subject work has been performed under Phase 1 of an SBIR program sponsored by Tyndall AFB. The effort concentrated on development of methods to quantify debris hazards from accidental explosions inside earth-bermed and unbermed aircraft shelters. The Phase 1 effort addressed shock loading, gas loading, debris breakup, and debris throw. The prediction model, Quantity-Distance Requirements for Aircraft Shelters (QDRACS), includes new programming which uses image charges and ray-tracing of shocks for the specific geometry of an aircraft shelter. Interior surfaces are divided into a grid of rectangular elements. Shock loads are calculated at each element for up to 20 munition stacks. Existing data were utilized to determine structural breakup dependence on load intensity and the formation of small or large debris. Venting is calculated using the FRANG program as a subroutine to QDRACS, but with special treatment for defining vent area and vent perimeter based on the breakup pattern, and venting provided by the door. The velocity of all missiles is calculated based on contributions from both the shock and gas pressure loading. Debris dispersion is calculated using MUDEMIMP as a subroutine. Model results were compared to the Q-D criteria based on DISTANT RUNNER tests. Hazard distances for Event 4 were predicted within 20 percent, and for Event 5, within 5 percent of the DISTANT RUNNER data. DTIC

N95-25399* Queensland Univ., Saint Lucia (Australia). Dept. of Mechanical Engineering.

THE SUPERORBITAL EXPANSION TUBE CONCEPT, EXPERIMENT AND ANALYSIS

A. J. NEELY and R. G. MORGAN *In its Shock Tunnel Studies of Scramjet Phenomena* 1993 p 97-105 Jan. 1995 Sponsored in cooperation with the Australian Research Council Avail: CASI HC A02/MF A02

In response to the need for ground testing facilities for super orbital re-entry research, a small scale facility has been set up at the University of Queensland to demonstrate the superorbital expansion tube concept. This unique device is a free piston driven, triple diaphragm, impulse shock facility which uses the enthalpy multiplication mechanism of the unsteady expansion process and the addition of a secondary shock driver to further heat the driver gas. The pilot facility has been operated to produce quasi-steady test flows in air with shock velocities in excess of 13 km/s and with a usable test flow duration of the order of 15 micro sec. an experimental condition produced in the facility with total enthalpy of 108 MJ/kg and a total pressure of 335 MPa is reported. A simple analytical flow model which accounts for non-ideal rupture of the light tertiary diaphragm and the resulting entropy increase in the test gas is discussed. It is shown that equilibrium calculations more accurately model the unsteady expansion process than calculations assuming frozen chemistry. This is because the high enthalpy flows produced in the facility can only be achieved if the chemical energy stored in the test flow during shock heating of the test gas is partially returned to the flow during the process of unsteady expansion. Measurements of heat transfer rates to a flat plate demonstrate the usability of test flow for aerothermodynamic testing and comparison of these rates with empirical calculations confirms the usable accuracy of the flow model. Author

N95-26053 Wright Lab., Wright-Patterson AFB, OH. **HEAT TRANSFER MEASUREMENTS IN SMALL SCALE WIND TUNNELS** Final Report, 1 Nov. 1983 - 1 Sep. 1987

JAMES R. HAYES Jun. 1994 36 p Limited Reproducibility: More than 20% of this document may be affected by microfiche quality (Contract(s)/Grant(s): AF PROJ. 2404) (AD-A288689; WL-TR-94-3097) Avail: Issuing Activity (Defense Technical Information Center (DTIC))

This report describes an effort at the Flight Dynamics Directorate to use small scale models, miniature instrumentation and small in-house hypersonic facilities to accomplish full configurational testing of vehicle concepts. The project included development of procedures for generating model geometry data and transmitting that data to 495th TW machine shops of model fabrication on NC machines. A discussion of problems peculiar to testing of small scale models is included. A comparison is presented of data taken under this effort with similar data taken in large production wind tunnels on large scale models. DTIC

10

ASTRONAUTICS

Includes astronautics (general); astrodynamics; ground support systems and facilities (space); launch vehicles and space vehicles; space transportation; spacecraft communications, command and tracking; spacecraft design, testing and performance; spacecraft instrumentation; and spacecraft propulsion and power.

A95-80389* National Aeronautics and Space Administration. Langley Research Center, Hampton, VA.

GUIDANCE AND CONTROL, 1993; ANNUAL ROCKY MOUNTAIN GUIDANCE AND CONTROL CONFERENCE, 16TH, KEYSTONE, CO, FEB. 6-10, 1993

ROBERT D. CULP, editor Colorado Univ., Boulder, CO, US and **GEORGE BICKLEY**, editor Ball Aerospace Systems Group, Boulder, CO, US San Diego, CA American Astronautical Society (Advances in the Astronautical Sciences, Vol. 81) (ISSN 0065-3438) 1993 630 p.

(ISBN-0-87703-365-X; HTN-95-A0314) Copyright

Papers from the sixteenth annual American Astronautical Society Rocky Mountain Guidance and Control Conference are presented. The topics covered include the following: advances in guidance, navigation, and control; control system videos; guidance, navigation and control embedded flight control systems; recent experiences; guidance and control storyboard displays; and applications of modern control, featuring the Hubble Space Telescope (HST) performance enhancement study. For individual titles, see A95-80390 through A95-80436. Hemer

A95-80390

APPLICATION OF FUZZY LOGIC TO OPTIMIZE PLACEMENT OF AN ACQUISITION, TRACKING, AND POINTING EXPERIMENT

JERRY BUKLEY TASC, Huntsville, AL, US *In Guidance and control, 1993; Annual Rocky Mountain Guidance and Control Conference, 16th, Keystone, CO, Feb. 6-10, 1993. A95-80389* San Diego, CA American Astronautical Society (Advances in the Astronautical Sciences, Vol. 81) (ISSN 0065-3438) 1993 p. 3-12 Copyright

The experiment is comprised of a 115,000 cubic meter helium balloon which lifts a 2,900 kg Acquisition, Tracking and Pointing (ATP) experiment package to an altitude of 26 km. The Phillips Laboratory High Altitude Balloon Experiment (HABE) has been developed as a cost-effective means of testing satellite ATP technologies in an environment similar to space. A major advantage of the concept is the flexibility in placement and timing afforded a balloon over a satellite. This flexibility allows HABE to engage targets-of-opportunity launched from the domestic ranges without requiring a dedicated or closely coordinated launch time. The placement of HABE is optimized to maximize active track time. A routine was developed to raster scan the mathematical model of

a flight corridor while accumulating the intervals of continuous engagement that satisfy a list of ten rules. Although successful, this method is unable to place priorities or make trades based on the relative importance of the rules. The use of fuzzy logic in the form of approximate reasoning to evaluate the rules, while also considering goals, enables key qualitative considerations to be factored into the overall evaluation. This paper describes the application of fuzzy logic to data analysis and compares the results to conventional Boolean techniques.

Author (Herner)

A95-80409

DESCRIBING AN ATTITUDE

D. I. KOLVE Boeing Defense and Space Group, Seattle, WA, US *In* Guidance and control, 1993; Annual Rocky Mountain Guidance and Control Conference, 16th, Keystone, CO, Feb. 6-10, 1993. A95-80389 San Diego, CA American Astronautical Society (Advances in the Astronautical Sciences, Vol. 81) (ISSN 0065-3438) 1993 p. 289-303

Copyright

Describing the orientation of one coordinate system relative to another is a common requirement in the fields of navigation, guidance and control. The intent of this paper is to summarize the fundamental relationships between the most commonly used descriptors of attitude: direction cosine matrices, quaternions, and Euler angles. Most of the relations included here are well known, but described in a more compact form. Other transforms are new, such as a completely general and direct method for determining Euler angles from quaternions without using the direction cosine matrix as an intermediate step, and a simple interpretation and application of quaternion subtraction. Also included are general case least squares solutions to finding direction cosine matrices and quaternions, and the derivations and solutions of their differential equations.

Author (Herner)

A95-80427

A NEW GUIDANCE AND FLIGHT CONTROL SYSTEM FOR THE DELTA 2 LAUNCH VEHICLE

R. PORDON Allied Signal Aerospace, Teterboro, NJ, US, K. TOMPETRINI Allied Signal Aerospace, Teterboro, NJ, US, S. WEINSTEIN Allied Signal Aerospace, Teterboro, NJ, US, and H. DHUYVETTER McDonnell Douglas Aerospace, Huntington Beach, CA, US *In* Guidance and control, 1993; Annual Rocky Mountain Guidance and Control Conference, 16th, Keystone, CO, Feb. 6-10, 1993. A95-80389 San Diego, CA American Astronautical Society (Advances in the Astronautical Sciences, Vol. 81) (ISSN 0065-3438) 1993 p. 455

Copyright

Because redundancy potentially offers significant improvements in the probability for launch success, it has been one of the most sought after capabilities for launch vehicles. Avionic designs offering this capability have, to date, been largely prohibited due to cost, weight and development schedules. The Redundant Inertial Flight Control Assembly (RIFCA) is a system which offers a practical implementation of fault tolerant avionics through redundancy. The RIFCA program is completing the development phase and will lead to the production of flight hardware, which will start flying on the DELTA 2 in late 1994. This paper presents the redundancy concepts used in both the RIFCA and the vehicle, describes the RIFCA hardware and its integration with the software to provide a fail-op capability within the framework of a cost effective, weight effective system design.

Author (revised by Herner)

A95-81093

DYNAMICS AND CONTROL OF A TETHERED FLIGHT VEHICLE

T. S. NO Auburn Univ, Auburn, AL, United States and J. E. COCHRAN, JR. *Journal of Guidance, Control, and Dynamics* (ISSN 0731-5090) vol. 18, no. 1 January-February 1995 p. 66-72 refs (BTN-95-EIX95242670754) Copyright

Certain types of the problems of dynamics and control of maneuverable tethered flight vehicles are dealt with. The numerically linearized equations of motion are used in a stability analysis

and to design control laws that may be used in station keeping and maneuvering of the vehicle. For motion in which deviations from the equilibrium states are small in magnitude and the maneuver of the vehicle is confined to a neighboring region, the use of a linear quadratic regulator (LQR) for the station keeping and a linear terminal controller for the maneuver is investigated. For the model and conditions used, it is shown that aerodynamic control may be used successfully for station keeping and maneuvering, and the aerodynamic control yields results comparable to those obtained by using reaction control.

Author (EI)

A95-81360* National Aeronautics and Space Administration. Langley Research Center, Hampton, VA.

LOAD ALLEVIATION MANEUVERS FOR A LAUNCH VEHICLE

HANS SEYWALD Analytical Mechanics Associates, Inc., Hampton, VA, US and ROBERT R. BLESS Lockheed Engineering and Sciences Co., Hampton, VA, US *In* Spaceflight mechanics, 1993; AAS/AIAA Spaceflight Mechanics Meeting, 3rd, Pasadena, CA, Feb. 22-24, 1993, Parts 1 & 2. A95-81344 San Diego, CA American Astronautical Society (Advances in the Astronautical Sciences, Vol. 82, Pts. 1 & 2) (ISSN 0065-3438) 1993 p. 257-269

(Contract(s)/Grant(s): NAS1-18935; NAS1-19000)

Copyright

This paper addresses the design of a forward-looking autopilot that is capable of employing a priori knowledge of wind gusts ahead of the flight path to reduce the bending loads experienced by a launch vehicle. The analysis presented in the present paper is only preliminary, employing a very simple vehicle dynamical model and restricting itself to wind gusts of the form of isolated spikes. The main result of the present study is that linear quadratic regulator (LQR) based feedback laws are inappropriate to handle spike-type wind perturbations with large amplitude and narrow base. The best performance is achieved with an interior-point penalty optimal control formulation which can be well approximated by a simple feedback control law. Reduction of the maximum bending loads by nearly 50% is demonstrated.

Author (Herner)

A95-81374

IDEAL PROPORTIONAL NAVIGATION

PIN-JAR YUAN Chung Shan Inst. of Science and Technology, Lungtan, Taiwan and JENG-SHING CHERN Chung Shan Inst. of Science and Technology, Lungtan, Taiwan *In* Spaceflight mechanics, 1993; AAS/AIAA Spaceflight Mechanics Meeting, 3rd, Pasadena, CA, Feb. 22-24, 1993, Parts 1 & 2. A95-81344 San Diego, CA American Astronautical Society (Advances in the Astronautical Sciences, Vol. 82, Pts. 1 & 2) (ISSN 0065-3438) 1993 p. 501-512

Copyright

Proportional navigation has been proved to be a useful guidance technique in several surface-to-air and air-to-air homing systems for interception of airborne targets. Besides the familiar pure, true, and generalized proportional navigation guidance laws, a new guidance scheme, named ideal proportional navigation with commanded acceleration applied in the direction normal to the relative velocity between interceptor and target, is presented. In this study, the closed-form solutions of ideal proportional navigation are completely derived for maneuvering and non-maneuvering target and some important characteristics related to the system performance are introduced and investigated. Under this scheme, the capture criterion is related to the effective proportional navigation constant only, no matter what the initial condition and target maneuver are. With some more cost of energy consumption, this new guidance scheme has a larger capture area and is much more effective than previous ones.

Author (Herner)

N95-25664# National Aerospace Lab., Tokyo (Japan). Aerodynamics Div.

AERODYNAMIC CHARACTERISTICS OF THE ORBITAL REENTRY VEHICLE EXPERIMENTAL PROBE FINS IN A SUPERSONIC FLOW

MITSUNORI WATANABE, HIDEO SEKINE, ATSUSHI TATE, and

JUNICHI NODA Apr. 1994 18 p In JAPANESE
(ISSN 0389-4010)

(NAL-TR-1232) Avail: CASI HC A03/MF A01

The aerodynamic characteristics of probe fins with a sweep angle of 60 deg, which are equipped on the Orbital Reentry Experiment (OREX) vehicle to measure the surrounding ionized gas temperature and electron number density distributions in the high temperature communication black out regions, have been measured in the supersonic wind tunnel of the National Aerospace Laboratory and compared with those of the fins of 0 deg sweep angles. Since the probes are to be embedded in the boundary layer where the local Mach number is less than 2.5 over the OREX surface at a hypersonic flight speed, the aerodynamic characteristics in supersonic regions are needed to estimate the rolling moments of fins caused by the error of the installation angles. The lift coefficient slope of the probe fins decreases as the Mach number increases, being less than the values for the 0 deg sweep fins. The drag coefficient depends highly on the sweep angle of the fins in Mach number regions less than 2.5.

Author

11

CHEMISTRY AND MATERIALS

Includes chemistry and materials (general); composite materials; inorganic and physical chemistry; metallic materials; nonmetallic materials; and propellants and fuels.

A95-78467

THEORETICAL AND EXPERIMENTAL STUDIES OF FRETTEING-INITIATED FATIGUE FAILURE OF AEROENGINE COMPRESSOR DISCS

P. PAPANIKOS Univ of Toronto, Toronto, Ont, Canada and S. A. MEGUID Fatigue and Fracture of Engineering Materials & Structures (ISSN 8756-758X) vol. 17, no. 5 May 1994 p. 539-550 refs (BTN-94-EIX94421372285) Copyright

A finite element analysis and fatigue crack growth studies are made of dovetail joints in aeroengine compressor discs. Three aspects are examined: the first deals with the finite element stress analysis of the critical geometrical features and interface conditions of different dovetail configurations, thus enabling an assessment to be made of the critically loaded regions in the disc. The second deals with the prediction of the direction of potential fatigue cracks, which were allowed to initiate in the finite element model at the regions where fretting damage is most likely to occur, using an incremental crack tracking criterion. The third is concerned with the verification of the above modelling techniques with fatigue tests on a uniaxial back-to-back arrangement, which attempts to simulate the stress fields of a rotating disc.

Author (EI)

N95-24220*# Virginia Univ., Charlottesville, VA. Dept. of Materials Science and Engineering.

NASA-UVA LIGHT AEROSPACE ALLOY AND STRUCTURES TECHNOLOGY PROGRAM (LA2ST)

Progress Report, 1 Jul. - 31 Dec. 1994

EDGAR A. STARKE, JR., RICHARD P. GANGLOFF, CARL T. HERAKOVICH, JOHN R. SCULLY, GARY J. SHIFLET, GLENN E. STONER, and JOHN A. WERT Mar. 1995 209 p

(Contract(s)/Grant(s): NAG1-745)

(NASA-CR-198041; NAS 1.26:198041; UVA/528266/MSE94/117) Avail: CASI HC A10/MF A03

The NASA-UVA Light Aerospace Alloy and Structures Technology (LA2ST) Program was initiated in 1986 and continues with a high level of activity. Projects are being conducted by graduate students and faculty advisors in the Department of Materials Science and Engineering, as well as in the Department of Civil Engineering and Applied Mechanics, at the University of Virginia. Here, we report on progress achieved between July 1 and December 31, 1994. The objective of the LA2ST Program is to conduct interdisciplinary graduate student research on the performance of next generation,

light-weight aerospace alloys, composites and thermal gradient structures in collaboration with NASA-Langley researchers. Specific technical objectives are presented for each research project. We generally aim to produce relevant data and basic understanding of material mechanical response, environmental/corrosion behavior, and microstructure; new monolithic and composite alloys; advanced processing methods; new solid and fluid mechanics analyses; measurement and modeling advances; and a pool of educated graduate students for aerospace technologies.

Author

N95-24878*# Virginia Univ. Hospital, Charlottesville, VA. School of Engineering and Applied Science.

NASA-UVA LIGHT AEROSPACE ALLOY AND STRUCTURES TECHNOLOGY PROGRAM SUPPLEMENT: ALUMINUM-BASED MATERIALS FOR HIGH SPEED AIRCRAFT

Semiannual Report, 1 Jul. - 31 Dec. 1992

E. A. STARKE, JR., ed. Feb. 1995 383 p

(Contract(s)/Grant(s): NAG1-745; RTOP 537-06-20-06)

(NASA-CR-4645; NAS 1.26:4645) Avail: CASI HC A17/MF A03

This report on the NASA-UVA light aerospace alloy and structure technology program supplement: Aluminum-Based Materials for High Speed Aircraft covers the period from July 1, 1992. The objective of the research is to develop aluminum alloys and aluminum matrix composites for the airframe which can efficiently perform in the HSCT environment for periods as long as 60,000 hours (certification for 120,000 hours) and, at the same time, meet the cost and weight requirements for an economically viable aircraft. Current industry baselines focus on flight at Mach 2.4. The research covers four major materials systems: (1) Ingot metallurgy 2XXX, 6XXX, and 8XXX alloys, (2) Powder metallurgy 2XXX alloys, (3) Rapidly solidified, dispersion strengthened Al-Fe-X alloys, and (4) Discontinuously reinforced metal matrix composites. There are ten major tasks in the program which also include evaluation and trade-off studies by Boeing and Douglas aircraft companies.

Author

N95-24989# National Aerospace Lab., Tokyo (Japan). Airframe Div.

STUDY ON TENSILE FATIGUE TESTING METHOD OF UNIDIRECTIONAL FIBER-RESIN MATRIX COMPOSITES

YOSHIO NOGUCHI Jul. 1994 13 p In JAPANESE

(ISSN 0389-4010)

(NAL-TR-1241) Avail: CASI HC A03/MF A01

The aim of the Versailles Project on advanced materials and standards (VAMAS) program is to evaluate the mechanical properties of advanced materials. In this study, as part of the polymer composites, the first phase of this round robin test was carried out to examine the tension-tension fatigue properties of unidirectional GFRP and CFRP. Fatigue tests were undertaken in a sinusoidal load-controlled testing mode, with a load ratio of 0.1. In the case of CFRP tests, the comparison of cold-setting epoxy resin and curing epoxy resin film as the end tab adhesive was made. It was found that the fatigue strength differed largely between the two types of tab adhesive. In another study, the effects of the end-tab configuration of the specimen and the testing frequency of fatigue behavior of unidirectional CFRP specimen were examined. As for the tab configuration, 10 deg tapered and untapered end-tab specimens were provided. On the testing frequency, fatigue tests were conducted with 2, 5 and 10Hz. The difference of fatigue strength under these testing conditions was found to be small in the present study.

Author

N95-26004# Lockheed Environmental Systems and Technologies Co., Las Vegas, NV.

PARTS WASHING ALTERNATIVES STUDY: UNITED STATES COAST GUARD. PROJECT SUMMARY AND REPORT

BRAD MONTGOMERY Jan. 1995 80 p

(Contract(s)/Grant(s): EPA-68-C4-0020)

(PB95-166146; EPA/600/R-95/006) Avail: CASI HC A05/MF A01

The report has been written to assist the United States Coast

11 CHEMISTRY AND MATERIALS

Guard (USCG) industrial managers in determining the most cost effective and environmentally acceptable parts washing alternatives for their specific applications. An evaluation was conducted on four different cleaners from three different USCG facilities. The following parts cleaners were evaluated: Bio seven, Penatone 724, Safety-Kleen 105, and Brulin 815GD. All four cleaners are effective cleaners for the specific applications described in this evaluation. The evaluation included the categories of process description; environmental, safety and health impacts; cost analysis; and the material and emission reduction opportunities. NTIS

N95-26119*# National Aeronautics and Space Administration. Lewis Research Center, Cleveland, OH.

THERMAL BARRIER COATING WORKSHOP Abstracts

W. J. BRINDLEY, comp., W. Y. LEE, comp. (Oak Ridge National Lab., TN.), J. G. GOEDJEN, comp., and S. J. DAPKUNAS, comp. (National Inst. of Standards and Technology, Gaithersburg, MD.) Mar. 1995 31 p Workshop held in Westlake, OH, 27-29 Mar. 1995; cosponsored by NASA, DOE, and NIST (Contract(s)/Grant(s): RTOP 505-63-52) (NASA-CP-10170; E-9509; NAS 1.55:10170) Avail: CASI HC A03/MF A01

This document contains the agenda and presentation abstracts for the Thermal Barrier Coating Workshop, sponsored by NASA, DOE, and NIST. The workshop covered thermal barrier coating (TBC) issues related to applications, processing, properties, and modeling. The intent of the workshop was to highlight the state of knowledge on TBC's and to identify critical gaps in knowledge that may hinder TBC use in advanced applications. The workshop goals were achieved through presentations by 22 speakers representing industry, academia, and government as well as through extensive discussion periods. For individual titles, see N95-26120 through N95-26140.

N95-26120*# Pratt and Whitney Aircraft, West Palm Beach, FL. **A DESIGN PERSPECTIVE ON THERMAL BARRIER COATINGS Abstract Only**

F. O. SOECHTING In NASA. Lewis Research Center, Thermal Barrier Coating Workshop p 3 Mar. 1995
Avail: CASI HC A01/MF A01

This technical paper addresses the challenges for maximizing the benefit of thermal barrier coatings for turbine engine applications. The perspective is from a customer's viewpoint, a turbine airfoil designer, who is continuously challenged to increase the turbine inlet temperature capability for new products while maintaining cooling flow levels or even reducing them. This is a fundamental requirement to achieve increased engine thrust levels. Developing advanced material systems for the turbine flowpath airfoils is one approach to solve this challenge, for example, high temperature nickel based superalloys or thermal barrier coatings to insulate the metal airfoil from the hot flowpath environment. The second approach is to increase the cooling performance of the turbine airfoil, which enables increased flowpath temperatures and reduced cooling flow levels. Thermal barrier coatings have been employed in jet engine applications for almost 30 years. The initial application was on augmentor lines to provide thermal protection during afterburner operation. However, the production use of thermal barrier coating in the turbine section has only occurred in the past 15 years. The application was limited to stationary parts, and only recently incorporated on the rotating turbine blades. This lack of endorsement of thermal barrier coatings resulted from the poor initial durability of these coatings in high heat flux environments. Significant improvements have been made to enhance spallation resistance and erosion resistance which has resulted in increased reliability of these coatings in turbine applications. Author

N95-26121*# National Aeronautics and Space Administration. Lewis Research Center, Cleveland, OH.

THERMAL BARRIER COATINGS FOR AIRCRAFT ENGINES: HISTORY AND DIRECTIONS Abstract Only

R. A. MILLER In its Thermal Barrier Coating Workshop p 5 Mar.

1995

Avail: CASI HC A01/MF A01

Thin thermal barrier coatings for protecting aircraft turbine section airfoils are examined. The discussion focuses on those advances that led first to their use for component life extension and more recently as an integral part of airfoil design. It is noted that development has been driven by laboratory rig and furnace testing corroborated by engine testing and engine field experience. The technology has also been supported by performance modeling to demonstrate benefits and life modeling for mission analysis. Factors which have led to the selection of the current state-of-the-art plasma sprayed and physical vapor deposited zirconia-yttria/MCraIY TBC's is emphasized in addition to observations fundamentally related to their behavior. Current directions in research into thermal barrier coatings and recent progress at NASA is also noted. Author

N95-26122*# Department of Energy, Washington, DC. Office of Industrial Technologies.

THERMAL BARRIER COATINGS ISSUES IN ADVANCED

LAND-BASED GAS TURBINES Abstract Only

W. P. PARKS, W. Y. LEE (Oak Ridge National Lab., TN.), and I. G. WRIGHT (Oak Ridge National Lab., TN.) In NASA. Lewis Research Center, Thermal Barrier Coating Workshop p 7 Mar. 1995
Avail: CASI HC A01/MF A01

The Department of Energy's Advanced Turbine System (ATS) program is aimed at forecasting the development of a new generation of land-based gas turbine systems with overall efficiencies significantly beyond those of current state-of-the-art machines, as well as greatly increased times between inspection and refurbishment, improved environmental impact, and decreased cost. The proposed duty cycle of ATS turbines will require the use of different criteria in the design of the materials for the critical hot gas path components. In particular, thermal barrier coatings will be an essential feature of the hot gas path components in these machines. While such coatings are routinely used in high-performance aircraft engines and are becoming established in land-based turbines, the requirements of the ATS turbine application are sufficiently different that significant improvements in thermal barrier coating technology will be necessary. In particular, it appears that thermal barrier coatings will have to function on all airfoil sections of the first stage vanes and blades to provide the significant temperature reduction required. In contrast, such coatings applied to the blades and vanes of advanced aircraft engines are intended primarily to reduce air cooling requirements and extend component lifetime; failure of those coatings can be tolerated without jeopardizing mechanical or corrosion performance. A major difference is that in ATS turbines these components will be totally reliant on thermal barrier coatings which will, therefore, need to be highly reliable even over the leading edges of first stage blades. Obviously, the ATS program provides a very challenging opportunity for TBC's, and involves some significant opportunities to extend this technology. Author

N95-26123*# National Inst. of Standards and Technology, Gaithersburg, MD.

MEASUREMENT METHODS AND STANDARDS FOR PROCESSING AND APPLICATION OF THERMAL BARRIER COATINGS Abstract Only

S. J. DAPKUNAS In NASA. Lewis Research Center, Thermal Barrier Coating Workshop p 9 Mar. 1995
Avail: CASI HC A01/MF A01

Application of thermal barrier coatings deposited by thermal spray, physical vapor and possibly other methods is expected to be extended from aircraft gas turbines to industrial and utility gas turbines as well as diesel engines. This increased usage implies the participation of greater numbers of processors and users, making the availability of standards for process control and property measurement more important. Available standards for processing and evaluation of thermal barrier coatings are identified as well as those needed in the future but currently unavailable. Author

N95-26124* Department of Energy, Washington, DC. Office of Transportation Technologies.

THERMAL BARRIER COATINGS APPLICATION IN DIESEL ENGINES Abstract Only

J. W. FAIRBANKS *In* NASA. Lewis Research Center, Thermal Barrier Coating Workshop p 11 Mar. 1995

Avail: CASI HC A01/MF A01

Commercial use of thermal barrier coatings in diesel engines began in the mid 70's by Dr. Ingard Kvernes at the Central Institute for Industrial Research in Oslo, Norway. Dr. Kvernes attributed attack on diesel engine valves and piston crowns encountered in marine diesel engines in Norwegian ships as hot-corrosion attributed to a reduced quality of residual fuel. His solution was to coat these components to reduce metal temperature below the threshold of aggressive hot-corrosion and also to provide protection. The Department of Energy has supported thermal barrier coating development for diesel engine applications. In the Clean Diesel - 50 Percent Efficient (CD-50) engine for the year 2000, thermal barrier coatings will be used on piston crowns and possibly other components. The primary purpose of the thermal barrier coatings will be to reduce thermal fatigue as the engine peak cylinder pressure will nearly be doubled. As the coatings result in higher available energy in the exhaust gas, efficiency gains are achieved through use of this energy by turbochargers, turbocompounding or thermoelectric generators. Author

N95-26125* Pratt and Whitney Aircraft, East Hartford, CT.
THERMAL BARRIER COATING EXPERIENCE IN THE GAS TURBINE ENGINE Abstract Only

S. BOSE and J. DEMASI-MARCIN *In* NASA. Lewis Research Center, Thermal Barrier Coating Workshop p 13 Mar. 1995

Avail: CASI HC A01/MF A01

Thermal Barrier Coatings (TBC), provide thermal insulation and oxidation resistance in an environment consisting of hot combustion gases. TBC's consist of a two layer system. The outer ceramic layer provides good thermal insulation due to the low thermal conductivity of the ceramic coatings used, while the inner metallic bond coat layer provides needed oxidation resistance to the underlying superalloy. Pratt & Whitney has over a decade of experience with several generations of TBC systems on turbine airfoils. This paper will focus on the latest TBC field experience along with a proposed durability model. Author

N95-26126* General Electric Co., Cincinnati, OH. Aircraft Engines.

PVD TBC EXPERIENCE ON GE AIRCRAFT ENGINES Abstract Only

A. BARTZ, A. MARIOCCHI, and D. J. WORTMAN *In* NASA. Lewis Research Center, Thermal Barrier Coating Workshop p 15 Mar. 1995

Avail: CASI HC A01/MF A01

The higher performance levels of modern gas turbine engines present significant challenges in the reliability of materials in the turbine. The increased engine temperatures required to achieve the higher performance levels reduce the strength of the materials used in the turbine sections of the engine. Various forms of Thermal Barrier Coatings (TBC's) have been used for many years to increase the reliability of gas turbine engine components. Recent experience with the Physical Vapor Deposition (PVD) process using ceramic material has demonstrated success in extending the service life of turbine blades and nozzles. Engine test results of turbine components with a 125 micrometer (0.005 in) PVD TBC have demonstrated component operating temperatures of 56-83 C (100-150 F) lower than uncoated components. Engine testing has also revealed the TBC is susceptible to high angle particle impact damage. Sand particles and other engine debris impact the TBC surface at the leading edge of airfoils and fracture the PVD columns. As the impacting continues the TBC erodes away in local areas. Analysis of the eroded areas has shown a slight increase in temperature over a fully coated area, however, a significant temperature reduction was realized over an airfoil without any TBC. Author

N95-26128* Solar Turbines, Inc. San Diego, CA.

PERSPECTIVE ON THERMAL BARRIER COATINGS FOR INDUSTRIAL GAS TURBINE APPLICATIONS Abstract only

Z. Z. MUTASIM, L. L. HSU, and W. D. BRENTNALL *In* NASA. Lewis Research Center, Thermal Barrier Coating Workshop p 19 Mar. 1995

Avail: CASI HC A01/MF A01

Thermal Barrier Coatings (TBC's) have been used in high thrust aircraft engines for many years, and have proved to be very effective in allowing higher turbine inlet temperatures. TBC life requirements for aircraft engines are typically less than those required in industrial gas turbines. The use of TBC's for industrial gas turbines can increase if durability and longer service life can be successfully demonstrated. This paper will describe current and future applications of TBC's in industrial gas turbine engines. Early testing and applications of TBC's will also be reviewed. This paper focuses on the key factors that are expected to influence utilization of TBC's in advanced industrial gas turbine engines. It is anticipated that reliable, durable and high effective coating systems will be produced that will ultimately improve engine efficiency and performance. Author

N95-26131* Pratt and Whitney Aircraft, West Palm Beach, FL.

JET ENGINE APPLICATIONS FOR MATERIALS WITH NANOMETER-SCALE DIMENSIONS Abstract Only

J. W. APPLEBY, JR. *In* NASA. Lewis Research Center, Thermal Barrier Coating Workshop p 27 Mar. 1995

Avail: CASI HC A01/MF A01

The performance of advanced military and commercial gas turbine engines is often linked to advances in materials technology. High performance gas turbine engines being developed require major material advances in strength, toughness, reduced density and improved temperature capability. The emerging technology of nanostructured materials has enormous potential for producing materials with significant improvements in these properties. Extraordinary properties demonstrated in the laboratory include material strengths approaching theoretical limit, ceramics that demonstrate ductility and toughness, and material with ultra-high hardness. Nanostructured materials and coatings have the potential for meeting future gas turbine engine requirements for improved performance, reduced weight and lower fuel consumption. Author

N95-26133* Oak Ridge National Lab., TN.

THERMAL CONDUCTIVITY OF ZIRCONIA THERMAL BARRIER COATINGS Abstract Only

R. B. DINWIDDIE, S. C. BEECHER, B. A. NAGARAJ (General Electric Co., Cincinnati, OH.), and C. S. MOORE (General Electric Co., Cincinnati, OH.) *In* NASA. Lewis Research Center, Thermal Barrier Coating Workshop p 31 Mar. 1995

Avail: CASI HC A01/MF A01

Thermal barrier coatings (TBC's) applied to the hot gas components of turbine engines lead to enhanced fuel efficiency and component reliability. Understanding the mechanisms which control the thermal transport behavior of the TBC's is of primary importance. Physical vapor deposition (PVD) and plasma spraying (PS) are the two most commonly used coating techniques. These techniques produce coatings with unique microstructures which control their performance and stability. The PS coatings were applied with either standard power or hollow sphere particles. The hollow sphere particles yielded a lower density and lower thermal conductivity coating. The thermal conductivity of both fully and partially stabilized zirconia, before and after thermal aging, will be compared. The thermal conductivity of the coatings permanently increase upon being exposed to high temperatures. These increases are attributed to microstructural changes within the coatings. Sintering of the as fabricated plasma sprayed lamellar structure is observed by scanning electron microscopy of coatings isothermally heat treated at temperatures greater than 1100 C. During this sintering process the planar porosity between lamella is converted to a series of small spherical pores. The change in pore morphology is the primary reason for the observed increase in thermal conductivity. This increase in thermal conductivity can be modeled using a relationship

which depends on both the temperature and time of exposure. Although the PVD coatings are less susceptible to thermal aging effects, preliminary results suggest that they have a higher thermal conductivity than PS coatings, both before and after thermal aging. The increases in thermal conductivity due to thermal aging for partially stabilized plasma sprayed zirconia have been found to be less than for fully stabilized plasma sprayed zirconia coatings. The high temperature thermal diffusivity data indicates that if these coatings reach a temperature above 1100 C during operation, they will begin to lose their effectiveness as a thermal barrier. Author

N95-26138* Purdue Univ., West Lafayette, IN.
**THERMAL FRACTURE MECHANISMS IN CERAMIC
THERMAL BARRIER COATINGS Abstract Only**
K. KOKINI, B. D. CHOULES, and Y. R. TAKEUCHI / In NASA. Lewis
Research Center, Thermal Barrier Coating Workshop p 41 Mar.
1995

Avail: CASI HC A01/MF A01

Ceramic thermal barrier coatings represent an attractive method of increasing the high temperature limits for systems such as diesel engines, gas turbines and aircraft engines. However, the dissimilarities between ceramics and metal, as well as the severe temperature gradients applied in such systems, cause thermal stresses which can lead to cracking and ultimately spalling of the coating. This paper reviews the research which considers initiation of surface cracks, interfacial edge cracks and the effect of a transient thermal load on interface cracks. The results of controlled experiments together with analytical models are presented. The implications of these findings to the differences between diesel engines and gas turbines are discussed. The importance of such work for determining the proper design criteria for thermal barrier coatings is underlined. Author

N95-26140* Pratt and Whitney Aircraft, East Hartford, CT.
**THERMAL BARRIER COATING LIFE MODELING IN
AIRCRAFT GAS TURBINE ENGINES Abstract Only**
D. M. NISSLEY / In NASA. Lewis Research Center, Thermal Barrier
Coating Workshop p 45 Mar. 1995

Avail: CASI HC A01/MF A01

Analytical models useful for predicting ceramic thermal barrier coating (TBC) spalling life in aircraft gas turbine engines are presented. Electron beam-physical vapor deposited (EB-PVD) and plasma sprayed TBC systems are discussed. TBC spalling was attributed to a combination of mechanisms such as metal oxidation at the ceramic-metal interface, ceramic-metal interface stress concentrations at free surfaces due to dissimilar materials, ceramic-metal interface stresses caused by local radius of curvature and interface roughness, material properties and mechanical behavior, transient temperature gradients across the ceramic layer and component design features. TBC spalling life analytical models were developed based on observations of TBC failure modes and plausible failure theories. TBC failure was assumed to occur when the imposed stresses exceeded the material strength (at or near the ceramic-metal interface). TBC failure knowledge gaps caused by lack of experimental evidence and analytical understanding are noted. The analytical models are considered initial engineering approaches that capture observed TBC failure trends. Author

N95-26251* National Aeronautics and Space Administration.
Langley Research Center, Hampton, VA.
**DESIGN AND EVALUATION OF A FOAM-FILLED HAT-
STIFFENED PANEL CONCEPT FOR AIRCRAFT PRIMARY
STRUCTURAL APPLICATIONS**
DAMODAR R. AMBUR Jan. 1995 21 p Presented at the Third
Advanced Composites Technology Conference, Jun. 1992
(Contract(s)/Grant(s): RTOP 505-63-50-08)
(NASA-TM-109175; NAS 1.15:109175) Avail: CASI HC A03/MF
A01

A structurally efficient hat-stiffened panel concept that utilizes a structural foam as stiffener core has been designed for aircraft

primary structural applications. This stiffener concept utilizes a manufacturing process that can be adapted readily to grid-stiffened structural configurations which possess inherent damage tolerance characteristics due to their multiplicity of load paths. The foam-filled hat-stiffener concept in a prismatically stiffened panel configuration is more efficient than most other stiffened panel configurations in a load range that is typical for both fuselage and wing structures. The prismatically stiffened panel concept investigated here has been designed using AS4/3502 prepregged tape and Rohacell foam core and evaluated for its buckling and postbuckling behavior with and without low-speed impact damage. The results from single-stiffener and multi-stiffener specimens suggest that this structural concept responds to loading as anticipated and has good damage tolerance characteristics. Author

12

ENGINEERING

Includes engineering (general); communications; electronics and electrical engineering; fluid mechanics and heat transfer; instrumentation and photography; lasers and masers; mechanical engineering; quality assurance and reliability; and structural mechanics.

A95-77379
**MODAL CHARACTERISTICS OF ROTORS USING A
CONICAL SHAFT FINITE ELEMENT**

M. A. MOHIUDDIN King Fahd Univ of Petroleum & Minerals,
Dhahran, Saudi Arabia and Y. A. KHULIEF Computer Methods in
Applied Mechanics and Engineering (ISSN 0045-7825) vol. 115,
no. 1-2 May 1994 p. 125-144 refs

(BTN-94-EIX94401359745) Copyright

A finite element formulation for a rotor-bearing system is presented. The equations of coupled bending and torsional motion of the rotating shaft are derived using the Lagrangian approach. A conical beam finite element for vibration analysis of rotating shafts including shear deformations and rotary inertia is derived. The finite beam element has ten degrees of freedom and accounts for linear tapering. Explicit expressions for the element mass, stiffness, and gyroscopic matrices are derived using consistent mass formulation. The finite element discretization is employed, the generalized eigenvalue problem is defined, and numerical solutions are obtained for a wide range of whirl ratios, spin speeds, and taper ratios. Comparisons are made wherever possible with exact solutions, and with other numerical results available in the literature. Extended numerical results are produced for a wider range of parameters for which solutions were not previously attempted. Author (EI)

A95-77921* National Aeronautics and Space Administration.
Langley Research Center, Hampton, VA.
**VISCOPLASTIC RESPONSE OF STRUCTURES FOR
INTENSE LOCAL HEATING**
EARL A. THORNTON University of Virginia, Charlottesville, VA, US
and J. D. KOLENSKI University of Virginia, Charlottesville, VA, US
Journal of Aerospace Engineering (ISSN 0893-1321) vol. 7, no. 1
January 1994 p. 50-71 Research sponsored by NASA Langley
(HTN-95-41540) Copyright

A thermoviscoplastic finite element method employing the Bodner-Partom constitutive model is used to investigate the response of simplified thermal-structural models to intense local heating. The computational method formulates the problem in rate and advances the solution in time by numerical integration. The thermoviscoplastic response of simplified structures with prescribed temperatures is investigated. With rapid rises of temperature, the nickel alloy structures display initially higher yield stresses due to strain rate effects. As temperatures approach elevated values, yield stress and stiffness degrade rapidly and pronounced plastic deformation occurs. Author (Hemer)

A95-78494

IMPINGEMENT COOLING OF AN ISOTHERMALLY HEATED SURFACE WITH A CONFINED SLOT JET

Y. J. CHOU Natl Tsing Hua Univ, Hsinchu, Taiwan, Province of China and Y. H. HUNG Journal of Heat Transfer, Transactions ASME (ISSN 0022-1481) vol. 116, no. 2 May 1994 p. 479-482 refs

(BTN-94-EIX94421348950) Copyright

The objectives of this study include: (1) to explore the effects of jet Reynolds number; (2) ratio of separation distance to jet width and jet exit-velocity profile on stagnation and local heat transfer characteristics in confined slot-jet impingement problems; and (3) to propose new Nu correlations for predicting stagnation and local heat transfer characteristics. EI

A95-78576

DYNAMIC IMAGING AND RCS MEASUREMENTS OF AIRCRAFT

ATUL JAIN Hughes Aircraft Co, Los Angeles, CA, United States and INDU PATEL IEEE Transactions on Aerospace and Electronic Systems (ISSN 0018-9251) vol. 31, no. 1 January 1995 p. 211-226 refs

(BTN-95-EIX95202637582) Copyright

Results on radar cross section (RCS) measurements and inverse synthetic aperture radar images of a Mooney 231 aircraft using a ground-to-air measurement system (GTAMS) and a KC-135 airplane using an airborne radar are presented. The Mooney 231 flew in a controlled path in both clockwise and counterclockwise orbits, and successively with the gear down, flaps in the take-off position and with the speed brakes up. The data indicates that RCS pattern measurements from both ground-based and airborne radar of flying aircraft are useful and that the inverse synthetic aperture radar (ISAR) images obtained are valuable for signature diagnostics. Author (EI)

A95-79236

STRUCTURE OF A DOUBLE-FIN TURBULENT INTERACTION AT HIGH SPEED

DATTA GAITONDE Wright Lab, Wright-Patterson Air Force Base, OH, United States, J. S. SHANG, and MIGUEL VISBAL AIAA Journal (ISSN 0001-1452) vol. 33, no. 2 February 1995 p. 193-200 refs

(BTN-95-EIX95222650780) Copyright

This study examines the interaction of a Mach 8.3 turbulent boundary layer with intersecting oblique shock waves generated by 15-deg sharp fins mounted symmetrically on a flat plate. The full three-dimensional mass-averaged compressible Navier-Stokes equations are solved with a high-resolution implicit finite-volume scheme. Turbulence closure is achieved with variations of the Baldwin-Lomax algebraic model. Excellent agreement with experimental data is observed for plate surface pressure. However, accurate heat transfer rates are obtained only near the plane of symmetry. Some quantitative details are dependent on the manner in which the turbulence model is implemented. Within this limitation, the overall computed mean flow structure remains similar and mesh independent and compares well with available field surveys. The incoming flat plate boundary layer separates along the entire spanwise width and does not reattach in the domain of computation. Beneath the separated boundary layer is a vortex interaction with an off-surface stagnation point, a centerline longitudinal vortex, and an entrainment flow originating from the essentially inviscid stream near the fin leading edge. Author (EI)

A95-80044

EXPERIMENTAL INVESTIGATION OF THE FLOW AROUND A CIRCULAR CYLINDER: INFLUENCE OF ASPECT RATIO

C. NORBERG Chalmers Univ of Technology, Goteborg, Sweden Journal of Fluid Mechanics (ISSN 0022-1120) vol. 258 January 10 1994 p. 287-316

(BTN-94-EIX95011441120) Copyright

The investigation is concentrated on two important quantities - the Strouhal number and the mean base suction coefficient, both

measured at the mid-span position. Reynolds numbers from about 50 to 4×10^4 (exp 4) were investigated. Different aspect ratios, at low blockage ratios, were achieved by varying the distance between circular end plates (end plate diameter ratios between 10 and 30). It was not possible, by using these end plates in uniform flow and at very large aspect ratios, to produce parallel shedding all over the laminar shedding regime. However, parallel shedding at around mid-span was observed throughout this regime in cases when there was a slight but symmetrical increase in the free-stream velocity towards both ends of the cylinder. At higher Re, the results at different aspect ratios were compared with those of a 'quasi-infinite cylinder' and the required aspect ratio to reach conditions independent of this parameter, within the experimental uncertainties, are given. For instance, aspect ratios as large as $L/D = 60-70$ were needed in the range Re approximately $= 4 \times 10^3 - 10^4$ (exp 4). With the smallest relative end plate diameter and for aspect ratios smaller than 7, a bi-stable flow switching between regular vortex shedding and 'irregular flow' was found at intermediate Reynolds number ranges in the subcritical regime (Re approximately $= 2 \times 10^3$)). Author (EI)

A95-81012

FLOW DUE TO AN OSCILLATING SPHERE AND AN EXPRESSION FOR UNSTEADY DRAG ON THE SPHERE AT FINITE REYNOLDS NUMBER

RENWEI MEI Univ of Florida, Gainesville, FL, United States Journal of Fluid Mechanics (ISSN 0022-1120) vol. 270 July 10 1994 p. 133-174 refs

(BTN-94-EIX95011441142) Copyright

Unsteady flow due to an oscillating sphere with a velocity $U(\sin \omega t)$, in which U and ω are the amplitude and frequency of the oscillation and t is time, is investigated at finite Reynolds number. The methods used are: (1) Fourier mode expansion in the frequency domain; (2) a time-dependent finite difference technique in the time domain; and (3) a matched asymptotic expansion for high-frequency oscillation. The flow fields of the steady streaming component, the second and third harmonic components are obtained with the fundamental component. The dependence of the unsteady drag on ω is examined at small and finite Reynolds numbers. For large Stokes number, $\epsilon = (\omega a / \nu)^2$ very much greater than 1, in which a is the radius of the sphere and ν is the kinematic viscosity, the numerical result for the unsteady drag agrees well with the high-frequency asymptotic solution; and the Stokes solution is valid for finite Re at ϵ very much greater than 1. For small Strouhal number, $St = \omega a / U$ very much less than 1, the imaginary component of the unsteady drag (scaled by $6\pi U(\sin \omega t) \rho a$, in which ρ is the fluid density) behaves as $D(\sin \omega t)$ approx. $(h(\sin \omega t) / St \log St - h(\sin \omega t) / St)$, $m = 1, 3, 5, \dots$. This is in direct contrast to an earlier result obtained for an unsteady flow over a stationary sphere with a small-amplitude oscillation in the free-stream velocity (hereinafter referred to as the SA case) in which $D(\sin \omega t)$ approx. $-h(\sin \omega t) / St$. Computations for flow over a sphere with a free-stream velocity $U(1 - \alpha \sin \omega t + \alpha \cos \omega t)$ at $Re = U(2a/\nu) = 0.2$ and St very much less than 1 show that $h(\sin \omega t)$ for the first mode varies from 0 (at $\alpha = 0$) to around 0.5 (at $\alpha = 1$) and that the SA case is a degenerated case in which the logarithmic dependence of the drag in St is suppressed by the strong mean uniform flow. The numerical results for the unsteady drag are used to examine an approximate particle dynamic equation proposed for spherical particles with finite Reynolds number. The equation includes a quasi-steady drag, an added-mass force, and a modified history force. The approximate expression for the history force in the time domain compares very well with the numerical results of the SA case for all frequencies; it compares favorably for the PO case for moderate and high frequencies; it underestimates slightly the history force for the PO case at low frequency. For a solid sphere settling in a stagnant liquid with zero initial velocity, the velocity history is computed using the proposed particle dynamic equation. The results compare very well with experimental data of Moorman over a large range of Reynolds numbers. The present particle dynamic equation at finite Re performs consistently better

than that proposed by Odar & Hamilton both qualitatively and quantitatively for three different types of spatially uniform unsteady flows.
Author (EI)

A95-81027

FLOW STRUCTURE IN THE LEE OF AN INCLINED 6:1 PROLATE SPHEROID

T. C. FU CD/NSWC, Bethesda, MD, United States, A. SHEKARRIZ, J. KATZ, and T. T. HUANG Journal of Fluid Mechanics (ISSN 0022-1120) vol. 269 June 25 1994 p. 79-106 refs (BTN-94-EIX95011441127) Copyright

The paper presents a study on the flow structure in the lee of an inclined 6:1 prolate spheroid with the use of particle displacement velocimetry. The aim is to determine the effects of boundary layer tripping, incidence angle, and Reynolds number on the flow structure. The vorticity distributions are also used for computing the lateral forces and rolling moments that occur when the flow is symmetric. Results show an agreement between the computed values and those by direct measurements.
EI

A95-81056

ON THE ROLE OF THE OUTER REGION IN THE TURBULENT-BOUNDARY-LAYER BURSTING PROCESS

ROY Y. MYOSE Wichita State Univ, Wichita, KS, United States and RON F. BLACKWELDER Journal of Fluid Mechanics (ISSN 0022-1120) vol. 259 January 25 1994 p. 345-373 (BTN-94-EIX95011441078) Copyright

The dynamics and interaction of turbulent-boundary-layer eddy structures was experimentally emulated. Counter-rotating streamwise vortices and low-speed streaks emulating turbulent-boundary-layer wall eddies were generated by a Gortler instability mechanism. Large-scale motions associated with the outer region of turbulent boundary layer were emulated with $-\omega(z)$ spanwise vortical eddies shed by a periodic non-sinusoidal oscillation of an airfoil. The scales of the resulting eddy structures were comparable to a moderate-Reynolds-number turbulent boundary layer. Results show that the emulated wall-eddy breakdown was triggered by streamwise acceleration associated with the outer region of turbulent boundary layer. This breakdown involved violent mixing between low-speed fluid from the wall eddy and accelerated fluid associated with the outer structure. Although wall eddies can break down autonomously, the presence of and interaction with outer-region- $-\omega(z)$ eddies hastened their breakdown. Increasing the $-\omega(z)$ eddy strength resulted in further hastening of the breakdown. Conversely, $+\omega(z)$ eddies were found to delay wall-eddy breakdown locally, with further delays resulting from stronger $+\omega(z)$ eddies. This suggests that the outer region of turbulent boundary layers plays a role in the bursting process.
Author (EI)

N95-24203 Defence Science and Technology Organisation, Melbourne (Australia). Airframes and Engines Div.

A PORTABLE TRANSMISSION VIBRATION ANALYSIS SYSTEM FOR THE S-70A-9 BLACK HAWK HELICOPTER

D. M. BLUNT, B. REBBECCHI, B. D. FORRESTER, and K. W. VAUGHAN Sep. 1994 45 p Original contains color illustrations (DSTO-TR-0072; AR-008-938) Copyright Avail: Issuing Activity (DSTO Aeronautical and Maritime Research Lab., GPO Box 4331, Melbourne, Victoria 3001, Australia)

The prototype portable transmission vibration analysis system developed by Aeronautical and Maritime Research Laboratory (AMRL) for the Black Hawk helicopter is described in detail, including the results of flight trials conducted at RAAF Base Edinburgh during July 1993. The results of these trials have proved the concept of the system and laid the foundations for the future development of smaller and lighter systems.
Author

N95-24211# Wichita State Univ., Wichita, KS. National Inst. for Aviation Research.

ANALYSIS OF WARPING EFFECTS ON THE STATIC AND DYNAMIC RESPONSE OF A SEAT-TYPE STRUCTURE Final Report

STEVEN J. HOOPER and MANOJ RAHEMATPURA May 1994 97 p (NIAR-94-12) Avail: CASI HC A05/MF A02

An experimental investigation was conducted to evaluate the significance of warping deformations in the dynamic response of a seat frame type structure subjected to impact loading. The test article design featured thin-walled open-section beams and was loaded inertially by a number of rigid weights which were attached to the 'seat frame' members. Strain gage data acquired during these tests were analyzed to whether these data are better represented by Vlasov beam theory or Euler-Bernoulli beam theory. Static tests of the test article were conducted to validate the data reduction techniques employed in the analysis of the dynamic data.
Derived from text

N95-24396*# National Aeronautics and Space Administration. Langley Research Center, Hampton, VA.

DSMC CALCULATIONS FOR 70-DEG BLUNTED CONE AT 3.2 KM/S IN NITROGEN

J. N. MOSS, J. M. PRICE, and V. K. DOGRA (Vigyan Research Associates, Inc., Hampton, VA.) Jan. 1995 54 p (Contract(s)/Grant(s): RTOP 242-80-01-01) (NASA-TM-109181; NAS 1.15:109181) Avail: CASI HC A04/MF A01

Numerical results obtained with the direct simulation Monte Carlo (DSMC) method are presented for Mach 15.6 nitrogen flow about a 70-deg spherically blunted cone at zero incidence. This flow condition is one of several generated in the Large Energy National Shock (LENS) tunnel during tests of a 15.24 cm diameter model with an afterbody sting. The freestream Knudsen number, based on model diameter, is 0.0023. The focus of the DSMC calculations is to characterize the near wake flow under conditions where rarefaction effects may influence afterbody aerothermal loads. This report provides information concerning computational details along with flowfield and surface quantities. Calculations show that the flow enveloping the test model is in thermal nonequilibrium and a sizable vortex develops in the near wake. Along the model baseplane the heating rates are about 0.6 percent of the forebody stagnation value while the maximum heating along the sting is about 4.2 percent of the forebody stagnation value. Comparison of a Navier-Stokes solution with the present calculations show good agreement for surface heating, pressure, and skin friction results.
Author

N95-24412*# California Univ., Los Angeles, CA. Dept. of Mechanical Aerospace and Nuclear Engineering.

EFFECT OF DENSITY GRADIENTS IN CONFINED SUPERSONIC SHEAR LAYERS, PART 1

OSHIN PEROOMIAN and R. E. KELLY 7 Nov. 1994 83 p (Contract(s)/Grant(s): NCC2-374) (NASA-CR-198029; NAS 1.26:198029) Avail: CASI HC A05/MF A01

The effect of density gradients on the supersonic wall modes (acoustic modes) of a 2-D confined compressible shear layer were investigated using linear analysis. Due to the inadequacies of the hyperbolic tangent profile, the boundary layer basic profiles were used. First a test case was taken with the same parameters as in Tam and Hu's analysis with convective Mach number $M(\text{sub } c) = 1.836$ and density ratio of 1.398. Three generalized inflection points were found giving rise to three modes. The first two show similar properties to the Class A and B modes, and the third is an 'inner mode' which will be called a Class C mode. As the density ratio is increased, the smallest of the three neutral phase speeds tends towards the speed of the lower velocity stream, and the other two eventually coalesce and then disappear. These two effects lead to a linear resonance between the Class B modes which increases the cutoff frequency and growth rate of the lowest mode. In fact, growth rates of 2-4 times the test case were found as the density ratio was increased to 7. A similar trend is observed for the Class A modes when the density ratio is decreased from the test case, but the growth rate is not changed by much from the test case.
Author

N95-24413* California Univ., Los Angeles, CA. Dept. of Mechanical Aerospace and Nuclear Engineering.
EFFECT OF DENSITY GRADIENTS IN CONFINED SUPERSONIC SHEAR LAYERS. PART 2: 3-D MODES
 OSHIN PEROOMIAN and R. E. KELLY 7 Nov. 1994 35 p
 (Contract(s)/Grant(s): NCC2-374)
 (NASA-CR-198030; NAS 1.26:198030) Avail: CASI HC A03/MF A01

The effect of basic flow density gradients on the supersonic wall modes were investigated in Part 1 of this analysis. In that investigation only the 2-D modes were studied. Tam and Hu investigated the 3-D modes in a confined vortex sheet and reported that the first 2-D Class A mode (A01) had the highest growth rate compared to all other 2-D and 3-D modes present in the vortex sheet for that particular set of flow patterns. They also showed that this result also held true for finite thickness shear layers with δ (sub w) less than 0.125. For free shear layers, Sandham and Reynolds showed that the 3-D K-H mode became the dominant mode for M (sub c) greater than 0.6. Jackson and Grosch investigated the effect of crossflow and obliqueness on the slow and fast modes present in a M (sub c) greater than 1 environment and showed that for certain combination of crossflow and wave angles the growth rates could be increased by up to a factor of 2 with respect to the 2-D case. The case studied here is a confined shear layer shown in Part 1. All solution procedures and basic flow profiles are the same as in Part 1. The effect of density gradients on the 3-D modes present in the density ratios considered in Part 1 are investigated. Author

N95-24461* Texas A&M Univ., College Station, TX. Dept. of Mechanical Engineering.
THERMOHYDRODYNAMIC ANALYSIS OF CRYOGENIC LIQUID TURBULENT FLOW FLUID FILM BEARINGS, PHASE 2 Annual Research Progress Report, 1 Jan. - 31 Dec. 1994
 LUIS SANANDRES 31 Dec. 1994 211 p
 (Contract(s)/Grant(s): NAG3-1434)
 (NASA-CR-197412; NAS 1.26:197412) Avail: CASI HC A10/MF A03

The Phase 2 (1994) Annual Progress Report presents two major report sections describing the thermal analysis of tilting- and flexure-pad hybrid bearings, and the unsteady flow and transient response of a point mass rotor supported on fluid film bearings. A literature review on the subject of two-phase flow in fluid film bearings and part of the proposed work for 1995 are also included. The programs delivered at the end of 1994 are named hydroflex and hydrotran. Both codes are fully compatible with the hydrosealt (1993) program. The new programs retain the same calculating options of hydrosealt plus the added bearing geometries, and unsteady flow and transient forced response. Refer to the hydroflex & hydrotran User's Manual and Tutorial for basic information on the analysis and instructions to run the programs. The Examples Handbook contains the test bearing cases along with comparisons with experimental data or published analytical values. The following major tasks were completed in 1994 (Phase 2): (1) extension of the thermohydrodynamic analysis and development of computer program hydroflex to model various bearing geometries, namely, tilting-pad hydrodynamic journal bearings, flexure-pad cylindrical bearings (hydrostatic and hydrodynamic), and cylindrical pad bearings with a simple elastic matrix (ideal foil bearings); (2) improved thermal model including radial heat transfer through the bearing stator; (3) calculation of the unsteady bulk-flow field in fluid film bearings and the transient response of a point mass rotor supported on bearings; and (4) a literature review on the subject of two-phase flows and homogeneous-mixture flows in thin-film geometries.

Derived from text

N95-24470* Joint Publications Research Service, Washington, DC.
JPRS REPORT: SCIENCE AND TECHNOLOGY. CENTRAL EURASIA

31 Oct. 1994 48 p Transl. into ENGLISH from various Central Eurasian articles
 (JPRS-UST-94-027) Avail: CASI HC A03/MF A01

Translated articles cover the following topics: delay effect and energy transfer through a turbulent atmosphere to a moving object; nonlinear phenomena in active phased arrays; linearizing modulation characteristics of microwave broadband avalanche transit time diode oscillators with varactor frequency tuning; microwave radiation absorption by edge-type Josephson junctions in wide-band detection mode; and localization of vibrations in the shrouded blade assembly of the rotor wheel of a turbomachine. Author

N95-24472* Joint Publications Research Service, Washington, DC.

JPRS REPORT: SCIENCE AND TECHNOLOGY. CENTRAL EURASIA

9 Sep. 1994 184 p Transl. into ENGLISH from various Central Eurasian articles
 (JPRS-UST-94-018) Avail: CASI HC A09/MF A02

Translated articles cover the following topics: estimating life of structural ceramic on basis of dynamic fatigue test results; numerical solution of 3-D problems of non-axisymmetrical deformation of laminated anisotropic rotation shells; edge effects in laminated plates; miniature high-temperature superconducting microwave antenna; device for diagnostic sounding of ionospheric plasma with neutralized effect of charge-carrying spacecraft; new types of diagnosis of ionospheric parameters by surface and remote radio sounding; development and use of new weldable structural alloys in the aircraft industry; aerodynamic characteristics of delta wing in hypersonic flow; interrelationship between acoustic properties of nozzle head and combustion chamber with exciting transverse gas oscillations; study of effect of refraction parallax on accuracy of measurements of angular coordinates of artificial earth satellite; assessment of possibility of observation of artificial earth satellite by passive optical means in a twilight and daylight conditions; experimental study of friction against fluid at high speeds; construction of airfoil profiles streamlined with separation of turbulent boundary layer; dependence of aerodynamic characteristics of circular cylinder in supersonic stream of ideal gas on temperature factor; optimum conditions for control of turbulence intensity in stream by means of honeycombs; ionospheric effects of spacecraft launches; and consequences of greenhouse effect: predictions and reality. Author

N95-24598* Westinghouse Savannah River Co., Aiken, SC.
RESIDUAL STRESS MEASUREMENTS WITH LASER SPECKLE CORRELATION INTERFEROMETRY AND LOCAL HEAT TREATING

M. J. PECHERSKY, R. F. MILLER, and C. S. VIKRAM (Alabama Univ., Huntsville, AL.) Jan. 1994 26 p Presented at the SPIE '95: SPIE Conference on Optics, Electro-optics, and Laser Application in Science, Engineering and Medicine, San Jose, CA, 5-10 Feb. 1995
 (Contract(s)/Grant(s): DE-AC09-89SR-18035)
 (DE95-060082; WSRC-MS-94-0632; CONF-950226-3) Avail: CASI HC A03/MF A01

A new experimental technique has been devised to measure residual stresses in ductile materials with a combination of laser speckle pattern interferometry and spot heating. The speckle pattern interferometer measures in-plane deformations while the heating provides for very localized stress relief. The residual stresses are determined by the amount of strain that is measured subsequent to the heating and cool-down of the region being interrogated. A simple lumped parameter model is presented to provide a description of the method. This description is followed by presentations of the results of finite element analyses and experimental results with uniaxial test specimens. Excellent agreement between the experiments and the computer analyses were obtained. DOE

N95-24759# Joint Publications Research Service, Washington, DC.

JPRS REPORT: SCIENCE AND TECHNOLOGY. CENTRAL EURASIA

25 Nov. 1994 79 p Transl. into ENGLISH from various Central Eurasian articles

(JPRS-UST-94-032) Avail: CASI HC A05/MF A01

Translated articles cover the following topics: synthesis of stabilization systems for unmanned aircraft using spatial states methods; synthesis of two-dimensional nonequidistant antenna arrays based on theory of difference sets; study of the stability of an elastic hull-fuel lines-engines system for liquid fuel packet arrangement rockets; determining parameters of strength kinetics and critical dimension of fracture of composite materials by recording electromagnetic radiation pulses recorded during fracture; air density distribution around supersonic cone at angle of attack; and transfer of laser energy through turbulent atmosphere to far moving objects.

CASI

N95-25394*# Queensland Univ., Saint Lucia (Australia). Dept. of Mechanical Engineering.

SHOCK TUNNEL STUDIES OF SCRAMJET PHENOMENA 1993

R. J. STALKER, R. J. BAKOS, R. G. MORGAN, L. PORTER, D. MEE, A. PAULL, S. TUTTLE, J. M. SIMMONS, M. WENDT, K. SKINNER et al. Jan. 1995 108 p Sponsored in cooperation with the Australian Research Council and the Queen Elizabeth 2nd Fellowship Scheme

(Contract(s)/Grant(s): NAGW-674; RTOP 505-70-62-04)

(NASA-CR-195038; NAS 1.26:195038) Avail: CASI HC A06/MF A02 Reports by the staff of the University of Queensland on various research studies related to the advancement of scramjet technology and hypervelocity pulse test facilities are presented. These reports document the tests conducted in the reflected shock tunnel T4 and supporting research facilities that have been used to study the injection, mixing, and combustion of hydrogen fuel in generic scramjets at flow conditions typical of hypersonic flight. In addition, topics include the development of instrumentation and measurement technology, such as combustor wall shear and stream composition in pulse facilities, and numerical studies and analyses of the scramjet combustor process and the test facility operation. This research activity is Supplement 10 under NASA Grant NAGW-674. For individual titles, see N95-25395 through N95-25400.

N95-25400*# Queensland Univ., Saint Lucia (Australia). Dept. of Mechanical Engineering.

BALANCES FOR THE MEASUREMENT OF MULTIPLE COMPONENTS OF FORCE IN FLOWS OF A MILLISECOND DURATION

D. J. MEE, W. J. DANIEL, S. L. TUTTLE, and J. M. SIMMONS *In Its Shock Tunnel Studies of Scramjet Phenomena 1993* p 107-112 Jan. 1995 Sponsored in cooperation with the Australian Research Council and the Queen Elizabeth 2nd Fellowship Scheme

Avail: CASI HC A02/MF A02

This paper reports a new balance for the measurement of three components of force - lift, drag and pitching moment - in impulsively starting flows which have a duration of about one millisecond. The basics of the design of the balance are presented and results of tests on a 15 deg semi-angle cone set at incidence in the T4 shock tunnel are compared with predictions. These results indicate that the prototype balance performs well for a 1.9 kg, 220 mm long model. Also presented are results from initial bench tests of another application of the deconvolution force balance to the measurement of thrust produced by a 2D scramjet nozzle.

Author

N95-25592* National Aeronautics and Space Administration. Lyndon B. Johnson Space Center, Houston, TX.

PRELOAD RELEASE MECHANISM Patent

ROBERT M. GENEROLI, inventor (to NASA) (McDonnell-Douglas Corp., Houston, TX.) and HARRY J. YOUNG, inventor (to NASA)

(McDonnell-Douglas Corp., Houston, TX.) 14 Mar. 1995 10 p Filed 20 Apr. 1994 Supersedes N94-36839 (32 - 12, p 4450)

(NASA-CASE-MS-C-22327-1; US-PATENT-5,397,244; US-PATENT-APPL-SN-230571; US-PATENT-CLASS-439-248; INT-PATENT-CLASS-H01R-13/629) Avail: US Patent and Trademark Office

This invention relates to a preload release mechanism comprising a preload spring assembly adapted to apply a preload to a first connector member which is mounted on a support structure and adapted for connection with a second connector member on an object. The assembly comprises telescoped bushings and a preload spring. A tubular shaft extends through the spring assembly and openings in the first connector member and support structure, on which it is clamped. A plunger rod in the shaft is provided with a tip end and a recess in the rod near the other end thereof. A retainer precludes passage of the rod through the shaft in one direction and an end cap closes the bore of the shaft at the other end and provides a shoulder which extends radially of the shaft. A plunger return spring biases the plunger rod against the plunger retainer with the plunger tip protruding from the shaft and a spring assembly return spring engages at its ends the shoulder of the end cap and one end of the spring assembly. Detents received in lateral openings in the tubular shaft are held captive by the plunger rod and one end of the spring assembly to lock the spring assembly on the tubular shaft and apply a preload to the first connector member. Upon completion of the connection, detents and spring assembly are released by plunger contact with the object to be connected, thereby releasing the preload while the connection is maintained.

Official Gazette of the U.S. Patent and Trademark Office

N95-25606 Army Research Lab., Aberdeen Proving Ground, MD. **WORKSHOP REPORT: MEASUREMENT TECHNIQUES IN HIGHLY TRANSIENT, SPECTRALLY RICH COMBUSTION ENVIRONMENTS Final Report, 1-30 Nov. 1993**

TODD E. ROSENBERGER Sep. 1994 204 p Limited Reproducibility: More than 20% of this document may be affected by microfiche quality

(AD-A288395; ARL-SR-18) Avail: Issuing Activity (Defense Technical Information Center (DTIC))

With the emergence of advanced propulsion systems such as liquid propellant (LP), electrothermal-chemical (ETC), electromagnetic (EM), conventional hypervelocity, and in-bore ramjet, the measurement of combustion phenomena has become more complex. The data associated with these systems can be rich in high-frequency components, and share similar transient behavior. Measurement techniques associated with conventional solid propellant systems are not always capable of accurately recording these phenomena. The accuracy of pressure and acceleration measurements in combustion chambers, barrels, and on-board projectiles has been compromised by the lack of a fundamental understanding of the effects of the mounting configuration and the mechanical and electrical components of the transducer on the integrity of the measurement. Consequently, the system development and technical understanding of the physical processes involved in the ignition and combustion of such advanced propulsion systems have been compromised. A workshop was needed to bring together experts from the aforementioned and related communities to disseminate knowledge of lessons learned and to discuss the techniques necessary to make high-fidelity pressure measurements in these environments. This report will state the objectives, identify the participants who met to address them, provide a list of the technical presentations made, present highlights from these presentations and the discussions that they prompted, and end with conclusions and recommendations which came out of the workshop.

DTIC

N95-25749 Research Inst. of National Defence, Linköping (Sweden). Dept. of Command and Control Warfare Technology.

ORIENTATION DETERMINATION OF AIRCRAFT USING VISUAL 3D MATCHING AND RADAR. CASE STUDY 2

H. A. OLSSON, M. BENGTSSON, and P. ROIVAINEN Aug. 1994 26 p

(PB95-165791) Avail: Issuing Activity (National Technical Information Service (NTIS))

This study is an application of a matching method using 3D models and images. In the earlier case study we combined radar data and visual matching for aircraft identification and orientation determination. We analyzed a video sequence of an aircraft together with radar data, where the radar has guided the tracking of the aircraft. The purpose of this case study is to test our new 3D model, composed of edge segments from the silhouette of an aircraft and to see if it is possible to analyze the video sequence only with visual matching, after the radar has given the initial start values. NTIS

13

GEOSCIENCES

Includes geosciences (general); earth resources; energy production and conversion; environment pollution; geophysics; meteorology and climatology; and oceanography.

A95-77982* National Aeronautics and Space Administration. Ames Research Center, Moffett Field, CA.

ANALYSIS OF THE PHYSICAL STATE OF ONE ARCTIC POLAR STRATOSPHERIC CLOUD BASED ON OBSERVATIONS

K. DRDLA Univ. of California at Los Angeles, Los Angeles, CA, US, A. TABAZADEH NASA. Ames Research Center, Moffett Field, CA, US, R. P. TURCO Univ. of California at Los Angeles, Los Angeles, CA, US, M. Z. JACOBSON Univ. of California at Los Angeles, Los Angeles, CA, US, J. E. DYE National Center for Atmospheric Research, Boulder, CO, US, C. TWOHY National Center for Atmospheric Research, Boulder, CO, US, and D. BAUMGARDNER National Center for Atmospheric Research, Boulder, CO, US Geophysical Research Letters (ISSN 0094-8276) vol. 21, no. 23 November 15, 1994 p. 2475-2478 Research sponsored by NCAR Advanced Study Program Graduate Fellowship (Contract(s)/Grant(s): NAGW-2183) (HTN-95-70917) Copyright

During the Arctic Airborne Stratospheric Expedition (AASE) simultaneous measurements of aerosol size distribution and NO(y) (HN03 + NO + NO2 + 2(N2O5)) were made along ER-2 flight paths. The flow characteristics of the NO(y) instrument allow us to derive the condensed NO(y) amount (assumed to be HN03) present during polar stratospheric cloud (PSC) events. Analysis of the January 24th flight indicates that this condensed HN03 amount does not agree well with the aerosol volume if the observed PSCs are composed of solid nitric acid trihydrate (NAT), as is generally assumed. However, the composition agrees well with that predicted for liquid H2SO4/HN03/H2O solution droplets using a new Aerosol Physical Chemistry Model (APCM). The agreement corresponds in detail to variations in temperature and humidity. The weight percentages of H2SO4, HN03, and H2O derived from the measurements all correspond to those predicted for ternary, liquid solutions.

Author (Herner)

A95-78000* National Aeronautics and Space Administration. Ames Research Center, Moffett Field, CA.

THE DISTRIBUTION OF HYDROGEN, NITROGEN, AND CHLORINE RADICALS IN THE LOWER STRATOSPHERE: IMPLICATIONS FOR CHANGES IN O3 DUE TO EMISSION OF NO(Y) FROM SUPERSONIC AIRCRAFT

R. J. SALAWITCH Harvard Univ., Cambridge, MA, US, S. C. WOFSY Harvard Univ., Cambridge, MA, US, P. O. WEINBERG Harvard Univ., Cambridge, MA, US, R. C. COHEN Harvard Univ., Cambridge, MA, US, J. G. ANDERSON Harvard Univ., Cambridge, MA, US, D. W. FAHEY NOAA Aeronomy Laboratory, Boulder, CO, US, R. S. GAO NOAA Aeronomy Laboratory, Boulder, CO, US, E. R. KEIM NOAA Aeronomy Laboratory, Boulder, CO, US, E. L. WOODBRIDGE, R. M. STIMPFLER Harvard Univ., Cambridge, MA, US et al. Geophysical Research Letters (ISSN 0094-8276) vol. 21,

no. 23 November 15, 1994 p. 2547-2550

(Contract(s)/Grant(s): NAG2-731; NAGW-1230; NAS1-19955; NSF ATM-89-21119)

(HTN-95-70935) Copyright

In situ measurements of hydrogen, nitrogen, and chlorine radicals obtained in the lower stratosphere during SPADE are compared to results from a photochemical model that assimilates measurements of radical precursors and environmental conditions. Models allowing for heterogeneous hydrolysis of N2O5 agree well with measured concentrations of NO and ClO, but concentrations of HO2 and OH are underestimated by 10 to 25%, concentrations of NO2 are overestimated by 10 to 30%, and concentrations of HCl are overestimated by a factor of 2. Discrepancies for (OH) and (HO2) are reduced if we allow for higher yields of O(1D) from O2 photolysis and for heterogeneous production of HNO2. The data suggest more efficient catalytic removal of O3 by hydrogen and halogen radicals relative to nitrogen oxide radicals than predicted by models using recommended rates and cross sections. Increased in (O3) in the lower stratosphere may be larger in response to inputs of NO(y) from supersonic aircraft than estimated by current assessment models.

Author (Herner)

A95-78006* National Aeronautics and Space Administration. Ames Research Center, Moffett Field, CA.

VERTICAL TRANSPORT RATES IN THE STRATOSPHERE IN 1993 FROM OBSERVATIONS OF CO2, N2O, AND CH4

STEVEN C. WOFSY Harvard Univ., Cambridge, MA, US, KRISTIE A. BOERING Harvard Univ., Cambridge, MA, US, BRUCE C. DAUBE, JR. Harvard Univ., Cambridge, MA, US, MICHAEL B. MCELROY Harvard Univ., Cambridge, MA, US, MAX LOEWENSTEIN NASA. Ames Research Center, Moffett Field, CA, US, JAMES R. PODOLSKIE NASA. Ames Research Center, Moffett Field, CA, US, JAMES W. ELKINS NOAA, Boulder, CO, US, GEOFFREY S. DUTTON NOAA, Boulder, CO, US, and DAVID W. FAHEY NOAA, Boulder, CO, US Geophysical Research Letters (ISSN 0094-8276) vol. 21, no. 23 November 15, 1994 p. 2571-2574 Research sponsored by DOE (Contract(s)/Grant(s): NCC2-694) (HTN-95-70941) Copyright

Measurements of CO2, N2O, and CH4 are analyzed to define hemispheric average vertical exchange rates in the lower stratosphere from November 1992 to October 1993. Effective vertical diffusion coefficients were small in summer, less than or equal to 1 sq m/s at altitudes below 25 km; values were similar near the tropopause in winter, but increased markedly with altitude. The analysis suggests possible longer residence times for exhaust from stratospheric aircraft, and more efficient transport from 20 km to the middle stratosphere, than predicted by many current models. Seasonally-resolved measurements of stratospheric CO2 and N2O provide significant new constraints on rates for global-scale vertical transport.

Author (Herner)

A95-78008* National Aeronautics and Space Administration. Langley Research Center, Hampton, VA.

AN ANALYSIS OF AIRCRAFT EXHAUST PLUMES FORM ACCIDENTAL ENCOUNTERS

J. ZHENG Univ. of Colorado, Boulder, CO, US, A. J. WEINHEIMER National Center for Atmospheric Research, Boulder, CO, US, B. A. RIDLEY National Center for Atmospheric Research, Boulder, CO, US, S. C. LIU Univ. of Colorado, Boulder, CO, US, G. W. SACHSE NASA. Langley Research Center, Hampton, VA, US, B. E. ANDERSON NASA. Langley Research Center, Hampton, VA, US, and J. E. COLLINS, JR. Geophysical Research Letters (ISSN 0094-8276) vol. 21, no. 23 November 15, 1994 p. 2579-2582 Research sponsored by NASA and NSF (HTN-95-70943) Copyright

An analysis of data obtained during the second Airborne Arctic Stratospheric Expedition (AASE-II) was made with emphasis on aircraft exhaust plumes accidentally encountered during the mission. Twenty spikes were found with peak NO(y) increments greater

than or equal to 1 ppbv. The examination of CO and CO₂ indicated that there was only one NO(y) spike having clearly corresponding spikes of both CO and CO₂ and another four with unambiguous CO₂ spikes. No significant increases were found for CH₄ and N₂O for these 5 spikes. The ratio of the excess CO₂ and NO(y) compares well with the ratio of published subsonic aircraft emission indices. The study of the selected spikes from the DC-8 and another two spikes observed during other missions shows that the odd nitrogen other than NO(x) accounts for a very small percentage of the NO(y) increase associated with the observed spikes. Author (Herner)

A95-78009* Jet Propulsion Lab., California Inst. of Tech., Pasadena, CA.

MERIDIONAL DISTRIBUTIONS OF NO(X), NO(Y), AND OTHER SPECIES IN THE LOWER STRATOSPHERE AND UPPER TROPOSPHERE DURING AASE 2

A. J. WEINHEIMER National Center for Atmospheric Research, Boulder, CO, US, J. G. WALEGA National Center for Atmospheric Research, Boulder, CO, US, B. A. RIDLEY National Center for Atmospheric Research, Boulder, CO, US, B. L. GARY Jet Propulsion Laboratory, Pasadena, CA, US, D. R. BLAKE Univ. of California, Irvine, CA, US, N. J. BLAKE Univ. of California, Irvine, CA, US, F. S. ROWLAND Univ. of California, Irvine, CA, US, G. W. SACHSE NASA. Langley Research Center, Hampton, VA, US, B. E. ANDERSON NASA. Langley Research Center, Hampton, VA, US, and J. E. COLLINS NASA. Langley Research Center, Hampton, VA, US Geophysical Research Letters (ISSN 0094-8276) vol. 21, no. 23 November 15, 1994 p. 2583-2586 Research sponsored by NASA and NSF

(HTN-95-70944) Copyright

The meridional distribution of NO(x) in the lower stratosphere and upper troposphere is inferred from 10 flights of the NASA DC-8 in the northern winter of 1992 along with like distributions of NO(y), NO(x)/NO(y), CO, and C₂H₄. In the lowest few km of the stratosphere there is little vertical gradient in NO(x) over the range of latitudes measured (40 deg-90 deg N). There is a substantial latitudinal gradient, with 50 pptv above the pole and 120 pptv near 40 deg N. In the uppermost few km of the troposphere, background values range from 30 pptv over the pole to 90 pptv near 40 deg N. On two occasions higher values, up to 140 pptv in the mean, were seen 2-3 km below the tropopause in association with frontal systems. The meridional distributions of CO and C₂H₄ show the same feature, suggesting that the source of the elevated NO(x) is near the earth's system. Author (Herner)

A95-78011* Jet Propulsion Lab., California Inst. of Tech., Pasadena, CA.

COMPARISON OF COLUMN ABUNDANCES FROM THREE INFRARED SPECTROMETERS DURING AASE 2

W. A. TRAUB Smithsonian Astrophysical Observatory, Cambridge, MA, US, K. W. JUCKS Smithsonian Astrophysical Observatory, Cambridge, MA, US, D. G. JOHNSON Smithsonian Astrophysical Observatory, Cambridge, MA, US, M. T. COFFEY National Center for Atmospheric Research, Boulder, CO, US, W. G. MANKIN National Center for Atmospheric Research, Boulder, CO, US, and G. C. TOON Jet Propulsion Laboratory, Pasadena, CA, US Geophysical Research Letters (ISSN 0094-8276) vol. 21, no. 23 November 15, 1994 p. 2591-2594 Research sponsored by NASA and NSF

(Contract(s)/Grant(s): NSG5-175)

(HTN-95-70946) Copyright

Three Fourier transform infrared (FTIR) spectrometers were based on board the NASA DC-8 during the second Airborne Arctic Stratospheric Expedition (AASE II) in 1992. Two FTIRs used solar absorption and one used thermal emission. We compare over 2000 measurements from these 3 FTIRs, on 12 DC-8 flights, for closely coincident air masses and times, both inside and outside the polar vortex. In the majority of cases the offset biases are quite small, in the range 1-4%, and comparable to the absolute precisions expected. In most cases the rms scatter is in the range 4-11%; this

scatter is unlikely to be geophysical, but rather is probably instrumental or analytical in origin.

Author (Herner)

A95-78012* National Aeronautics and Space Administration. Goddard Space Flight Center, Greenbelt, MD.

CHEMICAL CHANGE IN THE ARCTIC VORTEX DURING AASE 2

WESLEY A. TRAUB Smithsonian Astrophysical Observatory, Cambridge, MA, US, KENNETH W. JUCKS Smithsonian Astrophysical Observatory, Cambridge, MA, US, DAVID G. JOHNSON Smithsonian Astrophysical Observatory, Cambridge, MA, US, and KELLY V. CHANCE Smithsonian Astrophysical Observatory, Cambridge, MA, US Geophysical Research Letters (ISSN 0094-8276) vol. 21, no. 23 November 15, 1994 p. 2595-2598

(Contract(s)/Grant(s): NSG5-175)

(HTN-95-70947) Copyright

We measured column abundances of HF, HCl, O₃, HNO₃, and H₂O on the NASA DC-8 during the AASE II campaign, using thermal emission spectroscopy. We made multiple traversals of the Arctic vortex and surroundings. Using HF as a tracer, we remove the effects of subsidence from the measured column abundances; perturbations in the resulting column abundances are attributed to chemical processing. We find that by January 1992 the stratospheric column in the vortex had been chemically depleted by about (55+/-10)% in HCl and (35+/-10)% in O₃, and enhanced by about (15+/-10)% in HNO₃ and (0+/-10)% in H₂O.

Author (Herner)

A95-78013* Jet Propulsion Lab., California Inst. of Tech., Pasadena, CA.

LATITUDE VARIATIONS OF STRATOSPHERIC TRACE GASES

G. C. TOON Jet Propulsion Laboratory, Pasadena, CA, US, J.-F. BLAVIER Jet Propulsion Laboratory, Pasadena, CA, US, and J. T. SZETO Jet Propulsion Laboratory, Pasadena, CA, US Geophysical Research Letters (ISSN 0094-8276) vol. 21, no. 23 November 15, 1994 p. 2599-2602

(HTN-95-70948) Copyright

We present vertical column abundances of H₂O, N₂O, HNO₃, NO₂, O₃, HF, HCl, and ClONO₂, determined from solar absorption spectra measured by the JPL MkIV interferometer from the NASA DC-8 aircraft. These observations, taken in 1987 and 1992, covered latitudes ranging from 85 deg S to 85 deg N. Although most gases display latitude symmetry, large asymmetries in H₂O, HNO₃, and O₃ are apparent, which can be ascribed to processes enhanced by the colder Antarctic winter temperatures.

Author (Herner)

A95-78014* National Aeronautics and Space Administration. Goddard Space Flight Center, Greenbelt, MD.

FINE-SCALE, POLEWARD TRANSPORT OF TROPICAL AIR DURING AASE 2

D. W. WAUGH Massachusetts Institute of Technology, Cambridge, MA, US, R. A. PLUMB Massachusetts Institute of Technology, Cambridge, MA, US, P. A. NEWMAN NASA. Goddard Space Flight Center, Greenbelt, MD, US, M. R. SCHOEBERL NASA. Goddard Space Flight Center, Greenbelt, MD, US, L. R. LAIT NASA. Goddard Space Flight Center, Greenbelt, MD, US, M. LOEWENSTEIN NASA. Ames Research Center, Moffett Field, CA, US, J. R. PODOLSKA NASA. Ames Research Center, Moffett Field, CA, US, J. W. ELKINS NOAA, Boulder, CO, US, and K. R. CHAN NASA. Ames Research Center, Moffett Field, CA, US Geophysical Research Letters (ISSN 0094-8276) vol. 21, no. 23 November 15, 1994 p. 2603-2606

(Contract(s)/Grant(s): NAGW-1727)

(HTN-95-70949) Copyright

The poleward transport of tropical air in the lower stratosphere during the winter period of the second Airborne Arctic Stratospheric Expedition (AASE 2) (December 1991-March 1992) is examined using contour advection calculations. These calculations show that filaments of tropical air extend into mid-latitudes, and are wrapped around the equatorward edge of the polar jet. Simultaneously filaments are drawn from the polar vortex and are intermingled with

the filaments of tropical air. The tropical filaments are consistent with measurements of chemical tracers taken aboard the ER-2 and DC-8 aircraft which show localized regions, in mid-latitudes, of air with the characteristics of tropical air. Author (Herner)

A95-78678

NITROUS OXIDE AND METHANE EMISSIONS FROM AERO ENGINES

P. WIESEN Univ.-GH Wuppertal, Wuppertal, Germany, J. KLEFFMANN Univ.-GH Wuppertal, Wuppertal, Germany, R. KURTENBACH Univ.-GH Wuppertal, Wuppertal, Germany, and K. H. BECKER Univ.-GH Wuppertal, Wuppertal, Germany *Geophysical Research Letters* (ISSN 0094-8276) vol. 21, no. 18 September 1, 1994 p. 2027-2030 Research sponsored by the EC (HTN-95-21363) Copyright

The emissions of nitrous oxide and methane from a Pratt & Whitney Canada PW 305 and a Rolls Royce RB 211 jet engine were measured under various flight conditions either on a ground level stationary test stand or in altitude test cells by using an off-line sampling technique. The concentrations of the gases were determined by long path infrared diode laser absorption spectroscopy in the laboratory. The calculated emission indices indicate that, at present, air traffic does not contribute significantly to the global budgets of methane and nitrous oxide. Author (Herner)

A95-78679

IMPACT OF PRESENT AIRCRAFT EMISSIONS OF NITROGEN OXIDES ON TROPOSPHERIC OZONE AND CLIMATE FORCING

D. A. HAUGLUSTAIN CNRS, Paris, France, C. GRANIER National Center for Atmospheric Research, Boulder, CO, US, G. P. BRASSEUR National Center for Atmospheric Research, Boulder, CO, US, and G. MEGIE CNRS, Paris, France *Geophysical Research Letters* (ISSN 0094-8276) vol. 21, no. 18 September 1, 1994 p. 2031-2034 Research sponsored by the NSF, CEC, and Gas Research Institute (HTN-95-21364) Copyright

A two-dimensional (2-D) model in which dynamics, radiation and chemistry are treated interactively is used to investigate the seasonal changes in tropospheric ozone due to current nitrogen oxide emissions from aircraft and to assess the associated radiative forcing on the climate system. Our results confirm the high efficiency of nitrogen oxide in-situ emissions in producing ozone in comparison to surface emissions. The ozone increase is characterized by a strong seasonal variation; it reaches more than 7 % during summer in the upper troposphere at northern mid-latitudes. On a global average basis, the radiative forcing associated with this ozone increase appears to be small in comparison to that of other greenhouse gases. However, it may play a significant role in the anthropogenic forcing on northern hemisphere climate. Author (Herner)

A95-79453

SENSITIVITY OF SUPERSONIC AIRCRAFT MODELLING STUDIES TO HNO₃ PHOTOLYSIS RATE

A. E. JONES Univ. of Cambridge, Cambridge, UK, S. BEKKI Univ. of Cambridge, Cambridge, UK, and J. A. PYLE Univ. of Cambridge, Cambridge, UK *Geophysical Research Letters* (ISSN 0094-8276) vol. 20, no. 20 October 22, 1993 p. 2231-2234 Research sponsored by the U.K. Univ. Global Atmospheric Modelling (UGAMP) programme (HTN-95-11475) Copyright

In the last few years the possibility of a second generation of supersonic aircraft flying mainly in the stratosphere has been discussed. This, and the increasing number of longhaul subsonic aircraft flying in the lower stratosphere, has caused the issue of possible ozone depletion due to nitrogen oxides emitted in the aircraft exhaust gases to be re-opened. Model calculations have indicated that significant ozone loss could occur if a large, economically viable fleet of supersonic aircraft were to be built. However, the results are sensitive to a number of assumptions and also to

uncertainties in photochemical data. We consider the sensitivity with respect to HNO₃ photolysis rates, which are dependent upon the assumed photochemical data. There is also considerable variability between models in the calculated photolysis rates. If temperature dependent absorption cross sections for HNO₃ are used in model simulations of supersonic aircraft exhaust impact, the calculated ozone loss at high latitudes is significantly reduced, and an ozone increase rather than a decrease is calculated for low to mid-latitudes. The result emphasized our current uncertainty about the impact of future supersonic aircraft on ozone chemistry and more generally, about processes operating in the lower stratosphere. Author (Herner)

A95-80525*

TRACER TRANSPORT FOR REALISTIC AIRCRAFT EMISSION SCENARIOS CALCULATED USING A THREE-DIMENSIONAL MODEL

CLARK J. WEAVER Applied Research Corporation, Landover, MD, US, ANNE R. DOUGLASS NASA, Goddard Space Flight Center, Greenbelt, MD, US, and RICHARD B. ROOD NASA, Goddard Space Flight Center, Greenbelt, MD, US *Journal of Geophysical Research* (ISSN 0148-0227) vol. 100, no. D3 March 20, 1995 p. 5203-5214 (HTN-95-41799) Copyright

A three-dimensional transport model, which uses winds from a stratospheric data assimilation system, is used to study the transport of supersonic aircraft exhaust in the lower stratosphere. A passive tracer is continuously injected into the transport model. The tracer source distribution is based on realistic scenarios for the daily emission rate of reactive nitrogen species for all forecasted flight routes. Winds are from northern hemisphere winter/spring months for 1979 and 1989; there are minimal differences between the tracer integrations for the 2 years. During the integration, peak tracer mixing ratios in the flight corridors are compared with the zonal mean and found to be greater by a factor of 2 or less. This implies that the zonal mean assumption used in two dimensional models is reasonable during winter and spring. There is a preference for pollutant buildup in the heavily traveled North Pacific and North Atlantic flight corridors. Pollutant concentration in the corridors depends on the position of the Aleutian anticyclone and the northern hemisphere polar vortex edge. Author (Herner)

A95-80559

COMPARISON OF WIND PROFILER AND AIRCRAFT WIND MEASUREMENTS AT CHEBOGUE POINT, NOVA SCOTIA

WAYNE M. ANGEVINE University of Colorado, Boulder, CO, US and J. IAN MACPHERSON National Research Council, Ottawa, Ontario, Canada *Journal of Atmospheric and Oceanic Technology* (ISSN 0739-0572) vol. 12, no. 2 April 1995 p. 421-426 Research sponsored by the U.S. Department of Energy and the Atmospheric Environment Service of Canada (HTN-95-41833) Copyright

In August 1993, a 915-MHz boundary layer wind-profiling radar was deployed at Chebogue Point, Nova Scotia, to provide wind, turbulence, and boundary layer structure information for the North Atlantic Regional Experiment summer 1993 intensive campaign. The National Research Council Canada (NRCC) Twin Otter atmospheric research aircraft was also part of that campaign. During the campaign, the Twin Otter flew 29 soundings over Chebogue Point. This paper describes a comparison of the wind speed and direction measured by the profiler and the aircraft. In the height range 300-2000 m above sea level, the random difference between the wind speed measurements is 0.9 m/s, and the random difference between the wind direction measurements is 9 deg. There is a small systematic difference in the wind speeds (0.14 m/s) that is probably due to uncertainty in the zenith angles of the radar beams and extremely good agreement (within 0.5 deg) in the wind direction. The Kalman filter-smoother technique used to remove drifts in the inertial navigation system is shown to be important in achieving these favorable results. Author (Herner)

A95-80829

NORTH ATLANTIC AIR TRAFFIC WITHIN THE LOWER STRATOSPHERE: CRUISING TIMES AND CORRESPONDING EMISSIONS

KLAUS P. HOINKA Institut fuer Physik der Atmosphere, Wessling, Germany, MANFRED E. REINHARDT Institut fuer Physik der Atmosphere, Wessling, Germany, and WERNER METZ Universitat Muenchen, Munich, Germany Journal of Geophysical Research (ISSN 0148-0227) vol. 98, no. D12 December 12, 1993 p. 23,113-23,131

(HTN-95-91841) Copyright

This study estimates cruising times and related pollutant emissions (NO(x), CO, HC) and H₂O of today's aircraft fleet within the troposphere and stratosphere performed for the North Atlantic region in between 45 deg N, 65 deg N, 10 deg W, and 50 deg W for the years 1989, 1990, and 1991. The tropopause surface distribution is determined through analysis of assimilated data. Both conventional lapse rate and potential vorticity criteria are employed to determine the location of the tropopause surface. These data combined with air traffic statistics are used to evaluate cruising times within the troposphere and stratosphere separately. The study shows an average of about 44% of the cruising time of the aircraft above the North Atlantic flown within the stratosphere. Based on emission indices of aircraft engines, the emission rates of NO(x) (in mass units of NO₂) into the stratosphere and troposphere in the given region result in 0.26 and 0.33 x 10^(exp -12) kg/q m/s, respectively.

Author (Herner)

A95-80830* National Aeronautics and Space Administration. Langley Research Center, Hampton, VA. EFFECTS ON STRATOSPHERIC OZONE FROM HIGH-SPEED CIVIL TRANSPORT: SENSITIVITY TO STRATOSPHERIC AEROSOL LOADING

DEBRA K. WEISENSTEIN Atmospheric and Environmental Research, Inc., Cambridge, MA, US, MALCOLM K. W. KO Atmospheric and Environmental Research, Inc., Cambridge, MA, US, JOSE M. RODRIGUEZ Atmospheric and Environmental Research, Inc., Cambridge, MA, US, and NIEN-DAK SZE Atmospheric and Environmental Research, Inc., Cambridge, MA, US Journal of Geophysical Research (ISSN 0148-0227) vol. 98, no. D12 December 12, 1993 p. 23,133-23,140

(Contract(s)/Grant(s): NAS1-19192)

(HTN-95-91842) Copyright

The potential impact of high-speed civil transport (HSCT) aircraft emissions on stratospheric ozone and the sensitivity of these results to changes in aerosol loading are examined with a two-dimensional model. With aerosols fixed at background levels, calculated ozone changes due to HSCT aircraft emissions range from negligible up to 4-6% depletions in column zone at northern high latitudes. The magnitude of the ozone change depends mainly on the NO(x) increase due to aircraft emissions, which depends on fleet size, cruise altitude, and engine design. The partitioning of the odd nitrogen species in the lower stratosphere among NO, NO₂, N₂O₅, is strongly dependent on the concentration of sulfuric acid aerosol particles, and thus the sensitivity of O₃ to NO(x) emissions changes when the stratospheric aerosol loading changes. Aerosol concentrations 4 times greater than background levels have not been unusual in the last 2 decades. Our model results show that a factor of 4 increase in aerosol loading would significantly reduce the calculated ozone depletion due to HSCT emissions. Because of the neutral variability of stratospheric aerosols, the possible impact of HSCT emissions on ozone must be viewed as a range of possible results.

Author (Herner)

A95-80831

HIGH-SPEED CIVIL TRANSPORT IMPACT: ROLE OF SULFATE, NITRIC ACID TRIHYDRATE, AND ICE AEROSOLS STUDIED WITH A TWO-DIMENSIONAL MODEL INCLUDING AEROSOL PHYSICS

G. PITARI Universita degli Studi, L'Aquila, Italy, V. RIZI Istituto Nazionale di Geofisica, Rome, Italy, L. RICCIARDULLI Universita degli Studi, L'Aquila, Italy, and G. VISCONTI Universita degli Studi, L'Aquila, Italy Journal of Geophysical Research (ISSN 0148-0227)

vol. 98, no. D12 December 12, 1993 p. 23,141-23,164 Research sponsored by the Italian Space Agency and the Commission of European Communities

(HTN-95-91843) Copyright

In this paper we describe a two-dimensional model covering the whole stratosphere and troposphere which includes photochemical reactions for the sulfur cycle and a microphysical code for sulfuric acid aerosols. Starting from these particles, the same code predicts also the size distribution for nitric trihydrate (NAT) and ice aerosols, covering globally a particle radius range between 0.01 micrometers and about 160 micrometers. A rather simple scheme is described for nucleation and condensation processes leading to the formation and growth of NAT and ice particles, still using grid point temperature data taken from the zonally averaged climatology of the lower stratosphere. A discussion is made of the high-speed civil transport (HSCT) impact on ozone adopting different scenarios for the aerosols. Model results for the aerosol size distribution and for the available surface densities appear reasonable when compared to satellite and balloon measurements and to independent numerical calculations. As pointed out also by previous research work and assessment panels, our calculation shows that the ozone sensitivity to HSCT emissions largely decreases when heterogeneous chemistry is included with respect to a pure gas phase chemistry case. In addition, our results indicate that the ozone sensitivity to HSCT emission decreases even more when NAT and ice aerosols are present: this is a consequence of the aerosol-induced stratospheric denitrification which makes the residence time of the injected odd nitrogen shorter and the relative weight of the NO(x) catalytic cycle smaller. Inclusion of the sulfur dioxide feedback with the sulfate aerosol surface does not change significantly the ozone depletion in our model simulation, at least in the pure sulfate case. The additional ozone change due to aircraft injection of SO₂ is larger when NAT and ice aerosols are allowed to form, due to the decreased ozone sensitivity to NO(x). In this version of the model no direct aircraft emission of particulate has been included as a possible source for additional condensation nuclei.

Author (Herner)

A95-80843* National Aeronautics and Space Administration. Langley Research Center, Hampton, VA.

AN INTERCOMPARISON OF AIRCRAFT INSTRUMENTATION FOR TROPOSPHERIC MEASUREMENTS OF SULFUR DIOXIDE

GERALD L. GREGORY NASA. Langley Research Center, Hampton, VA, US, DOUGLAS D. DAVIS Georgia Institute of Technology, Atlanta, GA, US, NOBERT BELTZ J.W. Goethe University, Frankfurt, Germany, ALAN R. BANDY Drexel University, Philadelphia, PA, US, RONALD J. FERREK University of Washington, Seattle, WA, US, and DONALD C. THORNTON Drexel University, Philadelphia, PA, US Journal of Geophysical Research (ISSN 0148-0227) vol. 98, no. D12 December 12, 1993 p. 23,325-23,352

(HTN-95-91855) Copyright

As part of the NASA Tropospheric Chemistry Program, a series of field intercomparisons have been conducted to evaluate the state-of-the-art for measuring key tropospheric species. One of the objectives of the third intercomparison campaign in this series, Chemical Instrumentation Test and Evaluation 3 (CITE 3), was to evaluate instrumentation for making reliable tropospheric aircraft measurements of sulfur dioxide, dimethyl sulfide, hydrogen sulfide, carbon disulfide, and carbonyl sulfide. This paper reports the results of the intercomparisons of five sulfur dioxide measurement methods ranging from filter techniques, in which samples collected in flight are returned to the laboratory for analyses (chemiluminescent or ion chromatographic), to near real-time, in-flight measurements via gas chromatographic, mass spectrometric, and chemiluminescent techniques. All techniques showed some tendency to track sizeable changes in ambient SO₂ such as those associated with altitude changes. For SO₂ mixing ratios in the range of 200 pptv to a few ppbv, agreement among the techniques varies from about 30% to several orders of magnitude, depending upon the pair of measurements intercompared. For SO₂ mixing ratios less than 200 pptv, measurements from the techniques are uncorrelated. In general, observed differences in the measurement of standards do not

account for the flight results. The CITE 3 results do not unambiguously identify one or more of the measurement techniques as providing valid or invalid SO₂ measurements, but identify the range of 'potential' uncertainty in SO₂ measurements reported by currently available instrumentation and as measured under realistic aircraft environments.

Author (Herner)

A95-80844* National Aeronautics and Space Administration. Langley Research Center, Hampton, VA.

AN INTERCOMPARISON OF AIRCRAFT INSTRUMENTATION FOR TROPOSPHERIC MEASUREMENTS OF CARBONYL SULFIDE, HYDROGEN SULFIDE, AND CARBON DISULFIDE

GERALD L. GREGORY NASA. Langley Research Center, Hampton, VA, US, DOUGLAS D. DAVIS Georgia Institute of Technology, Atlanta, GA, US, DONALD C. THORNTON Drexel University, Philadelphia, PA, US, JAMES E. JOHNSON NOAA, Seattle, WA, US, ALAN R. BANDY Drexel University, Philadelphia, PA, US, ERIC S. SALTZMAN University of Miami, Miami, FL, US, MEINRAT O. ANDREA Max-Planck-Institute für Chemie, Mainz, Germany, and JOHN D. BARRICK NASA. Langley Research Center, Hampton, VA, US *Journal of Geophysical Research* (ISSN 0148-0227) vol. 98, no. D12 December 12, 1993 p. 23,353-23,372 (HTN-95-91856) Copyright

This paper reports results of NASA's Chemical Instrumentation and Test Evaluation (CITE 3) during which airborne measurements for carbonyl sulfide (COS), hydrogen sulfide (H₂S), and carbon disulfide (CS₂) were intercompared. Instrumentation included a gas chromatograph using flame photometric detection (COS, H₂S, and CS₂), a gas chromatograph using mass spectrometric detection (COS) and CS₂), a gas chromatograph using fluorination and subsequent SF₆ detection via electron capture (COS and CS₂), and the Natusch technique (H₂S). The measurements were made over the Atlantic Ocean east of North and South America during flights from NASA's Wallops Flight Center, Virginia, and Natal, Brazil, in August/September 1989. Most of the intercomparisons for H₂S and CS₂ were at mixing ratios less than 25 pptv and less than 10 pptv, respectively, with a maximum mixing ratio of about 100 pptv and 50 pptv, respectively. Carbonyl sulfide intercomparisons were at mixing ratios between 400 and 600 pptv. Measurements were intercompared from data bases constructed from time periods of simultaneous or overlapping measurements. Agreement among the COS techniques averaged about 5%, and individual measurements were generally within 10%. For H₂S and at mixing ratio greater than 25 pptv, the instruments agreed on average to about 15%. At mixing ratios less than 25 pptv the agreement was about 5 pptv. For CS₂ (mixing ratios less than 50 pptv), two techniques agreed on average to about 4 pptv, and the third exhibited a bias (relative to the other two) that varied in the range of 3-7 pptv. CS₂ mixing ratios over the ocean east of Natal as measured by the gas chromatograph-mass spectrometer technique were only a few pptv and were below the detection limits of the other two techniques. The CITE 3 data are used to estimate the current uncertainty associated with aircraft measurements of COS, H₂S, and CS₂ in the remote troposphere.

Author (Herner)

A95-80845* National Aeronautics and Space Administration. Langley Research Center, Hampton, VA.

AN INTERCOMPARISON OF INSTRUMENTATION FOR TROPOSPHERIC MEASUREMENTS OF DIMETHYL SULFIDE: AIRCRAFT RESULTS FOR CONCENTRATIONS AT THE PARTS-PER-TRILLION LEVEL

GERALD L. GREGORY NASA. Langley Research Center, Hampton, VA, US, LINDA S. WARREN NASA. Langley Research Center, Hampton, VA, US, DOUGLAS D. DAVIS Georgia Institute of Technology, Atlanta, GA, US, MEINRAT O. ANDREA Max-Planck-Institut für Chemie, Mainz, Germany, ALAN R. BANDY Drexel University, Philadelphia, PA, US, RONALD J. FERREK University of Washington, Seattle, WA, US, JAMES E. JOHNSON NOAA, Seattle, WA, US, ERIC S. SALTZMAN University of Miami, Miami, FL, US, and DAVID J. COOPER University of Miami, Miami, FL, US

Journal of Geophysical Research (ISSN 0148-0227) vol. 98, no. D12 December 12, 1993 p. 23,373-23,388 (HTN-95-91857) Copyright

This paper reports results from NASA's Chemical Instrumentation and Test Evaluation (CITE 3) during which airborne measurements of dimethyl sulfide (DMS) from six instruments were intercompared. Represented by the six instruments are three fundamentally different detection principles (flame photometric, mass spectrometric, and electron capture after fluorination); three collection/preconcentration methods (cryogenic, gold wool absorption, and polymer absorbent); and three types of oxidant scrubbers (solid phase alkaline, aqueous reactor, and cotton). The measurements were made over the Atlantic Ocean in August/September 1989 during flights from NASA's Wallops Flight Center, Virginia, and Natal, Brazil. The majority of the intercomparisons are at DMS mixing ratios less than 50 pptv. Results show that instrument agreement is of the order of a few pptv for mixing ratios less than 50 pptv and to within about 15% above 50 pptv. Statistically significant (95% confidence) measurement biases were noted among some of the techniques. However, in all cases, any bias is small and within the accuracy of the measurements and prepared DMS standards. Thus, we conclude that the techniques intercompared during CITE 3 provide equally valid measurements of DMS in the range of a few pptv to 100 pptv (upper range of the intercomparisons).

Author (Herner)

A95-80860

DYNAMICS OF AIRCRAFT EXHAUST PLUMES IN THE JET-REGIME

B. KAERCHER Univ. Muenchen, Freising, Germany and P. FABIAN Univ. Muenchen, Freising, Germany *Annales Geophysicae* (ISSN 0992-7689) vol. 12, no. 10-11 November 1994 p. 911-919 (HTN-95-51275) Copyright

A computational model describing the two-dimensional, turbulent mixing of a single jet of exhaust gas from aircraft engines with the ambient atmosphere is presented. The underlying assumptions and governing equations are examined and supplemented by a discussion of analytical solutions. As an application, the jet dynamics of a B747-400 aircraft engine in cruise and its dependence on key parameters is investigated in detail. The computer code for this dynamical model is computationally fast and can easily be coupled to complex chemical and microphysical models in order to perform comprehensive studies of atmospheric effects from aircraft exhaust emissions in the jet regime.

Author (Herner)

A95-80861

MODELING OF AIRCRAFT EXHAUST EMISSIONS AND INFRARED SPECTRA FOR REMOTE MEASUREMENT OF NITROGEN OXIDES

K. BEIER DLR, Oberpfaffenhofen, Germany and F. SCHREIER DLR, Oberpfaffenhofen, Germany *Annales Geophysicae* (ISSN 0992-7689) vol. 12, no. 10-11 November 1994 p. 920-943 (HTN-95-51276) Copyright

Infrared (IR) molecular spectroscopy is proposed to performed remote measurements of NO(x) concentrations in the exhaust plume and wake of aircraft. The computer model NIRATAM is applied to simulate the physical and chemical properties of the exhaust plume and to generate low resolution IR spectra and syntheical thermal images of the aircraft in its natural surroundings. High-resolution IR spectra of the plume, including atmospheric absorption and emission, are simulated using the molecular line-by-line radiation model FASCODE2. Simulated IR spectra of a Boeing 747-400 at cruising altitude for different axial and radial positions in the jet region of the exhaust plume are presented. A number of spectral lines of NO can be identified that can be discriminated from lines of other exhaust gases and the natural atmospheric background in the region around 5.2 microns. These lines can be used to determine NO concentration profiles in the plume. The possibility of measuring nitrogen dioxide NO₂ is also discussed briefly, although measurements turn out to be substantially less likely than those of NO. This feasibility study compiles fundamental data for the optical

13 GEOSCIENCES

and radiometric design of an airborne Fourier transform spectrometer and the preparation of in-flight measurements for monitoring of aircraft pollutants.

Author (Herner)

A95-80862

CHEMICAL COMPOSITION AND PHOTOCHEMICAL REACTIVITY OF EXHAUST FROM AIRCRAFT TURBINE ENGINES

C. W. SPICER Battelle, Columbus, OH, US, M. W. HOLDREN Battelle, Columbus, OH, US, R. M. RIGGIN Eli Lilly and Company, Indianapolis, IN, US, and T. F. LYON General Electric Company, Evendale, OH, US *Annales Geophysicae* (ISSN 0992-7689) vol. 12, no. 10-11 November 1994 p. 944-955 (Contract(s)/Grant(s): F08635-82-C-0131) (HTN-95-51277) Copyright

Assessment of the environmental impact of aircraft emissions is required by planners and policy makers. Several areas of concern are: (1) exposure of airport workers and urban residents to toxic chemicals emitted when the engines operate at low power (idle and taxi) on the ground; (2) contributions to urban photochemical air pollution of aircraft volatile organic and nitrogen oxides emissions from operations around airports; and (3) emissions of nitrogen oxides and particles during high-altitude operation. The environmental impact of chemicals emitted from jet aircraft turbine engines has not been firmly established due to lack of data regarding emission rates and identities of the compounds emitted. This paper describes an experimental study of two different aircraft turbine engines designed to determine detailed organic emissions, as well as emissions of inorganic gases. Emissions were measured at several engine power settings. Measurements were made of detailed organic composition from C-1 through C-17, CO, CO₂, NO, NO(x) and polycyclic aromatic hydrocarbons. Measurements were made using a multi-port sampling probe positioned directly behind the engine in the exhaust exit plane. The emission measurements have been used to determine the organic distribution by carbon number and the distribution by compound class at each engine power level. The sum of the organic species was compared with an independent measurement of total organic carbon to assess the carbon mass balance. A portion of the exhaust was captured and irradiated in outdoor smog chambers to assess the photochemical reactivity of the emissions with respect to ozone formation.

Author (Herner)

A95-80867

POTENTIAL EFFECTS ON OZONE OF FUTURE SUPERSONIC AIRCRAFT/2D SIMULATION

R. RAMAROSON Office Nat. d'Etudes et de Recherches Aérospatiales, Chatillon, France and N. LOUISNARD Office Nat. d'Etudes et de Recherches Aérospatiales, Chatillon, France *Annales Geophysicae* (ISSN 0992-7689) vol. 12, no. 10-11 November 1994 p. 986-995 Research sponsored by the French Ministry of Transport and the Committee Avion-Ozone (HTN-95-51282) Copyright

In a previous work, the stratospheric effect of a future supersonic aircraft fleet on ozone has been simulated, by using a photochemical diffusive 1D model and a 2D photochemical, radiative dynamical model. The fleet scenario was defined by Aérospatiale and Snecma for a current technology Mach-2 aircraft; the models were limited to simplified homogeneous phase reactions. The results indicated a global ozone decrease of about 1.5% in steady-state conditions. Now the 2D model has been upgraded and includes the classical heterogeneous reactions with Polar Stratospheric Clouds (PSC) and aerosol. It also takes into account the natural or anthropogenic evolution of the background atmosphere. The scenario has been optimized to meet more realistic conditions. Thus, new results are presented. The main conclusion concerning the calculated impact of a realistic fleet for the next 20-50 years is still weaker than in the previous work: the decrease for the total ozone would always be lower than 0.3%. These results are commented, with the help of a parametric study, pointing out the importance of the background atmosphere and especially the total chlorine loading and the aerosol surface area.

Author (Herner)

A95-80868

IMPACT ON OZONE OF HIGH-SPEED STRATOSPHERIC AIRCRAFT: EFFECTS OF THE EMISSION SCENARIO

G. PITARI Univ. degli Studi, L'Aquila, Italy, S. PALERMI Univ. degli Studi, L'Aquila, Italy, and G. VISCONTI Univ. degli Studi, L'Aquila, Italy *Annales Geophysicae* (ISSN 0992-7689) vol. 12, no. 10-11 November 1994 p. 996-1005 Research sponsored by the Italian Space Agency

(HTN-95-51283) Copyright

A photochemical-transport two-dimensional model has been used to assess the impact of a projected fleet of high-speed stratospheric aircraft using different emissions scenarios. It is shown that the presence in the background atmosphere of nitric acid trihydrate aerosols is responsible for a lower stratospheric denoxification in addition to that caused by the sulfate aerosol later. This has the effect of further decreasing the relative role of the odd nitrogen catalytic cycle for ozone destruction, so that the lower stratosphere is primarily controlled by chlorine species. The effect of aircraft injection of nitric oxides is that of decreasing the level of ClO, so that the lower stratospheric ozone (below about 20-25 km altitude) increases. The net effect on global ozone is that of a small increase even at Mach 2.4, and is enhanced by adopting emission scenarios including altitude restriction at 15 or 18 km. Reductions of the emission index (EI) of nitric oxides below relatively small values (about 15) are shown to reduce the aircraft-induced ozone increase, because of the associated smaller decrease of ClO. This conclusion is no more valid when the emission index is raised at the present values (about 45).

Author (Herner)

A95-80908

IDENTIFICATION OF AVIATION WEATHER HAZARDS BASED ON THE INTEGRATION OF RADAR AND LIGHTNING DATA

ANDREW D. STERN NOAA, Sterling, VA, US, RAYMOND H. BRADY, III NOAA, Sterling, VA, US, PATRICK D. MOORE NOAA, Sterling, VA, US, and GARY M. CARTER NOAA, Bohemia, NY, US *American Meteorological Society, Bulletin* (ISSN 0003-0007) vol. 75, no. 12 December 1994 p. 2269-2280 (HTN-95-51323) Copyright

The National Weather Service (NWS) Eastern Region is carrying out a national risk-reduction exercise at the Baltimore-Washington Forecast Office in Sterling, Virginia. The primary objective of this project is to integrate information from remote sensor technologies to produce comprehensive state-of-the-atmosphere reports that promote aviation safety. Techniques have been developed and tested to identify aviation-oriented hazardous weather based on data from conventional radars, a national lightning detection network, and collateral observations from new Automated Surface Observing System (ASOS) sites that are being deployed throughout the nation. Integration of information from several products generated by the new Doppler radar at Sterling with lightning network data is being pursued for the second phase of the project. The National Weather Service will determine the viability of this approach to generate products to routinely supplement the information provided by ASOS on either a national or a local basis.

Author (revised by Herner)

A95-81648

AERODYNAMIC PARAMETERS OF CROP CANOPIES ESTIMATED WITH A CENTER-OF-PRESSURE TECHNIQUE

QIN WENHAN Academia Sinica, Beijing, China *Acta Meteorologica Sinica* (ISSN 0577-6619) vol. 52, no. 1 February 1994 p. 99-106 In CHINESE

(HTN-95-41901) Copyright

The Center-of-Pressure technique (CPT), originally proposed by Thom in 1971, is firstly verified in the field, based on the canopy architecture and microclimate data of four crops. The comparison of u^* estimated by CPT with that by eddy-correlation method shows that CPT not only works well in the field, but also gives more steady and accurate results, which are hardly affected by atmospheric stratification stability, than that of the log-profile fitting method which is frequently used in practice. In addition, a physical model for directly calculating d is approximately developed. The results yield

that the ratio of d , $z(\text{sub } 0)$ to h , in general, varies with the canopy structure, turbulence intensity and the stability of flow above and within the canopy; d/h increases with the increase of α (the relative height of the maximum foliage density layer) and $\gamma(\text{sub } u)$ (the wind extinction coefficient within canopies). Only for short stem crops and when their canopies reach the moderate foliage density and stable structure, d and $z(\text{sub } 0)$ approximately and steadily approach to 0.64 h and 0.08 h , respectively. Besides, with very sparse or tall crops, the fairly large stresses at the soil surface and variability of m undoubtedly influence the accuracy of CPT to a certain extent.

Author (Herner)

N95-24219* North Dakota Univ., Grand Forks, ND. Dept. of Atmospheric Sciences.

PRELIMINARY ANALYSIS OF UNIVERSITY OF NORTH DAKOTA AIRCRAFT DATA FROM THE FIRE CIRrus IFO-2 Final Report

MICHAEL R. POELLT 30 Mar. 1995 14 p

(Contract(s)/Grant(s): NAG1-1351)

(NASA-CR-198038; NAS 1.26:198038) Avail: CASI HC A03/MF A01

The stated goals of the First ISCCP (International Satellite Cloud Climatology Project) Regional Experiment (FIRE) are 'to promote the development of improved cloud and radiation parameterization for use in climate models, and to provide for assessment and improvement of ISCCP projects'. FIRE Phase 2 has focused on the formation, maintenance and dissipation of cirrus and marine stratocumulus cloud systems. These objectives have been approached through a combination of modeling, extended-time observations and intensive field observation (IFO) periods. The work under this grant was associated with the FIRE Cirrus IFO 2. This field measurement program was conducted to obtain observations of cirrus cloud systems on a range of scales from the synoptic to the microscale, utilizing simultaneous measurements from a variety of ground-based, satellite and airborne platforms. By combining these remote and in situ measurements a more complete picture of cirrus systems can be obtained. The role of the University of North Dakota in Phase 2 was three-fold: to collect in situ microphysical data during the Cirrus IFO 2; to process and archive these data; and to collaborate in analyses of IFO data. This report will summarize the activities and findings of the work performed under this grant; detailed description of the data sets available and of the analyses are contained in the Semi-annual Status Reports submitted to NASA.

Derived from text

N95-24274* National Aeronautics and Space Administration, Washington, DC.

THE ATMOSPHERIC EFFECTS OF STRATOSPHERIC AIRCRAFT: A FOURTH PROGRAM REPORT

RICHARD S. STOLARSKI, ed. (National Aeronautics and Space Administration, Goddard Space Flight Center, Greenbelt, MD.), HOWARD L. WESOKY, ed., STEVEN C. WOFSY (Harvard Univ., Cambridge, MA.), A. R. RAVISHANKARA (National Oceanic and Atmospheric Administration, Boulder, CO.), JOSE M. RODRIGUEZ (Atmospheric and Environmental Research, Inc., Cambridge, MA.), and WILLIAM L. GROSE (National Aeronautics and Space Administration, Langley Research Center, Hampton, VA.) Jan. 1995 234 p

(NASA-RP-1359; NAS 1.61:1359) Avail: CASI HC A11/MF A03

This document presents the fourth report from the Atmospheric Effects of Stratospheric Aircraft (AESA) component of NASA's High-Speed Research Program (HSRP). Market and technology considerations continue to provide an impetus for high-speed civil transport research. A recent AESA interim assessment report and a review of that report have shown that considerable uncertainty still exists about the possible impact of aircraft on the atmosphere. The AESA has been designed to develop the body of scientific knowledge necessary for the evaluation of the impact of stratospheric aircraft on the atmosphere. The first Program report presented the basic objectives and plans for AESA. This fourth report comes after the interim assessment and sets forth directions for the 1995 assess-

ment at the end of AESA Phase 1. It also sets forth the goals and directions for AESA Phase 2, as reported at the 1994 Atmospheric Effects of Aviation Project (AEAP) annual meeting held in June. The focus of the Phase 2 effort is to obtain the best possible closure on the outstanding problems identified in the interim assessment and NASA/NRC review. Topics discussed in this report include how high-speed civil transports (HSCT) might affect stratospheric ozone, emissions scenarios and databases to assess potential atmospheric effects from HSCT's, calculated results from 2-D zonal mean models using emissions data, engine trace constituent measurements.

Author

N95-24853# National Renewable Energy Lab., Golden, CO. **USING DIGITAL FILTERING TECHNIQUES AS AN AID IN WIND TURBINE DATA ANALYSIS**

TERESA YOUNG Nov. 1994 9 p Presented at the AIAA Region 5 Student Conference, Ft. Collins, CO, 21-24 Apr. 1993

(Contract(s)/Grant(s): DE-AC36-83CH-10093)

(DE94-011862; NREL/TP-441-7077; CONF-9304280-1) Avail: CASI HC A02/MF A01

Research involving very large sets of digital data is often difficult due to the enormity of the database. In the case of a wind turbine operating under varying environmental conditions, determining which data are representative of the blade aerodynamics and which are due to transient flow ingestion effects or errors in instrumentation, operation, and data collection is of primary concern to researchers. The National Renewable Energy Laboratory in Golden, Colorado collected extensive data on a downwind horizontal axis wind turbine (HAWT) during a turbine test project called the Combined Experiment. A principal objective of this experiment was to provide a means to predict HAWT aerodynamic, mechanical, and electrical operational loads based upon analytical models of aerodynamic performance related to blade design and inflow conditions. In a collaborative effort with the Aerospace Engineering Department at the University of Colorado at Boulder, a team of researchers has evolved and utilized various digital filtering techniques in analyzing the data from the Combined Experiment. A preliminary analysis of the data set was performed to determine how to best approach the data. The reduced data set emphasized selection of inflow conditions such that the aerodynamic data could be compared directly to wind tunnel data obtained for the same airfoil design as used for the HAWT's blades. It will be shown that this reduced data set has yielded valid, reproducible results that a simple averaging technique or a random selection approach cannot achieve. These findings provide a stable baseline against which operational HAWT data can be compared.

DOE

N95-24882# National Renewable Energy Lab., Golden, CO.

NREL AIRFOIL FAMILIES FOR HAWTS

J. L. TANGLER and D. M. SOMERS (Airfoils, Inc., State College, PA.) Jan. 1995 10 p

(Contract(s)/Grant(s): DE-AC36-83CH-10093)

(DE95-000267; NREL/TP-442-7109) Avail: CASI HC A02/MF A01

The development of special-purpose airfoils for horizontal-axis wind turbines (HAWTs) began in 1984 as a joint effort between the National Renewable Energy Laboratory (NREL), formerly the Solar Energy Research Institute (SERI), and Airfoils, Incorporated. Since that time seven airfoil families have been designed for various size rotors using the Eppler Airfoil Design and Analysis Code. A general performance requirement of the new airfoil families is that they exhibit a maximum lift coefficient ($c(\text{sub } l, \text{max})$) which is relatively insensitive to roughness effects. The airfoil families address the needs of stall-regulated, variable-pitch, and variable-rpm wind turbines. For stall-regulated rotors, better peak-power control is achieved through the design of tip airfoils that restrain the maximum lift coefficient. Restrained maximum lift coefficient allows the use of more swept disc area for a given generator size. Also, for stall-regulated rotors, tip airfoils with high thickness are used to accommodate overspeed control devices. For variable-pitch and variable-rpm rotors, tip airfoils having a high maximum lift coefficient lend themselves to lightweight blades with low solidity. Tip airfoils

having low thickness result in less drag for blades having full-span pitch control. Annual energy improvements from the NREL airfoil families are projected to be 23% to 35% for stall-regulated turbines, 8% to 20% for variable-pitch turbines, and 8% to 10% for variable-rpm turbines. The improvement for stall-regulated turbines has been verified in field tests. DOE

N95-25110 EG and G Energy Measurements, Inc., Goleta, CA. **TURBINE-ENGINE APPLICATIONS OF THERMOGRAPHIC-PHOSPHOR TEMPERATURE MEASUREMENTS** BRUCE W. NOEL (Noel Associates, Espanola, NM.), W. DALE TURLEY, and STEPHEN W. ALLISON (Martin Marietta Energy Systems, Inc., Oak Ridge, TN.) 1995 24 p Presented at the Remote Temperature Sensing Workshop, Cleveland, OH, 27-28 Oct. 1994 Limited Reproducibility: More than 20% of this document may be affected by microfiche quality (Contract(s)/Grant(s): DE-AC08-93NV-11265) (DE95-003625; EGG-11265-3011; UC-706; CONF-9410259-1) Avail: CASI HC A03

The thermographic-phosphor (TP) method can measure temperature, heat flux, strain, and other physical quantities remotely in hostile and/or inaccessible environments such as the first-stage turbine components in turbine engines. It is especially useful in situations in which no other known method works well. This paper is a brief review of engine tests that demonstrated the utility of the TP method. For the most part, the results presented here are discussed only qualitatively. The papers in the bibliography describe these and other experiments and results in detail. The first viewgraph summarizes the many desirable features of the TP method. The second viewgraph describes TP's, and the third summarizes how the TP method works. To measure single-point temperatures in turbine-engine applications, we use the decay-time method, which depends on the fact that the luminescence following an impulse of ultraviolet excitation decays, with a characteristic decay time that is a monotonically decreasing function of temperature over some range of temperatures. The viewgraph is a set of calibration curves showing the behavior of some useful emission lines for ten important TP's. Consider $\text{LuPO}_4:\text{Eu}$ as an example. Below the 'quenching' temperature near 900 K, the decay time is nearly constant. Above it, the decay time decreases exponentially with the temperature. This strong functional dependence means that one can have a fairly large error in the lifetime measurement, as in environments with poor signal-to-noise ratios (SNR's), yet still obtain high accuracy in the temperature measurement. Our more-recent data up to 1900 K show the same behavior. DOE

N95-26005# Radian Corp., Research Triangle Park, NC. **NITROGEN OXIDE EMISSIONS AND THEIR CONTROL FROM UNINSTALLED AIRCRAFT ENGINES IN ENCLOSED TEST CELLS: JOINT REPORT TO CONGRESS ON THE ENVIRONMENTAL PROTECTION AGENCY - DEPARTMENT OF TRANSPORTATION STUDY Final Report** Oct. 1994 196 p Prepared in cooperation with Energy and Environmental Research Corp., Durham, NC Sponsored in cooperation with FAA (Contract(s)/Grant(s): EPA-68-D1-0177) (PB95-166237; EPA/453/R-94/068) Avail: CASI HC A09/MF A03

The report was submitted to the Congress under mandate of Section 233 of the Clean Air Act Amendments of 1990. The report provides a characterization of aircraft engine test cells and their emissions. Various NOx control technologies that have been applied to combustion sources other than test cells are examined in the report for their applicability to test cells. Effects of NOx controls on the aircraft engine and aircraft engine test are also addressed. Finally, annual emissions from test cells are estimated and compared to total NOx emissions in the applicable ozone non-attainment areas. NTIS

N95-26090# National Renewable Energy Lab., Golden, CO. **WIND TECHNOLOGY DEVELOPMENT: LARGE AND SMALL TURBINES**

R. W. THRESHER, S. M. HOCK, R. R. LOOSE, and P. GOLDMAN Dec. 1994 13 p Presented at the Power Generation Conference, Orlando, FL, 7-9 Dec. 1994

(Contract(s)/Grant(s): DE-AC36-83CH-10093) (DE95-000286; NREL/TP-440-7224; CONF-941210-2) Avail: CASI HC A03/MF A01

Wind technology has developed rapidly over the last decade with the design and development of advanced systems with improved performance, higher reliability, and lower costs. During the past several years, substantial gains have been made in wind turbine designs, lowering costs to an average of \$0.05/kWh while further technology development is expected to allow the cost to drop below \$0.04/kWh by 2000. As a result, wind is expected to be one of the least expensive forms of new electric generation in the next century. This paper will present the technology developments for both utility-scale wind turbines and remote, small-village wind turbines that are currently available or in development. Technology innovations are being adapted for remote and stand-alone power applications with smaller wind turbines. Hybrid power systems using smaller 1 to 50 (kW) wind turbines are being developed for non-grid-connected electrical generation applications. These village power systems typically use wind energy, photovoltaics, battery storage, and conventional diesel generators to power remote communities. Smaller turbines are being explored for application as distributed generation sources on utility grids to supply power during periods of peak demand, avoiding costly upgrades in distribution equipment. New turbine designs now account for turbulence-induced loads, unsteady aerodynamic stall effects, and complex fatigue loads, making use of new technology developments such as advanced airfoils. The new airfoils increase the energy capture, improve the operating efficiency, and reduce the sensitivity of the airfoils to operation roughness. Electronic controls are allowing variable rotor speed operation; while aerodynamic control devices, such as ailerons and flaps, are used to modulate power or stop the rotor in high-speed conditions. These technology trends and future turbine configurations are being sponsored and explored by the U.S. Department of Energy's Wind Energy Program. DOE

15

MATHEMATICAL AND COMPUTER SCIENCES

Includes mathematical and computer sciences (general); computer operations and hardware; computer programming and software; computer systems; cybernetics; numerical analysis; statistics and probability; systems analysis; and theoretical mathematics.

A95-79238 **QUANTITATIVE COMPARISON BETWEEN INTERFEROMETRIC MEASUREMENTS AND EULER COMPUTATIONS FOR SUPERSONIC CONE FLOWS**

T. A. W. M. LANEN Delft Univ of Technology, Delft, Netherlands, E. M. HOUTMAN, and P. G. BAKKER AIAA Journal (ISSN 0001-1452) vol. 33, no. 2 February 1995 p. 210-216 refs (BTN-95-EIX95222650782) Copyright

Dual-reference-beam, plane-wave digital holographic interferometry has been applied to obtain quantitative interferometric data in the three-dimensional supersonic flow over circular cones. The interferometric data are compared quantitatively on a two-dimensional grid with the postprocessed results of an Euler code that simulates three-dimensional inviscid compressible flows. The comparison involves two different combinations of cone angle and angle of incidence. The maximum deviations between the interferometric data and the numerical data are found to lie in the error interval (-2.0%, +2.0%). Author (EI)

A95-80405* Jet Propulsion Lab., California Inst. of Tech., Pasadena, CA.

THE CASSINI SPACECRAFT: OBJECT ORIENTED FLIGHT CONTROL SOFTWARE

JOHN C. HACKNEY Jet Propulsion Lab., California Inst. of Tech., Pasadena, CA, US, DOUGLAS E. BERNARD Jet Propulsion Lab., California Inst. of Tech., Pasadena, CA, US, and ROBERT D. RASMUSSEN Jet Propulsion Lab., California Inst. of Tech., Pasadena, CA, US In Guidance and control, 1993; Annual Rocky Mountain Guidance and Control Conference, 16th, Keystone, CO, Feb. 6-10, 1993. A95-80389 San Diego, CA American Astronautical Society (Advances in the Astronautical Sciences, Vol. 81) (ISSN 0065-3438) 1993 p. 211-236 Copyright

The Cassini Attitude and Articulation Control Subsystem (AACS) is responsible for determining and controlling the spacecraft attitude including instrument pointing, antenna pointing, and thrust vector pointing during velocity change maneuvers. The 12 year mission life, long round-trip light time, and extended periods of coast without continuous ground control drive the AACS flight software design in the directions of autonomy, fault tolerance, and modularity to accommodate planned upgrades in flight. The Cassini AACS Flight Software is depicted in increasing levels of detail using a Context Diagram, Architecture Diagrams (i.e., Dependency Diagrams), an Object Diagram for each object, and a Statechart (i.e., State Transition Diagram) for each object. The detail contained in the diagrams is enhanced and refined during the Requirements and Design Phases of both Subsystem and Software Development. Examples of all the diagrams as well as the criteria for object selection, the advantages of statecharts, and the ease of modifying the design to accommodate changes in scope are described. Author (revised by Herner)

A95-81079

ON-LINE LEARNING NONLINEAR DIRECT NEUROCONTROLLERS FOR RESTRUCTURABLE CONTROL SYSTEMS

MARCELLO R. NAPOLITANO West Virginia Univ, Morgantown, WV, United States, STEVE NAYLOR, CHARLES NEPPACH, and VAN CASDORPH Journal of Guidance, Control, and Dynamics (ISSN 0731-5090) vol. 18, no. 1 January-February 1995 p. 170-176 refs (BTN-95-EIX95242670768) Copyright

This paper describes an innovative approach to the problem of the on-line determination of a control law in order to achieve a dynamic reconfiguration of an aircraft that has sustained extensive damage to a vital control surface. The approach consists of the use of on-line learning neural network controllers that have the capability of bringing an aircraft, whose dynamics can become unstable after a substantial damage, back to an equilibrium condition. This goal has been achieved through the use of a specific training algorithm, the extended back-propagation algorithm (EBPA), and proper selection of the architectures for the neural network controllers. The EBPA has recently shown remarkable improvements over the back-propagation algorithm in terms of convergence time and local minimum problems. The methodology is illustrated through a nonlinear dynamic simulation of a typical combat maneuver for a high-performance aircraft. Author (EI)

A95-81081

APPLICATION OF DIRECT TRANSCRIPTION TO COMMERCIAL AIRCRAFT TRAJECTORY OPTIMIZATION

JOHN T. BETTS Boeing Computer Services, Seattle, WA, United States and EVIN J. CRAMER Journal of Guidance, Control, and Dynamics (ISSN 0731-5090) vol. 18, no. 1 January-February 1995 p. 151-159 refs (BTN-95-EIX95242670766) Copyright

One of the most effective numerical techniques for the solution of trajectory optimization and optimal control problems is the direct transcription method. This approach combines a nonlinear programming algorithm with a discretization of the trajectory dynamics. When the resulting mathematical programming problem is solved

using a sparse sequential quadratic programming algorithm, the technique produces solutions very rapidly and has demonstrated considerable robustness when applied to atmospheric and orbital trajectories. This paper describes the application of the direct transcription technique to the optimal design of a commercial aircraft trajectory, subject to realistic constraints on the aircraft flight path. A primary result of the paper is to demonstrate that the transcription formulation leads to a very natural treatment of realistic Federal Aviation Administration (FAA) imposed path constraints within a high fidelity simulation. A second important result is to demonstrate that modeling tabular data using smooth approximations significantly improves the speed of convergence. Author (EI)

A95-81088

IMPACT OF NEAR-COINCIDENT FAULTS ON DIGITAL FLIGHT CONTROL SYSTEMS

CRISTIAN CONSTANTINESCU Duke Univ, Durham, NC, United States Journal of Guidance, Control, and Dynamics (ISSN 0731-5090) vol. 18, no. 1 January-February 1995 p. 102-107 refs (BTN-95-EIX95242670759) Copyright

The effects of near-coincident faults must be taken into account in designing highly reliable digital flight control systems. In this paper closed-form solutions for permanent and transient near-coincident fault factors are derived, based on the behavioral decomposition/aggregation technique and Markov version of the CARE 3 coverage model. Parameters of the model are assumed to be exponentially distributed. The influence of fault detection rate, fault detectability, error production and propagation rates, error detectability, and transient fault/error transition rate on the near-coincident fault factors is discussed. Eventually, a homogeneous, continuous-time Markov chain is used for describing a triple modular redundant (TMR) system. The near-coincident fault factors are employed for analyzing the effect of the interfering faults on reliability of the TMR computer. System reliability and near-coincident fault unreliability are plotted as functions of mission time, fault detectability, and weight of permanent and transient fault/errors. The impact of near-coincident faults can be curbed by increasing fault detectability. That impact is also lower when the percentage of transients is higher. Author (EI)

A95-81100

ROBUST DYNAMIC INVERSION FOR CONTROL OF HIGHLY MANEUVERABLE AIRCRAFT

JACOB REINER Univ of Minnesota, Minneapolis, MN, United States, GARY J. BALAS, and WILLIAM L. GARRARD Journal of Guidance, Control, and Dynamics (ISSN 0731-5090) vol. 18, no. 1 January-February 1995 p. 18-24 refs (BTN-95-EIX95242670747) Copyright

This paper presents a methodology for the design of flight controllers for aircraft operating over large ranges of angle of attack. The methodology is a combination of dynamic inversion and structured singular value (μ) synthesis. An inner-loop controller, designed by dynamic inversion, is used to linearize the aircraft dynamics. This inner-loop controller lacks guaranteed robustness to uncertainties in the system model and the measurements; therefore, a robust, linear outer-loop controller is designed using μ synthesis. This controller minimizes the weighted $H(\infty)$ norm of the error between the aircraft response and the specified handling quality model while maximizing robustness to model uncertainties and sensor noise. The methodology is applied to the design of a pitch rate command system for longitudinal control of a high-performance aircraft. Nonlinear simulations demonstrate that the controller satisfies handling quality requirements, provides good tracking of pilot inputs, and exhibits excellent robustness over a wide range of angles of attack and Mach number. The linear controller requires no scheduling with flight conditions. Author (EI)

A95-81253

FAULT DETECTION IN MULTIPROCESSOR SYSTEMS AND ARRAY PROCESSORS

MARK G. KARPOVSKY Boston Univ Coll of Engineering, Boston,

MA, United States, TATYANA D. ROZINER, and CLAUDIO MORAGA
IEEE Transactions on Computers (ISSN 0018-9340) vol. 44, no. 3
March 1995 p. 383-392 refs
(BTN-95-EIX95242679097) Copyright

Off-line testing of large multiprocessor networks or VLSI chips with many outputs requires a large volume of memory for reference data storage. Space compaction combined with time compression of test responses can essentially reduce an over-head required for testing and diagnosis. In this paper, we discuss the problem of optimal design for space compactors (compactors), to minimize the number of observation points for detection of single faulty components in multiprocessor networks. A space compactor is assumed to be followed by a time compressor, to detect a fault not necessarily manifesting itself for a single test pattern. We formulate the rules of design for a space compaction matrix for the topology of the circuit-under-test (CUT) modeled by an arbitrary acyclic graph. Tree arrays and Fourier transform networks are considered as examples. The lower and upper bounds on the number of space compactor outputs are obtained, and optimal space compaction matrices are determined for above mentioned CUT topologies. Simple procedures for design of off-line testing devices with built-in self-testing are presented. Estimations on a complexity of proposed designs are given. Author (EI)

N95-25264*# Air Force Academy, CO.

APPLICATION OF NEURAL NETWORKS TO UNSTEADY AERODYNAMIC CONTROL

WILLIAM E. FALLER, SCOTT J. SCHRECK, and MARVIN W. LUTTGES (Colorado Univ., Boulder, CO.) In JPL, A Decade of Neural Networks: Practical Applications and Prospects p 107-126
11 May 1994

Avail: CASI HC A03/MF A03

The problem under consideration in this viewgraph presentation is to understand, predict, and control the fluid mechanics of dynamic maneuvers, unsteady boundary layers, and vortex dominated flows. One solution is the application of neural networks demonstrating closed-loop control. Neural networks offer unique opportunities: simplify modeling of three dimensional, vortex dominated, unsteady separated flow fields; are effective means for controlling unsteady aerodynamics; and address integration of sensors, controllers, and time lags into adaptive control systems. CASI

N95-25797*# Overset Methods, Inc., Los Altos, CA.

THE COUPLING OF FLUIDS, DYNAMICS, AND CONTROLS ON ADVANCED ARCHITECTURE COMPUTERS Final Report, 1 Jun. 1994 - 31 May 1995

CHRISTOPHER ATWOOD May 1995 32 p Original contains color illustrations

(Contract(s)/Grant(s): NCC2-799)

(NASA-CR-197727; NAS 1.26:197727) Avail: CASI HC A03/MF A01; 1 functional color page

This grant provided for the demonstration of coupled controls, body dynamics, and fluids computations in a workstation cluster environment; and an investigation of the impact of peer-peer communication on flow solver performance and robustness. The findings of these investigations were documented in the conference articles. The attached publication, 'Towards Distributed Fluids/Controls Simulations', documents the solution and scaling of the coupled Navier-Stokes, Euler rigid-body dynamics, and state feedback control equations for a two-dimensional canard-wing. The poor scaling shown was due to serialized grid connectivity computation and Ethernet bandwidth limits. The scaling of a peer-to-peer communication flow code on an IBM SP-2 was also shown. The scaling of the code on the switched fabric-linked nodes was good, with a 2.4 percent loss due to communication of intergrid boundary point information. The code performance on 30 worker nodes was 1.7 (mu)s/point/iteration, or a factor of three over a Cray C-90 head. The attached paper, 'Nonlinear Fluid Computations in a Distributed Environment', documents the effect of several computational rate enhancing methods on convergence. For the cases shown, the

highest throughput was achieved using boundary updates at each step, with the manager process performing communication tasks only. Constrained domain decomposition of the implicit fluid equations did not degrade the convergence rate or final solution. The scaling of a coupled body/fluid dynamics problem on an Ethernet-linked cluster was also shown. Derived from text

N95-25803*# Texas Technological Univ., Lubbock, TX.

A BRIEF SURVEY OF CONSTRAINED MECHANICS AND VARIATIONAL PROBLEMS IN TERMS OF DIFFERENTIAL FORMS

ROBERT HERMANN In *its* Hierarchical Control and Trajectory Planning 15 p 31 Dec. 1994

Avail: CASI HC A03/MF A03

There has been considerable interest recently in constrained mechanics and variational problems. This is in part due to applied interests (such as 'non-holonomic mechanics in robotics') and in other part due to the fact that several schools of 'pure' mathematics have found that this classical subject is of importance for what they are trying to do. I have made various attempts at developing these subjects since my Lincoln lab days of the late 1950's. In this Chapter, I will sketch a Unified point of view, using Cartan's approach with differential forms. This has the advantage from the C-O-R viewpoint being developed in this Volume that the extension from 'smooth' to 'generalized' data is very systematic and algebraic. (I will only deal with the 'smooth' point of view in this Chapter; I will develop the 'generalized function' material at a later point.) The material presented briefly here about Variational Calculus and Constrained Mechanics can be found in more detail in my books, 'Differential Geometry and the Calculus of Variations', 'Lie Algebras and Quantum Mechanics', and 'Geometry, Physics and Systems'. Author

N95-25805*# Texas Technological Univ., Lubbock, TX.

HOW TO FLY AN AIRCRAFT WITH CONTROL THEORY AND SPLINES

ANDERS KARLSSON In *its* Hierarchical Control and Trajectory Planning 108 p 31 Dec. 1994

Avail: CASI HC A06/MF A03

When trying to fly an aircraft as smoothly as possible it is a good idea to use the derivatives of the pilot command instead of using the actual control. This idea was implemented with splines and control theory, in a system that tries to model an aircraft. Computer calculations in Matlab show that it is impossible to receive enough smooth control signals by this way. This is due to the fact that the splines not only try to approximate the test function, but also its derivatives. A perfect traction is received but we have to pay in very peaky control signals and accelerations. Author

N95-25894# Linköping Univ. (Sweden).

ASPECT ESTIMATION OF AN AIRCRAFT USING LIBRARY MODEL SILHOUETTES

A. LAUBERTS Jun. 1994 23 p

(PB95-141834; FOA-C-30763-8.4.3.4) Avail: CASI HC A03/MF A01

This matching method uses a library of silhouettes of a model aircraft with 512 uniformly distributed orientations. The library contains silhouettes of aircraft aspects stored as chain code in a look-up table. Scaled model silhouettes are matched to a distance transform map of the object silhouette. The scaling is according to the apparent major diameter, being a relatively rotation invariant quantity. After translation to a common center of area, the silhouettes are rotated in discrete angular steps until best fit model-object. The best matched views, constrained within a small group of nearby aspect directions, are added vectorially using inverse fit errors as weights to yield an optimum aspect direction. The corresponding aspect angles define the model orientation, and therefore give an estimate of the object orientation. Optionally, radar gives position and velocity of the object, restricting the number of possible views. However, only the aspect matching method supplies the instantaneous 3D orientation needed for accurate prediction of an evasive flight maneuver. NTIS

N95-26085* Institute for Computer Applications in Science and Engineering, Hampton, VA.

CUMULATIVE REPORTS AND PUBLICATIONS THROUGH DECEMBER 31, 1994 Final Report, 1975 - Dec. 1994

Hampton, VA NASA Mar. 1995 109 p

(Contract(s)/Grant(s): NAS1-19480; NAS1-18605; NAS1-17070; NAS1-17130; NAS1-15810; NAS1-16394; NAS1-14101; NAS1-14472; RTOP 505-90-52-01)

(NASA-CR-195043; NAS 1.26:195043) Avail: CASI HC A06/MF A02

This document contains a complete list of Institute for Computer Applications in Science and Engineering (ICASE) reports. Since ICASE reports are intended to be preprints of articles that will appear in journals or conference proceedings, the published reference is included when it is available. Author

N95-26330 Polish Academy of Sciences, Warsaw (Poland). Inst. of Basic Problems of Technology.

ACTUATING SIGNALS IN ADAPTIVE CONTROL SYSTEMS [SYGNALY POBUDZAJACE W ADAPTACYJNYCH UKLADACH STEROWANIA]

DARIUSZ JANECKI 1994 180 p In POLISH

(ISSN 0208-5658)

(IFTR-13/1994) Avail: Issuing Activity (Polish Academy of Sciences, Warsaw, Poland)

This dissertation discusses the properties of selected adaptive control systems and describes the methods used to analyze these systems. The author places particular emphasis on the theoretical problems associated with the stability, convergence, and immunity of adaptive systems, especially on the significance of uniform actuation of a controlled system for the properties in question. In addition to existing results which are already rooted in the theory, the author presents new results concerning the immunity of adaptive systems published for the first time. The author supplements and illustrates his theoretical solutions with an example of the use of adaptive controllers to control the vibrations of flexible rotors.

Transl. by SCITRAN

16

PHYSICS

Includes physics (general); acoustics; atomic and molecular physics; nuclear and high-energy physics; optics; plasma physics; solid-state physics; and thermodynamics and statistical physics.

A95-79988

IMPACT, FRICTION, AND WEAR TESTING OF MICROSAMPLES OF POLYCRYSTALLINE SILICON

ABRAHAM P. LEE California Univ., Berkeley, CA, US, ALBERT P. PISANO California Univ., Berkeley, CA, US, and MARTIN G. LIM Xerox Palo Alto Research Center, Palo Alto, CA, US In Smart materials fabrication and materials for micro-electro-mechanical systems; Symposium Proceedings, San Francisco, CA, Apr. 28-30, 1992. A95-79980 Pittsburgh, PA Materials Research Society (MRS) Symposium Proceedings, Vol. 276) (ISSN 0272-9172) 1992 p. 67-78

Copyright

This paper gives an overview of the recent developments in impact, friction, and wear testing of polycrystalline silicon (polysilicon) based microelectromechanical structures. Impact-friction actuated micromechanisms form a new type of actuators. In this type of actuators, lateral resonant structures are retracted by electrostatic comb drives and are propelled forward toward the actuated micromechanism by elastic forces generated by folded beam flexures at frequencies ranging from 10 kHz to 20 kHz. This sequence generates normal impact and tangential friction contact between the two microstructures, raising wear concerns. Two sorts of impact test structures are introduced in this paper. One with a resonant micro impact bumper (MIB) striking a stationary impact wall anchored on

the substrate. Another is a testing of two MIBs driven to impact each other. Two types of impact actuators are also described, an impact actuated micro angular oscillator (MAO) and a polysilicon micro vibromotor. The vibromotor is a rotor driven by oblique impact on the rim by a converter pointer tip attached to a lateral resonator. Some initial results of impact wear testing as well as static and dynamic friction done by researchers in the field are also described in the paper. Finally, many areas where material scientists can contribute to this field are suggested. Author (Hemer)

A95-80633

LASER DEVICE FOR MEASURING A VESSEL'S SPEED

A. Z. ZURABYAN S.I. Vavilov State Optical Inst., St. Petersburg, Russia, V. K. KACHURIN S.I. Vavilov State Optical Inst., St. Petersburg, Russia, and V. A. YAKOVLEV S.I. Vavilov State Optical Inst., St. Petersburg, Russia Journal of Optical Technology (ISSN 1070-9762) vol. 61, no. 10 October 1994 p. 738-740

(HTN-95-60992) Copyright

This paper considers a new remote optical method for determining the speed of vessels (ships and seaplanes) with respect to the water surface. The error in measuring the speed is estimated, and a description is given of a prototype of the device that has been created. Results are presented of full-scale tests of the resulting laser device for measuring a vessel's speed. Author (Hemer)

A95-81690

EMPIRICAL CORRECTIONS OF THE RIGID ROTOR INTERACTION POTENTIAL OF H₂-H₂ IN THE ATTRACTIVE REGION: DIMER FEATURES IN THE FIR ABSORPTION SPECTRA

J. SCHAEFER Max-Planck-Institut fuer Astrophysik, Garching, Germany Astronomy and Astrophysics (ISSN 0004-6361) vol. 284, no. 3 April 1994 p. 1015-1025

(HTN-95-41943) Copyright

An improved rigid rotor potential of the H₂-H₂ system has been determined for reproducing measured quantities which are especially sensitive to the full non-spherical interaction in the attractive region. The leading potential terms have been fitted one after the other: the isotropic term $V(\text{sub } 000)$ has been adapted to two sets of measured second virial coefficients of para-H₂, at temperatures up to 200 K, the anisotropic term $V(\text{sub } 022)$ ($=V(\text{sub } 202)$) has been adapted to reproduce measured hyperfine transition frequencies of the ortho-H₂ - para-H₂ dimers observed in a molecular beam magnetic resonance experiment by Verberne (1979) and Verberne & Reuss (1980, 1981), and additional observed data for the ortho-H₂ - ortho-H₂ dimers have been used to adapt the quadrupole-quadrupole interaction term $V(\text{sub } 224)$ as well. Satisfying quantitative agreement has been achieved in all these fits. The sensitive (rather small) empirical improvements of the anisotropic potential parts provide now improved dimer binding energies. The possible dimer features in the far infrared (less than 30/cm) spectrum hydrogen gas at very low temperature are shown by discussing a few examples, under the assumption of dimerization equilibrium: normal-H₂ at 20 K, equilibrium-H₂ at 60 and 120 K, and a highly speculative model of cold interstellar molecular hydrogen at about 5 K. Author (Hemer)

N95-24879* Georgia Tech Research Inst., Atlanta, GA. Acoustics, Aerodynamics, and Advanced Vehicles Div.

EFFECTS OF CAVITY DIMENSIONS, BOUNDARY LAYER, AND TEMPERATURE ON CAVITY NOISE WITH EMPHASIS ON BENCHMARK DATA TO VALIDATE COMPUTATIONAL AEROACOUSTIC CODES

K. K. AHUJA and J. MENDOZA Apr. 1995 278 p

(Contract(s)/Grant(s): NAS1-19061; RTOP 505-59-52-01)

(NASA-CR-4653; NAS 1.26:4653) Avail: CASI HC A13/MF A03

This report documents the results of an experimental investigation on the response of a cavity to external flowfields. The primary objective of this research was to acquire benchmark of data on the effects of cavity length, width, depth, upstream boundary layer, and flow temperature on cavity noise. These data were to be used for

validation of computational aeroacoustic (CAA) codes on cavity noise. To achieve this objective, a systematic set of acoustic and flow measurements were made for subsonic turbulent flows approaching a cavity. These measurements were conducted in the research facilities of the Georgia Tech research institute. Two cavity models were designed, one for heated flow and another for unheated flow studies. Both models were designed such that the cavity length (L) could easily be varied while holding fixed the depth (D) and width (W) dimensions of the cavity. Depth and width blocks were manufactured so that these dimensions could be varied as well. A wall jet issuing from a rectangular nozzle was used to simulate flows over the cavity. Author

N95-25004# National Aerospace Lab., Tokyo (Japan). Control Systems Div.

PRELIMINARY EXPERIMENTS OF AN OPTICAL FIBER DISPLAY

KAORU WAKAIRO, AKIRA WATANABE, and HIROYASU KAWAHARA Jan. 1995 20 p In JAPANESE (ISSN 0389-4010)

(NAL-TR-1257) Avail: CASI HC A03/MF A01

At the National Aerospace Laboratory, the technological feasibility study of a dome screen display, which is able to give simulator pilots a very wide field of outside view, has been conducted. To provide this wide field of view, we designed a new display screen which itself could emit the light. We call this kind of screen 'a self-luminescence display.' For the self-luminescence display, we can use not only a CRT or a liquid crystal display, but also optical fibers. To investigate the applicability of plastic fibers for a self-luminescence display for use in flight simulators, we prepared a trial display. We made two displays of the same size, both of which were 900 mm in height and 1200 mm in length. The fiber's diameter is 0.75 mm, and the total number of fibers is 34,400 per display. We tested the validities of a fiber display and reached the following conclusions: (1) brightness is sufficient; (2) angle of view is limited and too narrow for practical use; and (3) picture quality is inferior. Author

N95-25978# International Centre for Theoretical Physics, Trieste (Italy).

DYNAMICS OF PHASE ORDERING OF NEMATICS IN A PORE

A. BHATTACHARYA, M. RAO, and A. CHAKRABARTI (Kansas State Univ., Manhattan, KS.) Jun. 1994 16 p (DE95-607662; IC-94/138) Avail: CASI HC A03/MF A01 (US Sales Only)

We study the kinetics of phase ordering of a nematic liquid crystal, modeled by a spin-rotor Hamiltonian, confined within a parallel piped pore. The dynamics of the rotor obeys the time-dependent Ginzburg-Landau equation. We study the generation and evolution of a variety of defect structures, and the growth of domains, with different anchoring conditions at the pore surface. Unlike in binary fluids, mere confinement with no anchoring field, does not result in slow dynamics. Homeotropic anchoring, however, leads to slow logarithmic growth. Interestingly, homogeneous anchoring dynamically generates wall defects, resulting in an Ising like structure factor at late times. DOE

N95-26015* National Aeronautics and Space Administration. Ames Research Center, Moffett Field, CA.

ANGULAR DISPLACEMENT MEASURING DEVICE Patent

H. LEE B. SEEGLER, inventor (to NASA) 11 Aug. 1992 7 p Filed 10 Oct. 1991

(NASA-CASE-ARC-11937-1; US-PATENT-5,137,353; US-PATENT-

APPL-SN-774490; US-PATENT-CLASS-356-152; US-PATENT-CLASS-356-34; US-PATENT-CLASS-250-225; INT-PATENT-CLASS-G01B-11/16) Avail: US Patent and Trademark Office

A system for measuring the angular displacement of a point of interest on a structure, such as aircraft model within a wind tunnel, includes a source of polarized light located at the point of interest. A remote detector arrangement detects the orientation of the plane of the polarized light received from the source and compares this orientation with the initial orientation to determine the amount or rate of angular displacement of the point of interest. The detector arrangement comprises a rotating polarizing filter and a dual filter and light detector unit. The latter unit comprises an inner aligned filter and photodetector assembly which is disposed relative to the periphery of the polarizer so as to receive polarized light passing the polarizing filter and an outer aligned filter and photodetector assembly which receives the polarized light directly, i.e., without passing through the polarizing filter. The purpose of the unit is to compensate for the effects of dust, fog and the like. A polarization preserving optical fiber conducts polarized light from a remote laser source to the point of interest.

Official Gazette of the U.S. Patent and Trademark Office

N95-26160* McDonnell-Douglas Aerospace, Long Beach, CA. **NOISE IMPACT OF ADVANCED HIGH LIFT SYSTEMS Final Report**

KEVIN R. ELMER and MAHENDRA C. JOSHI Mar. 1995 66 p

(Contract(s)/Grant(s): NAS1-20103; RTOP 538-03-15-01)

(NASA-CR-195028; NAS 1.26:195028; CRAD-9310-TR-0127) Avail: CASI HC A04/MF A01

The impact of advanced high lift systems on aircraft size, performance, direct operating cost and noise were evaluated for short-to-medium and medium-to-long range aircraft with high bypass ratio and very high bypass ratio engines. The benefit of advanced high lift systems in reducing noise was found to be less than 1 effective-perceived-noise decibel level (EPNdB) when the aircraft were sized to minimize takeoff gross weight. These aircraft did, however, have smaller wings and lower engine thrusts for the same mission than aircraft with conventional high lift systems. When the advanced high lift system was implemented without reducing wing size and simultaneously using lower flap angles that provide higher L/D at approach a cumulative noise reduction of as much as 4 EPNdB was obtained. Comparison of aircraft configurations that have similar approach speeds showed cumulative noise reduction of 2.6 EPNdB that is purely the result of incorporating advanced high lift system in the aircraft design. Author

N95-26187* National Aeronautics and Space Administration. Lewis Research Center, Cleveland, OH.

JET MIXER NOISE SUPPRESSOR USING ACOUSTIC FEEDBACK Patent

EDWARD J. RICE, inventor (to NASA) 28 Feb. 1995 12 p Filed 10 Feb. 1994 Division of US-Patent-5,325,661 (US Patent-Appl-SN-46256, filed 14 Apr. 1993)

(NASA-CASE-LEW-15170-2; US-PATENT-5,392,597; US-PATENT-APPL-SN-194654; US-PATENT-APPL-SN-046256; US-PATENT-CLASS-60-204; US-PATENT-CLASS-60-271; INT-PATENT-CLASS-F02C-7/00) Avail: US Patent and Trademark Office

The present invention generally relates to providing an improved jet mixer noise suppressor for high speed jets that rapidly mixes high speed air flow with a lower speed air flow, and more particularly, relates to an improved jet mixer noise suppressor that uses feedback of acoustic waves produced by the interaction of shear flow instability waves with an obstacle downstream of the jet nozzle. Official Gazette of the U.S. Patent and Trademark Office

17

SOCIAL SCIENCES

Includes social sciences (general); administration and management; documentation and information science; economics and cost analysis; law and political science; and urban technology and transportation.

N95-24202# Federal Aviation Administration, Washington, DC.
**FEDERAL AVIATION ADMINISTRATION PLAN FOR
 RESEARCH, ENGINEERING AND DEVELOPMENT, 1995**
 Dec. 1994 216 p

Avail: CASI HC A10/MF A03

The Federal Aviation Administration (FAA) manages and operates the National Airspace System (NAS), a significant national resource. However, the demands on this system are continuously growing, and changing technologies provide the opportunity to improve system effectiveness and efficiency. Today, 23 of the country's largest airports are plagued by more than 20,000 hours of delay per year, which is projected to grow to 40 major airports by 2000. Nationally, air traffic delays cost the economy an estimated \$6 billion in passenger delays and \$3 billion in airline operating costs in 1990. At current trends, these costs will increase 50 percent within 10 years. The FAA must accommodate the increasing demand on limited airport and airspace capacity, deal with crucial airport security issues, and cope with the unforeseen problems of an aging aircraft fleet. These requirements pose unprecedented challenges, which can only be met through a major investment in research, engineering and development (R&E&D). The projects in this Plan are those needed to bring the FAA's vision of the future system to reality in the context of a continuing top-level system engineering process. The Plan has enjoyed contributions from across the spectrum of scientific, operational, and user communities. Plan contents: capacity and air traffic management technology; communications, navigation, and surveillance; weather; airport technology; aircraft safety technology; system security technology; human factors and aviation medicine; environment and energy, and innovative/cooperative research. Derived from text

N95-24238# National Aeronautics and Space Administration, Washington, DC.

NASA VIDEO CATALOG

1995 69 p

(NASA-SP-7109(01); NAS 1.21:7109(01))

Avail: Issuing Activity (NASA Center for AeroSpace Information (NASA CASI) (301) 621-0390))

This issue of the NASA Video Catalog lists 463 video productions announced in the NASA STI Database. The videos listed in this catalog have been developed by the NASA Centers covering Shuttle mission press conferences; fly-bys of planets; aircraft design, testing and performance; environmental pollution; lunar and planetary exploration; and many other categories related to manned and unmanned space exploration. Each entry in the publication consists of a standard bibliographic citation accompanied by an abstract. The listing of the entries is arranged by STAR categories. A complete Table of contents describes the scope of each entry. Three indexes - title, report number, and accession number - are included. NASA guidelines, ordering information, and order form are located at the back of this issue. Derived from text

N95-24439# Native American Services, Huntsville, AL.
NLS FLIGHT SIMULATION LABORATORY (FSL)

DOCUMENTATION Final Report

1995 24 p

(Contract(s)/Grant(s): NAS8-37925)

(NASA-CR-196564; NAS 1.26:196564) Avail: CASI HC A03/MF A01

The Flight Simulation Laboratory (FSL) Electronic Documentation System design consists of modification and utilization of the MSFC Integrated Engineering System (IES), translation of the existing FSL documentation to an electronic format, and generation of new drawings to represent the Engine Flight Simulation Laboratory design and implementation. The intent of the electronic documentation is to provide ease of access, local print/plot capabilities, as well as the ability to correct and/or modify the stored data by network users who are authorized to access this information.

Derived from text

18

SPACE SCIENCES

Includes space sciences (general); astronomy; astrophysics; lunar and planetary exploration; solar physics; and space radiation.

A95-81583* National Aeronautics and Space Administration. Ames Research Center, Moffett Field, CA.

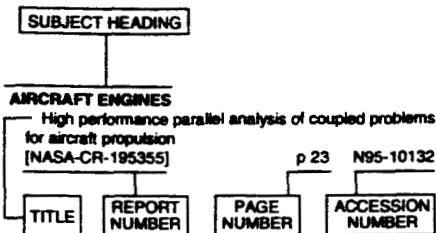
SOFIA: STRATOSPHERIC OBSERVATORY FOR INFRARED ASTRONOMY

E. F. ERICKSON NASA. Ames Research Center, Moffett Field, CA, US and J. A. DAVIDSON NASA. Ames Research Center, Moffett Field, CA, US Space astronomy; Symposium E2 and Meetings E10, E8 and E9 of the COSPAR, Plenary Meeting, 29th, Washington, DC, USA, Aug. 28 - Sep. 5, 1992. A95-81512 Advances in Space Research (ISSN 0273-1177) vol. 13, no. 12 December 1993 p. (12)549-(12)556

Copyright

SOFIA, (Stratospheric Observatory for Infrared Astronomy) is a planned 2.5 meter telescope to be installed in a Boeing 747 aircraft and operated at altitudes from 41,000 to 46,000 feet. It will permit routine measurement of infrared radiation inaccessible from the ground-based sites, and observation of astronomical objects and transient events from anywhere in the world. The concept is based on 18 years of experience with NASA's Kuiper Airborne Observatory (KAO), which SOFIA would replace. Author (Hemer)

Typical Subject Index Listing



The subject heading is a key to the subject content of the document. The title is used to provide a description of the subject matter. When the title is insufficiently descriptive of document content, a title extension is added, separated from the title by three hyphens. The accession number and the page number are included in each entry to assist the user in locating the abstract in the abstract section. If applicable, a report number is also included as an aid in identifying the document. Under any one subject heading, the accession numbers are arranged in sequence.

A

ABSORPTION SPECTRA

- Chemical change in the arctic vortex during AASE 2 [HTN-95-70947] p 352 A95-78012
- Latitude variations of stratospheric trace gases [HTN-95-70948] p 352 A95-78013
- Empirical corrections of the rigid rotor interaction potential of H₂-H₂ in the attractive region: Dimer features in the FIR absorption spectra [HTN-95-41943] p 361 A95-81690

ABUNDANCE

- Comparison of column abundances from three infrared spectrometers during AASE 2 [HTN-95-70946] p 352 A95-78011
- Chemical change in the arctic vortex during AASE 2 [HTN-95-70947] p 352 A95-78012
- Latitude variations of stratospheric trace gases [HTN-95-70948] p 352 A95-78013

ACOUSTIC EMISSION

- Emerging nondestructive inspection for aging aircraft [PB95-143053] p 328 N95-25401

ACOUSTIC PROPERTIES

- Effect of density gradients in confined supersonic shear layers, part 1 [NASA-CR-198029] p 348 N95-24412
- Effect of density gradients in confined supersonic shear layers. Part 2: 3-D modes [NASA-CR-198030] p 349 N95-24413

ACTION

- Actuating signals in adaptive control systems [IFTR-13/1994] p 361 N95-26330

ACTUATORS

- Fundamental mechanisms of aeroelastic control with control surface and strain actuation [BTN-95-EIX95242670746] p 327 A95-81101
- The 1994 Fiber Optic Sensors for Aerospace Technology (FOSAT) Workshop [NASA-CP-10166] p 337 N95-24207

- Actuating signals in adaptive control systems [IFTR-13/1994] p 361 N95-26330

ADAPTIVE CONTROL

- On-line learning nonlinear direct neurocontrollers for restructurable control systems [BTN-95-EIX95242670768] p 359 A95-81079
- Direct adaptive and neural control of wing-rock motion of slender delta wings [BTN-95-EIX95242670748] p 327 A95-81099
- Application of neural networks to unsteady aerodynamic control p 360 N95-25264
- Actuating signals in adaptive control systems [IFTR-13/1994] p 361 N95-26330

ADVECTION

- Fine-scale, poleward transport of tropical air during AASE 2 [HTN-95-70949] p 352 A95-78014

AEROACOUSTICS

- Effects of cavity dimensions, boundary layer, and temperature on cavity noise with emphasis on benchmark data to validate computational aeroacoustic codes [NASA-CR-4653] p 361 N95-24879
- Noise impact of advanced high lift systems [NASA-CR-195028] p 362 N95-26160
- Jet mixer noise suppressor using acoustic feedback [NASA-CASE-LEW-15170-2] p 362 N95-26187

AERODYNAMIC BALANCE

- Balances for the measurement of multiple components of force in flows of a millisecond duration p 350 N95-25400

AERODYNAMIC CHARACTERISTICS

- Performance of an aerodynamic yaw controller mounted on the space shuttle orbiter body flap at Mach 10 [NASA-TM-109179] p 330 N95-24397
- Experimental study of the effects of Reynolds number on high angle of attack aerodynamic characteristics of forebodies during rotary motion [NASA-CR-195033] p 330 N95-24443
- Exploratory flow visualization investigation of mast-mounted sights in presence of a rotor [NASA-TM-4634] p 330 N95-24566
- Low speed aerodynamic characteristics of delta wings with vortex flaps: 60 deg and 70 deg delta wings [NAL-TR-1245] p 331 N95-25105

AERODYNAMIC COEFFICIENTS

- NREL airfoil families for HAWTs [DE95-000267] p 357 N95-24882
- Measurements of longitudinal static aerodynamic coefficients by the cable mount system [NAL-TR-1226] p 331 N95-25761

AERODYNAMIC CONFIGURATIONS

- Aerodynamic shape optimization of wing and wing-body configurations using control theory [NASA-CR-198024] p 335 N95-25334
- Configuration and other differences between Black Hawk and Seahawk helicopters in military service in the USA and Australia [AR-008-386] p 336 N95-25935

AERODYNAMIC DRAG

- Dynamic stall control for advanced rotorcraft application [BTN-95-EIX95222650793] p 334 A95-79249
- Flow due to an oscillating sphere and an expression for unsteady drag on the sphere at finite Reynolds number [BTN-94-EIX95011441142] p 347 A95-81012
- Numerical and experimental study of drag characteristics of two-dimensional HLFC airfoils in high subsonic, high Reynolds number flow [NAL-TR-1244T] p 331 N95-24998
- Thrust measurements of a complete axisymmetric scramjet in an impulse facility p 339 N95-25395
- A theoretical and experimental investigation of the flow over supersonic leading edge wing/body configurations [DRA-TM-AERO-PROP-41] p 331 N95-25649
- Aerodynamic characteristics of the orbital reentry vehicle experimental probe fins in a supersonic flow [NAL-TR-1232] p 342 N95-25664

AERODYNAMIC FORCES

- Flow structure in the lee of an inclined 6:1 prolate spheroid [BTN-94-EIX95011441127] p 348 A95-81027

AERODYNAMIC HEATING

- Viscoplastic response of structures for intense local heating [HTN-95-41540] p 346 A95-77921
- Heat transfer measurements in small scale wind tunnels [AD-A288689] p 341 N95-26053

AERODYNAMIC LOADS

- Integrated development of the equations of motion for elastic hypersonic flight vehicles [BTN-95-EIX95242670755] p 327 A95-81092
- Dynamics and control of a tethered flight vehicle [BTN-95-EIX95242670754] p 342 A95-81093
- Balances for the measurement of multiple components of force in flows of a millisecond duration p 350 N95-25400

AERODYNAMIC NOISE

- Effects of cavity dimensions, boundary layer, and temperature on cavity noise with emphasis on benchmark data to validate computational aeroacoustic codes [NASA-CR-4653] p 361 N95-24879
- Noise impact of advanced high lift systems [NASA-CR-195028] p 362 N95-26160

AERODYNAMIC STABILITY

- Rotorcraft handling qualities in turbulence [BTN-95-EIX95242670750] p 334 A95-81097
- Direct adaptive and neural control of wing-rock motion of slender delta wings [BTN-95-EIX95242670748] p 327 A95-81099

AERODYNAMIC STALLING

- Dynamic stall control for advanced rotorcraft application [BTN-95-EIX95222650793] p 334 A95-79249

AERODYNAMICS

- Experimental investigation of the flow around a circular cylinder: influence of aspect ratio [BTN-94-EIX95011441120] p 347 A95-80044
- Determination of plotting feedback structures for an altitude tracking task [BTN-95-EIX95242670770] p 327 A95-81077
- Aerodynamic parameters of crop canopies estimated with a center-of-pressure technique [HTN-95-41901] p 356 A95-81648
- Aeronautical engineering: A continuing bibliography with indexes (supplement 316) [NASA-SP-7037(316)] p 328 N95-24465
- Aerodynamic parameter estimation via Fourier modulating function techniques [NASA-CR-4654] p 335 N95-24630
- Using digital filtering techniques as an aid in wind turbine data analysis [DE94-011862] p 357 N95-24853
- Aeronautical engineering: A continuing bibliography with indexes (supplement 317) [NASA-SP-7037(317)] p 328 N95-25798
- Cumulative reports and publications through December 31, 1994 [NASA-CR-195043] p 361 N95-26085

AEROELASTICITY

- Multilevel decomposition procedure for efficient design optimization of helicopter rotor blades [BTN-95-EIX95222650784] p 334 A95-79240
- Fundamental mechanisms of aeroelastic control with control surface and strain actuation [BTN-95-EIX95242670746] p 327 A95-81101

AERONAUTICAL ENGINEERING

- Aeronautical engineering: A continuing bibliography with indexes (supplement 316) [NASA-SP-7037(316)] p 328 N95-24465
- JPRS report: Science and technology. Central Eurasia [JPRS-UST-94-027] p 349 N95-24470
- JPRS report: Science and technology. Central Eurasia [JPRS-UST-94-018] p 349 N95-24472
- Aeronautical engineering: A continuing bibliography with indexes (supplement 317) [NASA-SP-7037(317)] p 328 N95-25798

AERONAUTICS

- NASA video catalog [NASA-SP-7109(01)] p 363 N95-24238
- Aeronautical engineering: A continuing bibliography with indexes (supplement 316) [NASA-SP-7037(316)] p 328 N95-24465

AEROSERVOELASTICITY

Aeroservoelastic aspects of wing/control surface platform shape optimization
[BTN-95-EIX9522650795] p 340 A95-79251

AEROSOLS

Effects on stratospheric ozone from high-speed civil transport: Sensitivity to stratospheric aerosol loading
[HTN-95-91842] p 354 A95-80830

High-speed civil transport impact: Role of sulfate, nitric acid trihydrate, and ice aerosols studied with a two-dimensional model including aerosol physics
[HTN-95-91843] p 354 A95-80831

Potential effects on ozone of future supersonic aircraft/2D simulation
[HTN-95-51282] p 356 A95-80867

Impact on ozone of high-speed stratospheric aircraft: Effects of the emission scenario
[HTN-95-51283] p 356 A95-80868

The atmospheric effects of stratospheric aircraft: A fourth program report
[NASA-RP-1359] p 357 N95-24274

AEROSPACE ENGINEERING

NASA-UVA light aerospace alloy and structures technology program (LA2ST)
[NASA-CR-198041] p 343 N95-24220

NASA video catalog
[NASA-SP-7109(01)] p 363 N95-24238

AEROSPACE PLANES

Measurements of longitudinal static aerodynamic coefficients by the cable mount system
[NAL-TR-1226] p 331 N95-25761

AEROSPACE SCIENCES

NASA video catalog
[NASA-SP-7109(01)] p 363 N95-24238

AEROTHERMODYNAMICS

DSMC calculations for 70-deg blunt cone at 3.2 km/s in nitrogen
[NASA-TM-109181] p 348 N95-24396

AGING (MATERIALS)

Proceedings of the 2d USAF Aging Aircraft Conference
[AD-A288217] p 336 N95-25578

AH-64 HELICOPTER

Identification and simulation evaluation of a combat helicopter in hover
[BTN-95-EIX95242670749] p 335 A95-81098

AIR LAUNCHING

SR-71 may launch targets for missile defense tests
[HTN-95-91872] p 335 A95-81974

AIR MASSES

Fine-scale, poleward transport of tropical air during AASE 2
[HTN-95-70949] p 352 A95-78014

AIR NAVIGATION

Describing an attitude p 342 A95-80409
Ideal proportional navigation p 342 A95-81374
Federal Aviation Administration plan for research, engineering and development, 1995 p 363 N95-24202

AIR POLLUTION

Vertical transport rates in the stratosphere in 1993 from observations of CO₂, N₂O, and CH₄
[HTN-95-70941] p 351 A95-78006

An analysis of aircraft exhaust plumes form accidental encounters
[HTN-95-70943] p 351 A95-78008

Meridional distributions of NO(X), NO(Y), and other species in the lower stratosphere and upper troposphere during AASE 2
[HTN-95-70944] p 352 A95-78009

Comparison of column abundances from three infrared spectrometers during AASE 2
[HTN-95-70946] p 352 A95-78011

Chemical change in the arctic vortex during AASE 2
[HTN-95-70947] p 352 A95-78012

Latitude variations of stratospheric trace gases
[HTN-95-70948] p 352 A95-78013

Fine-scale, poleward transport of tropical air during AASE 2
[HTN-95-70949] p 352 A95-78014

North Atlantic air traffic within the lower stratosphere: Cruising times and corresponding emissions
[HTN-95-91841] p 354 A95-80829

Chemical composition and photochemical reactivity of exhaust from aircraft turbine engines
[HTN-95-51277] p 356 A95-80862

Potential effects on ozone of future supersonic aircraft/2D simulation
[HTN-95-51282] p 356 A95-80867

Impact on ozone of high-speed stratospheric aircraft: Effects of the emission scenario
[HTN-95-51283] p 356 A95-80868

The atmospheric effects of stratospheric aircraft: A fourth program report
[NASA-RP-1359] p 357 N95-24274

Nitrogen oxide emissions and their control from uninstalled aircraft engines in enclosed test cells: Joint report to Congress on the Environmental Protection Agency - Department of Transportation study
[PB95-166237] p 358 N95-26005

AIR QUALITY

Nitrogen oxide emissions and their control from uninstalled aircraft engines in enclosed test cells: Joint report to Congress on the Environmental Protection Agency - Department of Transportation study
[PB95-166237] p 358 N95-26005

AIR SAMPLING

Vertical transport rates in the stratosphere in 1993 from observations of CO₂, N₂O, and CH₄
[HTN-95-70941] p 351 A95-78006

An analysis of aircraft exhaust plumes form accidental encounters
[HTN-95-70943] p 351 A95-78008

Meridional distributions of NO(X), NO(Y), and other species in the lower stratosphere and upper troposphere during AASE 2
[HTN-95-70944] p 352 A95-78009

Comparison of column abundances from three infrared spectrometers during AASE 2
[HTN-95-70946] p 352 A95-78011

Chemical change in the arctic vortex during AASE 2
[HTN-95-70947] p 352 A95-78012

Latitude variations of stratospheric trace gases
[HTN-95-70948] p 352 A95-78013

Fine-scale, poleward transport of tropical air during AASE 2
[HTN-95-70949] p 352 A95-78014

Chemical composition and photochemical reactivity of exhaust from aircraft turbine engines
[HTN-95-51277] p 356 A95-80862

AIR TO AIR MISSILES

Ideal proportional navigation p 342 A95-81374

AIR TRAFFIC

North Atlantic air traffic within the lower stratosphere: Cruising times and corresponding emissions
[HTN-95-91841] p 354 A95-80829

Aviation system capacity improvements through technology
[NASA-TM-109165] p 333 N95-24633

AIR TRAFFIC CONTROL

Federal Aviation Administration plan for research, engineering and development, 1995 p 363 N95-24202

Aviation system capacity improvements through technology
[NASA-TM-109165] p 333 N95-24633

AIR TRANSPORTATION

Federal Aviation Administration plan for research, engineering and development, 1995 p 363 N95-24202

Aviation system capacity improvements through technology
[NASA-TM-109165] p 333 N95-24633

AIRBORNE RADAR

Dynamic imaging and RCS measurements of aircraft
[BTN-95-EIX95202637582] p 347 A95-78576

AIRBORNE/SPACEBORNE COMPUTERS

Guidance and control, 1993: Annual Rocky Mountain Guidance and Control Conference, 16th, Keystone, CO, Feb. 6-10, 1993
[ISBN-0-87703-365-X] p 341 A95-80389

AIRCRAFT ACCIDENT INVESTIGATION

Aircraft accident report: Impact with blast fence upon landing rollout Action Air Charters flight 990 Piper PA-31-350, N990RA, Stratford, Connecticut, 27 April 1994
[PB94-910410] p 333 N95-24206

AIRCRAFT ACCIDENTS

Real-time decision aiding: Aircraft guidance for wind shear avoidance
[BTN-95-EIX95202637575] p 332 A95-78583

Aircraft accident report: Impact with blast fence upon landing rollout Action Air Charters flight 990 Piper PA-31-350, N990RA, Stratford, Connecticut, 27 April 1994
[PB94-910410] p 333 N95-24206

AIRCRAFT APPROACH SPACING

Characterizing the wake vortex signature for an active line of sight remote sensor
[NASA-CR-197697] p 333 N95-24391

AIRCRAFT CONFIGURATIONS

Aerodynamics model for a generic ASTOVL lift-fan aircraft
[NASA-TM-110347] p 332 N95-26302

AIRCRAFT CONSTRUCTION MATERIALS

NASA-UVA light aerospace alloy and structures technology program supplement: Aluminum-based materials for high speed aircraft
[NASA-CR-46445] p 343 N95-24878

Jet engine applications for materials with nanometer-scale dimensions p 345 N95-26131

AIRCRAFT CONTROL

Determination of piloting feedback structures for an altitude tracking task
[BTN-95-EIX95242670770] p 327 A95-81077

On-line learning nonlinear direct neurocontrollers for restructurable control systems
[BTN-95-EIX95242670768] p 359 A95-81079

Robust dynamic inversion for control of highly maneuverable aircraft
[BTN-95-EIX95242670747] p 359 A95-81100

Application of neural networks to unsteady aerodynamic control p 360 N95-25264

AIRCRAFT DESIGN

Aeroservoelastic aspects of wing/control surface platform shape optimization
[BTN-95-EIX9522650795] p 340 A95-79251

NASA video catalog
[NASA-SP-7109(01)] p 363 N95-24238

Advanced subsonic airplane design and economic studies
[NASA-CR-195443] p 338 N95-24304

A crew-centered flight deck design philosophy for High-Speed Civil Transport (HSCT) aircraft
[NASA-TM-109171] p 335 N95-24582

Geometric analysis of wing sections
[NASA-TM-110346] p 335 N95-24629

Aerodynamic shape optimization of wing and wing-body configurations using control theory
[NASA-CR-198024] p 335 N95-25334

The coupling of fluids, dynamics, and controls on advanced architecture computers
[NASA-CR-197727] p 360 N95-25797

A quiet STOL Research Aircraft Development program
[NAL-TR-1223] p 336 N95-25862

Noise impact of advanced high lift systems
[NASA-CR-195028] p 362 N95-26160

Aerodynamics model for a generic ASTOVL lift-fan aircraft
[NASA-TM-110347] p 332 N95-26302

AIRCRAFT DETECTION

Visual contrast detection thresholds for aircraft contrails
[AD-A288618] p 328 N95-25607

Orientation determination of aircraft using visual 3D matching and radar. Case study 2
[PB95-165791] p 350 N95-25749

AIRCRAFT ENGINES

Theoretical and experimental studies of fretting-initiated fatigue failure of aeroengine compressor discs
[BTN-94-EIX94421372285] p 343 A95-78467

Nitrous oxide and methane emissions from aero engines
[HTN-95-21363] p 353 A95-78678

Impact of present aircraft emissions of nitrogen oxides on tropospheric ozone and climate forcing
[HTN-95-21364] p 353 A95-78679

The effect of altitude conditions on the particle emissions of a J85-GE-5L turbojet engine
[NASA-TM-106669] p 339 N95-24561

Bird ingestion into large turbofan engines
[DOT/FAA/CT-93/14] p 333 N95-24631

Nitrogen oxide emissions and their control from uninstalled aircraft engines in enclosed test cells: Joint report to Congress on the Environmental Protection Agency - Department of Transportation study
[PB95-166237] p 358 N95-26005

Thermal Barrier Coating Workshop
[NASA-CP-10170] p 344 N95-26119

Natural barrier coatings for aircraft engines: History and directions
[NASA-CP-10170] p 344 N95-26121

Thermal barrier coatings issues in advanced land-based gas turbines
[NASA-CP-10170] p 344 N95-26122

PVD TBC experience on GE aircraft engines
[NASA-CP-10170] p 345 N95-26126

Thermal barrier coating life modeling in aircraft gas turbine engines
[NASA-CP-10170] p 346 N95-26140

AIRCRAFT EQUIPMENT

Analysis of warping effects on the static and dynamic response of a seat-type structure
[NAR-94-12] p 348 N95-24211

AIRCRAFT GUIDANCE

Real-time decision aiding: Aircraft guidance for wind shear avoidance
[BTN-95-EIX95202637575] p 332 A95-78583

How to fly an aircraft with control theory and spines
[NASA-CR-195067] p 360 N95-25805

AIRCRAFT HAZARDS

Identification of aviation weather hazards based on the integration of radar and lightning data
[HTN-95-51323] p 356 A95-80908

Characterizing the wake vortex signature for an active line of sight remote sensor
[NASA-CR-197697] p 333 N95-24391

Consistent approach to describing aircraft HIRF protection
[NASA-CR-195067] p 334 N95-25341

AIRCRAFT INSTRUMENTS

An intercomparison of aircraft instrumentation for tropospheric measurements of sulfur dioxide
[HTN-95-91855] p 354 A95-80843

An intercomparison of aircraft instrumentation for tropospheric measurements of carbonyl sulfide, hydrogen sulfide, and carbon disulfide
[HTN-95-91856] p 355 A95-80844

An intercomparison of instrumentation for tropospheric measurements of dimethyl sulfide: Aircraft results for concentrations at the parts-per-trillion level
[HTN-95-91857] p 355 A95-80845

AIRCRAFT LANDING

Aircraft accident report: Impact with blast fence upon landing rollout Action Air Charters flight 990 Piper PA-31-350, N990RA, Stratford, Connecticut, 27 April 1994
[PB94-910410] p 333 N95-24206

Characterizing the wake vortex signature for an active line of sight remote sensor
[NASA-CR-197697] p 333 N95-24391

AIRCRAFT MAINTENANCE

An overview of Health and Usage Monitoring Systems (HUMS) for military helicopters
[DSTO-TR-0061] p 327 N95-24200

Helicopter life substantiation: Review of some USA and UK initiatives
[DSTO-TR-0062] p 328 N95-24201

Estimate of probability of crack detection from service difficulty report data
[PB95-149381] p 328 N95-24295

Emerging nondestructive inspection for aging aircraft
[PB95-143053] p 328 N95-25401

Proceedings of the 2d USAF Aging Aircraft Conference
[AD-A288217] p 336 N95-25578

AIRCRAFT MANEUVERS

Load alleviation maneuvers for a launch vehicle
p 342 A95-81360

AIRCRAFT MODELS

Aspect estimation of an aircraft using library model silhouettes
[PB95-141834] p 360 N95-25894

AIRCRAFT NOISE

Aviation system capacity improvements through technology
[NASA-TM-109165] p 333 N95-24633

AIRCRAFT PARTS

JPRS report: Science and technology, Central Eurasia [JPRS-UST-95-011] p 335 N95-24541

AIRCRAFT PILOTS

Determination of piloting feedback structures for an altitude tracking task
[BTN-95-EIX95242670770] p 327 A95-81077

Visual contrast detection thresholds for aircraft contrails
[AD-A288618] p 328 N95-25607

AIRCRAFT PRODUCTION

Report to Congressional Committees. Tactical Aircraft: Concurrence in development and production of F-22 aircraft should be reduced
[GAO/NSAID-95-59] p 336 N95-26338

AIRCRAFT SAFETY

Real-time decision aiding: Aircraft guidance for wind shear avoidance
[BTN-95-EIX95202637575] p 332 A95-78583

Federal Aviation Administration plan for research, engineering and development, 1995
p 363 N95-24202

Development of an intervention program to encourage shoulder harness use and aircraft retrofit in general aviation aircraft, phases 1 and 2
[DOT/FAA/AM-95/2] p 333 N95-24384

Quantity-distance requirements for earth-bermed aircraft shelters
[AD-A279692] p 341 N95-24424

Bird ingestion into large turbofan engines
[DOT/FAA/CT-93/14] p 333 N95-24631

AIRCRAFT STABILITY

Rotorcraft handling qualities in turbulence
[BTN-95-EIX95242670750] p 334 A95-81097

Identification and simulation evaluation of a combat helicopter in hover
[BTN-95-EIX95242670749] p 335 A95-81098

AIRCRAFT STRUCTURES

Viscoplastic response of structures for intense local heating
[HTN-95-41540] p 346 A95-77921

NASA-UVA light aerospace alloy and structures technology program (LA2ST)
[NASA-CR-198041] p 343 N95-24220

JPRS report: Science and technology, Central Eurasia [JPRS-UST-95-011] p 335 N95-24541

Proceedings of the 2d USAF Aging Aircraft Conference
[AD-A288217] p 336 N95-25578

Design and evaluation of a foam-filled hat-stiffened panel concept for aircraft primary structural applications
[NASA-TM-109175] p 346 N95-26251

AIRCRAFT WAKES

Three-dimensional interaction of wake/boundary-layer and vortex/boundary-layer data report
[CUE/A-AEREO/TR-23] p 329 N95-24210

Characterizing the wake vortex signature for an active line of sight remote sensor
[NASA-CR-197697] p 333 N95-24391

AIRFOIL PROFILES

Geometric analysis of wing sections
[NASA-TM-110346] p 335 N95-24629

AIRFOILS

On the role of the outer region in the turbulent-boundary-layer bursting process
[BTN-94-EIX95011441078] p 348 A95-81056

NREL airfoil families for HAWTs
[DE95-000267] p 357 N95-24882

Wind technology development: Large and small turbines
[DE95-000286] p 358 N95-26090

Thermal barrier coatings for aircraft engines: History and directions
p 344 N95-26121

AIRFRAMES

Advanced subsonic airplane design and economic studies
[NASA-CR-195443] p 338 N95-24304

AIRPORT SECURITY

Federal Aviation Administration plan for research, engineering and development, 1995
p 363 N95-24202

AIRPORTS

Federal Aviation Administration plan for research, engineering and development, 1995
p 363 N95-24202

Aviation system capacity improvements through technology
[NASA-TM-109165] p 333 N95-24633

AIRSHIPS

Long endurance stratospheric solar powered airship
[PB95-178729] p 336 N95-26009

AIRSPACE

Aviation system capacity improvements through technology
[NASA-TM-109165] p 333 N95-24633

ALGORITHMS

On-line learning nonlinear direct neurocontrollers for restructurable control systems
[BTN-95-EIX95242670768] p 359 A95-81079

Aerodynamic parameter estimation via Fourier modulating function techniques
[NASA-CR-4654] p 335 N95-24630

ALTITUDE TESTS

The effect of altitude conditions on the particle emissions of a J85-GE-5L turbojet engine
[NASA-TM-106869] p 339 N95-24561

ALUMINUM ALLOYS

NASA-UVA light aerospace alloy and structures technology program supplement: Aluminum-based materials for high speed aircraft
[NASA-CR-4645] p 343 N95-24878

AMBIENT TEMPERATURE

Similarity rule for jet-temperature effects on transonic base pressure
[BTN-95-EIX95222650791] p 329 A95-79247

ANGLE OF ATTACK

Flow structure in the lee of an inclined 6:1 prolate spheroid
[BTN-94-EIX95011441127] p 348 A95-81027

Robust dynamic inversion for control of highly maneuverable aircraft
[BTN-95-EIX95242670747] p 359 A95-81100

Experimental study of the effects of Reynolds number on high angle of attack aerodynamic characteristics of forebodies during rotary motion
[NASA-CR-195033] p 330 N95-24443

ANGULAR CORRELATION

Angular displacement measuring device
[NASA-CASE-ARC-11937-1] p 362 N95-26015

ANTIMISSILE DEFENSE

SR-71 may launch targets for missile defense tests
[HTN-95-91872] p 335 A95-81974

APPLICATIONS OF MATHEMATICS

Cumulative reports and publications through December 31, 1994
[NASA-CR-195043] p 361 N95-26085

APPLICATIONS PROGRAMS (COMPUTERS)

Thermohydrodynamic analysis of cryogenic liquid turbulent flow fluid film bearings, phase 2
[NASA-CR-197412] p 349 N95-24461

APPROACH INDICATORS

Flight reference display for powered-lift STOL aircraft
[NAL-TR-1251] p 337 N95-25005

ARCHITECTURE (COMPUTERS)

A new guidance and flight control system for the DELTA 2 launch vehicle --- Abstract only
p 342 A95-80427

ARCTIC REGIONS

Analysis of the physical state of one Arctic polar stratospheric cloud based on observations
[HTN-95-70917] p 351 A95-77982

Comparison of column abundances from three infrared spectrometers during AASE 2
[HTN-95-70946] p 352 A95-78011

Chemical change in the arctic vortex during AASE 2
[HTN-95-70947] p 352 A95-78012

ARTIFICIAL INTELLIGENCE

Real-time decision aiding: Aircraft guidance for wind shear avoidance
[BTN-95-EIX95202637575] p 332 A95-78583

ASPECT RATIO

Experimental investigation of the flow around a circular cylinder: Influence of aspect ratio
[BTN-94-EIX95011441120] p 347 A95-80044

ASTRONAUTICS

NASA video catalog
[NASA-SP-7109(01)] p 363 N95-24238

ASTRONOMY

NASA video catalog
[NASA-SP-7109(01)] p 363 N95-24238

ATLANTIC OCEAN

North Atlantic air traffic within the lower stratosphere: Cruising times and corresponding emissions
[HTN-95-91841] p 354 A95-80829

ATMOSPHERIC BOUNDARY LAYER

Comparison of wind profiler and aircraft wind measurements at Chebogue Point, Nova Scotia
[HTN-95-41833] p 353 A95-80559

ATMOSPHERIC CHEMISTRY

The distribution of hydrogen, nitrogen, and chlorine radicals in the lower stratosphere: Implications for changes in O₃ due to emission of NO(y) from supersonic aircraft
[HTN-95-70935] p 351 A95-78000

Vertical transport rates in the stratosphere in 1993 from observations of CO₂, N₂O, and CH₄
[HTN-95-70941] p 351 A95-78006

Meridional distributions of NO(X), NO(Y), and other species in the lower stratosphere and upper troposphere during AASE 2
[HTN-95-70944] p 352 A95-78009

Comparison of column abundances from three infrared spectrometers during AASE 2
[HTN-95-70946] p 352 A95-78011

Chemical change in the arctic vortex during AASE 2
[HTN-95-70947] p 352 A95-78012

Latitude variations of stratospheric trace gases
[HTN-95-70948] p 352 A95-78013

Fine-scale, poleward transport of tropical air during AASE 2
[HTN-95-70949] p 352 A95-78014

High-speed civil transport impact: Role of sulfate, nitric acid trihydrate, and ice aerosols studied with a two-dimensional model including aerosol physics
[HTN-95-91843] p 354 A95-80831

ATMOSPHERIC CIRCULATION

Meridional distributions of NO(X), NO(Y), and other species in the lower stratosphere and upper troposphere during AASE 2
[HTN-95-70944] p 352 A95-78009

Chemical change in the arctic vortex during AASE 2
[HTN-95-70947] p 352 A95-78012

Fine-scale, poleward transport of tropical air during AASE 2
[HTN-95-70949] p 352 A95-78014

Tracer transport for realistic aircraft emission scenarios calculated using a three-dimensional model
[HTN-95-41799] p 353 A95-80525

ATMOSPHERIC COMPOSITION

Effects on stratospheric ozone from high-speed civil transport: Sensitivity to stratospheric aerosol loading
[HTN-95-91842] p 354 A95-80830

An intercomparison of aircraft instrumentation for tropospheric measurements of sulfur dioxide
[HTN-95-91855] p 354 A95-80843

An intercomparison of aircraft instrumentation for tropospheric measurements of carbonyl sulfide, hydrogen sulfide, and carbon disulfide
[HTN-95-91856] p 355 A95-80844

An intercomparison of instrumentation for tropospheric measurements of dimethyl sulfide: Aircraft results for concentrations at the parts-per-trillion level
[HTN-95-91857] p 355 A95-80845

Preliminary analysis of University of North Dakota aircraft data from the FIRE Cirrus IFO-2
[NASA-CR-198038] p 357 N95-24219

ATMOSPHERIC CONDUCTIVITY

Fine-scale, poleward transport of tropical air during AASE 2
[HTN-95-70949] p 352 A95-78014

ATMOSPHERIC EFFECTS

- The distribution of hydrogen, nitrogen, and chlorine radicals in the lower stratosphere: implications for changes in O₃ due to emission of NO(y) from supersonic aircraft [HTN-95-70935] p 351 A95-78000
- Dynamics of aircraft exhaust plumes in the jet-regime [HTN-95-51275] p 355 A95-80860

ATMOSPHERIC MODELS

- Sensitivity of supersonic aircraft modelling studies to HNO₃ photolysis rate [HTN-95-11475] p 353 A95-79453
- Tracer transport for realistic aircraft emission scenarios calculated using a three-dimensional model [HTN-95-41799] p 353 A95-80525
- Effects on stratospheric ozone from high-speed civil transport: Sensitivity to stratospheric aerosol loading [HTN-95-91842] p 354 A95-80830
- Potential effects on ozone of future supersonic aircraft/2D simulation [HTN-95-51282] p 356 A95-80867
- Impact on ozone of high-speed stratospheric aircraft: Effects of the emission scenario [HTN-95-51283] p 356 A95-80868

ATMOSPHERIC PRESSURE

- Comparison of column abundances from three infrared spectrometers during AASE 2 [HTN-95-70946] p 352 A95-78011
- Aerodynamic parameters of crop canopies estimated with a center-of-pressure technique [HTN-95-41901] p 356 A95-81648

ATMOSPHERIC SOUNDING

- Comparison of wind profiler and aircraft wind measurements at Chebogue Point, Nova Scotia [HTN-95-41833] p 353 A95-80559

ATMOSPHERIC TEMPERATURE

- Comparison of column abundances from three infrared spectrometers during AASE 2 [HTN-95-70946] p 352 A95-78011

ATMOSPHERIC TURBULENCE

- Comparison of wind profiler and aircraft wind measurements at Chebogue Point, Nova Scotia [HTN-95-41833] p 353 A95-80559
- Aerodynamic parameters of crop canopies estimated with a center-of-pressure technique [HTN-95-41901] p 356 A95-81648

ATTITUDE (INCLINATION)

- Describing an attitude p 342 A95-80409

ATTITUDE CONTROL

- The Cassini spacecraft: Object oriented flight control software p 359 A95-80405

ATTITUDE INDICATORS

- Flight reference display for powered-lift STOL aircraft [NAL-TR-1251] p 337 N95-25005

AUTOMATIC CONTROL

- Partial camera automation in a simulated Unmanned Air Vehicle [AD-A288786] p 337 N95-26190

AUTOMATIC PILOTS

- High-performance, robust, bank-to-turn missile autopilot design [BTN-95-EIX95242670751] p 336 A95-81096
- Load alleviation maneuvers for a launch vehicle p 342 A95-81360

AUTONOMOUS NAVIGATION

- Interfacing a digital compass to a remote-controlled helicopter [PB95-164927] p 340 N95-24260

AVIONICS

- Assessment of avionics technology in European aerospace organizations [NASA-CR-189201] p 337 N95-24624
- Preload release mechanism [NASA-CASE-MSC-22327-1] p 350 N95-25592
- Configuration and other differences between Black Hawk and Seahawk helicopters in military service in the USA and Australia [AR-008-386] p 336 N95-25935

AXIAL STRESS

- Thrust measurement in a 2-D scramjet nozzle p 339 N95-25397

B**BALLOON-BORNE INSTRUMENTS**

- Application of fuzzy logic to optimize placement of an acquisition, tracking, and pointing experiment p 341 A95-80390

BASE FLOW

- Study of subsonic base cavity flowfield structure using particle image velocimetry [BTN-95-EIX95222650781] p 327 A95-79237

BASE PRESSURE

- Similarity rule for jet-temperature effects on transonic base pressure [BTN-95-EIX95222650791] p 329 A95-79247

BENDING

- Modal characteristics of rotors using a conical shaft finite element [BTN-94-EIX94401359745] p 346 A95-77379
- Load alleviation maneuvers for a launch vehicle p 342 A95-81360

BENDING FATIGUE

- Thrust measurement in a 2-D scramjet nozzle p 339 N95-25397

BIAS

- An intercomparison of instrumentation for tropospheric measurements of dimethyl sulfide: Aircraft results for concentrations at the parts-per-trillion level [HTN-95-91857] p 355 A95-80845

BIBLIOGRAPHIES

- NASA video catalog [NASA-SP-7109(01)] p 363 N95-24238
- Aeronautical engineering: A continuing bibliography with indexes (supplement 316) [NASA-SP-7037(316)] p 328 N95-24465
- Aeronautical engineering: A continuing bibliography with indexes (supplement 317) [NASA-SP-7037(317)] p 328 N95-25798
- Cumulative reports and publications through December 31, 1994 [NASA-CR-195043] p 361 N95-26085

BIOTECHNOLOGY

- JPRS Report: Science and technology. Central Eurasia [JPRS-UST-94-032] p 350 N95-24759

BIRD-AIRCRAFT COLLISIONS

- Bird ingestion into large turbofan engines [DOT/FAA/CT-93/14] p 333 N95-24631

BIRDS

- Bird ingestion into large turbofan engines [DOT/FAA/CT-93/14] p 333 N95-24631

BLADE TIPS

- Unsteady lift on a swept blade tip [BTN-94-EIX95011441154] p 329 A95-80030

BLADE-VORTEX INTERACTION

- Unsteady lift on a swept blade tip [BTN-94-EIX95011441154] p 329 A95-80030

BLAST LOADS

- Quantity-distance requirements for earth-bermed aircraft shelters [AD-A279692] p 341 N95-24424

BLUNT BODIES

- DSMC calculations for 70-deg blunted cone at 3.2 km/s in nitrogen [NASA-TM-109181] p 348 N95-24396

BODY-WING CONFIGURATIONS

- Aerodynamic shape optimization of wing and wing-body configurations using control theory [NASA-CR-198024] p 335 N95-25334
- A theoretical and experimental investigation of the flow over supersonic leading edge wing/body configurations [DRA-TM-AERO-PROP-41] p 331 N95-25649

BOEING 747 AIRCRAFT

- Dynamics of aircraft exhaust plumes in the jet-regime [HTN-95-51275] p 355 A95-80860
- Modeling of aircraft exhaust emissions and infrared spectra for remote measurement of nitrogen oxides [HTN-95-51276] p 355 A95-80861
- SOFIA: Stratospheric Observatory for Infrared Astronomy p 363 A95-81583

BOUNDARY LAYER CONTROL

- Flow structure in the lee of an inclined 6:1 prolate spheroid [BTN-94-EIX95011441127] p 348 A95-81027

BOUNDARY LAYER EQUATIONS

- Supersonic quiet-tunnel development for laminar-turbulent transition research [NASA-CR-198040] p 340 N95-24302

BOUNDARY LAYER SEPARATION

- Experimental study of flow separation on an oscillating flap at Mach 2.4 [BTN-95-EIX95222650792] p 329 A95-79248

BOUNDARY LAYER TRANSITION

- Supersonic quiet-tunnel development for laminar-turbulent transition research [NASA-CR-198040] p 340 N95-24302

BOUNDARY LAYERS

- Three-dimensional interaction of wake/boundary-layer and vortex/boundary-layer data report [CUED/A-AERO/TR-23] p 329 N95-24210

BUCKLING

- Design and evaluation of a foam-filled hat-stiffened panel concept for aircraft primary structural applications [NASA-TM-109175] p 346 N95-26251

C**C-135 AIRCRAFT**

- Dynamic imaging and RCS measurements of aircraft [BTN-95-EIX95202637582] p 347 A95-78576

CABLES (ROPES)

- Measurements of longitudinal static aerodynamic coefficients by the cable mount system [NAL-TR-1226] p 331 N95-25761

CALCULUS OF VARIATIONS

- A brief survey of constrained mechanics and variational problems in terms of differential forms p 360 N95-25803

CAMERAS

- Partial camera automation in a simulated Unmanned Air Vehicle [AD-A288786] p 337 N95-26190

CANOPIES (VEGETATION)

- Aerodynamic parameters of crop canopies estimated with a center-of-pressure technique [HTN-95-41901] p 356 A95-81648

CARBON DIOXIDE

- Vertical transport rates in the stratosphere in 1993 from observations of CO₂, N₂O, and CH₄ [HTN-95-70941] p 351 A95-78006

CARBON DISULFIDE

- An intercomparison of aircraft instrumentation for tropospheric measurements of carbonyl sulfide, hydrogen sulfide, and carbon disulfide [HTN-95-91856] p 355 A95-80844

CARBON FIBER REINFORCED PLASTICS

- Study on tensile fatigue testing method of unidirectional fiber-resin matrix composites [NAL-TR-1241] p 343 N95-24989

CARBONYL COMPOUNDS

- An intercomparison of aircraft instrumentation for tropospheric measurements of carbonyl sulfide, hydrogen sulfide, and carbon disulfide [HTN-95-91856] p 355 A95-80844

CASSINI MISSION

- The Cassini spacecraft: Object oriented flight control software p 359 A95-80405

CATALOGS (PUBLICATIONS)

- NASA video catalog [NASA-SP-7109(01)] p 363 N95-24238

CAVITIES

- Effects of cavity dimensions, boundary layer, and temperature on cavity noise with emphasis on benchmark data to validate computational aeroacoustic codes [NASA-CR-4653] p 361 N95-24879

CAVITY FLOW

- Study of subsonic base cavity flowfield structure using particle image velocimetry [BTN-95-EIX95222650781] p 327 A95-79237
- Effects of cavity dimensions, boundary layer, and temperature on cavity noise with emphasis on benchmark data to validate computational aeroacoustic codes [NASA-CR-4653] p 361 N95-24879

CENTER OF PRESSURE

- Aerodynamic parameters of crop canopies estimated with a center-of-pressure technique [HTN-95-41901] p 356 A95-81648

CERAMIC COATINGS

- PVD TBC experience on GE aircraft engines p 345 N95-26126
- Thermal fracture mechanisms in ceramic thermal barrier coatings p 346 N95-26138
- Thermal barrier coating life modeling in aircraft gas turbine engines p 346 N95-26140

CERTIFICATION

- Consistent approach to describing aircraft HIRF protection [NASA-CR-195067] p 334 N95-25341

CHEMICAL ANALYSIS

- An intercomparison of aircraft instrumentation for tropospheric measurements of sulfur dioxide [HTN-95-91855] p 354 A95-80843
- An intercomparison of aircraft instrumentation for tropospheric measurements of carbonyl sulfide, hydrogen sulfide, and carbon disulfide [HTN-95-91856] p 355 A95-80844

- An intercomparison of instrumentation for tropospheric measurements of dimethyl sulfide: Aircraft results for concentrations at the parts-per-trillion level [HTN-95-91857] p 355 A95-80845

CHEMICAL CLEANING

- Parts washing alternatives study: United States Coast Guard. Project summary and report [PB95-166146] p 343 N95-26004

CHEMICAL COMPOSITION

- Analysis of the physical state of one Arctic polar stratospheric cloud based on observations [HTN-95-70917] p 351 A95-77982

- Effects on stratospheric ozone from high-speed civil transport: Sensitivity to stratospheric aerosol loading [HTN-95-91842] p 354 A95-80830

- An intercomparison of aircraft instrumentation for tropospheric measurements of sulfur dioxide [HTN-95-91855] p 354 A95-80843

- An intercomparison of aircraft instrumentation for tropospheric measurements of carbonyl sulfide, hydrogen sulfide, and carbon disulfide
[HTN-95-91856] p 355 A95-80844
- An intercomparison of instrumentation for tropospheric measurements of dimethyl sulfide: Aircraft results for concentrations at the parts-per-trillion level
[HTN-95-91857] p 355 A95-80845
- Chemical composition and photochemical reactivity of exhaust from aircraft turbine engines
[HTN-95-51277] p 356 A95-80862
- CHEMICAL TESTS**
- Chemical composition and photochemical reactivity of exhaust from aircraft turbine engines
[HTN-95-51277] p 356 A95-80862
- CHLORINE**
- The distribution of hydrogen, nitrogen, and chlorine radicals in the lower stratosphere: Implications for changes in O₃ due to emission of NO(y) from supersonic aircraft
[HTN-95-70935] p 351 A95-78000
- Impact on ozone of high-speed stratospheric aircraft: Effects of the emission scenario
[HTN-95-51283] p 356 A95-80868
- CIRCULAR CONES**
- Quantitative comparison between interferometric measurements and Euler computations for supersonic cone flows
[BTN-95-EIX95222650782] p 358 A95-79238
- CIRCULAR CYLINDERS**
- Experimental investigation of the flow around a circular cylinder: Influence of aspect ratio
[BTN-94-EIX95011441120] p 347 A95-80044
- CIRCULAR PLATES**
- Experimental investigation of the flow around a circular cylinder: Influence of aspect ratio
[BTN-94-EIX95011441120] p 347 A95-80044
- CIRRUS CLOUDS**
- Preliminary analysis of University of North Dakota aircraft data from the FIRE Cirrus IFO-2
[NASA-CR-198038] p 357 A95-24219
- CLEANERS**
- Parts washing alternatives study: United States Coast Guard. Project summary and report
[PB95-166146] p 343 A95-26004
- CLIMATOLOGY**
- Preliminary analysis of University of North Dakota aircraft data from the FIRE Cirrus IFO-2
[NASA-CR-198038] p 357 A95-24219
- CLOUD COVER**
- Analysis of the physical state of one Arctic polar stratospheric cloud based on observations
[HTN-95-70917] p 351 A95-77982
- Preliminary analysis of University of North Dakota aircraft data from the FIRE Cirrus IFO-2
[NASA-CR-198038] p 357 A95-24219
- CLOUD PHYSICS**
- Preliminary analysis of University of North Dakota aircraft data from the FIRE Cirrus IFO-2
[NASA-CR-198038] p 357 A95-24219
- CLOUDS**
- Analysis of the physical state of one Arctic polar stratospheric cloud based on observations
[HTN-95-70917] p 351 A95-77982
- COCKPITS**
- A crew-centered flight deck design philosophy for High-Speed Civil Transport (HSCT) aircraft
[NASA-TM-109171] p 335 A95-24582
- COGENERATION**
- Small gas turbine component evaluation study
[PB95-147542] p 338 A95-24293
- COLLISIONS**
- Aircraft accident report: Impact with blast fence upon landing rollout Action Air Charters flight 990 Piper PA-31-350, N990RA, Stratford, Connecticut, 27 April 1994
[PB94-910410] p 333 A95-24206
- COMBUSTION**
- Workshop report: Measurement techniques in highly transient, spectrally rich combustion environments
[AD-A288395] p 350 A95-25606
- COMBUSTION CHAMBERS**
- Effect of density gradients in confined supersonic shear layers, part 1
[NASA-CR-198029] p 348 A95-24412
- Effect of density gradients in confined supersonic shear layers. Part 2: 3-D modes
[NASA-CR-198030] p 348 A95-24413
- COMBUSTION PHYSICS**
- Workshop report: Measurement techniques in highly transient, spectrally rich combustion environments
[AD-A288395] p 350 A95-25606
- COMMERCIAL AIRCRAFT**
- Application of direct transcription to commercial aircraft trajectory optimization
[BTN-95-EIX95242670766] p 359 A95-81081
- Consistent approach to describing aircraft HIRF protection
[NASA-CR-195067] p 334 A95-25341
- Emerging nondestructive inspection for aging aircraft
[PB95-143053] p 328 A95-25401
- COMMUTER AIRCRAFT**
- Emerging nondestructive inspection for aging aircraft
[PB95-143053] p 328 A95-25401
- COMPARISON**
- Comparison of wind profiler and aircraft wind measurements at Chebogue Point, Nova Scotia
[HTN-95-41833] p 353 A95-80559
- An intercomparison of aircraft instrumentation for tropospheric measurements of sulfur dioxide
[HTN-95-91855] p 354 A95-80843
- An intercomparison of aircraft instrumentation for tropospheric measurements of carbonyl sulfide, hydrogen sulfide, and carbon disulfide
[HTN-95-91856] p 355 A95-80844
- An intercomparison of instrumentation for tropospheric measurements of dimethyl sulfide: Aircraft results for concentrations at the parts-per-trillion level
[HTN-95-91857] p 355 A95-80845
- COMPASSES**
- Interfacing a digital compass to a remote-controlled helicopter
[PB95-164927] p 340 A95-24260
- COMPOSITE MATERIALS**
- NASA-UVA light aerospace alloy and structures technology program (LA2ST)
[NASA-CR-198041] p 343 A95-24220
- JPRS report: Science and technology. Central Eurasia
[JPRS-UST-94-018] p 349 A95-24472
- COMPRESSIBLE FLOW**
- Study of compressible flow through a rectangular-to-semiannular transition duct
[NASA-CR-4660] p 338 A95-24392
- Effect of density gradients in confined supersonic shear layers, part 1
[NASA-CR-198029] p 348 A95-24412
- COMPRESSORS**
- Theoretical and experimental studies of fretting-initiated fatigue failure of aeroengine compressor discs
[BTN-94-EIX94421372285] p 343 A95-78467
- COMPUTATIONAL FLUID DYNAMICS**
- Verification of computational aerodynamic predictions for complex hypersonic vehicles using the INCA(trademark) code
[DE95-004757] p 330 A95-24308
- Aerodynamic optimization studies on advanced architecture computers
[NASA-CR-198045] p 330 A95-24379
- DSMC calculations for 70-deg blunted cone at 3.2 km/s in nitrogen
[NASA-TM-109181] p 348 A95-24396
- Aerodynamic shape optimization of wing and wing-body configurations using control theory
[NASA-CR-198024] p 335 A95-25334
- The coupling of fluids, dynamics, and controls on advanced architecture computers
[NASA-CR-197727] p 360 A95-25797
- Recent improvements to and validation of the one dimensional NASA wave rotor model
[NASA-TM-106913] p 332 A95-25962
- A combined geometric approach for solving the Navier-Stokes equations on dynamic grids
[NASA-TM-106919] p 332 A95-26075
- Cumulative reports and publications through December 31, 1994
[NASA-CR-195043] p 361 A95-26085
- COMPUTATIONAL GRIDS**
- A combined geometric approach for solving the Navier-Stokes equations on dynamic grids
[NASA-TM-106919] p 332 A95-26075
- COMPUTER AIDED DESIGN**
- Modeling of aircraft exhaust emissions and infrared spectra for remote measurement of nitrogen oxides
[HTN-95-51276] p 355 A95-80861
- Aerodynamic optimization studies on advanced architecture computers
[NASA-CR-198045] p 330 A95-24379
- Aspect estimation of an aircraft using library model silhouettes
[PB95-141834] p 360 A95-25894
- COMPUTER NETWORKS**
- The coupling of fluids, dynamics, and controls on advanced architecture computers
[NASA-CR-197727] p 360 A95-25797
- COMPUTER PROGRAMMING**
- Cumulative reports and publications through December 31, 1994
[NASA-CR-195043] p 361 A95-26085
- COMPUTER PROGRAMS**
- The Cassini spacecraft: Object oriented flight control software
[AD-A288786] p 337 A95-26190
- Verification of computational aerodynamic predictions for complex hypersonic vehicles using the INCA(trademark) code
[DE95-004757] p 330 A95-24308
- COMPUTER VISION**
- Aspect estimation of an aircraft using library model silhouettes
[PB95-141834] p 360 A95-25894
- COMPUTERIZED SIMULATION**
- Modeling of aircraft exhaust emissions and infrared spectra for remote measurement of nitrogen oxides
[HTN-95-51276] p 355 A95-80861
- Estimate of probability of crack detection from service difficulty report data
[PB95-149381] p 328 A95-24295
- The coupling of fluids, dynamics, and controls on advanced architecture computers
[NASA-CR-197727] p 360 A95-25797
- CONFERENCES**
- Guidance and control, 1993; Annual Rocky Mountain Guidance and Control Conference, 16th, Keystone, CO, Feb. 6-10, 1993
[ISBN-0-87703-365-X] p 341 A95-80389
- The 1994 Fiber Optic Sensors for Aerospace Technology (FOSAT) Workshop
[NASA-CP-10166] p 337 A95-24207
- Proceedings of the 2d USAF Aging Aircraft Conference
[AD-A288217] p 336 A95-25578
- Thermal Barrier Coating Workshop
[NASA-CP-10170] p 344 A95-26119
- CONFINEMENT**
- Dynamics of phase ordering of nematics in a pore
[DE95-807662] p 362 A95-25978
- CONGRESSIONAL REPORTS**
- Nitrogen oxide emissions and their control from uninstalled aircraft engines in enclosed test cells: Joint report to Congress on the Environmental Protection Agency - Department of Transportation study
[PB95-166237] p 358 A95-26005
- Report to Congressional Committees. Tactical Aircraft: Concurrence in development and production of F-22 aircraft should be reduced
[GAO/NSIAD-95-59] p 336 A95-26338
- CONICAL BODIES**
- DSMC calculations for 70-deg blunted cone at 3.2 km/s in nitrogen
[NASA-TM-109181] p 348 A95-24396
- CONSTRAINTS**
- A brief survey of constrained mechanics and variational problems in terms of differential forms
p 360 A95-25803
- CONTRAILS**
- Visual contrast detection thresholds for aircraft contrails
[AD-A288618] p 328 A95-25607
- CONTROL SURFACES**
- Aeroservoelastic aspects of wing/control surface platform shape optimization
[BTN-95-EIX95222650795] p 340 A95-79251
- On-line learning nonlinear direct neurocontrollers for restructurable control systems
[BTN-95-EIX95242670768] p 359 A95-81079
- Fundamental mechanisms of aeroelastic control with control surface and strain actuation
[BTN-95-EIX95242670746] p 327 A95-81101
- CONTROL SYSTEMS DESIGN**
- Guidance and control, 1993; Annual Rocky Mountain Guidance and Control Conference, 16th, Keystone, CO, Feb. 6-10, 1993
[ISBN-0-87703-365-X] p 341 A95-80389
- The Cassini spacecraft: Object oriented flight control software
[AD-A288786] p 337 A95-26190
- A new guidance and flight control system for the DELTA 2 launch vehicle - Abstract only
[BTN-95-EIX95242670754] p 342 A95-81093
- On-line learning nonlinear direct neurocontrollers for restructurable control systems
[BTN-95-EIX95242670768] p 359 A95-81079
- Dynamics and control of a tethered flight vehicle
[BTN-95-EIX95242670754] p 342 A95-81093
- High-performance, robust, bank-to-turn missile autopilot design
[BTN-95-EIX95242670751] p 336 A95-81096
- Direct adaptive and neural control of wing-rock motion of slender delta wings
[BTN-95-EIX95242670748] p 327 A95-81099
- Robust dynamic inversion for control of highly maneuverable aircraft
[BTN-95-EIX95242670747] p 359 A95-81100
- Application of neural networks to unsteady aerodynamic control
p 360 A95-25264
- Partial camera automation in a simulated Unmanned Air Vehicle
[AD-A288786] p 337 A95-26190

CONTROL THEORY

- Aerodynamic shape optimization of wing and wing-body configurations using control theory
[NASA-CR-198024] p 335 N95-25334
- How to fly an aircraft with control theory and splines
p 360 N95-25805
- Actuating signals in adaptive control systems
[IFTR-13/1994] p 361 N95-26330
- CONTROLLABILITY**
Determination of piloting feedback structures for an altitude tracking task
[BTN-95-EIX95242670770] p 327 A95-81077
- Rotorcraft handling qualities in turbulence
[BTN-95-EIX95242670750] p 334 A95-81097
- CONTROLLERS**
Actuating signals in adaptive control systems
[IFTR-13/1994] p 361 N95-26330
- CONVERGENT-DIVERGENT NOZZLES**
Internal performance characteristics of thrust-vectoring axisymmetric ejector nozzles
[NASA-TM-4610] p 331 N95-25338
- COOLANTS**
Effect of film cooling/regenerative cooling on scramjet engine performances
[NAL-TR-1242] p 339 N95-24990
- COOLING**
Impingement cooling of an isothermally heated surface with a confined slot jet
[BTN-94-EIX9421348950] p 347 A95-78494
- COOLING SYSTEMS**
Effect of film cooling/regenerative cooling on scramjet engine performances
[NAL-TR-1242] p 339 N95-24990
- COORDINATE TRANSFORMATIONS**
Describing an attitude p 342 A95-80409
- COPPER ALLOYS**
NASA-UVA light aerospace alloy and structures technology program supplement: Aluminum-based materials for high speed aircraft
[NASA-CR-4645] p 343 N95-24878
- CORIOLIS EFFECT**
Integrated development of the equations of motion for elastic hypersonic flight vehicles
[BTN-95-EIX95242670755] p 327 A95-81092
- CORROSION**
Proceedings of the 2d USAF Aging Aircraft Conference
[AD-A288217] p 336 N95-25578
- COSINE SERIES**
Describing an attitude p 342 A95-80409
- COST ANALYSIS**
Small gas turbine component evaluation study
[PB95-147542] p 338 N95-24293
- CRACK INITIATION**
Estimate of probability of crack detection from service difficulty report data
[PB95-149381] p 328 N95-24295
- Thermal fracture mechanisms in ceramic thermal barrier coatings p 346 N95-26138
- CRACK PROPAGATION**
Theoretical and experimental studies of fretting-initiated fatigue failure of aeroengine compressor discs
[BTN-94-EIX94421372285] p 343 A95-78467
- Estimate of probability of crack detection from service difficulty report data
[PB95-149381] p 328 N95-24295
- CRACKS**
Theoretical and experimental studies of fretting-initiated fatigue failure of aeroengine compressor discs
[BTN-94-EIX94421372285] p 343 A95-78467
- CRASHWORTHINESS**
Analysis of warping effects on the static and dynamic response of a seat-type structure
[NIAR-94-12] p 348 N95-24211
- CREW WORKSTATIONS**
A crew-centered flight deck design philosophy for High-Speed Civil Transport (HSCT) aircraft
[NASA-TM-109171] p 335 N95-24582
- CRITICAL FLOW**
High frequency flow-structural interaction in dense subsonic fluids
[NASA-CR-4652] p 330 N95-24217
- CROSS FLOW**
Three-dimensional interaction of wake/boundary-layer and vortex/boundary-layer data report
[CUED/A-AERO/TR-23] p 329 N95-24210
- Crossflow mixing of noncircular jets
[NASA-TM-106865] p 338 N95-24390
- Effect of density gradients in confined supersonic shear layers. Part 2: 3-D modes
[NASA-CR-198030] p 349 N95-24413
- CRUISING FLIGHT**
North Atlantic air traffic within the lower stratosphere: Cruising times and corresponding emissions
[HTN-95-91841] p 354 A95-80829

CRYOGENIC FLUIDS

- Thermohydrodynamic analysis of cryogenic liquid turbulent flow fluid film bearings, phase 2
[NASA-CR-197412] p 349 N95-24461
- CRYOGENIC WIND TUNNELS**
Similarity rule for jet-temperature effects on transonic base pressure
[BTN-95-EIX95222650791] p 329 A95-79247

D

DAMAGE

- On-line learning nonlinear direct neurocontrollers for restructurable control systems
[BTN-95-EIX95242670768] p 359 A95-81079
- Bird ingestion into large turbofan engines
[DOT/FAA/CT-93/14] p 333 N95-24631

DAMAGE ASSESSMENT

- Emerging nondestructive inspection for aging aircraft
[PB95-143053] p 328 N95-25401
- Proceedings of the 2d USAF Aging Aircraft Conference
[AD-A288217] p 336 N95-25578

DATA ACQUISITION

- An overview of Health and Usage Monitoring Systems (HUMS) for military helicopters
[DSTO-TR-0061] p 327 N95-24200

DATA BASES

- NLS Flight Simulation Laboratory (FSL) documentation
[NASA-CR-196564] p 363 N95-24439

DATA COLLECTION PLATFORMS

- Long endurance stratospheric solar powered airship
[PB95-178729] p 336 N95-26009

DATA COMPRESSION

- Fault detection in multiprocessor systems and array processors
[BTN-95-EIX95242679097] p 359 A95-81253

DATA PROCESSING

- Using digital filtering techniques as an aid in wind turbine data analysis
[DE94-011862] p 357 N95-24853

DATA PROCESSING EQUIPMENT

- Fault detection in multiprocessor systems and array processors
[BTN-95-EIX95242679097] p 359 A95-81253

DATA REDUCTION

- Identification of aviation weather hazards based on the integration of radar and lightning data
[HTN-95-51323] p 356 A95-80908
- Using digital filtering techniques as an aid in wind turbine data analysis
[DE94-011862] p 357 N95-24853

DATA SMOOTHING

- A brief survey of constrained mechanics and variational problems in terms of differential forms
p 360 N95-25803

DATA STRUCTURES

- Determination of piloting feedback structures for an altitude tracking task
[BTN-95-EIX95242670770] p 327 A95-81077

DEBRIS

- Quantity-distance requirements for earth-bermed aircraft shelters
[AD-A279692] p 341 N95-24424

DECISION MAKING

- Real-time decision aiding: Aircraft guidance for wind shear avoidance
[BTN-95-EIX95202637575] p 332 A95-78583

DEFECTS

- Dynamics of phase ordering of nematics in a pore
[DE95-607662] p 362 N95-25978

DEFORMATION

- Analysis of warping effects on the static and dynamic response of a seat-type structure
[NIAR-94-12] p 348 N95-24211

- Residual Stress Measurements with Laser Speckle Correlation Interferometry and Local Heat Treating
[DE95-060082] p 349 N95-24598

DELMARVA PENINSULA (DE-MD-VA)

- Identification of aviation weather hazards based on the integration of radar and lightning data
[HTN-95-51323] p 356 A95-80908

DELTA LAUNCH VEHICLE

- A new guidance and flight control system for the DELTA 2 launch vehicle — Abstract only p 342 A95-80427

DELTA WINGS

- Direct adaptive and neural control of wing-rock motion of slender delta wings
[BTN-95-EIX95242670748] p 327 A95-81099
- Low speed aerodynamic characteristics of delta wings with vortex flaps: 60 deg and 70 deg delta wings
[NAL-TR-1245] p 331 N95-25105

DENSITY (MASS/VOLUME)

- Effect of density gradients in confined supersonic shear layers, part 1
[NASA-CR-198029] p 348 N95-24412
- Effect of density gradients in confined supersonic shear layers. Part 2: 3-D modes
[NASA-CR-198030] p 349 N95-24413

DENSITY DISTRIBUTION

- Aerodynamic characteristics of the orbital reentry vehicle experimental probe fins in a supersonic flow
[NAL-TR-1232] p 342 N95-25664

DESIGN ANALYSIS

- Development of a model protection and dynamic response monitoring system for the national transonic facility
[NASA-CR-195041] p 340 N95-24388
- A crew-centered flight deck design philosophy for High-Speed Civil Transport (HSCT) aircraft
[NASA-TM-109171] p 335 N95-24582
- Long endurance stratospheric solar powered airship
[PB95-178729] p 336 N95-26009
- A design perspective on thermal barrier coatings
p 344 N95-26120

DIESEL ENGINES

- Thermal Barrier Coating Workshop
[NASA-CP-10170] p 344 N95-26119
- Thermal barrier coatings application in diesel engines
p 345 N95-26124

DIFFERENTIAL EQUATIONS

- Aerodynamic parameter estimation via Fourier modulating function techniques
[NASA-CR-4654] p 335 N95-24630

DIGITAL DATA

- Using digital filtering techniques as an aid in wind turbine data analysis
[DE94-011862] p 357 N95-24853

DIGITAL FILTERS

- Using digital filtering techniques as an aid in wind turbine data analysis
[DE94-011862] p 357 N95-24853

DIGITAL NAVIGATION

- Interfacing a digital compass to a remote-controlled helicopter
[PB95-164927] p 340 N95-24260

DIGITAL SYSTEMS

- Impact of near-coincident faults on digital flight control systems
[BTN-95-EIX95242670759] p 359 A95-81088

DIMERIZATION

- Empirical corrections of the rigid rotor interaction potential of H₂-H₂ in the attractive region: Dimer features in the FIR absorption spectra
[HTN-95-41943] p 361 A95-81690

DIMETHYL COMPOUNDS

- An intercomparison of instrumentation for tropospheric measurements of dimethyl sulfide: Aircraft results for concentrations at the parts-per-trillion level
[HTN-95-91857] p 355 A95-80845

DIRECTIONAL CONTROL

- Performance of an aerodynamic yaw controller mounted on the space shuttle orbiter body flap at Mach 10
[NASA-TM-109179] p 330 N95-24397

DISPLACEMENT MEASUREMENT

- Angular displacement measuring device
[NASA-CASE-ARC-11937-1] p 362 N95-26015

DISPLAY DEVICES

- Preliminary experiments of an optical fiber display
[NAL-TR-1257] p 362 N95-25004

DISTRIBUTED PROCESSING

- The coupling of fluids, dynamics, and controls on advanced architecture computers
[NASA-CR-197727] p 360 N95-25797

DOCUMENT STORAGE

- NLS Flight Simulation Laboratory (FSL) documentation
[NASA-CR-196564] p 363 N95-24439

DOCUMENTATION

- NLS Flight Simulation Laboratory (FSL) documentation
[NASA-CR-196564] p 363 N95-24439

DOPPLER RADAR

- Identification of aviation weather hazards based on the integration of radar and lightning data
[HTN-95-51323] p 356 A95-80908

DRAG REDUCTION

- Study of subsonic base cavity flowfield structure using particle image velocimetry
[BTN-95-EIX95222650781] p 327 A95-79237
- Numerical and experimental study of drag characteristics of two-dimensional HLFC airfoils in high subsonic, high Reynolds number flow
[NAL-TR-12447] p 331 N95-24998
- A theoretical and experimental investigation of the flow over supersonic leading edge wing/body configurations
[DRA-TM-AERO-PROP-41] p 331 N95-25649

DUCTED FLOW

- Study of compressible flow through a rectangular-to-semiannular transition duct
[NASA-CR-4660] p 338 N95-24392
- Recent improvements to and validation of the one dimensional NASA wave rotor model
[NASA-TM-106913] p 332 N95-25962

DYNAMIC CHARACTERISTICS

- High frequency flow-structural interaction in dense subsonic fluids
[NASA-CR-4652] p 330 N95-24217
- Experimental study of the effects of Reynolds number on high angle of attack aerodynamic characteristics of forebodies during rotary motion
[NASA-CR-195033] p 330 N95-24443

DYNAMIC RESPONSE

- Analysis of warping effects on the static and dynamic response of a seat-type structure
[NIAR-94-12] p 348 N95-24211
- Development of a model protection and dynamic response monitoring system for the national transonic facility
[NASA-CR-195041] p 340 N95-24388

DYNAMIC STRUCTURAL ANALYSIS

- Modal characteristics of rotors using a conical shaft finite element
[BTN-94-EIX94401359745] p 346 A95-77379

DYNAMIC TESTS

- Analysis of warping effects on the static and dynamic response of a seat-type structure
[NIAR-94-12] p 348 N95-24211

DYNAMICAL SYSTEMS

- Actuating signals in adaptive control systems
[IFTR-13/1994] p 361 N95-26330

E**EARTH SCIENCES**

- JPRS report: Science and technology. Central Eurasia
[JPRS-UST-94-018] p 349 N95-24472

ECONOMIC ANALYSIS

- Small gas turbine component evaluation study
[PB95-147542] p 338 N95-24293
- Advanced subsonic airplane design and economic studies
[NASA-CR-195443] p 338 N95-24304

EDDY CURRENTS

- Emerging nondestructive inspection for aging aircraft
[PB95-143053] p 328 N95-25401

EFFLUENTS

- Potential effects on ozone of future supersonic aircraft/2D simulation
[HTN-95-51282] p 356 A95-80867

EJECTORS

- Internal performance characteristics of thrust-vectoring axisymmetric ejector nozzles
[NASA-TM-4610] p 331 N95-25338

ELASTIC DEFORMATION

- Integrated development of the equations of motion for elastic hypersonic flight vehicles
[BTN-95-EIX95242670755] p 327 A95-81092

ELECTRIC CONNECTORS

- Preload release mechanism
[NASA-CASE-MSC-22327-1] p 350 N95-25592

ELECTRIC GENERATORS

- Wind technology development: Large and small turbines
[DE95-000286] p 358 N95-26090

ELECTRICAL ENGINEERING

- JPRS report: Science and technology. Central Eurasia
[JPRS-UST-94-027] p 349 N95-24470
- JPRS report: Science and technology. Central Eurasia
[JPRS-UST-94-018] p 349 N95-24472

ELECTROMAGNETIC FIELDS

- Consistent approach to describing aircraft HIRF protection
[NASA-CR-195067] p 334 N95-25341

ELECTRONIC CONTROL

- Wind technology development: Large and small turbines
[DE95-000286] p 358 N95-26090

ELECTRONIC EQUIPMENT

- Real-time decision aiding: Aircraft guidance for wind shear avoidance
[BTN-95-EIX95202637575] p 332 A95-78583

ELECTRONIC EQUIPMENT TESTS

- Fault detection in multiprocessor systems and array processors
[BTN-95-EIX95242679097] p 359 A95-81253

EMISSION

- Nitrous oxide and methane emissions from aero engines
[HTN-95-21363] p 353 A95-78678

EMISSION SPECTRA

- Analysis of the physical state of one Arctic polar stratospheric cloud based on observations
[HTN-95-70917] p 351 A95-77982
- An analysis of aircraft exhaust plumes from accidental encounters
[HTN-95-70943] p 351 A95-78008
- Comparison of column abundances from three infrared spectrometers during AASE 2
[HTN-95-70946] p 352 A95-78011

ENERGY CONVERSION EFFICIENCY

- NREL airfoil families for HAWTs
[DE95-000267] p 357 N95-24882

ENERGY POLICY

- Wind technology development: Large and small turbines
[DE95-000286] p 358 N95-26090

ENGINE AIRFRAME INTEGRATION

- Advanced subsonic airplane design and economic studies
[NASA-CR-195443] p 338 N95-24304

ENGINE DESIGN

- Small gas turbine component evaluation study
[PB95-147542] p 338 N95-24293

ENGINE INLETS

- Prediction of supersonic inlet unstart caused by freestream disturbances
[BTN-95-EIX95222650790] p 329 A95-79246
- Study of compressible flow through a rectangular-to-semiannular transition duct
[NASA-CR-4660] p 338 N95-24392

ENGINE NOISE

- Noise impact of advanced high lift systems
[NASA-CR-195028] p 362 N95-26160
- Jet mixer noise suppressor using acoustic feedback
[NASA-CASE-LEW-15170-2] p 362 N95-26187

ENGINE PARTS

- Small gas turbine component evaluation study
[PB95-147542] p 338 N95-24293

ENGINE TESTS

- Turbine-engine applications of thermographic-phosphor temperature measurements
[DE95-003625] p 358 N95-25110
- Assessment of overhaul surge margin tests applied to the T53 engines in ADF Iroquois helicopters
[AR-008-389] p 339 N95-25936
- Nitrogen oxide emissions and their control from uninstalled aircraft engines in enclosed test cells: Joint report to Congress on the Environmental Protection Agency - Department of Transportation study
[PB95-166237] p 358 N95-26005
- Perspective on thermal barrier coatings for industrial gas turbine applications
p 345 N95-26128

ENTHALPY

- The Supersonic Expansion Tube concept, experiment and analysis
p 341 N95-25399

ENVIRONMENT EFFECTS

- Impact of present aircraft emissions of nitrogen oxides on tropospheric ozone and climate forcing
[HTN-95-21364] p 353 A95-78679
- The atmospheric effects of stratospheric aircraft: A fourth program report
[NASA-RP-1359] p 357 N95-24274
- Parts washing alternatives study: United States Coast Guard. Project summary and report
[PB95-166146] p 343 N95-26004

ENVIRONMENT PROTECTION

- Nitrogen oxide emissions and their control from uninstalled aircraft engines in enclosed test cells: Joint report to Congress on the Environmental Protection Agency - Department of Transportation study
[PB95-166237] p 358 N95-26005

EQUATIONS OF MOTION

- Integrated development of the equations of motion for elastic hypersonic flight vehicles
[BTN-95-EIX95242670755] p 327 A95-81092

ERRORS

- Aspect estimation of an aircraft using library model silhouettes
[PB95-141834] p 360 N95-25894

ESTIMATING

- Aerodynamic parameter estimation via Fourier modulating function techniques
[NASA-CR-4654] p 335 N95-24630

EULER EQUATIONS OF MOTION

- Quantitative comparison between interferometric measurements and Euler computations for supersonic cone flows
[BTN-95-EIX95222650782] p 358 A95-79238
- Effect of density gradients in confined supersonic shear layers, part 1
[NASA-CR-198029] p 348 N95-24412

EUROPE

- Assessment of avionics technology in European aerospace organizations
[NASA-CR-189201] p 337 N95-24624

EXHAUST EMISSION

- The distribution of hydrogen, nitrogen, and chlorine radicals in the lower stratosphere: Implications for changes in O₃ due to emission of NO_x from supersonic aircraft
[HTN-95-70935] p 351 A95-78000
- An analysis of aircraft exhaust plumes from accidental encounters
[HTN-95-70943] p 351 A95-78008
- Chemical change in the arctic vortex during AASE 2
[HTN-95-70947] p 352 A95-78012
- Impact of present aircraft emissions of nitrogen oxides on tropospheric ozone and climate forcing
[HTN-95-21364] p 353 A95-78679
- Sensitivity of supersonic aircraft modelling studies to HNO₃ photolysis rate
[HTN-95-11475] p 353 A95-79453
- Tracer transport for realistic aircraft emission scenarios calculated using a three-dimensional model
[HTN-95-41799] p 353 A95-80525
- Modeling of aircraft exhaust emissions and infrared spectra for remote measurement of nitrogen oxides
[HTN-95-51276] p 355 A95-80861
- Chemical composition and photochemical reactivity of exhaust from aircraft turbine engines
[HTN-95-51277] p 356 A95-80862
- Impact on ozone of high-speed stratospheric aircraft: Effects of the emission scenario
[HTN-95-51283] p 356 A95-80868
- Small gas turbine component evaluation study
[PB95-147542] p 338 N95-24293
- The effect of altitude conditions on the particle emissions of a J85-GE-5L turbojet engine
[NASA-TM-106669] p 339 N95-24561

EXHAUST GASES

- North Atlantic air traffic within the lower stratosphere: Cruising times and corresponding emissions
[HTN-95-91841] p 354 A95-80829
- Effects on stratospheric ozone from high-speed civil transport: Sensitivity to stratospheric aerosol loading
[HTN-95-91842] p 354 A95-80830
- The atmospheric effects of stratospheric aircraft: A fourth program report
[NASA-RP-1359] p 357 N95-24274

EXHAUST NOZZLES

- Internal performance characteristics of thrust-vectoring axisymmetric ejector nozzles
[NASA-TM-4610] p 331 N95-25338

EXPERIMENT DESIGN

- SOFIA: Stratospheric Observatory for Infrared Astronomy
p 363 A95-81583

EXPLOSIONS

- Quantity-distance requirements for earth-bermed aircraft shelters
[AD-A279692] p 341 N95-24424

F**F-22 AIRCRAFT**

- Report to Congressional Committees. Tactical Aircraft: Concurrency in development and production of F-22 aircraft should be reduced
[GAO/NSIAD-95-59] p 336 N95-26338

FAILURE

- Theoretical and experimental studies of fretting-initiated fatigue failure of aeroengine compressor discs
[BTN-94-EIX94421372285] p 343 A95-78467

FAILURE ANALYSIS

- Fault detection in multiprocessor systems and array processors
[BTN-95-EIX95242679097] p 359 A95-81253

FAR INFRARED RADIATION

- Empirical corrections of the rigid rotor interaction potential of H₂-H₂ in the attractive region: Dimer features in the FIR absorption spectra
[HTN-95-41943] p 361 A95-81690

FATIGUE (MATERIALS)

- Theoretical and experimental studies of fretting-initiated fatigue failure of aeroengine compressor discs
[BTN-94-EIX94421372285] p 343 A95-78467

FATIGUE LIFE

- Helicopter life substantiation: Review of some USA and UK initiatives
[DSTO-TR-0062] p 328 N95-24201
- Proceedings of the 2d USAF Aging Aircraft Conference
[AD-A288217] p 336 N95-25578

FATIGUE TESTS

- Study on tensile fatigue testing method of unidirectional fiber-resin matrix composites
[NAL-TR-1241] p 343 N95-24989

FAULT DETECTION

- Impact of near-coincident faults on digital flight control systems
[BTN-95-EIX95242670759] p 359 A95-81088

- Fault detection in multiprocessor systems and array processors
[BTN-95-EIX95242679097] p 359 A95-81253
- A portable transmission vibration analysis system for the S-70A-9 Black Hawk helicopter
[DSTO-TR-0072] p 348 N95-24203
- FAULT TOLERANCE**
Impact of near-coincident faults on digital flight control systems
[BTN-95-EIX95242670759] p 359 A95-81088
- FEASIBILITY ANALYSIS**
Modeling of aircraft exhaust emissions and infrared spectra for remote measurement of nitrogen oxides
[HTN-95-51276] p 355 A95-80861
- FEEDBACK**
Determination of piloting feedback structures for an altitude tracking task
[BTN-95-EIX9524267077C] p 327 A95-81077
- FEEDBACK CONTROL**
Load alleviation maneuvers for a launch vehicle
p 342 A95-81360
Application of neural networks to unsteady aerodynamic control
p 360 N95-25264
- FENCES (BARRIERS)**
Aircraft accident report: Impact with blast fence upon landing rollout Action Air Charters flight 990 Piper PA-31-350, N990RA, Stratford, Connecticut, 27 April 1994
[PB94-910410] p 333 N95-24206
- FIBER OPTICS**
The 1994 Fiber Optic Sensors for Aerospace Technology (FOSAT) Workshop
[NASA-CP-10166] p 337 N95-24207
Workshop report: Measurement techniques in highly transient, spectrally rich combustion environments
[AD-A288395] p 350 N95-25606
- FIELD OF VIEW**
Preliminary experiments of an optical fiber display
[NAL-TR-1257] p 362 N95-25004
- FILM COOLING**
Effect of film cooling/regenerative cooling on scramjet engine performances
[NAL-TR-1242] p 339 N95-24990
- FINITE ELEMENT METHOD**
Modal characteristics of rotors using a conical shaft finite element
[BTN-94-EIX94401359745] p 346 A95-77379
Viscoplastic response of structures for intense local heating
[HTN-95-41540] p 346 A95-77921
Theoretical and experimental studies of fretting-initiated fatigue failure of aeroengine compressor discs
[BTN-94-EIX94421372285] p 343 A95-78467
Dynamic behavior of a magnetic bearing supported jet engine rotor with auxiliary bearings
[NASA-CR-197860] p 338 N95-24213
- FINS**
Structure of a double-fin turbulent interaction at high speed
[BTN-95-EIX95222650780] p 347 A95-79236
Aerodynamic characteristics of the orbital reentry vehicle experimental probe fins in a supersonic flow
[NAL-TR-1232] p 342 N95-25664
Fundamental wind tunnel experiments on low-speed flutter of a tip-fin configuration wing
[NAL-TR-1228] p 332 N95-25762
- FIRE (CLIMATOLOGY)**
Preliminary analysis of University of North Dakota aircraft data from the FIRE Cirrus IFO-2
[NASA-CR-198038] p 357 N95-24219
- FLAPS (CONTROL SURFACES)**
Experimental study of flow separation on an oscillating flap at Mach 2.4
[BTN-95-EIX95222650792] p 329 A95-79248
Performance of an aerodynamic yaw controller mounted on the space shuttle orbiter body flap at Mach 10
[NASA-TM-109179] p 330 N95-24397
- FLIGHT CHARACTERISTICS**
Determination of piloting feedback structures for an altitude tracking task
[BTN-95-EIX95242670770] p 327 A95-81077
Rotorcraft handling qualities in turbulence
[BTN-95-EIX95242670750] p 334 A95-81097
Aerodynamic characteristics of the orbital reentry vehicle experimental probe fins in a supersonic flow
[NAL-TR-1232] p 342 N95-25664
- FLIGHT CONTROL**
Dynamic imaging and RCS measurements of aircraft
[BTN-95-EIX95202637582] p 347 A95-78576
Dynamic stall control for advanced rotorcraft application
[BTN-95-EIX95222650793] p 334 A95-79249
Guidance and control, 1993: Annual Rocky Mountain Guidance and Control Conference, 16th, Keystone, CO, Feb. 6-10, 1993
[ISBN-0-87703-365-X] p 341 A95-80389

- The Cassini spacecraft: Object oriented flight control software
p 359 A95-80405
- A new guidance and flight control system for the DELTA 2 launch vehicle --- Abstract only
p 342 A95-80427
- On-line learning nonlinear direct neurocontrollers for restructurable control systems
[BTN-95-EIX95242670768] p 359 A95-81079
- Impact of near-coincident faults on digital flight control systems
[BTN-95-EIX95242670759] p 359 A95-81088
- Dynamics and control of a tethered flight vehicle
[BTN-95-EIX95242670754] p 342 A95-81093
- High-performance, robust, bank-to-turn missile autopilot design
[BTN-95-EIX95242670751] p 336 A95-81096
- Robust dynamic inversion for control of highly maneuverable aircraft
[BTN-95-EIX95242670747] p 359 A95-81100
- Assessment of avionics technology in European aerospace organizations
[NASA-CR-189201] p 337 N95-24624
- FLIGHT CREWS**
A crew-centered flight deck design philosophy for High-Speed Civil Transport (HSCT) aircraft
[NASA-TM-109171] p 335 N95-24582
- FLIGHT HAZARDS**
Bird ingestion into large turbofan engines
[DOT/FAA/CT-93/14] p 333 N95-24631
- FLIGHT MECHANICS**
NASA-UVA light aerospace alloy and structures technology program (LA2ST)
[NASA-CR-198041] p 343 N95-24220
- FLIGHT PATHS**
Dynamic imaging and RCS measurements of aircraft
[BTN-95-EIX95202637582] p 347 A95-78576
Application of direct transcription to commercial aircraft trajectory optimization
[BTN-95-EIX95242670766] p 359 A95-81081
- FLIGHT SIMULATION**
Identification and simulation evaluation of a combat helicopter in hover
[BTN-95-EIX95242670749] p 335 A95-81098
NLS Flight Simulation Laboratory (FSL) documentation
[NASA-CR-196564] p 363 N95-24439
Flight reference display for powered-lift STOL aircraft
[NAL-TR-1251] p 337 N95-25005
- FLIGHT SIMULATORS**
Preliminary experiments of an optical fiber display
[NAL-TR-1257] p 362 N95-25004
Visual contrast detection thresholds for aircraft controls
[AD-A288618] p 328 N95-25607
- FLIGHT TEST VEHICLES**
Reentry guidance for hypersonic Flight Experiment (HYFLEX) vehicle
[NAL-TR-1235] p 334 N95-25764
- FLIGHT TESTS**
Flight reference display for powered-lift STOL aircraft
[NAL-TR-1251] p 337 N95-25005
- FLIGHT TIME**
North Atlantic air traffic within the lower stratosphere: Cruising times and corresponding emissions
[HTN-95-91841] p 354 A95-80829
- FLOW CHARACTERISTICS**
Supersonic quiet-tunnel development for laminar-turbulent transition research
[NASA-CR-198040] p 340 N95-24302
Aerodynamic characteristics of the orbital reentry vehicle experimental probe fins in a supersonic flow
[NAL-TR-1232] p 342 N95-25664
- FLOW DISTRIBUTION**
Exploratory flow visualization investigation of mast-mounted sights in presence of a rotor
[NASA-TM-4634] p 330 N95-24566
Low speed aerodynamic characteristics of delta wings with vortex flaps: 60 deg and 70 deg delta wings
[NAL-TR-1245] p 331 N95-25105
- FLOW MEASUREMENT**
Quantitative comparison between interferometric measurements and Euler computations for supersonic cone flows
[BTN-95-EIX95222650782] p 358 A95-79238
Supersonic quiet-tunnel development for laminar-turbulent transition research
[NASA-CR-198040] p 340 N95-24302
- FLOW VISUALIZATION**
Exploratory flow visualization investigation of mast-mounted sights in presence of a rotor
[NASA-TM-4634] p 330 N95-24566
- FLUID FILMS**
Thermohydrodynamic analysis of cryogenic liquid turbulent flow fluid film bearings, phase 2
[NASA-CR-197412] p 349 N95-24461

- FLUID FLOW**
Experimental investigation of the flow around a circular cylinder: Influence of aspect ratio
[BTN-94-EIX95011441120] p 347 A95-80044
- FLUID MECHANICS**
NASA-UVA light aerospace alloy and structures technology program (LA2ST)
[NASA-CR-198041] p 343 N95-24220
JPRS report: Science and technology. Central Eurasia
[JPRS-UST-94-018] p 349 N95-24472
- FLUID-SOLID INTERACTIONS**
On the role of the outer region in the turbulent-boundary-layer bursting process
[BTN-94-EIX95011441078] p 348 A95-81056
High frequency flow-structural interaction in dense subsonic fluids
[NASA-CR-4652] p 330 N95-24217
- FLUTTER ANALYSIS**
Fundamental wind tunnel experiments on low-speed flutter of a tip-fin configuration wing
[NAL-TR-1228] p 332 N95-25762
- FOAMS**
Design and evaluation of a foam-filled hat-stiffened panel concept for aircraft primary structural applications
[NASA-TM-109175] p 346 N95-26251
- FORCE DISTRIBUTION**
Thrust measurements of a complete axisymmetric scramjet in an impulse facility
p 339 N95-25395
Balances for the measurement of multiple components of force in flows of a millisecond duration
p 350 N95-25400
- FOREBODIES**
Experimental study of the effects of Reynolds number on high angle of attack aerodynamic characteristics of forebodies during rotary motion
[NASA-CR-195033] p 330 N95-24443
- FOURIER ANALYSIS**
Aerodynamic parameter estimation via Fourier modulating function techniques
[NASA-CR-4654] p 335 N95-24630
- FRACTURING**
Thermal fracture mechanisms in ceramic thermal barrier coatings
p 346 N95-26138
- FRAGMENTATION**
Quantity-distance requirements for earth-bermed aircraft shelters
[AD-A279692] p 341 N95-24424
- FRAMES**
Analysis of warping effects on the static and dynamic response of a seat-type structure
[NIAIR-94-12] p 348 N95-24211
- FREE FLOW**
Exploratory flow visualization investigation of mast-mounted sights in presence of a rotor
[NASA-TM-4634] p 330 N95-24566
- FRICTION**
Impact, friction, and wear testing of microsamples of polycrystalline silicon
p 361 A95-79988
- FUEL COMBUSTION**
Shock tunnel studies of scramjet phenomena 1993
[NASA-CR-195038] p 350 N95-25394
- FUEL CONSUMPTION**
Small gas turbine component evaluation study
[PB95-147542] p 338 N95-24293
- FUEL INJECTION**
Shock tunnel studies of scramjet phenomena 1993
[NASA-CR-195038] p 350 N95-25394
Scramjet thrust measurement in a shock tunnel
p 339 N95-25396
- FUNCTIONAL DESIGN SPECIFICATIONS**
SOFIA: Stratospheric Observatory for Infrared Astronomy
p 363 A95-81583
- FUSELAGES**
Estimate of probability of crack detection from service difficulty report data
[PB95-149381] p 328 N95-24295
- FUSION WELDING**
JPRS report: Science and technology. Central Eurasia
[JPRS-UST-95-011] p 335 N95-24541
- FUZZY SETS**
Application of fuzzy logic to optimize placement of an acquisition, tracking, and pointing experiment
p 341 A95-80390
- FUZZY SYSTEMS**
Application of fuzzy logic to optimize placement of an acquisition, tracking, and pointing experiment
p 341 A95-80390

- GAS INJECTION**
High-speed civil transport impact: Role of sulfate, nitric acid trihydrate, and ice aerosols studied with a two-dimensional model including aerosol physics
[HTN-95-91843] p 354 A95-80831

GAS JETS

- Similarity rule for jet-temperature effects on transonic base pressure
[BTN-95-EIX95222650791] p 329 A95-79247

GAS TEMPERATURE

- Aerodynamic characteristics of the orbital reentry vehicle experimental probe fins in a supersonic flow
[NAL-TR-1232] p 342 N95-25664

GAS TURBINE ENGINES

- Small gas turbine component evaluation study
[PB95-147542] p 338 N95-24293
- Thermal barrier coatings for aircraft engines: History and directions
p 344 N95-26121
- Thermal barrier coatings application in diesel engines
p 345 N95-26124
- Thermal barrier coating experience in the gas turbine engine
p 345 N95-26125
- PVD TBC experience on GE aircraft engines
p 345 N95-26126
- Perspective on thermal barrier coatings for industrial gas turbine applications
p 345 N95-26128
- Jet engine applications for materials with nanometer-scale dimensions
p 345 N95-26131
- Thermal conductivity of zirconia thermal barrier coatings
p 345 N95-26133
- Thermal barrier coating life modeling in aircraft gas turbine engines
p 346 N95-26140

GAS TURBINES

- Thermal Barrier Coating Workshop
[NASA-CP-10170] p 344 N95-26119
- Thermal barrier coatings issues in advanced land-based gas turbines
p 344 N95-26122

GASEOUS DIFFUSION

- Vertical transport rates in the stratosphere in 1993 from observations of CO₂, N₂O, and CH₄
[HTN-95-70941] p 351 A95-78006

GENERAL AVIATION AIRCRAFT

- Development of an intervention program to encourage shoulder harness use and aircraft retrofit in general aviation aircraft, phases 1 and 2
[DOT/FAA/AM-95/2] p 333 N95-24384

GLASS FIBER REINFORCED PLASTICS

- Study on tensile fatigue testing method of unidirectional fiber-resin matrix composites
[NAL-TR-1241] p 343 N95-24989

GLOBAL AIR POLLUTION

- Nitrous oxide and methane emissions from aero engines
[HTN-95-21363] p 353 A95-78678
- Impact of present aircraft emissions of nitrogen oxides on tropospheric ozone and climate forcing
[HTN-95-21364] p 353 A95-78679

GLOBAL POSITIONING SYSTEM

- Real-time testing and demonstration of the US Army Corps of Engineers' Real-Time On-The-Fly positioning system
[AD-A288624] p 334 N95-25609

GOVERNMENT PROCUREMENT

- Report to Congressional Committees. Tactical Aircraft: Concurrency in development and production of F-22 aircraft should be reduced
[GAO/NSIAD-95-59] p 336 N95-26338

GRID GENERATION (MATHEMATICS)

- Aerodynamic shape optimization of wing and wing-body configurations using control theory
[NASA-CR-198024] p 335 N95-25334
- A combined geometric approach for solving the Navier-Stokes equations on dynamic grids
[NASA-TM-106919] p 332 N95-26075

GROUND TESTS

- The Superoorbital Expansion Tube concept, experiment and analysis
p 341 N95-25399

H

H-60 HELICOPTER

- Configuration and other differences between Black Hawk and Seahawk helicopters in military service in the USA and Australia
[AR-008-386] p 336 N95-25935

HAMILTONIAN FUNCTIONS

- Dynamics of phase ordering of nematics in a pore
[DE95-807662] p 362 N95-25978

HARNESSES

- Development of an intervention program to encourage shoulder harness use and aircraft retrofit in general aviation aircraft, phases 1 and 2
[DOT/FAA/AM-95/2] p 333 N95-24384

HEAT FLUX

- Hypersonic model testing in a shock tunnel
[BTN-95-EIX95222650789] p 329 A95-79245
- Turbine-engine applications of thermographic-phosphor temperature measurements
[DE95-003625] p 358 N95-25110

HEAT TRANSFER

- Impingement cooling of an isothermally heated surface with a confined slot jet
[BTN-94-EIX94421348950] p 347 A95-78494

HEATING

- Residual Stress Measurements with Laser Speckle Correlation Interferometry and Local Heat Treating
[DE95-060082] p 349 N95-24598

HELICOPTER DESIGN

- Multilevel decomposition procedure for efficient design optimization of helicopter rotor blades
[BTN-95-EIX95222650784] p 334 A95-79240

HELICOPTER PERFORMANCE

- Dynamic stall control for advanced rotorcraft application
[BTN-95-EIX95222650793] p 334 A95-79249
- Rotorcraft handling qualities in turbulence
[BTN-95-EIX95242670750] p 334 A95-81097

HELICOPTER PROPELLER DRIVE

- A portable transmission vibration analysis system for the S-70A-9 Black Hawk helicopter
[DSTO-TR-0072] p 348 N95-24203

HELICOPTERS

- Interfacing a digital compass to a remote-controlled helicopter
[PB95-164927] p 340 N95-24260

HIGH ALTITUDE BALLOONS

- Application of fuzzy logic to optimize placement of an acquisition, tracking, and pointing experiment
p 341 A95-80390

HIGH REYNOLDS NUMBER

- Numerical and experimental study of drag characteristics of two-dimensional HLFC airfoils in high subsonic, high Reynolds number flow
[NAL-TR-1244T] p 331 N95-24998

HIGH SPEED

- Impact on ozone of high-speed stratospheric aircraft: Effects of the emission scenario
[HTN-95-51283] p 356 A95-80868

HIGH TEMPERATURE ENVIRONMENTS

- Aerodynamic characteristics of the orbital reentry vehicle experimental probe fins in a supersonic flow
[NAL-TR-1232] p 342 N95-25664

HIGH TEMPERATURE GASES

- High frequency flow-structural interaction in dense subsonic fluids
[NASA-CR-4652] p 330 N95-24217

HIGHLY MANEUVERABLE AIRCRAFT

- Robust dynamic inversion for control of highly maneuverable aircraft
[BTN-95-EIX95242670747] p 359 A95-81100

HOLOGRAPHIC INTERFEROMETRY

- Quantitative comparison between interferometric measurements and Euler computations for supersonic cone flows
[BTN-95-EIX95222650782] p 358 A95-79238

HOMING DEVICES

- Ideal proportional navigation
p 342 A95-81374

HOVERING

- Identification and simulation evaluation of a combat helicopter in hover
[BTN-95-EIX95242670749] p 335 A95-81098

HUBBLE SPACE TELESCOPE

- Guidance and control, 1993: Annual Rocky Mountain Guidance and Control Conference, 16th, Keystone, CO, Feb. 6-10, 1993
[ISBN-0-87703-365-X] p 341 A95-80389

HUMAN FACTORS ENGINEERING

- A crew-centered flight deck design philosophy for High-Speed Civil Transport (HSCT) aircraft
[NASA-TM-109171] p 335 N95-24582

HYDRATES

- Analysis of the physical state of one Arctic polar stratospheric cloud based on observations
[HTN-95-70917] p 351 A95-77982

- High-speed civil transport impact: Role of sulfate, nitric acid trihydrate, and ice aerosols studied with a two-dimensional model including aerosol physics
[HTN-95-91843] p 354 A95-80831

HYDROGEN

- The distribution of hydrogen, nitrogen, and chlorine radicals in the lower stratosphere: Implications for changes in O₃ due to emission of NO(y) from supersonic aircraft
[HTN-95-70935] p 351 A95-78000

HYDROGEN FUELS

- Shock tunnel studies of scramjet phenomena 1993
[NASA-CR-195038] p 350 N95-25384

HYDROGEN SULFIDE

- Analysis of the physical state of one Arctic polar stratospheric cloud based on observations
[HTN-95-70917] p 351 A95-77982

- An intercomparison of aircraft instrumentation for tropospheric measurements of carbonyl sulfide, hydrogen sulfide, and carbon disulfide
[HTN-95-91856] p 355 A95-80844

HYDROGRAPHY

- Real-time testing and demonstration of the US Army Corps of Engineers' Real-Time On-The-Fly positioning system
[AD-A288624] p 334 N95-25609

HYPERSONIC BOUNDARY LAYER

- Structure of a double-fin turbulent interaction at high speed
[BTN-95-EIX95222650780] p 347 A95-79236

HYPERSONIC FLIGHT

- Integrated development of the equations of motion for elastic hypersonic flight vehicles
[BTN-95-EIX95242670755] p 327 A95-81092

HYPERSONIC FLOW

- Structure of a double-fin turbulent interaction at high speed
[BTN-95-EIX95222650780] p 347 A95-79236

- Hypersonic model testing in a shock tunnel
[BTN-95-EIX95222650789] p 329 A95-79245

- Supercooling in hypersonic nitrogen wind tunnels
[BTN-94-EIX95011441134] p 340 A95-81020

- Verification of computational aerodynamic predictions for complex hypersonic vehicles using the INCA(trademark) code
[DE95-004757] p 330 N95-24308

- DSMC calculations for 70-deg blunt cone at 3.2 km/s in nitrogen
[NASA-TM-109181] p 348 N95-24396

HYPERSONIC HEAT TRANSFER

- Heat transfer measurements in small scale wind tunnels
[AD-A288689] p 341 N95-26053

HYPERSONIC SPEED

- Performance of an aerodynamic yaw controller mounted on the space shuttle orbiter body flap at Mach 10
[NASA-TM-109179] p 330 N95-24397

HYPERSONIC VEHICLES

- Integrated development of the equations of motion for elastic hypersonic flight vehicles
[BTN-95-EIX95242670755] p 327 A95-81092

- Verification of computational aerodynamic predictions for complex hypersonic vehicles using the INCA(trademark) code
[DE95-004757] p 330 N95-24308

- Reentry guidance for hypersonic Flight Experiment (HYFLEX) vehicle
[NAL-TR-1235] p 334 N95-25764

- Heat transfer measurements in small scale wind tunnels
[AD-A288689] p 341 N95-26053

HYPERSONIC WIND TUNNELS

- Supercooling in hypersonic nitrogen wind tunnels
[BTN-94-EIX95011441134] p 340 A95-81020

HYPERSONICS

- Hypersonic model testing in a shock tunnel
[BTN-95-EIX95222650789] p 329 A95-79245

- Integrated development of the equations of motion for elastic hypersonic flight vehicles
[BTN-95-EIX95242670755] p 327 A95-81092

ICE

- High-speed civil transport impact: Role of sulfate, nitric acid trihydrate, and ice aerosols studied with a two-dimensional model including aerosol physics
[HTN-95-91843] p 354 A95-80831

IDEAL GAS

- Recent improvements to and validation of the one dimensional NASA wave rotor model
[NASA-TM-106913] p 332 N95-25962

IMAGE ANALYSIS

- Aspect estimation of an aircraft using library model silhouettes
[PB95-141834] p 360 N95-25894

IMAGING TECHNIQUES

- Dynamic imaging and RCS measurements of aircraft
[BTN-95-EIX95202637582] p 347 A95-78576

IMPACT LOADS

- Analysis of warping effects on the static and dynamic response of a seat-type structure
[NIAR-94-12] p 348 N95-24211

IMPACT RESISTANCE

- Design and evaluation of a foam-filled hat-stiffened panel concept for aircraft primary structural applications
[NASA-TM-109175] p 346 N95-26251

IMPACT TESTS

- Impact, friction, and wear testing of microsamples of polycrystalline silicon
p 361 A95-79988

IMPULSES

- Thrust measurements of a complete axisymmetric scramjet in an impulse facility
p 339 N95-25395

IN-FLIGHT MONITORING

An overview of Health and Usage Monitoring Systems (HUMS) for military helicopters
[DSTO-TR-0061] p 327 N95-24200

INCOMPRESSIBLE FLUIDS

Dynamics of aircraft exhaust plumes in the jet-regime
[HTN-95-51275] p 355 A95-80860

INDEXES (DOCUMENTATION)

Aeronautical engineering: A continuing bibliography with indexes (supplement 316)
[NASA-SP-7037(316)] p 328 N95-24465

Aeronautical engineering: A continuing bibliography with indexes (supplement 317)
[NASA-SP-7037(317)] p 328 N95-25798

INFINITE SPAN WINGS

Three-dimensional interaction of wake/boundary-layer and vortex/boundary-layer data report
[CUED/A-AERO/TR-23] p 329 N95-24210

INFORMATION SYSTEMS

NLS Flight Simulation Laboratory (FSL) documentation
[NASA-CR-196564] p 363 N95-24439

INFRARED ASTRONOMY

SOFIA: Stratospheric Observatory for Infrared Astronomy
p 363 A95-81583

INFRARED SPECTRA

Modeling of aircraft exhaust emissions and infrared spectra for remote measurement of nitrogen oxides
[HTN-95-51276] p 355 A95-80861

INFRARED TELESCOPES

SOFIA: Stratospheric Observatory for Infrared Astronomy
p 363 A95-81583

INGESTION (ENGINES)

Bird ingestion into large turbofan engines
[DOT/FAA/CT-93/14] p 333 N95-24631

INLET FLOW

Prediction of supersonic inlet unstart caused by freestream disturbances
[BTN-95-EIX95222650790] p 329 A95-79246
Study of compressible flow through a rectangular-to-semiannular transition duct
[NASA-CR-4660] p 338 N95-24392

INLET NOZZLES

Study of compressible flow through a rectangular-to-semiannular transition duct
[NASA-CR-4660] p 338 N95-24392

INSPECTION

Estimate of probability of crack detection from service difficulty report data
[PB95-149381] p 328 N95-24295

INTERACTIONAL AERODYNAMICS

Structure of a double-lin turbulent interaction at high speed
[BTN-95-EIX95222650780] p 347 A95-79236

Three-dimensional interaction of wake/boundary-layer and vortex/boundary-layer data report
[CUED/A-AERO/TR-23] p 329 N95-24210

INTERFEROMETRY

Emerging nondestructive inspection for aging aircraft
[PB95-143053] p 328 N95-25401

INTERNAL FLOW

High frequency flow-structural interaction in dense subsonic fluids
[NASA-CR-4652] p 330 N95-24217

IONIZED GASES

Aerodynamic characteristics of the orbital reentry vehicle experimental probe fins in a supersonic flow
[NAL-TR-1232] p 342 N95-25664

IRON ALLOYS

NASA-UVA light aerospace alloy and structures technology program supplement: Aluminum-based materials for high speed aircraft
[NASA-CR-4645] p 343 N95-24878

ISCCP PROJECT

Preliminary analysis of University of North Dakota aircraft data from the FIRE Cirrus IFO-2
[NASA-CR-198038] p 357 N95-24219

ISOTHERMAL FLOW

Crossflow mixing of noncircular jets
[NASA-TM-106865] p 338 N95-24390

ISOTHERMAL PROCESSES

Impingement cooling of an isothermally heated surface with a confined slot jet
[BTN-94-EIX94421348950] p 347 A95-78494

J

J-85 ENGINE

The effect of altitude conditions on the particle emissions of a J85-GE-5L turbojet engine
[NASA-TM-106669] p 339 N95-24561

JET AIRCRAFT

Impact on ozone of high-speed stratospheric aircraft: Effects of the emission scenario
[HTN-95-51283] p 356 A95-80868

JET AIRCRAFT NOISE

Noise impact of advanced high lift systems
[NASA-CR-195028] p 362 N95-26160
Jet mixer noise suppressor using acoustic feedback
[NASA-CASE-LEW-15170-2] p 362 N95-26187

JET ENGINES

Nitrous oxide and methane emissions from aero engines
[HTN-95-21363] p 353 A95-78678

North Atlantic air traffic within the lower stratosphere: Cruising times and corresponding emissions
[HTN-95-91841] p 354 A95-80829

Effects on stratospheric ozone from high-speed civil transport: Sensitivity to stratospheric aerosol loading
[HTN-95-91842] p 354 A95-80830

Dynamics of aircraft exhaust plumes in the jet-regime
[HTN-95-51275] p 355 A95-80860

Dynamic behavior of a magnetic bearing supported jet engine rotor with auxiliary bearings
[NASA-CR-197860] p 338 N95-24213

A design perspective on thermal barrier coatings
p 344 N95-26120
Jet engine applications for materials with nanometer-scale dimensions
p 345 N95-26131

JET EXHAUST

Sensitivity of supersonic aircraft modeling studies to HNO₃ photolysis rate
[HTN-95-11475] p 353 A95-79453

Tracer transport for realistic aircraft emission scenarios calculated using a three-dimensional model
[HTN-95-41799] p 353 A95-80525

North Atlantic air traffic within the lower stratosphere: Cruising times and corresponding emissions
[HTN-95-91841] p 354 A95-80829

Effects on stratospheric ozone from high-speed civil transport: Sensitivity to stratospheric aerosol loading
[HTN-95-91842] p 354 A95-80830

Dynamics of aircraft exhaust plumes in the jet-regime
[HTN-95-51275] p 355 A95-80860

JET FLOW

Impingement cooling of an isothermally heated surface with a confined slot jet
[BTN-94-EIX94421348950] p 347 A95-78494

Dynamics of aircraft exhaust plumes in the jet-regime
[HTN-95-51275] p 355 A95-80860

Jet mixer noise suppressor using acoustic feedback
[NASA-CASE-LEW-15170-2] p 362 N95-26187

JET IMPINGEMENT

Impingement cooling of an isothermally heated surface with a confined slot jet
[BTN-94-EIX94421348950] p 347 A95-78494

JET MIXING FLOW

Crossflow mixing of noncircular jets
[NASA-TM-106865] p 338 N95-24390

Jet mixer noise suppressor using acoustic feedback
[NASA-CASE-LEW-15170-2] p 362 N95-26187

JET THRUST

Scramjet thrust measurement in a shock tunnel
p 339 N95-25396

JOURNAL BEARINGS

Thermohydrodynamic analysis of cryogenic liquid turbulent flow fluid film bearings, phase 2
[NASA-CR-197412] p 349 N95-24461

K

K-EPSILON TURBULENCE MODEL

Dynamics of aircraft exhaust plumes in the jet-regime
[HTN-95-51275] p 355 A95-80860

KAWASAKI AIRCRAFT

A quiet STOL Research Aircraft Development program
[NAL-TR-1223] p 336 N95-25862

KINETICS

Dynamics of phase ordering of nematics in a pore
[DE95-607662] p 362 N95-25978

L

LABOR

Partial camera automation in a simulated Unmanned Air Vehicle
[AD-A288786] p 337 N95-26190

LABORATORIES

NLS Flight Simulation Laboratory (FSL) documentation
[NASA-CR-196564] p 363 N95-24439

LAMINAR FLOW

Impingement cooling of an isothermally heated surface with a confined slot jet
[BTN-94-EIX94421348950] p 347 A95-78494

Numerical and experimental study of drag characteristics of two-dimensional HLFC airfoils in high subsonic, high Reynolds number flow
[NAL-TR-1244T] p 331 N95-24998

LAMINAR FLOW AIRFOILS

Numerical and experimental study of drag characteristics of two-dimensional HLFC airfoils in high subsonic, high Reynolds number flow
[NAL-TR-1244T] p 331 N95-24998

LAP JOINTS

Estimate of probability of crack detection from service difficulty report data
[PB95-149381] p 328 N95-24295

LASER APPLICATIONS

Residual Stress Measurements with Laser Speckle Correlation Interferometry and Local Heat Treating
[DE95-060082] p 349 N95-24598

LASERS

Laser device for measuring a vessel's speed
[HTN-95-60992] p 361 A95-80633

LATITUDE MEASUREMENT

Latitude variations of stratospheric trace gases
[HTN-95-70948] p 352 A95-78013

LAUNCH VEHICLES

Load alleviation maneuvers for a launch vehicle
p 342 A95-81360

LEADING EDGE SLATS

Dynamic stall control for advanced rotorcraft application
[BTN-95-EIX95222650793] p 334 A95-79249

Three-dimensional interaction of wake/boundary-layer and vortex/boundary-layer data report
[CUED/A-AERO/TR-23] p 329 N95-24210

LEADING EDGES

Dynamic stall control for advanced rotorcraft application
[BTN-95-EIX95222650793] p 334 A95-79249

A theoretical and experimental investigation of the flow over supersonic leading edge wing/body configurations
[DRA-TM-AERO-PROP-41] p 331 N95-25649

LEAST SQUARES METHOD

Describing an attitude
p 342 A95-80409
Aerodynamic parameter estimation via Fourier modulating function techniques
[NASA-CR-4654] p 335 N95-24630

LIBRARIES

Aspect estimation of an aircraft using library model silhouettes
[PB95-141834] p 360 N95-25894

LIFE (DURABILITY)

Thermal barrier coating life modeling in aircraft gas turbine engines
p 346 N95-26140

LIFE SCIENCES

NASA video catalog
[NASA-SP-7109(01)] p 363 N95-24238

JPRS Report: Science and technology. Central Eurasia
[JPRS-UST-94-032] p 350 N95-24759

LIFT

Dynamic stall control for advanced rotorcraft application
[BTN-95-EIX95222650793] p 334 A95-79249

Unsteady lift on a swept blade tip
[BTN-94-EIX95011441154] p 329 A95-80030

NREL airfoil families for HAWTs
[DE95-000267] p 357 N95-24882

Aerodynamic characteristics of the orbital reentry vehicle experimental probe fins in a supersonic flow
[NAL-TR-1232] p 342 N95-25664

Noise impact of advanced high lift systems
[NASA-CR-195028] p 362 N95-26160

LIFT DRAG RATIO

Low speed aerodynamic characteristics of delta wings with vortex flaps: 60 deg and 70 deg delta wings
[NAL-TR-1245] p 331 N95-25105

LIFT FANS

Aerodynamics model for a generic ASTOVL lift-fan aircraft
[NASA-TM-110347] p 332 N95-26302

LIGHT ALLOYS

NASA-UVA light aerospace alloy and structures technology program (LA2ST)
[NASA-CR-198041] p 343 N95-24220

LIGHTNING

Identification of aviation weather hazards based on the integration of radar and lightning data
[HTN-95-51323] p 356 A95-80908

LINE OF SIGHT

Characterizing the wake vortex signature for an active line of sight remote sensor
[NASA-CR-197697] p 333 N95-24391

LINEAR QUADRATIC REGULATOR

Dynamics and control of a tethered flight vehicle
[BTN-95-EIX95242670754] p 342 A95-81093

Fundamental mechanisms of aeroelastic control with control surface and strain actuation
[BTN-95-EIX95242670746] p 327 A95-81101

Load alleviation maneuvers for a launch vehicle
p 342 A95-81360

LIQUID CRYSTALS

- Dynamics of phase ordering of nematics in a pore
[DE95-607662] p 362 N95-25978

LIQUID FLOW

- Thermohydrodynamic analysis of cryogenic liquid turbulent flow fluid film bearings, phase 2
[NASA-CR-197412] p 349 N95-24461

LITHIUM ALLOYS

- NASA-UVA light aerospace alloy and structures technology program supplement: Aluminum-based materials for high speed aircraft
[NASA-CR-4645] p 343 N95-24878

LOADS (FORCES)

- Load alleviation maneuvers for a launch vehicle
p 342 A95-81360

LOCAL AREA NETWORKS

- NLS Flight Simulation Laboratory (FSL) documentation
[NASA-CR-198564] p 363 N95-24439

LONGITUDINAL CONTROL

- Robust dynamic inversion for control of highly maneuverable aircraft
[BTN-95-EIX95242670747] p 359 A95-81100

LOW SPEED

- Low speed aerodynamic characteristics of delta wings with vortex flaps: 60 deg and 70 deg delta wings
[NAL-TR-1245] p 331 N95-25105

M

MACH NUMBER

- Study of subsonic base cavity flowfield structure using particle image velocimetry
[BTN-95-EIX95222650781] p 327 A95-79237

MACHINE LEARNING

- On-line learning nonlinear direct neurocontrollers for restructurable control systems
[BTN-95-EIX95242670768] p 359 A95-81079

MAGNESIUM ALLOYS

- NASA-UVA light aerospace alloy and structures technology program supplement: Aluminum-based materials for high speed aircraft
[NASA-CR-4645] p 343 N95-24878

MAGNETIC BEARINGS

- Dynamic behavior of a magnetic bearing supported jet engine rotor with auxiliary bearings
[NASA-CR-197860] p 338 N95-24213

MAN MACHINE SYSTEMS

- A crew-centered flight deck design philosophy for High-Speed Civil Transport (HSCT) aircraft
[NASA-TM-109171] p 335 N95-24582

MANEUVERABILITY

- Determination of piloting feedback structures for an altitude tracking task
[BTN-95-EIX95242670770] p 327 A95-81077
Rotorcraft handling qualities in turbulence
[NASA-CR-197860] p 334 A95-81097
Robust dynamic inversion for control of highly maneuverable aircraft
[BTN-95-EIX95242670747] p 359 A95-81100

MANNED SPACE FLIGHT

- NASA video catalog
[NASA-SP-7109(01)] p 363 N95-24238

MARINE ENVIRONMENTS

- An intercomparison of instrumentation for tropospheric measurements of dimethyl sulfide: Aircraft results for concentrations at the parts-per-trillion level
[HTN-95-91857] p 355 A95-80845

MARINER MARK 2 SPACECRAFT

- The Cassini spacecraft: Object oriented flight control software
p 359 A95-80405

MATCHING

- Orientation determination of aircraft using visual 3D matching and radar. Case study 2
[PB95-165791] p 350 N95-25749

MATERIALS SCIENCE

- JPRS report: Science and technology. Central Eurasia
[JPRS-UST-94-018] p 349 N95-24472

MATHEMATICAL LOGIC

- Application of fuzzy logic to optimize placement of an acquisition, tracking, and pointing experiment
p 341 A95-80390

MATHEMATICAL MODELS

- Viscoplastic response of structures for intense local heating
[HTN-95-41540] p 346 A95-77921
Theoretical and experimental studies of fretting-initiated fatigue failure of aeroengine compressor discs
[BTN-94-EIX94421372285] p 343 A95-78467
Modeling of aircraft exhaust emissions and infrared spectra for remote measurement of nitrogen oxides
[HTN-95-51276] p 355 A95-80861
Chemical composition and photochemical reactivity of exhaust from aircraft turbine engines
[HTN-95-51277] p 356 A95-80862

- Impact of near-coincident faults on digital flight control systems
[BTN-95-EIX95242670759] p 359 A95-81088

- Effect of density gradients in confined supersonic shear layers, part 1
[NASA-CR-198029] p 348 N95-24412

- Effect of density gradients in confined supersonic shear layers. Part 2: 3-D modes
[NASA-CR-198030] p 349 N95-24413

- Aerodynamic parameter estimation via Fourier modulating function techniques
[NASA-CR-4654] p 335 N95-24630

- Recent improvements to and validation of the one dimensional NASA wave rotor model
[NASA-TM-106913] p 332 N95-25962

- Thermal barrier coating life modeling in aircraft gas turbine engines
p 346 N95-26140

- Aerodynamics model for a generic ASTOVL lift-fan aircraft
[NASA-TM-110347] p 332 N95-26302

MATRICES (MATHEMATICS)

- Describing an attitude
p 342 A95-80409

MAXIMUM LIKELIHOOD ESTIMATES

- Estimate of probability of crack detection from service difficulty report data
[PB95-149381] p 328 N95-24295

MEASURING INSTRUMENTS

- An intercomparison of aircraft instrumentation for tropospheric measurements of sulfur dioxide
[HTN-95-91855] p 354 A95-80643

- An intercomparison of aircraft instrumentation for tropospheric measurements of carbonyl sulfide, hydrogen sulfide, and carbon disulfide
[HTN-95-91856] p 355 A95-80644

- An intercomparison of instrumentation for tropospheric measurements of dimethyl sulfide: Aircraft results for concentrations at the parts-per-trillion level
[HTN-95-91857] p 355 A95-80845

- Workshop report: Measurement techniques in highly transient, spectrally rich combustion environments
[AD-A288395] p 350 N95-25606

MECHANICAL DEVICES

- Preload release mechanism
[NASA-CASE-MSC-22327-1] p 350 N95-25592

MECHANICAL ENGINEERING

- NASA-UVA light aerospace alloy and structures technology program (LA2ST)
[NASA-CR-198041] p 343 N95-24220

- JPRS report: Science and technology. Central Eurasia
[JPRS-UST-94-027] p 349 N95-24470

MEDICAL SCIENCE

- JPRS Report: Science and technology. Central Eurasia
[JPRS-UST-94-032] p 350 N95-24759

MERIDIONAL FLOW

- Meridional distributions of NO(X), NO(Y), and other species in the lower stratosphere and upper troposphere during AASE 2
[HTN-95-70944] p 352 A95-78009

METAL FATIGUE

- Proceedings of the 2d USAF Aging Aircraft Conference
[AD-A288217] p 336 N95-25578

METAL MATRIX COMPOSITES

- NASA-UVA light aerospace alloy and structures technology program supplement: Aluminum-based materials for high speed aircraft
[NASA-CR-4645] p 343 N95-24878

METASTABLE STATE

- Supercooling in hypersonic nitrogen wind tunnels
[BTN-94-EIX95011441134] p 340 A95-81020

METEOROLOGY

- Vertical transport rates in the stratosphere in 1993 from observations of CO₂, N₂O, and CH₄
[HTN-95-70941] p 351 A95-78006

- Chemical change in the arctic vortex during AASE 2
[HTN-95-70947] p 352 A95-78012

METHANE

- Vertical transport rates in the stratosphere in 1993 from observations of CO₂, N₂O, and CH₄
[HTN-95-70941] p 351 A95-78006

- Nitrous oxide and methane emissions from aero engines
[HTN-95-21363] p 353 A95-78678

MICROMECHANICS

- Impact, friction, and wear testing of microsamples of polycrystalline silicon
p 361 A95-79988

MICROSTRUCTURE

- NASA-UVA light aerospace alloy and structures technology program (LA2ST)
[NASA-CR-198041] p 343 N95-24220

MILITARY HELICOPTERS

- Rotorcraft handling qualities in turbulence
[BTN-95-EIX95242670750] p 334 A95-81097

- An overview of Health and Usage Monitoring Systems (HUMS) for military helicopters
[DSTO-TR-0061] p 327 N95-24200

- Helicopter life substantiation: Review of some USA and UK initiatives
[DSTO-TR-0062] p 328 N95-24201

MISSILE CONTROL

- High-performance, robust, bank-to-turn missile autopilot design
[BTN-95-EIX95242670751] p 336 A95-81096

- Ideal proportional navigation
p 342 A95-81374

MISSILE LAUNCHERS

- SR-71 may launch targets for missile defense tests
[HTN-95-91872] p 335 A95-81974

MISSILE SYSTEMS

- SR-71 may launch targets for missile defense tests
[HTN-95-91872] p 335 A95-81974

MISSILES

- High-performance, robust, bank-to-turn missile autopilot design
[BTN-95-EIX95242670751] p 336 A95-81096

MIXERS

- Jet mixer noise suppressor using acoustic feedback
[NASA-CASE-LEW-15170-2] p 362 N95-26187

MIXING RATIOS

- An analysis of aircraft exhaust plumes from accidental encounters
[HTN-95-70943] p 351 A95-78008

MODES (STANDING WAVES)

- Effect of density gradients in confined supersonic shear layers. Part 2: 3-D modes
[NASA-CR-198030] p 349 N95-24413

MODULATION

- Aerodynamic parameter estimation via Fourier modulating function techniques
[NASA-CR-4654] p 335 N95-24630

MOLECULAR INTERACTIONS

- Empirical corrections of the rigid rotor interaction potential of H₂-H₂ in the attractive region: Dimer features in the FIR absorption spectra
[HTN-95-41943] p 361 A95-81690

MONTE CARLO METHOD

- DSMC calculations for 70-deg blunted cone at 3.2 km/s in nitrogen
[NASA-TM-109181] p 348 N95-24396

MOTION PICTURES

- NASA video catalog
[NASA-SP-7109(01)] p 363 N95-24238

MOTION STABILITY

- Determination of piloting feedback structures for an altitude tracking task
[BTN-95-EIX95242670770] p 327 A95-81077

MULTIDISCIPLINARY DESIGN OPTIMIZATION

- Multilevel decomposition procedure for efficient design optimization of helicopter rotor blades
[BTN-95-EIX95222650784] p 334 A95-79240

- Aeroservoelastic aspects of wing/control surface platform shape optimization
[BTN-95-EIX95222650795] p 340 A95-79251

- Aerodynamic optimization studies on advanced architecture computers
[NASA-CR-198045] p 330 N95-24379

MULTIVARIABLE CONTROL

- High-performance, robust, bank-to-turn missile autopilot design
[BTN-95-EIX95242670751] p 336 A95-81096

N

NATIONAL AIRSPACE SYSTEM

- Federal Aviation Administration plan for research, engineering and development, 1995
p 363 N95-24202

- Aviation system capacity improvements through technology
[NASA-TM-109165] p 333 N95-24633

NAVIER-STOKES EQUATION

- Verification of computational aerodynamic predictions for complex hypersonic vehicles using the INCA(trademark) code
[DE95-004757] p 330 N95-24308

- A combined geometric approach for solving the Navier-Stokes equations on dynamic grids
[NASA-TM-106919] p 332 N95-26075

NEAR WAKES

- Study of subsonic base cavity flowfield structure using particle image velocimetry
[BTN-95-EIX95222650781] p 327 A95-79237

- DSMC calculations for 70-deg blunted cone at 3.2 km/s in nitrogen
[NASA-TM-109181] p 348 N95-24396

NEURAL NETS

- On-line learning nonlinear direct neurocontrollers for restructurable control systems
[BTN-95-EIX95242670768] p 359 A95-81079

- Direct adaptive and neural control of wing-rock motion of slender delta wings
[BTN-95-EIX95242670748] p 327 A95-81099
Application of neural networks to unsteady aerodynamic control p 360 N95-25264

NICKEL ALLOYS

- Viscoplastic response of structures for intense local heating
[HTN-95-41540] p 346 A95-77921

NITRIC ACID

- Analysis of the physical state of one Arctic polar stratospheric cloud based on observations
[HTN-95-70917] p 351 A95-77982
Sensitivity of supersonic aircraft modelling studies to HNO₃ photolysis rate
[HTN-95-11475] p 353 A95-79453
High-speed civil transport impact: Role of sulfate, nitric acid trihydrate, and ice aerosols studied with a two-dimensional model including aerosol physics
[HTN-95-91843] p 354 A95-80831
Impact on ozone of high-speed stratospheric aircraft: Effects of the emission scenario
[HTN-95-51283] p 356 A95-80868

NITROGEN

- The distribution of hydrogen, nitrogen, and chlorine radicals in the lower stratosphere: Implications for changes in O₃ due to emission of NO(y) from supersonic aircraft
[HTN-95-70935] p 351 A95-78000
Supercooling in hypersonic nitrogen wind tunnels
[BTN-94-EIX95011441134] p 340 A95-81020
DSMC calculations for 70-deg blunted cone at 3.2 km/s in nitrogen
[NASA-TM-109181] p 348 N95-24396

NITROGEN OXIDES

- Analysis of the physical state of one Arctic polar stratospheric cloud based on observations
[HTN-95-70917] p 351 A95-77982
The distribution of hydrogen, nitrogen, and chlorine radicals in the lower stratosphere: Implications for changes in O₃ due to emission of NO(y) from supersonic aircraft
[HTN-95-70935] p 351 A95-78000
Vertical transport rates in the stratosphere in 1993 from observations of CO₂, N₂O, and CH₄
[HTN-95-70941] p 351 A95-78006
Meridional distributions of NO(X), NO(Y), and other species in the lower stratosphere and upper troposphere during AASE 2
[HTN-95-70944] p 352 A95-78009
Impact of present aircraft emissions of nitrogen oxides on tropospheric ozone and climate forcing
[HTN-95-21364] p 353 A95-78679
Sensitivity of supersonic aircraft modelling studies to HNO₃ photolysis rate
[HTN-95-11475] p 353 A95-79453
Tracer transport for realistic aircraft emission scenarios calculated using a three-dimensional model
[HTN-95-41799] p 353 A95-80525
Modeling of aircraft exhaust emissions and infrared spectra for remote measurement of nitrogen oxides
[HTN-95-51276] p 355 A95-80861
Potential effects on ozone of future supersonic aircraft/2D simulation
[HTN-95-51282] p 356 A95-80867
Impact on ozone of high-speed stratospheric aircraft: Effects of the emission scenario
[HTN-95-51283] p 356 A95-80868
Nitrogen oxide emissions and their control from uninstalled aircraft engines in enclosed test cells: Joint report to Congress on the Environmental Protection Agency - Department of Transportation study
[PB95-166237] p 358 N95-26005

NITROUS OXIDES

- Nitrous oxide and methane emissions from aero engines
[HTN-95-21363] p 353 A95-78678

NOISE PREDICTION

- Unsteady lift on a swept blade tip
[BTN-94-EIX95011441154] p 329 A95-80030

NOISE REDUCTION

- Noise impact of advanced high lift systems
[NASA-CR-195028] p 362 N95-26160
Jet mixer noise suppressor using acoustic feedback
[NASA-CASE-LEW-15170-2] p 362 N95-26187

NONDESTRUCTIVE TESTS

- Emerging nondestructive inspection for aging aircraft
[PB95-143053] p 328 N95-25401
Proceedings of the 2d USAF Aging Aircraft Conference
[AD-A288217] p 336 N95-25578

NONLINEAR PROGRAMMING

- Application of direct transcription to commercial aircraft trajectory optimization
[BTN-95-EIX95242670766] p 359 A95-81081

NORTHERN HEMISPHERE

- North Atlantic air traffic within the lower stratosphere: Cruising times and corresponding emissions
[HTN-95-91841] p 354 A95-80829

NOZZLE DESIGN

- Internal performance characteristics of thrust-vectoring axisymmetric ejector nozzles
[NASA-TM-4610] p 331 N95-25338

NOZZLE EFFICIENCY

- Internal performance characteristics of thrust-vectoring axisymmetric ejector nozzles
[NASA-TM-4610] p 331 N95-25338

NOZZLE GEOMETRY

- Thrust measurement in a 2-D scramjet nozzle
p 339 N95-25397

NOZZLE WALLS

- Supersonic quiet-tunnel development for laminar-turbulent transition research
[NASA-CR-198040] p 340 N95-24302

NUMERICAL CONTROL

- Guidance and control, 1993: Annual Rocky Mountain Guidance and Control Conference, 16th, Keystone, CO, Feb. 6-10, 1993
[ISBN-0-87703-365-X] p 341 A95-80389
The Cassini spacecraft: Object oriented flight control software p 359 A95-80405
A new guidance and flight control system for the DELTA 2 launch vehicle --- Abstract only p 342 A95-80427

O**OBJECT-ORIENTED PROGRAMMING**

- The Cassini spacecraft: Object oriented flight control software p 359 A95-80405

OBLIQUE SHOCK WAVES

- Structure of a double-fin turbulent interaction at high speed
[BTN-95-EIX95222650780] p 347 A95-79236

ONE DIMENSIONAL FLOW

- Recent improvements to and validation of the one dimensional NASA wave rotor model
[NASA-TM-106913] p 332 N95-25962

OPERATIONAL HAZARDS

- Quantity-distance requirements for earth-bermed aircraft shelters
[AD-A279692] p 341 N95-24424

OPTICAL FIBERS

- Preliminary experiments of an optical fiber display
[NAL-TR-1257] p 362 N95-25004

OPTICAL MEASUREMENT

- Laser device for measuring a vessel's speed
[HTN-95-60992] p 361 A95-80633
Angular displacement measuring device
[NASA-CASE-ARC-11937-1] p 362 N95-26015

OPTICAL MEASURING INSTRUMENTS

- The 1994 Fiber Optic Sensors for Aerospace Technology (FOSAT) Workshop
[NASA-CP-10166] p 337 N95-24207

OPTICAL TRACKING

- Orientation determination of aircraft using visual 3D matching and radar. Case study 2
[PB95-165791] p 350 N95-25749

OPTICS

- JPRS report: Science and technology. Central Eurasia
[JPRS-UST-94-018] p 349 N95-24472

OPTIMAL CONTROL

- Application of direct transcription to commercial aircraft trajectory optimization
[BTN-95-EIX95242670766] p 359 A95-81081
Fundamental mechanisms of aeroelastic control with control surface and strain actuation
[BTN-95-EIX95242670746] p 327 A95-81101

OPTIMIZATION

- Aerodynamic optimization studies on advanced architecture computers
[NASA-CR-198045] p 330 N95-24379
Geometric analysis of wing sections
[NASA-TM-110346] p 335 N95-24629
Aerodynamic shape optimization of wing and wing-body configurations using control theory
[NASA-CR-198024] p 335 N95-25334

ORTHO HYDROGEN

- Empirical corrections of the rigid rotor interaction potential of H₂-H₂ in the attractive region: Dimer features in the FIR absorption spectra
[HTN-95-41943] p 361 A95-81690

OSCILLATING FLOW

- Experimental study of flow separation on an oscillating flap at Mach 2.4
[BTN-95-EIX95222650792] p 329 A95-79248
On the role of the outer region in the turbulent-boundary-layer bursting process
[BTN-94-EIX95011441078] p 348 A95-81056

OSCILLATIONS

- Flow due to an oscillating sphere and an expression for unsteady drag on the sphere at finite Reynolds number
[BTN-94-EIX95011441142] p 347 A95-81012

OXIDATION RESISTANCE

- Thermal barrier coating experience in the gas turbine engine p 345 N95-26125

OZONE

- The distribution of hydrogen, nitrogen, and chlorine radicals in the lower stratosphere: Implications for changes in O₃ due to emission of NO(y) from supersonic aircraft
[HTN-95-70935] p 351 A95-78000
Meridional distributions of NO(X), NO(Y), and other species in the lower stratosphere and upper troposphere during AASE 2
[HTN-95-70944] p 352 A95-78009
Effects on stratospheric ozone from high-speed civil transport: Sensitivity to stratospheric aerosol loading
[HTN-95-91842] p 354 A95-80830
Potential effects on ozone of future supersonic aircraft/2D simulation
[HTN-95-51282] p 356 A95-80867
Impact on ozone of high-speed stratospheric aircraft: Effects of the emission scenario p 356 A95-80868
The atmospheric effects of stratospheric aircraft: A fourth program report
[NASA-RP-1359] p 357 N95-24274

OZONE DEPLETION

- An analysis of aircraft exhaust plumes form accidental encounters
[HTN-95-70943] p 351 A95-78008
Meridional distributions of NO(X), NO(Y), and other species in the lower stratosphere and upper troposphere during AASE 2
[HTN-95-70944] p 352 A95-78009
Sensitivity of supersonic aircraft modelling studies to HNO₃ photolysis rate
[HTN-95-11475] p 353 A95-79453
Effects on stratospheric ozone from high-speed civil transport: Sensitivity to stratospheric aerosol loading
[HTN-95-91842] p 354 A95-80830
High-speed civil transport impact: Role of sulfate, nitric acid trihydrate, and ice aerosols studied with a two-dimensional model including aerosol physics
[HTN-95-91843] p 354 A95-80831

OZONOSPHERE

- Impact of present aircraft emissions of nitrogen oxides on tropospheric ozone and climate forcing
[HTN-95-21364] p 353 A95-78679

P**PANELS**

- Design and evaluation of a foam-filled hat-stiffened panel concept for aircraft primary structural applications
[NASA-TM-109175] p 346 N95-26251

PARA HYDROGEN

- Empirical corrections of the rigid rotor interaction potential of H₂-H₂ in the attractive region: Dimer features in the FIR absorption spectra
[HTN-95-41943] p 361 A95-81690

PARALLEL COMPUTERS

- Fault detection in multiprocessor systems and array processors
[BTN-95-EIX95242679097] p 359 A95-81253

PARALLEL PROCESSING (COMPUTERS)

- Fault detection in multiprocessor systems and array processors
[BTN-95-EIX95242679097] p 359 A95-81253
Aerodynamic optimization studies on advanced architecture computers
[NASA-CR-198045] p 330 N95-24379
The coupling of fluids, dynamics, and controls on advanced architecture computers
[NASA-CR-197727] p 360 N95-25797

PARAMETER IDENTIFICATION

- Impact of near-concurrent faults on digital flight control systems
[BTN-95-EIX95242670759] p 359 A95-81088
Identification and simulation evaluation of a combat helicopter in hover
[BTN-95-EIX95242670749] p 335 A95-81098
Aerodynamic parameter estimation via Fourier modulating function techniques
[NASA-CR-4654] p 335 N95-24630
Actuating signals in adaptive control systems
[IFTR-13/1994] p 361 N95-26330

PARTICLE IMAGE VELOCIMETRY

- Study of subsonic base cavity flowfield structure using particle image velocimetry
[BTN-95-EIX95222650781] p 327 A95-79237

- Flow structure in the lee of an inclined 6:1 prolate spheroid
[BTN-94-EIX95011441127] p 348 A95-81027
- PARTICLE SIZE DISTRIBUTION**
The effect of altitude conditions on the particle emissions of a J85-GE-5L turbojet engine
[NASA-TM-106669] p 339 N95-24561
- PASSENGER AIRCRAFT**
Noise impact of advanced high lift systems
[NASA-CR-195028] p 362 N95-26160
- PERFORMANCE PREDICTION**
SOFIA: Stratospheric Observatory for Infrared Astronomy p 363 A95-81583
Effect of film cooling/regenerative cooling on scramjet engine performances
[NAL-TR-1242] p 339 N95-24990
- PERFORMANCE TESTS**
Flight reference display for powered-lift STOL aircraft
[NAL-TR-1251] p 337 N95-25005
Internal performance characteristics of thrust-vectorized axisymmetric ejector nozzles
[NASA-TM-4610] p 331 N95-25338
Wind technology development: Large and small turbines
[DE95-000286] p 358 N95-26090
- PHASE TRANSFORMATIONS**
High-speed civil transport impact: Role of sulfate, nitric acid trihydrate, and ice aerosols studied with a two-dimensional model including aerosol physics
[HTN-95-91843] p 354 A95-80831
- PHOTOCHEMICAL REACTIONS**
High-speed civil transport impact: Role of sulfate, nitric acid trihydrate, and ice aerosols studied with a two-dimensional model including aerosol physics
[HTN-95-91843] p 354 A95-80831
Chemical composition and photochemical reactivity of exhaust from aircraft turbine engines
[HTN-95-51277] p 356 A95-80862
The atmospheric effects of stratospheric aircraft: A fourth program report
[NASA-RP-1359] p 357 N95-24274
- PHOTOLYSIS**
Sensitivity of supersonic aircraft modelling studies to HNO₃ photolysis rate
[HTN-95-11475] p 353 A95-79453
- PHOTOMETERS**
Angular displacement measuring device
[NASA-CASE-ARC-11937-1] p 362 N95-26015
- PHOTONS**
The 1994 Fiber Optic Sensors for Aerospace Technology (FOSAT) Workshop
[NASA-CP-10166] p 337 N95-24207
- PHOTOVOLTAIC CONVERSION**
Wind technology development: Large and small turbines
[DE95-000286] p 358 N95-26090
- PIPER AIRCRAFT**
Aircraft accident report: Impact with blast fence upon landing rollout Action Air Charters flight 990 Piper PA-31-350, N990RA, Stratford, Connecticut, 27 April 1994
[PB94-910410] p 333 N95-24206
- PITCHING MOMENTS**
Dynamic stall control for advanced rotorcraft application
[BTN-95-EIX95222650793] p 334 A95-79249
- PLASMA SPRAYING**
Thermal conductivity of zirconia thermal barrier coatings
p 345 N95-26133
- PLUMES**
An analysis of aircraft exhaust plumes from accidental encounters
[HTN-95-70943] p 351 A95-78008
Dynamics of aircraft exhaust plumes in the jet-regime
[HTN-95-51275] p 355 A95-80860
The atmospheric effects of stratospheric aircraft: A fourth program report
[NASA-RP-1359] p 357 N95-24274
- POINTING CONTROL SYSTEMS**
Application of fuzzy logic to optimize placement of an acquisition, tracking, and pointing experiment
p 341 A95-80390
- POLAR REGIONS**
Latitude variations of stratospheric trace gases
[HTN-95-70948] p 352 A95-78013
Fine-scale, poleward transport of tropical air during AASE 2
[HTN-95-70949] p 352 A95-78014
- POLARIZED LIGHT**
Angular displacement measuring device
[NASA-CASE-ARC-11937-1] p 362 N95-26015
- POLLUTION CONTROL**
Small gas turbine component evaluation study
[PB95-147542] p 338 N95-24293
- Parts washing alternatives study: United States Coast Guard. Project summary and report
[PB95-166146] p 343 N95-26004
- POLLUTION MONITORING**
An analysis of aircraft exhaust plumes from accidental encounters
[HTN-95-70943] p 351 A95-78008
Comparison of column abundances from three infrared spectrometers during AASE 2
[HTN-95-70946] p 352 A95-78011
Chemical change in the arctic vortex during AASE 2
[HTN-95-70947] p 352 A95-78012
Fine-scale, poleward transport of tropical air during AASE 2
[HTN-95-70949] p 352 A95-78014
Chemical composition and photochemical reactivity of exhaust from aircraft turbine engines
[HTN-95-51277] p 356 A95-80862
Nitrogen oxide emissions and their control from uninstalled aircraft engines in enclosed test cells: Joint report to Congress on the Environmental Protection Agency - Department of Transportation study
[PB95-166237] p 358 N95-26005
- POLLUTION TRANSPORT**
Tracer transport for realistic aircraft emission scenarios calculated using a three-dimensional model
[HTN-95-41799] p 353 A95-80525
Effects on stratospheric ozone from high-speed civil transport: Sensitivity to stratospheric aerosol loading
[HTN-95-91842] p 354 A95-80830
- POLYCRYSTALS**
Impact, friction, and wear testing of microsamples of polycrystalline silicon
p 361 A95-79988
- PORTABLE EQUIPMENT**
A portable transmission vibration analysis system for the S-70A-9 Black Hawk helicopter
[DSTO-TR-0072] p 348 N95-24203
- POSITION INDICATORS**
Real-time testing and demonstration of the US Army Corps of Engineers' Real-Time On-The-Fly positioning system
[AD-A288624] p 334 N95-25609
- POTENTIAL ENERGY**
Empirical corrections of the rigid rotor interaction potential of H₂-H₂ in the attractive region: Dimer features in the FIR absorption spectra
[HTN-95-41943] p 361 A95-81690
- POWER PLANTS**
Wind technology development: Large and small turbines
[DE95-000286] p 358 N95-26090
- POWERED LIFT AIRCRAFT**
Flight reference display for powered-lift STOL aircraft
[NAL-TR-1251] p 337 N95-25005
A quiet STOL Research Aircraft Development program
[NAL-TR-1223] p 336 N95-25862
- PRESSURE DISTRIBUTION**
Hypersonic model testing in a shock tunnel
[BTN-95-EIX95222650789] p 329 A95-79245
Experimental study of the effects of Reynolds number on high angle of attack aerodynamic characteristics of forebodies during rotary motion
[NASA-CR-195033] p 330 N95-24443
- PRESSURE DRAG**
A theoretical and experimental investigation of the flow over supersonic leading edge wing/body configurations
[DRA-TM-AERO-PROP-41] p 331 N95-25649
- PRESSURE EFFECTS**
Prediction of supersonic inlet unstart caused by freestream disturbances
[BTN-95-EIX95222650790] p 329 A95-79246
- PRESSURE MEASUREMENT**
Workshop report: Measurement techniques in highly transient, spectrally rich combustion environments
[AD-A288395] p 350 N95-25606
- PRESSURE RATIO**
Internal performance characteristics of thrust-vectorized axisymmetric ejector nozzles
[NASA-TM-4610] p 331 N95-25338
- PROBLEM SOLVING**
Aerodynamic parameter estimation via Fourier modulating function techniques
[NASA-CR-4654] p 335 N95-24630
- PRODUCT DEVELOPMENT**
A quiet STOL Research Aircraft Development program
[NAL-TR-1223] p 336 N95-25862
- PROGRAM VERIFICATION (COMPUTERS)**
Verification of computational aerodynamic predictions for complex hypersonic vehicles using the INCA(trademark) code
[DE95-004757] p 330 N95-24308
- PROLATE SPHEROIDS**
Flow structure in the lee of an inclined 6:1 prolate spheroid
[BTN-94-EIX95011441127] p 348 A95-81027
- PROPORTIONAL CONTROL**
Ideal proportional navigation p 342 A95-81374
- PROPULSION**
Advanced subsonic airplane design and economic studies
[NASA-CR-195443] p 338 N95-24304
Workshop report: Measurement techniques in highly transient, spectrally rich combustion environments
[AD-A288395] p 350 N95-25606
- PROTECTION**
Development of a model protection and dynamic response monitoring system for the national transonic facility
[NASA-CR-195041] p 340 N95-24388
- PUBLIC HEALTH**
JPRS Report: Science and technology. Central Eurasia
[JPRS-UST-94-032] p 350 N95-24759
- Q**
- QUADRATIC PROGRAMMING**
Application of direct transcription to commercial aircraft trajectory optimization
[BTN-95-EIX95242670766] p 359 A95-81081
- R**
- RADAR CROSS SECTIONS**
Dynamic imaging and RCS measurements of aircraft
[BTN-95-EIX95202637582] p 347 A95-78576
- RADAR DETECTION**
Identification of aviation weather hazards based on the integration of radar and lightning data
[HTN-95-51323] p 356 A95-80908
Characterizing the wake vortex signature for an active line of sight remote sensor
[NASA-CR-197697] p 333 N95-24391
- RADAR IMAGERY**
Dynamic imaging and RCS measurements of aircraft
[BTN-95-EIX95202637582] p 347 A95-78576
- RADAR MEASUREMENT**
Dynamic imaging and RCS measurements of aircraft
[BTN-95-EIX95202637582] p 347 A95-78576
- RADAR SIGNATURES**
Characterizing the wake vortex signature for an active line of sight remote sensor
[NASA-CR-197697] p 333 N95-24391
- RADAR TRACKING**
Orientation determination of aircraft using visual 3D matching and radar. Case study 2
[PB95-165791] p 350 N95-25749
Aspect estimation of an aircraft using library model silhouettes
[PB95-141834] p 360 N95-25894
- RADIATION EFFECTS**
Consistent approach to describing aircraft HIRF protection
[NASA-CR-195067] p 334 N95-25341
- RADIATION PROTECTION**
Consistent approach to describing aircraft HIRF protection
[NASA-CR-195067] p 334 N95-25341
- RADICALS**
The distribution of hydrogen, nitrogen, and chlorine radicals in the lower stratosphere: Implications for changes in O₃ due to emission of NO(y) from supersonic aircraft
[HTN-95-70935] p 351 A95-78000
- RAMJET ENGINES**
Workshop report: Measurement techniques in highly transient, spectrally rich combustion environments
[AD-A288395] p 350 N95-25606
- RAREFIED GAS DYNAMICS**
DSMC calculations for 70-deg blunted cone at 3.2 km/s in nitrogen
[NASA-TM-109181] p 348 N95-24396
- RATES (PER TIME)**
Vertical transport rates in the stratosphere in 1993 from observations of CO₂, N₂O, and CH₄
[HTN-95-70941] p 351 A95-78006
- REAL GASES**
Hypersonic model testing in a shock tunnel
[BTN-95-EIX95222650789] p 329 A95-79245
- REAL TIME OPERATION**
Real-time decision aiding: Aircraft guidance for wind shear avoidance
[BTN-95-EIX95202637575] p 332 A95-78583
Real-time testing and demonstration of the US Army Corps of Engineers' Real-Time On-The-Fly positioning system
[AD-A288624] p 334 N95-25609
- REDUNDANCY**
A new guidance and flight control system for the DELTA 2 launch vehicle — Abstract only p 342 A95-80427

REENTRY GUIDANCE

- Reentry guidance for hypersonic Flight Experiment (HYFLEX) vehicle [NAL-TR-1235] p 334 N95-25764
- REENTRY VEHICLES**
- Hypersonic model testing in a shock tunnel [BTN-95-EIX95222650789] p 329 A95-79245
- REGENERATIVE COOLING**
- Effect of film cooling/regenerative cooling on scramjet engine performances [NAL-TR-1242] p 339 N95-24990
- REINFORCEMENT (STRUCTURES)**
- Design and evaluation of a foam-filled hat-stiffened panel concept for aircraft primary structural applications [NASA-TM-109175] p 346 N95-26251
- RELIABILITY ANALYSIS**
- Impact of near-coincident faults on digital flight control systems [BTN-95-EIX95242670759] p 359 A95-81088
- REMOTE CONTROL**
- Interfacing a digital compass to a remote-controlled helicopter [PB95-164927] p 340 N95-24260
- REMOTE SENSING**
- Laser device for measuring a vessel's speed [HTN-95-60992] p 361 A95-80633
- Modeling of aircraft exhaust emissions and infrared spectra for remote measurement of nitrogen oxides [HTN-95-51276] p 355 A95-80861
- Preliminary analysis of University of North Dakota aircraft data from the FIRE Cirrus IFO-2 [NASA-CR-198038] p 357 N95-24219
- Turbine-engine applications of thermographic-phosphor temperature measurements [DE95-003625] p 358 N95-25110
- REMOTE SENSORS**
- Characterizing the wake vortex signature for an active line of sight remote sensor [NASA-CR-197697] p 333 N95-24391
- REMOTELY PILOTED VEHICLES**
- Interfacing a digital compass to a remote-controlled helicopter [PB95-164927] p 340 N95-24260
- RESEARCH AIRCRAFT**
- A quiet STOL Research Aircraft Development program [NAL-TR-1223] p 336 N95-25862
- RESEARCH AND DEVELOPMENT**
- Federal Aviation Administration plan for research, engineering and development, 1995 p 363 N95-24202
- JPRS report: Science and technology. Central Eurasia [JPRS-UST-94-027] p 349 N95-24470
- JPRS report: Science and technology. Central Eurasia [JPRS-UST-94-018] p 349 N95-24472
- JPRS report: Science and technology. Central Eurasia [JPRS-UST-95-011] p 335 N95-24541
- Assessment of avionics technology in European aerospace organizations [NASA-CR-189201] p 337 N95-24624
- JPRS Report: Science and technology. Central Eurasia [JPRS-UST-94-032] p 350 N95-24759
- RESIDUAL STRESS**
- Residual Stress Measurements with Laser Speckle Correlation Interferometry and Local Heat Treating [DE95-060082] p 349 N95-24598
- REYNOLDS NUMBER**
- Flow due to an oscillating sphere and an expression for unsteady drag on the sphere at finite Reynolds number [BTN-94-EIX95011441127] p 347 A95-81012
- Flow structure in the lee of an inclined 6:1 prolate spheroid [BTN-94-EIX95011441127] p 348 A95-81027
- Experimental study of the effects of Reynolds number on high angle of attack aerodynamic characteristics of forebodies during rotary motion [NASA-CR-195033] p 330 N95-24443
- RISK**
- Report to Congressional Committees. Tactical Aircraft: Concurrence in development and production of F-22 aircraft should be reduced [GAO/NSIAD-95-59] p 336 N95-26338
- RIVETED JOINTS**
- Estimate of probability of crack detection from service difficulty report data [PB95-149381] p 328 N95-24295
- ROBOT CONTROL**
- Guidance and control, 1993: Annual Rocky Mountain Guidance and Control Conference, 18th, Keystone, CO, Feb. 6-10, 1993 [ISBN-0-87703-365-X] p 341 A95-80389
- ROBUSTNESS (MATHEMATICS)**
- High-performance, robust, bank-to-turn missile autopilot design [BTN-95-EIX95242670751] p 336 A95-81096

- Robust dynamic inversion for control of highly maneuverable aircraft [BTN-95-EIX95242670747] p 359 A95-81100
- ROLLING MOMENTS**
- Flow structure in the lee of an inclined 6:1 prolate spheroid [BTN-94-EIX95011441127] p 348 A95-81027
- ROTARY STABILITY**
- Experimental study of the effects of Reynolds number on high angle of attack aerodynamic characteristics of forebodies during rotary motion [NASA-CR-195033] p 330 N95-24443
- ROTARY WING AIRCRAFT**
- Dynamic stall control for advanced rotorcraft application [BTN-95-EIX95222650793] p 334 A95-79249
- ROTARY WINGS**
- Multilevel decomposition procedure for efficient design optimization of helicopter rotor blades [BTN-95-EIX95222650784] p 334 A95-79240
- Dynamic stall control for advanced rotorcraft application [BTN-95-EIX95222650793] p 334 A95-79249
- ROTATING SHAFTS**
- Modal characteristics of rotors using a conical shaft finite element [BTN-94-EIX94401359745] p 346 A95-77379
- ROTATION**
- Aspect estimation of an aircraft using library model silhouettes [PB95-141834] p 360 N95-25894
- ROTOR AERODYNAMICS**
- Multilevel decomposition procedure for efficient design optimization of helicopter rotor blades [BTN-95-EIX95222650784] p 334 A95-79240
- Recent improvements to and validation of the one dimensional NASA wave rotor model [NASA-TM-106913] p 332 N95-25962
- ROTOR DYNAMICS**
- Multilevel decomposition procedure for efficient design optimization of helicopter rotor blades [BTN-95-EIX95222650784] p 334 A95-79240
- Dynamic behavior of a magnetic bearing supported jet engine rotor with auxiliary bearings [NASA-CR-197860] p 338 N95-24213
- Thermohydrodynamic analysis of cryogenic liquid turbulent flow fluid film bearings, phase 2 [NASA-CR-197412] p 349 N95-24461
- ROTORS**
- Modal characteristics of rotors using a conical shaft finite element [BTN-94-EIX94401359745] p 346 A95-77379
- Dynamic behavior of a magnetic bearing supported jet engine rotor with auxiliary bearings [NASA-CR-197860] p 338 N95-24213
- Exploratory flow visualization investigation of mast-mounted sights in presence of a rotor [NASA-TM-4634] p 330 N95-24566
- Recent improvements to and validation of the one dimensional NASA wave rotor model [NASA-TM-106913] p 332 N95-25962
- Dynamics of phase ordering of nematics in a pore [DE95-607662] p 362 N95-25978
- RUNWAYS**
- Aircraft accident report: Impact with blast fence upon landing rollout Action Air Charters flight 990 Piper PA-31-350, N990RA, Stratford, Connecticut, 27 April 1994 [PB94-910410] p 333 N95-24206
- RUSSIAN FEDERATION**
- JPRS report: Science and technology. Central Eurasia [JPRS-UST-94-027] p 349 N95-24470
- JPRS report: Science and technology. Central Eurasia [JPRS-UST-94-018] p 349 N95-24472
- JPRS Report: Science and technology. Central Eurasia [JPRS-UST-94-032] p 350 N95-24759
- S**
- SATELLITE TRACKING**
- Application of fuzzy logic to optimize placement of an acquisition, tracking, and pointing experiment p 341 A95-80390
- SCALE MODELS**
- Heat transfer measurements in small scale wind tunnels [AD-A288689] p 341 N95-26053
- SEAT BELTS**
- Development of an intervention program to encourage shoulder harness use and aircraft retrofit in general aviation aircraft, phases 1 and 2 [DOT/FAA/AM-95/2] p 333 N95-24384

- SEATS**
- Analysis of warping effects on the static and dynamic response of a seat-type structure [NIAR-94-12] p 348 N95-24211
- SECONDARY FLOW**
- Internal performance characteristics of thrust-vectorized axisymmetric ejector nozzles [NASA-TM-4610] p 331 N95-25338
- SENSORS**
- The 1994 Fiber Optic Sensors for Aerospace Technology (FOSAT) Workshop [NASA-CP-10166] p 337 N95-24207
- SERVICE LIFE**
- An overview of Health and Usage Monitoring Systems (HUMS) for military helicopters [DSTO-TR-0061] p 327 N95-24200
- Helicopter life substantiation: Review of some USA and UK initiatives [DSTO-TR-0062] p 328 N95-24201
- Proceedings of the 2d USAF Aging Aircraft Conference [AD-A288217] p 336 N95-25578
- PVD TBC experience on GE aircraft engines p 345 N95-26126
- SHAPE FUNCTIONS**
- Geometric analysis of wing sections [NASA-TM-110346] p 335 N95-24629
- SHEAR LAYERS**
- Effect of density gradients in confined supersonic shear layers, part 1 [NASA-CR-198029] p 348 N95-24412
- Effect of density gradients in confined supersonic shear layers, Part 2: 3-D modes [NASA-CR-198030] p 349 N95-24413
- SHELTERS**
- Quantity-distance requirements for earth-bermed aircraft shelters [AD-A279692] p 341 N95-24424
- SHOCK HEATING**
- The Superorbital Expansion Tube concept, experiment and analysis p 341 N95-25399
- SHOCK TESTS**
- Shock tunnel studies of scramjet phenomena 1993 [NASA-CR-195038] p 350 N95-25394
- The Superorbital Expansion Tube concept, experiment and analysis p 341 N95-25399
- SHOCK TUBES**
- The Superorbital Expansion Tube concept, experiment and analysis p 341 N95-25399
- SHOCK TUNNELS**
- Shock tunnel studies of scramjet phenomena 1993 [NASA-CR-195038] p 350 N95-25394
- Thrust measurements of a complete axisymmetric scramjet in an impulse facility p 339 N95-25395
- Scramjet thrust measurement in a shock tunnel p 339 N95-25396
- Balances for the measurement of multiple components of force in flows of a millisecond duration p 350 N95-25400
- SHOCK WAVE INTERACTION**
- Structure of a double-fin turbulent interaction at high speed [BTN-95-EIX95222650780] p 347 A95-79236
- SHOCK WAVES**
- Shock tunnel studies of scramjet phenomena 1993 [NASA-CR-195038] p 350 N95-25394
- Scramjet thrust measurement in a shock tunnel p 339 N95-25396
- SHORT TAKEOFF AIRCRAFT**
- Flight reference display for powered-lift STOL aircraft [NAL-TR-1251] p 337 N95-25005
- A quiet STOL Research Aircraft Development program [NAL-TR-1223] p 336 N95-25862
- SILICON COMPOUNDS**
- Impact, friction, and wear testing of microsamples of polycrystalline silicon p 361 A95-79988
- SILVER ALLOYS**
- NASA-UVA light aerospace alloy and structures technology program supplement: Aluminum-based materials for high speed aircraft [NASA-CR-4645] p 343 N95-24878
- SIMILARITY NUMBERS**
- Similarity rule for jet-temperature effects on transonic base pressure [BTN-95-EIX95222650791] p 329 A95-79247
- SLENDER WINGS**
- Direct adaptive and neural control of wing-rock motion of slender delta wings [BTN-95-EIX95242670748] p 327 A95-81099
- SOFIA (AIRBORNE OBSERVATORY)**
- SOFIA: Stratospheric Observatory for Infrared Astronomy p 363 A95-81583
- SOLAR POWERED AIRCRAFT**
- Long endurance stratospheric solar powered airship [PB95-178729] p 336 N95-26009

SOLID MECHANICS

- NASA-UVA light aerospace alloy and structures technology program (LA2ST)
[NASA-CR-198041] p 343 N95-24220

SOOT

- The effect of altitude conditions on the particle emissions of a J85-GE-5L turbojet engine
[NASA-TM-106669] p 339 N95-24561

SPACE EXPLORATION

- NASA video catalog
[NASA-SP-7109(01)] p 363 N95-24238

SPACE NAVIGATION

- Guidance and control, 1993; Annual Rocky Mountain Guidance and Control Conference, 16th, Keystone, CO, Feb. 6-10, 1993
[ISBN-0-87703-365-X] p 341 A95-80389
Describing an attitude p 342 A95-80409

SPACE SHUTTLE ORBITERS

- Performance of an aerodynamic yaw controller mounted on the space shuttle orbiter body flap at Mach 10
[NASA-TM-109179] p 330 N95-24397

SPACECRAFT CONTROL

- Guidance and control, 1993; Annual Rocky Mountain Guidance and Control Conference, 16th, Keystone, CO, Feb. 6-10, 1993
[ISBN-0-87703-365-X] p 341 A95-80389
The Cassini spacecraft: Object oriented flight control software p 359 A95-80405
Performance of an aerodynamic yaw controller mounted on the space shuttle orbiter body flap at Mach 10
[NASA-TM-109179] p 330 N95-24397

SPACECRAFT DESIGN

- Guidance and control, 1993; Annual Rocky Mountain Guidance and Control Conference, 16th, Keystone, CO, Feb. 6-10, 1993
[ISBN-0-87703-365-X] p 341 A95-80389

SPACECRAFT GUIDANCE

- Guidance and control, 1993; Annual Rocky Mountain Guidance and Control Conference, 16th, Keystone, CO, Feb. 6-10, 1993
[ISBN-0-87703-365-X] p 341 A95-80389

SPACECRAFT INSTRUMENTS

- Guidance and control, 1993; Annual Rocky Mountain Guidance and Control Conference, 16th, Keystone, CO, Feb. 6-10, 1993
[ISBN-0-87703-365-X] p 341 A95-80389

SPACECRAFT MANEUVERS

- Dynamics and control of a tethered flight vehicle
[BTN-95-EIX95242670754] p 342 A95-81093

SPACECRAFT PERFORMANCE

- Guidance and control, 1993; Annual Rocky Mountain Guidance and Control Conference, 16th, Keystone, CO, Feb. 6-10, 1993
[ISBN-0-87703-365-X] p 341 A95-80389

SPACECRAFT REENTRY

- The Superoorbital Expansion Tube concept, experiment and analysis p 341 N95-25399

SPALLING

- Thermal barrier coating life modeling in aircraft gas turbine engines p 346 N95-26140

SPECIFIC HEAT

- Similarity rule for jet-temperature effects on transonic base pressure
[BTN-95-EIX9522650791] p 329 A95-79247

SPECKLE INTERFEROMETRY

- Residual Stress Measurements with Laser Speckle Correlation Interferometry and Local Heat Treating
[DE95-060082] p 349 N95-24598

SPECKLE PATTERNS

- Residual Stress Measurements with Laser Speckle Correlation Interferometry and Local Heat Treating
[DE95-060082] p 349 N95-24598

SPECTROSCOPIC ANALYSIS

- Comparison of column abundances from three infrared spectrometers during AASE 2
[HTN-95-70946] p 352 A95-78011
Chemical change in the arctic vortex during AASE 2
[HTN-95-70947] p 352 A95-78012

SPEED INDICATORS

- Flight reference display for powered-lift STOL aircraft
[NAL-TR-1251] p 337 N95-25005

SPHERES

- Flow due to an oscillating sphere and an expression for unsteady drag on the sphere at finite Reynolds number
[BTN-94-EIX95011441142] p 347 A95-81012

SPLINES

- How to fly an aircraft with control theory and splines p 360 N95-25805

SPRAYED COATINGS

- JPRS report: Science and technology. Central Eurasia
[JPRS-UST-95-011] p 335 N95-24541

SPRAYING

- Measurement methods and standards for processing and application of thermal barrier coatings p 344 N95-26123

SR-71 AIRCRAFT

- SR-71 may launch targets for missile defense tests
[HTN-95-91872] p 335 A95-81974

STABILITY AUGMENTATION

- Identification and simulation evaluation of a combat helicopter in hover
[BTN-95-EIX95242670749] p 335 A95-81098

STANTON NUMBER

- Hypersonic model testing in a shock tunnel
[BTN-95-EIX9522650789] p 329 A95-79245

STATIC AERODYNAMIC CHARACTERISTICS

- Measurements of longitudinal static aerodynamic coefficients by the cable mount system
[NAL-TR-1226] p 331 N95-25761

STATIC TESTS

- Analysis of warping effects on the static and dynamic response of a seat-type structure
[NIAR-94-12] p 348 N95-24211

STRATOSPHERIC

- Dynamics and control of a tethered flight vehicle
[BTN-95-EIX95242670754] p 342 A95-81093

STEELS

- JPRS report: Science and technology. Central Eurasia
[JPRS-UST-95-011] p 335 N95-24541

STIFFNESS

- Design and evaluation of a foam-filled hat-stiffened panel concept for aircraft primary structural applications
[NASA-TM-109175] p 346 N95-26251

STOVL AIRCRAFT

- Aerodynamics model for a generic ASTOVL lift-fan aircraft
[NASA-TM-110347] p 332 N95-26302

STRAIN MEASUREMENT

- Scramjet thrust measurement in a shock tunnel p 339 N95-25396

- Angular displacement measuring device
[NASA-CASE-ARC-11937-1] p 362 N95-26015

STRAPDOWN INERTIAL GUIDANCE

- A new guidance and flight control system for the DELTA 2 launch vehicle — Abstract only p 342 A95-80427

STRATOSPHERE

- Analysis of the physical state of one Arctic polar stratospheric cloud based on observations
[HTN-95-70917] p 351 A95-77982

- The distribution of hydrogen, nitrogen, and chlorine radicals in the lower stratosphere: Implications for changes in O₃ due to emission of NO_y from supersonic aircraft
[HTN-95-70935] p 351 A95-78000

- Vertical transport rates in the stratosphere in 1993 from observations of CO₂, N₂O, and CH₄
[HTN-95-70941] p 351 A95-78006

- Mentional distributions of NO(X), NO₂(Y), and other species in the lower stratosphere and upper troposphere during AASE 2
[HTN-95-70944] p 352 A95-78009

- Chemical change in the arctic vortex during AASE 2
[HTN-95-70947] p 352 A95-78012

- Latitude variations of stratospheric trace gases
[HTN-95-70948] p 352 A95-78013

- Sensitivity of supersonic aircraft modelling studies to HNO₃ photolysis rate
[HTN-95-11475] p 353 A95-79453

- Tracer transport for realistic aircraft emission scenarios calculated using a three-dimensional model
[HTN-95-41799] p 353 A95-80525

- North Atlantic air traffic within the lower stratosphere: Cruising times and corresponding emissions
[HTN-95-91841] p 354 A95-80829

- Effects on stratospheric ozone from high-speed civil transport: Sensitivity to stratospheric aerosol loading
[HTN-95-91842] p 354 A95-80830

- Potential effects on ozone of future supersonic aircraft/2D simulation
[HTN-95-51282] p 356 A95-80867

- Impact on ozone of high-speed stratospheric aircraft: Effects of the emission scenario
[HTN-95-51283] p 356 A95-80868

- The atmospheric effects of stratospheric aircraft: A fourth program report
[NASA-RP-1359] p 357 N95-24274

- Long endurance stratospheric solar powered airship
[PB95-178729] p 336 N95-26009

STRESS ANALYSIS

- Theoretical and experimental studies of fretting-initiated fatigue failure of aeroengine compressor discs
[BTN-94-EIX94421372285] p 343 A95-78467

- Residual Stress Measurements with Laser Speckle Correlation Interferometry and Local Heat Treating
[DE95-060082] p 349 N95-24598

STRESS MEASUREMENT

- Residual Stress Measurements with Laser Speckle Correlation Interferometry and Local Heat Treating
[DE95-060082] p 349 N95-24598

STRESS WAVES

- Thrust measurement in a 2-D scramjet nozzle p 339 N95-25397

STROUHAL NUMBER

- Experimental investigation of the flow around a circular cylinder: Influence of aspect ratio
[BTN-94-EIX95011441120] p 347 A95-80044

- Flow due to an oscillating sphere and an expression for unsteady drag on the sphere at finite Reynolds number
[BTN-94-EIX95011441142] p 347 A95-81012

STRUCTURAL ANALYSIS

- Aeroservoelastic aspects of wing/control surface planform shape optimization
[BTN-95-EIX9522650795] p 340 A95-79251

STRUCTURAL DESIGN

- Multilevel decomposition procedure for efficient design optimization of helicopter rotor blades
[BTN-95-EIX9522650784] p 334 A95-79240

- Design and evaluation of a foam-filled hat-stiffened panel concept for aircraft primary structural applications
[NASA-TM-109175] p 346 N95-26251

STRUCTURAL ENGINEERING

- NASA-UVA light aerospace alloy and structures technology program (LA2ST)
[NASA-CR-198041] p 343 N95-24220
JPRS report: Science and technology. Central Eurasia
[JPRS-UST-94-027] p 349 N95-24470

STRUCTURAL VIBRATION

- Modal characteristics of rotors using a conical shaft finite element
[BTN-94-EIX94401359745] p 346 A95-77379

SUBSONIC AIRCRAFT

- An analysis of aircraft exhaust plumes form accidental encounters
[HTN-95-70943] p 351 A95-78008

- Advanced subsonic airplane design and economic studies
[NASA-CR-195443] p 338 N95-24304

SUBSONIC FLOW

- Study of subsonic base cavity flowfield structure using particle image velocimetry
[BTN-95-EIX9522650781] p 327 A95-79237

- Unsteady lift on a swept blade tip
[BTN-94-EIX95011441154] p 329 A95-80030

- High frequency flow-structural interaction in dense subsonic fluids
[NASA-CR-4652] p 330 N95-24217

- Effects of cavity dimensions, boundary layer, and temperature on cavity noise with emphasis on benchmark data to validate computational aeroacoustic codes
[NASA-CR-4653] p 361 N95-24879

- Numerical and experimental study of drag characteristics of two-dimensional HLFC airfoils in high subsonic, high Reynolds number flow
[NAL-TR-12447] p 331 N95-24998

SUBSONIC FLUTTER

- Fundamental wind tunnel experiments on low-speed flutter of a tip-fin configuration wing
[NAL-TR-1228] p 332 N95-25762

SUBSONIC SPEED

- Noise impact of advanced high lift systems
[NASA-CR-195028] p 362 N95-26160

SUCTION

- Experimental investigation of the flow around a circular cylinder: Influence of aspect ratio
[BTN-94-EIX95011441120] p 347 A95-80044

SULFATES

- High-speed civil transport impact: Role of sulfate, nitric acid trihydrate, and ice aerosols studied with a two-dimensional model including aerosol physics
[HTN-95-91843] p 354 A95-80831

SULFIDES

- An intercomparison of instrumentation for tropospheric measurements of dimethyl sulfide: Aircraft results for concentrations at the parts-per-trillion level
[HTN-95-91857] p 355 A95-80845

SULFUR DIOXIDES

- An intercomparison of aircraft instrumentation for tropospheric measurements of sulfur dioxide
[HTN-95-91855] p 354 A95-80843

SUPERCOOLING

- Supercooling in hypersonic nitrogen wind tunnels
[BTN-94-EIX95011441134] p 340 A95-81020

SUPersonic AIRCRAFT

- The distribution of hydrogen, nitrogen, and chlorine radicals in the lower stratosphere: Implications for changes in O₃ due to emission of NO_y from supersonic aircraft
[HTN-95-70935] p 351 A95-78000

- Sensitivity of supersonic aircraft modelling studies to HNO₃ photolysis rate
[HTN-95-11475] p 353 A95-79453

- Effects on stratospheric ozone from high-speed civil transport: Sensitivity to stratospheric aerosol loading
[HTN-95-91842] p 354 A95-80830

- High-speed civil transport impact: Role of sulfate, nitric acid trihydrate, and ice aerosols studied with a two-dimensional model including aerosol physics
[HTN-95-91843] p 354 A95-80831

Potential effects on ozone of future supersonic aircraft/2D simulation
[HTN-95-51282] p 356 A95-80867

SUPERSONIC COMBUSTION

Effect of density gradients in confined supersonic shear layers, part 1
[NASA-CR-198029] p 348 N95-24412
Effect of density gradients in confined supersonic shear layers. Part 2: 3-D modes
[NASA-CR-198030] p 349 N95-24413

SUPERSONIC COMBUSTION RAMJET ENGINES

Effect of film cooling/regenerative cooling on scramjet engine performances
[NAL-TR-1242] p 339 N95-24990
Shock tunnel studies of scramjet phenomena 1993
[NASA-CR-195038] p 350 N95-25394
Thrust measurements of a complete axisymmetric scramjet in an impulse facility p 339 N95-25395
Scramjet thrust measurement in a shock tunnel p 339 N95-25396
Thrust measurement in a 2-D scramjet nozzle p 339 N95-25397
Balances for the measurement of multiple components of force in flows of a millisecond duration p 350 N95-25400

SUPERSONIC FLOW

Quantitative comparison between interferometric measurements and Euler computations for supersonic cone flows
[BTN-95-EIX95222650782] p 358 A95-79238
Experimental study of flow separation on an oscillating flap at Mach 2.4
[BTN-95-EIX95222650792] p 329 A95-79248
Unsteady lift on a swept blade tip
[BTN-94-EIX95011441154] p 329 A95-80030
Effect of film cooling/regenerative cooling on scramjet engine performances
[NAL-TR-1242] p 339 N95-24990
A theoretical and experimental investigation of the flow over supersonic leading edge wing/body configurations
[DRA-TM-AERO-PROP-41] p 331 N95-25649
Aerodynamic characteristics of the orbital reentry vehicle experimental probe fins in a supersonic flow
[NAL-TR-1232] p 342 N95-25664

SUPERSONIC INLETS

Prediction of supersonic inlet unstart caused by freestream disturbances
[BTN-95-EIX95222650790] p 329 A95-79246

SUPERSONIC SPEED

Effect of density gradients in confined supersonic shear layers, part 1
[NASA-CR-198029] p 348 N95-24412

SUPERSONIC TRANSPORTS

The atmospheric effects of stratospheric aircraft: A fourth program report
[NASA-RP-1359] p 357 N95-24274
Study of compressible flow through a rectangular-to-semiannular transition duct
[NASA-CR-4660] p 338 N95-24392
A crew-centered flight deck design philosophy for High-Speed Civil Transport (HSCT) aircraft
[NASA-TM-109171] p 335 N95-24582
NASA-UVA light aerospace alloy and structures technology program supplement: Aluminum-based materials for high speed aircraft
[NASA-CR-4645] p 343 N95-24878

SUPERSONIC WIND TUNNELS

Supersonic quiet-tunnel development for laminar-turbulent transition research
[NASA-CR-198040] p 340 N95-24302

SUPPORTS

Measurements of longitudinal static aerodynamic coefficients by the cable mount system
[NAL-TR-1226] p 331 N95-25761

SUPPRESSORS

Jet mixer noise suppressor using acoustic feedback
[NASA-CASE-LEW-15170-2] p 362 N95-26187

SURFACE CRACKS

Thermal fracture mechanisms in ceramic thermal barrier coatings p 346 N95-26138

SURFACE REACTIONS

High-speed civil transport impact: Role of sulfate, nitric acid trihydrate, and ice aerosols studied with a two-dimensional model including aerosol physics
[HTN-95-91843] p 354 A95-80831

SURFACE TO AIR MISSILES

Ideal proportional navigation p 342 A95-81374

SURVEYS

Development of an intervention program to encourage shoulder harness use and aircraft retrofit in general aviation aircraft, phases 1 and 2
[DOT/FAA/AM-95/2] p 333 N95-24384

SWEPT WINGS

Three-dimensional interaction of wake/boundary-layer and vortex/boundary-layer data report
[CUED/A-AEREO/TR-23] p 329 N95-24210

Aerodynamic shape optimization of wing and wing-body configurations using control theory
[NASA-CR-198024] p 335 N95-25334

SYNTHETIC APERTURE RADAR

Dynamic imaging and RCS measurements of aircraft
[BTN-95-EIX95202637582] p 347 A95-78576

SYSTEMS ANALYSIS

Determination of piloting feedback structures for an altitude tracking task
[BTN-95-EIX95242670770] p 327 A95-81077
Application of direct transcription to commercial aircraft trajectory optimization
[BTN-95-EIX95242670766] p 359 A95-81081

SYSTEMS STABILITY

Actuating signals in adaptive control systems
[IFTR-13/1994] p 361 N95-26330

T

T-53 ENGINE

Assessment of overhaul surge margin tests applied to the T53 engines in ADF Iroquois helicopters
[AR-008-389] p 339 N95-25936

TARGET ACQUISITION

Application of fuzzy logic to optimize placement of an acquisition, tracking, and pointing experiment p 341 A95-80390

TARGET DRONE AIRCRAFT

SR-71 may launch targets for missile defense tests
[HTN-95-91872] p 335 A95-81974

TECHNOLOGIES

JPRS report: Science and technology. Central Eurasia
[JPRS-UST-94-027] p 349 N95-24470
JPRS report: Science and technology. Central Eurasia
[JPRS-UST-94-018] p 349 N95-24472
JPRS Report: Science and technology. Central Eurasia
[JPRS-UST-94-032] p 350 N95-24759

TECHNOLOGY ASSESSMENT

Assessment of avionics technology in European aerospace organizations
[NASA-CR-198201] p 337 N95-24624
Wind technology development: Large and small turbines
[DE95-000286] p 358 N95-26090

TECHNOLOGY UTILIZATION

Aviation system capacity improvements through technology
[NASA-TM-109165] p 333 N95-24633

TELEROBOTICS

Guidance and control, 1993: Annual Rocky Mountain Guidance and Control Conference, 16th, Keystone, CO, Feb. 6-10, 1993
[ISBN-0-87703-365-X] p 341 A95-80389

TEMPERATURE EFFECTS

Prediction of supersonic inlet unstart caused by freestream disturbances
[BTN-95-EIX95222650790] p 329 A95-79246
Similarity rule for jet-temperature effects on transonic base pressure
[BTN-95-EIX95222650791] p 329 A95-79247
Effects of cavity dimensions, boundary layer, and temperature on cavity noise with emphasis on benchmark data to validate computational aeroacoustic codes
[NASA-CR-4653] p 361 N95-24879

TEMPERATURE MEASUREMENT

Turbine-engine applications of thermographic-phosphor temperature measurements
[DE95-003625] p 358 N95-25110

TENSILE STRENGTH

Study on tensile fatigue testing method of unidirectional fiber-resin matrix composites
[NAL-TR-1241] p 343 N95-24989

TERRAIN

Partial camera automation in a simulated Unmanned Air Vehicle
[AD-A288786] p 337 N95-26190

TEST FACILITIES

The Superorbital Expansion Tube concept, experiment and analysis p 341 N95-25399

TETHERED SATELLITES

Dynamics and control of a tethered flight vehicle
[BTN-95-EIX95242670754] p 342 A95-81093

TETHERING

Dynamics and control of a tethered flight vehicle
[BTN-95-EIX95242670754] p 342 A95-81093

THERMAL ANALYSIS

Thermohydrodynamic analysis of cryogenic liquid turbulent flow fluid film bearings, phase 2
[NASA-CR-197412] p 349 N95-24461

THERMAL CONDUCTIVITY

Thermal conductivity of zirconia thermal barrier coatings p 345 N95-26133

THERMAL PROTECTION COATINGS

Thermal Barrier Coating Workshop
[NASA-CP-10170] p 344 N95-26119
A design perspective on thermal barrier coatings p 344 N95-26120
Thermal barrier coatings for aircraft engines: History and directions p 344 N95-26121
Thermal barrier coatings issues in advanced land-based gas turbines p 344 N95-26122
Measurement methods and standards for processing and application of thermal barrier coatings p 344 N95-26123
Thermal barrier coatings application in diesel engines p 345 N95-26124
Thermal barrier coating experience in the gas turbine engine p 345 N95-26125
PVD TBC experience on GE aircraft engines p 345 N95-26126
Perspective on thermal barrier coatings for industrial gas turbine applications p 345 N95-26128
Thermal conductivity of zirconia thermal barrier coatings p 345 N95-26133
Thermal fracture mechanisms in ceramic thermal barrier coatings p 346 N95-26138
Thermal barrier coating life modeling in aircraft gas turbine engines p 346 N95-26140

THERMAL INSULATION

Thermal barrier coating experience in the gas turbine engine p 345 N95-26125

THERMAL STRESSES

Thermal fracture mechanisms in ceramic thermal barrier coatings p 346 N95-26138

THERMOGRAPHY

Turbine-engine applications of thermographic-phosphor temperature measurements
[DE95-003625] p 358 N95-25110
Emerging nondestructive inspection for aging aircraft
[PB95-143053] p 328 N95-25401

THREAT EVALUATION

Consistent approach to describing aircraft HIRF protection
[NASA-CR-195067] p 334 N95-25341

THREE DIMENSIONAL FLOW

Quantitative comparison between interferometric measurements and Euler computations for supersonic cone flows
[BTN-95-EIX95222650782] p 358 A95-79238
Three-dimensional interaction of wake/boundary-layer and vortex/boundary-layer data report
[CUED/A-AEREO/TR-23] p 329 N95-24210

THREE DIMENSIONAL MODELS

Tracer transport for realistic aircraft emission scenarios calculated using a three-dimensional model
[HTN-95-41799] p 353 A95-80525
Orientation determination of aircraft using visual 3D matching and radar. Case study 2
[PB95-165791] p 350 N95-25749

THREE DIMENSIONAL MOTION

Effect of density gradients in confined supersonic shear layers. Part 2: 3-D modes
[NASA-CR-198030] p 349 N95-24413

THRESHOLDS (PERCEPTION)

Visual contrast detection thresholds for aircraft contrails
[AD-A288618] p 328 N95-25607

THRUST

Thrust measurement in a 2-D scramjet nozzle p 339 N95-25397

THRUST MEASUREMENT

Thrust measurements of a complete axisymmetric scramjet in an impulse facility p 339 N95-25395
Scramjet thrust measurement in a shock tunnel p 339 N95-25396
Thrust measurement in a 2-D scramjet nozzle p 339 N95-25397
Balances for the measurement of multiple components of force in flows of a millisecond duration p 350 N95-25400

THRUST VECTOR CONTROL

Internal performance characteristics of thrust-vectorized axisymmetric ejector nozzles
[NASA-TM-4610] p 331 N95-25338

THUNDERSTORMS

Identification of aviation weather hazards based on the integration of radar and lightning data
[HTN-95-51323] p 356 A95-80908

TIME DEPENDENCE

Dynamics of phase ordering of nematics in a pore
[DE95-607662] p 362 N95-25978

TOMOGRAPHY

Emerging nondestructive inspection for aging aircraft
[PB95-143053] p 328 N95-25401

TOPOGRAPHY

Partial camera automation in a simulated Unmanned Air Vehicle
[AD-A288786] p 337 N95-26190

TORSION

- Modal characteristics of rotors using a conical shaft finite element
[BTN-94-EIX94401359745] p 346 A95-77379

TOXIC HAZARDS

- Chemical composition and photochemical reactivity of exhaust from aircraft turbine engines
[HTN-95-51277] p 356 A95-80862

TRACE CONTAMINANTS

- Latitude variations of stratospheric trace gases
[HTN-95-70948] p 352 A95-78013
- Tracer transport for realistic aircraft emission scenarios calculated using a three-dimensional model
[HTN-95-41799] p 353 A95-80525

TRACKING (POSITION)

- Determination of piloting feedback structures for an altitude tracking task
[BTN-95-EIX95242670770] p 327 A95-81077

TRAJECTORY CONTROL

- Ideal proportional navigation p 342 A95-81374

TRAJECTORY OPTIMIZATION

- Application of direct transcription to commercial aircraft trajectory optimization
[BTN-95-EIX95242670766] p 358 A95-81061

TRANSDUCERS

- Workshop report: Measurement techniques in highly transient, spectrally rich combustion environments
[AD-A288395] p 350 N95-25606

TRANSFER FUNCTIONS

- Aerodynamic parameter estimation via Fourier modulating function techniques
[NASA-CR-4654] p 335 N95-24630

TRANSITION FLOW

- Study of compressible flow through a rectangular-to-semiannular transition duct
[NASA-CR-4660] p 338 N95-24392

TRANSLATING

- Partial camera automation in a simulated Unmanned Air Vehicle
[AD-A288786] p 337 N95-26190

TRANSMISSIONS (MACHINE ELEMENTS)

- A portable transmission vibration analysis system for the S-70A-9 Black Hawk helicopter
[DSTO-TR-0072] p 348 N95-24203

TRANSONIC FLOW

- Similarity rule for jet-temperature effects on transonic base pressure
[BTN-95-EIX95222650791] p 329 A95-79247

TRANSONIC WIND TUNNELS

- Development of a model protection and dynamic response monitoring system for the national transonic facility
[NASA-CR-195041] p 340 N95-24388

TRANSPORT AIRCRAFT

- Emerging nondestructive inspection for aging aircraft
[PB95-143053] p 328 N95-25401
- A quiet STOL Research Aircraft Development program
[NAL-TR-1223] p 336 N95-25862

TROPICAL REGIONS

- Fine-scale, poleward transport of tropical air during AASE 2
[HTN-95-70949] p 352 A95-78014

TROPOSPHERE

- Mendocino distributions of NO(X), NO(Y), and other species in the lower stratosphere and upper troposphere during AASE 2
[HTN-95-70944] p 352 A95-78009

- Impact of present aircraft emissions of nitrogen oxides on tropospheric ozone and climate forcing
[HTN-95-21364] p 353 A95-78679

- An intercomparison of aircraft instrumentation for tropospheric measurements of sulfur dioxide
[HTN-95-91855] p 354 A95-80843

- An intercomparison of aircraft instrumentation for tropospheric measurements of carbonyl sulfide, hydrogen sulfide, and carbon disulfide
[HTN-95-91856] p 355 A95-80844

TURBINE BLADES

- Using digital filtering techniques as an aid in wind turbine data analysis
[DE94-011862] p 357 N95-24853

- NREL airfoil families for HAWTs
[DE95-000267] p 357 N95-24882

TURBINE ENGINES

- Chemical composition and photochemical reactivity of exhaust from aircraft turbine engines
[HTN-95-51277] p 356 A95-80862

- Turbine-engine applications of thermographic-phosphor temperature measurements
[DE95-003625] p 358 N95-25110

- A design perspective on thermal barrier coatings p 344 N95-26120

TURBOFAN ENGINES

- Bird ingestion into large turbofan engines
[DOT/FAA/CT-93/14] p 333 N95-24631

TURBULENCE

- Structure of a double-fin turbulent interaction at high speed
[BTN-95-EIX95222650780] p 347 A95-79236

- On the role of the outer region in the turbulent-boundary-layer bursting process
[BTN-94-EIX95011441078] p 348 A95-81056

TURBULENCE EFFECTS

- Rotorcraft handling qualities in turbulence
[BTN-95-EIX95242670750] p 334 A95-81097

TURBULENCE MODELS

- Structure of a double-fin turbulent interaction at high speed
[BTN-95-EIX95222650780] p 347 A95-79236

TURBULENT BOUNDARY LAYER

- Structure of a double-fin turbulent interaction at high speed
[BTN-95-EIX95222650780] p 347 A95-79236

- Experimental study of flow separation on an oscillating flap at Mach 2.4
[BTN-95-EIX95222650792] p 329 A95-79248

- On the role of the outer region in the turbulent-boundary-layer bursting process
[BTN-94-EIX95011441078] p 348 A95-81056

- Effects of cavity dimensions, boundary layer, and temperature on cavity noise with emphasis on benchmark data to validate computational aeroacoustic codes
[NASA-CR-4653] p 361 N95-24879

TURBULENT FLOW

- On the role of the outer region in the turbulent-boundary-layer bursting process
[BTN-94-EIX95011441078] p 348 A95-81056

- Thermohydrodynamic analysis of cryogenic liquid turbulent flow fluid film bearings, phase 2
[NASA-CR-197412] p 349 N95-24461

TURBULENT JETS

- Crossflow mixing of noncircular jets
[NASA-TM-106865] p 338 N95-24390

TWO DIMENSIONAL FLOW

- Study of subsonic base cavity flowfield structure using particle image velocimetry
[BTN-95-EIX95222650781] p 327 A95-79237

- Thrust measurement in a 2-D scramjet nozzle
[NASA-TM-106865] p 338 N95-24390

TWO DIMENSIONAL MODELS

- High-speed civil transport impact: Role of sulfate, nitric acid trihydrate, and ice aerosols studied with a two-dimensional model including aerosol physics
[HTN-95-91843] p 354 A95-80831

- Dynamics of aircraft exhaust plumes in the jet-regime
[HTN-95-51275] p 355 A95-80860

- Potential effects on ozone of future supersonic aircraft/2D simulation
[HTN-95-51282] p 356 A95-80867

- Impact on ozone of high-speed stratospheric aircraft: Effects of the emission scenario
[HTN-95-51283] p 356 A95-80868

U

UH-1 HELICOPTER

- Assessment of overhaul surge margin tests applied to the T53 engines in ADF Iroquois helicopters
[AR-008-389] p 339 N95-25936

UH-60A HELICOPTER

- A portable transmission vibration analysis system for the S-70A-9 Black Hawk helicopter
[DSTO-TR-0072] p 348 N95-24203

ULTRASONIC TESTS

- Emerging nondestructive inspection for aging aircraft
[PB95-143053] p 328 N95-25401

UNIFORM FLOW

- Experimental investigation of the flow around a circular cylinder: Influence of aspect ratio
[BTN-94-EIX95011441120] p 347 A95-80044

UNITED KINGDOM

- Helicopter life substantiation: Review of some USA and UK initiatives
[DSTO-TR-0062] p 328 N95-24201

UNITED STATES

- Helicopter life substantiation: Review of some USA and UK initiatives
[DSTO-TR-0062] p 328 N95-24201

UNSTEADY AERODYNAMICS

- Aeroservoelastic aspects of wing/control surface planform shape optimization
[BTN-95-EIX95222650795] p 340 A95-79251

- Application of neural networks to unsteady aerodynamic control p 360 N95-25264

UNSTEADY FLOW

- Prediction of supersonic inlet unstart caused by freestream disturbances
[BTN-95-EIX95222650790] p 329 A95-79246

- Unsteady lift on a swept blade tip
[BTN-94-EIX95011441154] p 329 A95-80030

- Flow due to an oscillating sphere and an expression for unsteady drag on the sphere at finite Reynolds number
[BTN-94-EIX95011441142] p 347 A95-81012

- High frequency flow-structural interaction in dense subsonic fluids
[NASA-CR-4652] p 330 N95-24217

- Thermohydrodynamic analysis of cryogenic liquid turbulent flow fluid film bearings, phase 2
[NASA-CR-197412] p 349 N95-24461

- Recent improvements to and validation of the one dimensional NASA wave rotor model
[NASA-TM-106913] p 332 N95-25962

- A combined geometric approach for solving the Navier-Stokes equations on dynamic grids
[NASA-TM-106919] p 332 N95-26075

UPPER SURFACE BLOWING

- Dynamic stall control for advanced rotorcraft application
[BTN-95-EIX95222650793] p 334 A95-79249

- A quiet STOL Research Aircraft Development program
[NAL-TR-1223] p 336 N95-25862

V

VAPOR DEPOSITION

- Measurement methods and standards for processing and application of thermal barrier coatings
[NASA-TM-106865] p 344 N95-26123

- PVD TBC experience on GE aircraft engines p 345 N95-26126

- Thermal conductivity of zirconia thermal barrier coatings p 345 N95-26133

VAPORS

- Supercooling in hypersonic nitrogen wind tunnels
[BTN-94-EIX95011441134] p 340 A95-81020

VARIATIONS

- Latitude variations of stratospheric trace gases
[HTN-95-70948] p 352 A95-78013

VECTORS (MATHEMATICS)

- Describing an attitude p 342 A95-80409

VELOCITY MEASUREMENT

- Laser device for measuring a vessel's speed
[HTN-95-60992] p 361 A95-80633

VERTICAL DISTRIBUTION

- Vertical transport rates in the stratosphere in 1993 from observations of CO₂, N₂O, and CH₄
[HTN-95-70941] p 351 A95-78006

- An analysis of aircraft exhaust plumes from accidental encounters
[HTN-95-70943] p 351 A95-78008

- Latitude variations of stratospheric trace gases
[HTN-95-70948] p 352 A95-78013

VERY LARGE SCALE INTEGRATION

- Fault detection in multiprocessor systems and array processors
[BTN-95-EIX95242679097] p 359 A95-81253

VIBRATION

- Exploratory flow visualization investigation of mast-mounted sights in presence of a rotor
[NASA-TM-4634] p 330 N95-24566

VIBRATION MEASUREMENT

- A portable transmission vibration analysis system for the S-70A-9 Black Hawk helicopter
[DSTO-TR-0072] p 348 N95-24203

VIBRATION SIMULATORS

- A portable transmission vibration analysis system for the S-70A-9 Black Hawk helicopter
[DSTO-TR-0072] p 348 N95-24203

VIDEO TAPES

- NASA video catalog
[NASA-SP-7109(011)] p 363 N95-24238

VIRIAL COEFFICIENTS

- Empirical corrections of the rigid rotor interaction potential of H₂-H₂ in the attractive region: Dimer features in the FIR absorption spectra
[HTN-95-41943] p 361 A95-81690

VISCOPLASTICITY

- Viscoplastic response of structures for intense local heating
[HTN-95-41540] p 346 A95-77921

VISUAL PERCEPTION

- Visual contrast detection thresholds for aircraft contrails
[AD-A288618] p 328 N95-25607

VORTEX AVOIDANCE

- Characterizing the wake vortex signature for an active line of sight remote sensor
[NASA-CR-197697] p 333 N95-24391

VORTEX FLAPS

Low speed aerodynamic characteristics of delta wings with vortex flaps: 60 deg and 70 deg delta wings [NASA-TR-1245] p 331 N95-25105

VORTEX SHEDDING

High frequency flow-structural interaction in dense subsonic fluids [NASA-CR-4652] p 330 N95-24217

VORTEX SHEETS

Effect of density gradients in confined supersonic shear layers. Part 2: 3-D modes [NASA-CR-198030] p 349 N95-24413

VORTICES

On the role of the outer region in the turbulent-boundary-layer bursting process [BTN-94-EIX95011441078] p 348 A95-81056

Three-dimensional interaction of wake/boundary-layer and vortex/boundary-layer data report [CUEP/A-AERO/TR-23] p 329 N95-24210

The atmospheric effects of stratospheric aircraft: A fourth program report [NASA-RP-1359] p 357 N95-24274

Characterizing the wake vortex signature for an active line of sight remote sensor [NASA-CR-197697] p 333 N95-24391

W

WAKES

Flow structure in the lee of an inclined 6:1 prolate spheroid [BTN-94-EIX95011441127] p 348 A95-81027

WALL FLOW

Supersonic quiet-tunnel development for laminar-turbulent transition research [NASA-CR-198040] p 340 N95-24302

WALL JETS

Effects of cavity dimensions, boundary layer, and temperature on cavity noise with emphasis on benchmark data to validate computational aeroacoustic codes [NASA-CR-4653] p 361 N95-24879

WALL PRESSURE

Experimental study of flow separation on an oscillating flap at Mach 2.4 [BTN-95-EIX95222650792] p 329 A95-79248

WARNING SYSTEMS

Real-time decision aiding: Aircraft guidance for wind shear avoidance [BTN-95-EIX95202637575] p 332 A95-78583

WARPAGE

Analysis of warping effects on the static and dynamic response of a seat-type structure [NIAR-94-12] p 348 N95-24211

WATER

Analysis of the physical state of one Arctic polar stratospheric cloud based on observations [HTN-95-70917] p 351 A95-77982

WEAPONS DEVELOPMENT

Report to Congressional Committees. Tactical Aircraft: Concurrency in development and production of F-22 aircraft should be reduced [GAO/NSIAD-95-59] p 336 N95-26338

WEAR RESISTANCE

Impact, friction, and wear testing of microsamples of polycrystalline silicon p 361 A95-79988

WEIGHTING FUNCTIONS

Aerodynamic parameter estimation via Fourier modulating function techniques [NASA-CR-4654] p 335 N95-24630

WELDED STRUCTURES

JPRS report: Science and technology. Central Eurasia [JPRS-UST-95-011] p 335 N95-24541

WIND EFFECTS

Real-time decision aiding: Aircraft guidance for wind shear avoidance [BTN-95-EIX95202637575] p 332 A95-78583

WIND PRESSURE

Load alleviation maneuvers for a launch vehicle p 342 A95-81360

WIND PROFILES

Comparison of wind profiler and aircraft wind measurements at Chebogue Point, Nova Scotia [HTN-95-41833] p 353 A95-80559

WIND SHEAR

Real-time decision aiding: Aircraft guidance for wind shear avoidance [BTN-95-EIX95202637575] p 332 A95-78583

WIND TUNNEL MODELS

Development of a model protection and dynamic response monitoring system for the national transonic facility [NASA-CR-195041] p 340 N95-24388

Angular displacement measuring device [NASA-CASE-ARC-11937-1] p 362 N95-26015

WIND TUNNEL NOZZLES

Supersonic quiet-tunnel development for laminar-turbulent transition research [NASA-CR-198040] p 340 N95-24302

WIND TUNNEL TESTS

Hypersonic model testing in a shock tunnel [BTN-95-EIX95222650789] p 329 A95-79245

Similarity rule for jet-temperature effects on transonic base pressure [BTN-95-EIX95222650791] p 329 A95-79247

Three-dimensional interaction of wake/boundary-layer and vortex/boundary-layer data report [CUEP/A-AERO/TR-23] p 329 N95-24210

Supersonic quiet-tunnel development for laminar-turbulent transition research [NASA-CR-198040] p 340 N95-24302

Study of compressible flow through a rectangular-to-semiannular transition duct [NASA-CR-4660] p 338 N95-24392

DSMC calculations for 70-deg blunted cone at 3.2 km/s in nitrogen [NASA-TM-109181] p 348 N95-24396

Performance of an aerodynamic yaw controller mounted on the space shuttle orbiter body flap at Mach 10 [NASA-TM-109179] p 330 N95-24397

Experimental study of the effects of Reynolds number on high angle of attack aerodynamic characteristics of forebodies during rotary motion [NASA-CR-195033] p 330 N95-24443

Exploratory flow visualization investigation of mast-mounted sights in presence of a rotor [NASA-TM-4634] p 330 N95-24566

Using digital filtering techniques as an aid in wind turbine data analysis [DE94-011862] p 357 N95-24853

Effects of cavity dimensions, boundary layer, and temperature on cavity noise with emphasis on benchmark data to validate computational aeroacoustic codes [NASA-CR-4653] p 361 N95-24879

Numerical and experimental study of drag characteristics of two-dimensional HLFC airfoils in high subsonic, high Reynolds number flow [NAL-TR-1244T] p 331 N95-24998

Low speed aerodynamic characteristics of delta wings with vortex flaps: 60 deg and 70 deg delta wings [NAL-TR-1245] p 331 N95-25105

Thrust measurements of a complete axisymmetric scramjet in an impulse facility p 339 N95-25395

Scramjet thrust measurement in a shock tunnel p 339 N95-25396

Balances for the measurement of multiple components of force in flows of a millisecond duration p 350 N95-25400

Aerodynamic characteristics of the orbital reentry vehicle experimental probe fins in a supersonic flow [NAL-TR-1232] p 342 N95-25664

Measurements of longitudinal static aerodynamic coefficients by the cable mount system [NAL-TR-1226] p 331 N95-25761

Fundamental wind tunnel experiments on low-speed flutter of a tip-fin configuration wing [NAL-TR-1228] p 332 N95-25762

Heat transfer measurements in small scale wind tunnels [AD-A288689] p 341 N95-26053

WIND TURBINES

Using digital filtering techniques as an aid in wind turbine data analysis [DE94-011862] p 357 N95-24853

NREL airfoil families for HAWTs [DE95-000267] p 357 N95-24882

Wind technology development: Large and small turbines [DE95-000286] p 358 N95-26090

WIND VELOCITY MEASUREMENT

Comparison of wind profiler and aircraft wind measurements at Chebogue Point, Nova Scotia [HTN-95-41833] p 353 A95-80559

WINDPOWER UTILIZATION

Wind technology development: Large and small turbines [DE95-000286] p 358 N95-26090

WING OSCILLATIONS

Direct adaptive and neural control of wing-rock motion of slender delta wings [BTN-95-EIX95242670748] p 327 A95-81099

Fundamental wind tunnel experiments on low-speed flutter of a tip-fin configuration wing [NAL-TR-1228] p 332 N95-25762

WING PLANFORMS

Aeroservoelastic aspects of wing/control surface planform shape optimization [BTN-95-EIX95222650795] p 340 A95-79251

WING PROFILES

A theoretical and experimental investigation of the flow over supersonic leading edge wing/body configurations [DRA-TM-AERO-PROP-41] p 331 N95-25649

WING SLOTS

Impingement cooling of an isothermally heated surface with a confined slot jet [BTN-94-EIX94421348950] p 347 A95-78494

WING TIPS

Fundamental wind tunnel experiments on low-speed flutter of a tip-fin configuration wing [NAL-TR-1228] p 332 N95-25762

WINGLETS

Fundamental wind tunnel experiments on low-speed flutter of a tip-fin configuration wing [NAL-TR-1228] p 332 N95-25762

WINGS

Aeroservoelastic aspects of wing/control surface planform shape optimization [BTN-95-EIX95222650795] p 340 A95-79251

Geometric analysis of wing sections [NASA-TM-110346] p 335 N95-24629

Fundamental wind tunnel experiments on low-speed flutter of a tip-fin configuration wing [NAL-TR-1228] p 332 N95-25762

X

X RAY INSPECTION

Emerging nondestructive inspection for aging aircraft [PB95-143053] p 328 N95-25401

Z

ZIRCONIUM OXIDES

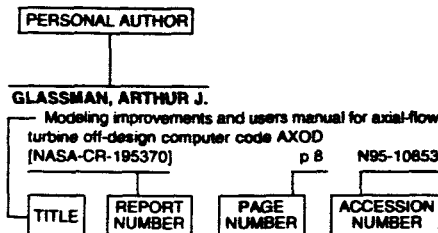
Thermal conductivity of zirconia thermal barrier coatings p 345 N95-26133

PERSONAL AUTHOR INDEX

AERONAUTICAL ENGINEERING / A Continuing Bibliography (Supplement 320)

August 1995

Typical Personal Author Index Listing



Listings in this index are arranged alphabetically by personal author. The title of the document is used to provide a brief description of the subject matter. The report number helps to indicate the type of document (e.g., NASA report, translation, NASA contractor report). The page and accession numbers are located beneath and to the right of the title. Under any one author's name the accession numbers are arranged in sequence.

A

- ABBOTT, TERENCE S.**
A crew-centered flight deck design philosophy for High-Speed Civil Transport (HSCT) aircraft
[NASA-TM-109171] p 335 N95-24582
- ADAMOVSKY, GRIGORY**
The 1994 Fiber Optic Sensors for Aerospace Technology (FOSAT) Workshop
[NASA-CP-10166] p 337 N95-24207
- AHUJA, K. K.**
Effects of cavity dimensions, boundary layer, and temperature on cavity noise with emphasis on benchmark data to validate computational aeroacoustic codes
[NASA-CR-4653] p 361 N95-24879
- ALLISON, STEPHEN W.**
Turbine-engine applications of thermographic-phosphor temperature measurements
[DE95-003625] p 358 N95-25110
- AMBUR, DAMODAR R.**
Design and evaluation of a foam-filled hat-stiffened panel concept for aircraft primary structural applications
[NASA-TM-109175] p 346 N95-26251
- ANDERSON, B. E.**
An analysis of aircraft exhaust plumes from accidental encounters
[HTN-95-70943] p 351 A95-78008
- Meridional distributions of NO(X), NO(Y), and other species in the lower stratosphere and upper troposphere during AASE 2
[HTN-95-70944] p 352 A95-78009
- ANDERSON, J. G.**
The distribution of hydrogen, nitrogen, and chlorine radicals in the lower stratosphere: Implications for changes in O₃ due to emission of NO(y) from supersonic aircraft
[HTN-95-70935] p 351 A95-78000
- ANDRASTEK, DONALD A.**
Advanced subsonic airplane design and economic studies
[NASA-CR-195443] p 338 N95-24304
- ANDREAE, MENIRAT O.**
An intercomparison of aircraft instrumentation for tropospheric measurements of carbonyl sulfide, hydrogen sulfide, and carbon disulfide
[HTN-95-91856] p 355 A95-80844

- An intercomparison of instrumentation for tropospheric measurements of dimethyl sulfide: Aircraft results for concentrations at the parts-per-trillion level
[HTN-95-91857] p 355 A95-80845
- ANGEVINE, WAYNE M.**
Comparison of wind profiler and aircraft wind measurements at Chebogue Point, Nova Scotia
[HTN-95-41833] p 353 A95-80559
- APPLEBY, J. W., JR.**
Jet engine applications for materials with nanometer-scale dimensions
p 345 N95-26131
- ASAI, KEISUKE**
Similarity rule for jet-temperature effects on transonic base pressure
[BTN-95-EIX95222650791] p 329 A95-79247
- ASHILL, P. R.**
A theoretical and experimental investigation of the flow over supersonic leading edge wing/body configurations [DRA-TM-AERO-PROP-41] p 331 N95-25649
- ATWOOD, CHRISTOPHER**
The coupling of fluids, dynamics, and controls on advanced architecture computers
[NASA-CR-197727] p 360 N95-25787

B

- BAKKER, P. G.**
Quantitative comparison between interferometric measurements and Euler computations for supersonic cone flows
[BTN-95-EIX95222650782] p 358 A95-79238
- BAKOS, R. J.**
Shock tunnel studies of scramjet phenomena 1993
[NASA-CR-195038] p 350 N95-25394
- BALAKRISHNA, S.**
Development of a model protection and dynamic response monitoring system for the national transonic facility
[NASA-CR-195041] p 340 N95-24388
- BALAS, GARY J.**
Robust dynamic inversion for control of highly maneuverable aircraft
[BTN-95-EIX95242670747] p 359 A95-81100
- BANDY, ALAN R.**
An intercomparison of aircraft instrumentation for tropospheric measurements of sulfur dioxide
[HTN-95-91855] p 354 A95-80843
- An intercomparison of aircraft instrumentation for tropospheric measurements of carbonyl sulfide, hydrogen sulfide, and carbon disulfide
[HTN-95-91856] p 355 A95-80844
- An intercomparison of instrumentation for tropospheric measurements of dimethyl sulfide: Aircraft results for concentrations at the parts-per-trillion level
[HTN-95-91857] p 355 A95-80845
- BANFLOWER, HOWARD**
Bird ingestion into large turbofan engines
[DOT/FAA/CT-83/14] p 333 N95-24631
- BARRICK, JOHN D.**
An intercomparison of aircraft instrumentation for tropospheric measurements of carbonyl sulfide, hydrogen sulfide, and carbon disulfide
[HTN-95-91856] p 355 A95-80844
- BARTZ, A.**
PVD TBC experience on GE aircraft engines
p 345 N95-26126
- BAUMICK, ROBERT**
The 1994 Fiber Optic Sensors for Aerospace Technology (FOSAT) Workshop
[NASA-CP-10166] p 337 N95-24207
- Assessment of avionics technology in European aerospace organizations
[NASA-CR-188201] p 337 N95-24624
- BAUMGARDNER, D.**
Analysis of the physical state of one Arctic polar stratospheric cloud based on observations
[HTN-95-70917] p 351 A95-77982
- BEATTIE, ALLAN**
Emerging nondestructive inspection for aging aircraft
[PB95-143053] p 328 N95-25401
- BECKER, K. H.**
Nitrous oxide and methane emissions from aero engines
[HTN-95-21363] p 353 A95-78678
- BEECHER, S. C.**
Thermal conductivity of zirconia thermal barrier coatings
p 345 N95-26133
- BEHEM, GLENN**
The 1994 Fiber Optic Sensors for Aerospace Technology (FOSAT) Workshop
[NASA-CP-10166] p 337 N95-24207
- BEIER, K.**
Modeling of aircraft exhaust emissions and infrared spectra for remote measurement of nitrogen oxides
[HTN-95-51276] p 355 A95-80861
- BEKKI, S.**
Sensitivity of supersonic aircraft modeling studies to HNO₃ photolysis rate
[HTN-95-11475] p 353 A95-79453
- BELTZ, NOBERT**
An intercomparison of aircraft instrumentation for tropospheric measurements of sulfur dioxide
[HTN-95-91855] p 354 A95-80843
- BENGTSSON, M.**
Orientation determination of aircraft using visual 3D matching and radar. Case study 2
[PB95-165791] p 350 N95-25749
- BERNARD, DOUGLAS E.**
The Cassini spacecraft: Object oriented flight control software
p 359 A95-80405
- BETTS, JOHN T.**
Application of direct transcription to commercial aircraft trajectory optimization
[BTN-95-EIX95242670766] p 359 A95-81081
- BHATTACHARYA, A.**
Dynamics of phase ordering of nematics in a pore
[DE95-607662] p 362 N95-25978
- BICKLEY, GEORGE**
Guidance and control, 1993; Annual Rocky Mountain Guidance and Control Conference, 16th, Keystone, CO, Feb. 6-10, 1993
[ISBN-0-87703-365-X] p 341 A95-80389
- BILIMORIA, KARL D.**
Integrated development of the equations of motion for elastic hypersonic flight vehicles
[BTN-95-EIX95242670755] p 327 A95-81092
- BIRCKELBAW, LOURDES G.**
Aerodynamics model for a generic ASTOVL lift-fan aircraft
[NASA-TM-110347] p 332 N95-26302
- BLACKWELDER, RON F.**
On the role of the outer region in the turbulent-boundary-layer bursting process
[BTN-94-EIX95011441078] p 348 A95-81056
- BLAKE, D. R.**
Meridional distributions of NO(X), NO(Y), and other species in the lower stratosphere and upper troposphere during AASE 2
[HTN-95-70944] p 352 A95-78009
- BLAKE, N. J.**
Meridional distributions of NO(X), NO(Y), and other species in the lower stratosphere and upper troposphere during AASE 2
[HTN-95-70944] p 352 A95-78009
- BLAVIER, J.-F.**
Latitude variations of stratospheric trace gases
[HTN-95-70948] p 352 A95-78013
- BLESS, ROBERT R.**
Load alleviation maneuvers for a launch vehicle
p 342 A95-81360
- BLUNT, D. M.**
A portable transmission vibration analysis system for the S-70A-9 Black Hawk helicopter
[DSTO-TR-0072] p 348 N95-24203
- BOERING, KRISTIE A.**
Vertical transport rates in the stratosphere in 1993 from observations of CO₂, N₂O, and CH₄
[HTN-95-70941] p 351 A95-78006
- BOSE, S.**
Thermal barrier coating experience in the gas turbine engine
p 345 N95-26125

- BRADY, RAYMOND H., III**
Identification of aviation weather hazards based on the integration of radar and lightning data
[HTN-95-51323] p 356 A95-80908
- BRASSEUR, G. P.**
Impact of present aircraft emissions of nitrogen oxides on tropospheric ozone and climate forcing
[HTN-95-21364] p 353 A95-78679
- BRENTNALL, W. D.**
Perspective on thermal barrier coatings for industrial gas turbine applications p 345 N95-26128
- BREWER, J. C.**
Estimate of probability of crack detection from service difficulty report data
[PB95-149381] p 328 N95-24295
- BRINDLEY, W. J.**
Thermal Barrier Coating Workshop
[NASA-CP-10170] p 344 N95-26119
- BUKLEY, JERRY**
Application of fuzzy logic to optimize placement of an acquisition, tracking, and pointing experiment p 341 A95-80390

C

- CARTER, GARY M.**
Identification of aviation weather hazards based on the integration of radar and lightning data
[HTN-95-51323] p 356 A95-80908
- CASDORPH, VAN**
On-line learning nonlinear direct neurocontrollers for restructurable control systems
[BTN-95-EIX95242670768] p 359 A95-81079
- CHAKRABARTI, A.**
Dynamics of phase ordering of nematics in a pore
[DE95-607662] p 362 N95-25978
- CHAN, K. R.**
Fine-scale, poleward transport of tropical air during AASE 2
[HTN-95-70949] p 352 A95-78014
- CHANCE, JOHN E.**
Real-time testing and demonstration of the US Army Corps of Engineers' Real-Time On-The-Fly positioning system
[AD-A288624] p 334 N95-25609
- CHANCE, KELLY V.**
Chemical change in the arctic vortex during AASE 2
[HTN-95-70947] p 352 A95-78012
- CHANG, C. I.**
Proceedings of the 2d USAF Aging Aircraft Conference
[AD-A288217] p 336 N95-25578
- CHANG, I.-CHUNG**
Geometric analysis of wing sections
[NASA-TM-110346] p 335 N95-24629
- CHAPMAN, GARY T.**
Experimental study of flow separation on an oscillating flap at Mach 2.4
[BTN-95-EIX95222650792] p 329 A95-79248
- CHATTOPADHYAY, ADITI**
Multilevel decomposition procedure for efficient design optimization of helicopter rotor blades
[BTN-95-EIX95222650784] p 334 A95-79240
- CHAU, JOHNNY**
Advanced subsonic airplane design and economic studies
[NASA-CR-195443] p 338 N95-24304
- CHAWLA, KALPANA**
Aerodynamic optimization studies on advanced architecture computers
[NASA-CR-198045] p 330 N95-24379
- CHERN, JENG-SHING**
Ideal proportional navigation p 342 A95-81374
- CHOU, Y. J.**
Impingement cooling of an isothermally heated surface with a confined slot jet
[BTN-94-EIX94421348950] p 347 A95-78494
- CHOULES, B. D.**
Thermal fracture mechanisms in ceramic thermal barrier coatings p 346 N95-26138
- CHRISTENSEN, DIANE G.**
Development of an intervention program to encourage shoulder harness use and aircraft retrofit in general aviation aircraft, phases 1 and 2
[DOT/FAA/AM-95/2] p 333 N95-24384
- CLOUTIER, JAMES R.**
High-performance, robust, bank-to-turn missile autopilot design
[BTN-95-EIX95242670751] p 336 A95-81096
- COCHRAN, J. E., JR.**
Dynamics and control of a tethered flight vehicle
[BTN-95-EIX95242670754] p 342 A95-81093

- COFFEY, M. T.**
Comparison of column abundances from three infrared spectrometers during AASE 2
[HTN-95-70946] p 352 A95-78011
- COHEN, R. C.**
The distribution of hydrogen, nitrogen, and chlorine radicals in the lower stratosphere: Implications for changes in O₃ due to emission of NO(y) from supersonic aircraft
[HTN-95-70935] p 351 A95-78000
- COLLINS, J. E.**
Meridional distributions of NO(X), NO(Y), and other species in the lower stratosphere and upper troposphere during AASE 2
[HTN-95-70944] p 352 A95-78009
- COLLINS, J. E., JR.**
An analysis of aircraft exhaust plumes from accidental encounters
[HTN-95-70943] p 351 A95-78008
- CONSTANTINESCU, CRISTIAN**
Impact of near-coincident faults on digital flight control systems
[BTN-95-EIX95242670759] p 359 A95-81088
- COON, MICHAEL D.**
Experimental study of flow separation on an oscillating flap at Mach 2.4
[BTN-95-EIX95222650792] p 329 A95-79248
- COOPER, DAVID J.**
An intercomparison of instrumentation for tropospheric measurements of dimethyl sulfide: Aircraft results for concentrations at the parts-per-trillion level
[HTN-95-91857] p 355 A95-80845
- CRAMER, EVIN J.**
Application of direct transcription to commercial aircraft trajectory optimization
[BTN-95-EIX95242670766] p 359 A95-81081
- CRAWLEY, EDWARD F.**
Fundamental mechanisms of aeroelastic control with control surface and strain actuation
[BTN-95-EIX95242670746] p 327 A95-81101
- CULP, ROBERT D.**
Guidance and control, 1993; Annual Rocky Mountain Guidance and Control Conference, 16th, Keystone, CO, Feb. 6-10, 1993
[ISBN-0-87703-365-X] p 341 A95-80389

D

- DAHLKE, LUTZ**
Emerging nondestructive inspection for aging aircraft
[PB95-143053] p 328 N95-25401
- DANIEL, W. J.**
Balances for the measurement of multiple components of force in flows of a millisecond duration p 350 N95-25400
- DAPKUNAS, S. J.**
Thermal Barrier Coating Workshop
[NASA-CP-10170] p 344 N95-26119
- Measurement methods and standards for processing and application of thermal barrier coatings p 344 N95-26123
- DAUBE, BRUCE C., JR.**
Vertical transport rates in the stratosphere in 1993 from observations of CO₂, N₂O, and CH₄
[HTN-95-70941] p 351 A95-78006
- DAVIDSON, J. A.**
SOFIA: Stratospheric Observatory for Infrared Astronomy p 363 A95-81583
- DAVIS, DOUGLAS D.**
An intercomparison of aircraft instrumentation for tropospheric measurements of sulfur dioxide
[HTN-95-91855] p 354 A95-80843
- An intercomparison of aircraft instrumentation for tropospheric measurements of carbonyl sulfide, hydrogen sulfide, and carbon disulfide p 355 A95-80844
- An intercomparison of instrumentation for tropospheric measurements of dimethyl sulfide: Aircraft results for concentrations at the parts-per-trillion level
[HTN-95-91857] p 355 A95-80845
- DEMASI-MARCIN, J.**
Thermal barrier coating experience in the gas turbine engine p 345 N95-26125
- DHUYVETTER, H.**
A new guidance and flight control system for the DELTA 2 launch vehicle p 342 A95-80427
- DICKES, E.**
Experimental study of the effects of Reynolds number on high angle of attack aerodynamic characteristics of forebodies during rotary motion
[NASA-CR-195033] p 330 N95-24443
- DINWIDDIE, R. B.**
Thermal conductivity of zirconia thermal barrier coatings p 345 N95-26133

- DOGRA, V. K.**
DSMC calculations for 70-deg blunted cone at 3.2 km/s in nitrogen
[NASA-TM-109181] p 348 N95-24396
- DOUGLASS, ANNE R.**
Tracer transport for realistic aircraft emission scenarios calculated using a three-dimensional model
[HTN-95-41799] p 353 A95-80525
- DOYAL, JEFFREY A.**
Visual contrast detection thresholds for aircraft contrails
[AD-A288618] p 328 N95-25607
- DRDLA, K.**
Analysis of the physical state of one Arctic polar stratospheric cloud based on observations
[HTN-95-70917] p 351 A95-77982
- DUTTON, CRAIG J.**
Study of subsonic base cavity flowfield structure using particle image velocimetry
[BTN-95-EIX95222650781] p 327 A95-79237
- DUTTON, GEOFFREY S.**
Vertical transport rates in the stratosphere in 1993 from observations of CO₂, N₂O, and CH₄
[HTN-95-70941] p 351 A95-78006
- DYE, J. E.**
Analysis of the physical state of one Arctic polar stratospheric cloud based on observations
[HTN-95-70917] p 351 A95-77982

E

- EKSTROM, C.**
Interfacing a digital compass to a remote-controlled helicopter
[PB95-164927] p 340 N95-24260
- ELKINS, J. W.**
Fine-scale, poleward transport of tropical air during AASE 2
[HTN-95-70949] p 352 A95-78014
- ELKINS, JAMES W.**
Vertical transport rates in the stratosphere in 1993 from observations of CO₂, N₂O, and CH₄
[HTN-95-70941] p 351 A95-78006
- ELMER, KEVIN R.**
Noise impact of advanced high lift systems
[NASA-CR-195028] p 362 N95-26160
- ERICKSON, E. F.**
SOFIA: Stratospheric Observatory for Infrared Astronomy p 363 A95-81583
- ESHOW, MICHELLE M.**
Identification and simulation evaluation of a combat helicopter in hover
[BTN-95-EIX95242670749] p 335 A95-81098
- EVERS, JOHNNY H.**
High-performance, robust, bank-to-turn missile autopilot design
[BTN-95-EIX95242670751] p 336 A95-81096

F

- FABIAN, P.**
Dynamics of aircraft exhaust plumes in the jet-regime
[HTN-95-51275] p 355 A95-80860
- FAHEY, D. W.**
The distribution of hydrogen, nitrogen, and chlorine radicals in the lower stratosphere: Implications for changes in O₃ due to emission of NO(y) from supersonic aircraft
[HTN-95-70935] p 351 A95-78000
- FAHEY, DAVID W.**
Vertical transport rates in the stratosphere in 1993 from observations of CO₂, N₂O, and CH₄
[HTN-95-70941] p 351 A95-78006
- FAIRBANKS, J. W.**
Thermal barrier coatings application in diesel engines p 345 N95-26124
- FALLER, WILLIAM E.**
Application of neural networks to unsteady aerodynamic control p 360 N95-25264
- FEREK, RONALD J.**
An intercomparison of aircraft instrumentation for tropospheric measurements of sulfur dioxide
[HTN-95-91855] p 354 A95-80843
- An intercomparison of instrumentation for tropospheric measurements of dimethyl sulfide: Aircraft results for concentrations at the parts-per-trillion level
[HTN-95-91857] p 355 A95-80845
- FLOWERS, G. T.**
Dynamic behavior of a magnetic bearing supported jet engine rotor with auxiliary bearings
[NASA-CR-197860] p 338 N95-24213
- FORRESTER, B. D.**
A portable transmission vibration analysis system for the S-70A-9 Black Hawk helicopter
[DSTO-TR-0072] p 348 N95-24203

FOSTER, JEFFRY

Study of compressible flow through a rectangular-to-semiannular transition duct
[NASA-CR-4660] p 338 N95-24392

FRASER, KEN F.

An overview of Health and Usage Monitoring Systems (HUMS) for military helicopters
[DSTO-TR-0061] p 327 N95-24200

Helicopter life substantiation: Review of some USA and UK initiatives
[DSTO-TR-0062] p 328 N95-24201

FRITH, P. C. W.

Assessment of overhaul surge margin tests applied to the T53 engines in ADF Iroquois helicopters
[AR-008-389] p 339 N95-25936

FRODGE, SALLY L.

Real-time testing and demonstration of the US Army Corps of Engineers' Real-Time On-The-Fly positioning system
[AD-A288624] p 334 N95-25609

FU, T. C.

Flow structure in the lee of an inclined 6:1 prolate spheroid
[BTN-94-EIX95011441127] p 348 A95-81027

FUJIEDA, HIROTOSHI

Low speed aerodynamic characteristics of delta wings with vortex flaps: 60 deg and 70 deg delta wings
[NAL-TR-1245] p 331 N95-25105

FUJITA, TOSHIMI

Low speed aerodynamic characteristics of delta wings with vortex flaps: 60 deg and 70 deg delta wings
[NAL-TR-1245] p 331 N95-25105

FULKER, J. L.

A theoretical and experimental investigation of the flow over supersonic leading edge wing/body configurations [DRA-TM-AERO-PROP-41] p 331 N95-25649

FUNABIKI, KOHEI

Fight reference display for powered-lift STOL aircraft [NAL-TR-1251] p 337 N95-25005

G

GAITONDE, DATTA

Structure of a double-fin turbulent interaction at high speed
[BTN-95-EIX95222650780] p 347 A95-79236

GANGLOFF, RICHARD P.

NASA-UVA light aerospace alloy and structures technology program (LA2ST)
[NASA-CR-198041] p 343 N95-24220

GAO, R. S.

The distribution of hydrogen, nitrogen, and chlorine radicals in the lower stratosphere: Implications for changes in O₃ due to emission of NO(y) from supersonic aircraft
[HTN-95-70935] p 351 A95-78000

GARRARD, WILLIAM L.

Robust dynamic inversion for control of highly maneuverable aircraft
[BTN-95-EIX95242670747] p 359 A95-81100

GARY, B. L.

Mentional distributions of NO(X), NO(Y), and other species in the lower stratosphere and upper troposphere during AASE 2
[HTN-95-70944] p 352 A95-78009

GENEROLI, ROBERT M.

Preload release mechanism
[NASA-CASE-MSC-22327-1] p 350 N95-25592

GHEE, TERENCE A.

Exploratory flow visualization investigation of mast-mounted sights in presence of a rotor
[NASA-TM-4634] p 330 N95-24566

GESKE, JOHN

Emerging nondestructive inspection for aging aircraft [PB95-143053] p 328 N95-25401

GIRVIN, RAQUEL

Advanced subsonic airplane design and economic studies
[NASA-CR-195443] p 338 N95-24304

GOEDJEN, J. G.

Thermal Barrier Coating Workshop
[NASA-CP-10170] p 344 N95-26119

GOLDMAN, P.

Wind technology development: Large and small turbines
[DE95-000286] p 358 N95-26090

GOODALL, COLIN

Bird ingestion into large turbofan engines
[DOT/FAA/CT-93/14] p 333 N95-24631

GOTO, NORIHIRO

Determination of piloting feedback structures for an altitude tracking task
[BTN-95-EIX95242670770] p 327 A95-81077

GRANIER, C.

Impact of present aircraft emissions of nitrogen oxides on tropospheric ozone and climate forcing
[HTN-95-21364] p 353 A95-78679

GREGORY, GERALD L.

An intercomparison of aircraft instrumentation for tropospheric measurements of sulfur dioxide
[HTN-95-91855] p 354 A95-80843

An intercomparison of aircraft instrumentation for tropospheric measurements of carbonyl sulfide, hydrogen sulfide, and carbon disulfide
[HTN-95-91856] p 355 A95-80844

An intercomparison of instrumentation for tropospheric measurements of dimethyl sulfide: Aircraft results for concentrations at the parts-per-trillion level
[HTN-95-91857] p 355 A95-80845

GRIFFITH, WAYLAND C.

Supercooling in hypersonic nitrogen wind tunnels
[BTN-94-EIX95011441134] p 340 A95-81020

GRONIG, H.

Hypersonic model testing in a shock tunnel
[BTN-95-EIX95222650789] p 329 A95-79245

GROSE, WILLIAM L.

The atmospheric effects of stratospheric aircraft: A fourth program report
[NASA-RP-1359] p 357 N95-24274

GUNN, WALTER J.

Development of an intervention program to encourage shoulder harness use and aircraft retrofit in general aviation aircraft, phases 1 and 2
[DOT/FAA/AM-95/2] p 333 N95-24384

H

HACKNEY, JOHN C.

The Cassini spacecraft: Object oriented flight control software
p 359 A95-80405

HANSCHKE, BRUCE

Emerging nondestructive inspection for aging aircraft [PB95-143053] p 328 N95-25401

HARVEY, W. DON

Aviation system capacity improvements through technology
[NASA-TM-109165] p 333 N95-24633

HAUGLUSTINE, D. A.

Impact of present aircraft emissions of nitrogen oxides on tropospheric ozone and climate forcing
[HTN-95-21364] p 353 A95-78679

HAYES, JAMES R.

Heat transfer measurements in small scale wind tunnels
[AD-A288689] p 341 N95-26053

HEIL, ROBERT MILTON

Characterizing the wake vortex signature for an active line of sight remote sensor
[NASA-CR-197697] p 333 N95-24391

HERAKOVICH, CARL T.

NASA-UVA light aerospace alloy and structures technology program (LA2ST)
[NASA-CR-198041] p 343 N95-24220

HERMANN, ROBERT

A brief survey of constrained mechanics and variational problems in terms of differential forms
p 360 N95-25803

HESS, R. A.

Rotorcraft handling qualities in turbulence
[BTN-95-EIX95242670750] p 334 A95-81097

HITT, ELLIS

Assessment of avionics technology in European aerospace organizations
[NASA-CR-189201] p 337 N95-24624

HOCK, S. M.

Wind technology development: Large and small turbines
[DE95-000286] p 358 N95-26090

HONKA, KLAUS P.

North Atlantic air traffic within the lower stratosphere: Cruising times and corresponding emissions
[HTN-95-91841] p 354 A95-80829

HOLDEMAN, J. D.

Crossflow mixing of noncircular jets
[NASA-TM-106865] p 338 N95-24390

HOLDREN, M. W.

Chemical composition and photochemical reactivity of exhaust from aircraft turbine engines
[HTN-95-51277] p 356 A95-80862

HOMAFAR, ABDOLLAH

Dynamic behavior of a magnetic bearing supported jet engine rotor with auxiliary bearings
[NASA-CR-197860] p 338 N95-24213

HOOPER, STEVEN J.

Analysis of warping effects on the static and dynamic response of a seat-type structure
[NIAR-94-12] p 348 N95-24211

HOUTMAN, E. M.

Quantitative comparison between interferometric measurements and Euler computations for supersonic cone flows
[BTN-95-EIX95222650782] p 358 A95-79238

HSU, L. L.

Perspective on thermal barrier coatings for industrial gas turbine applications
p 345 N95-26128

HUANG, T. T.

Flow structure in the lee of an inclined 6:1 prolate spheroid
[BTN-94-EIX95011441127] p 348 A95-81027

HUNG, Y. H.

Impingement cooling of an isothermally heated surface with a confined slot jet
[BTN-94-EIX94421348950] p 347 A95-78494

I

INAGAKI, TOSHIHARU

Flight reference display for powered-lift STOL aircraft [NAL-TR-1251] p 337 N95-25005

ISHIDA, YOJI

Numerical and experimental study of drag characteristics of two-dimensional HLFC airfoils in high subsonic, high Reynolds number flow
[NAL-TR-1244T] p 331 N95-24998

IWASAKI, AKIHIRO

Low speed aerodynamic characteristics of delta wings with vortex flaps: 60 deg and 70 deg delta wings
[NAL-TR-1245] p 331 N95-25105

IWASAKI, KAZUO

Fundamental wind tunnel experiments on low-speed flutter of a tip-fin configuration wing
[NAL-TR-1228] p 332 N95-25762

J

JACKSON, R. W.

Configuration and other differences between Black Hawk and Seahawk helicopters in military service in the USA and Australia
[AR-008-386] p 336 N95-25935

JACOBSON, M. Z.

Analysis of the physical state of one Arctic polar stratospheric cloud based on observations
[HTN-95-70917] p 351 A95-77982

JAIN, ATUL

Dynamic imaging and RCS measurements of aircraft
[BTN-95-EIX95202637582] p 347 A95-78576

JAMESON, ANTONY

Aerodynamic shape optimization of wing and wing-body configurations using control theory
[NASA-CR-198024] p 335 N95-25334

JANECKI, DARIUSZ

Actuating signals in adaptive control systems
[IFTR-13/1994] p 361 N95-26330

JOHNSON, D. G.

Comparison of column abundances from three infrared spectrometers during AASE 2
[HTN-95-70946] p 352 A95-78011

JOHNSON, DAVID G.

Chemical change in the arctic vortex during AASE 2
[HTN-95-70947] p 352 A95-78012

JOHNSON, JAMES E.

An intercomparison of aircraft instrumentation for tropospheric measurements of carbonyl sulfide, hydrogen sulfide, and carbon disulfide
[HTN-95-91856] p 355 A95-80844

An intercomparison of instrumentation for tropospheric measurements of dimethyl sulfide: Aircraft results for concentrations at the parts-per-trillion level
[HTN-95-91857] p 355 A95-80845

JONES, A. E.

Sensitivity of supersonic aircraft modelling studies to HNO₃ photolysis rate
[HTN-95-11475] p 353 A95-79453

JOSHI, MAHENDRA C.

Noise impact of advanced high lift systems
[NASA-CR-195028] p 362 N95-26160

JUCKS, K. W.

Comparison of column abundances from three infrared spectrometers during AASE 2
[HTN-95-70946] p 352 A95-78011

JUCKS, KENNETH W.

Chemical change in the arctic vortex during AASE 2
[HTN-95-70947] p 352 A95-78012

K

KACHURIN, V. K.

Laser device for measuring a vessel's speed
[HTN-95-60992] p 361 A95-80633

KAERCHER, B.

Dynamics of aircraft exhaust plumes in the jet-regime
[HTN-95-51275] p 355 A95-80860

KANDA, HIROSHI

Numerical and experimental study of drag characteristics of two-dimensional HLFC airfoils in high subsonic, high Reynolds number flow
[NAL-TR-1244T] p 331 N95-24998

KANDA, TAKESHI

Effect of film cooling/regenerative cooling on scramjet engine performances
[NAL-TR-1242] p 339 N95-24990

KARLSSON, ANDERS

How to fly an aircraft with control theory and splines
p 360 N95-25805

KARPOVSKY, MARK G.

Fault detection in multiprocessor systems and array processors
[BTN-95-EIX9524267097] p 359 A95-81253

KATZ, J.

Flow structure in the lee of an inclined 6:1 prolate spheroid
[BTN-94-EIX95011441127] p 348 A95-81027

KAWAHARA, HIROYASU

Preliminary experiments of an optical fiber display
[NAL-TR-1257] p 362 N95-25004
Flight reference display for powered-lift STOL aircraft
[NAL-TR-1251] p 337 N95-25005

KEIM, E. R.

The distribution of hydrogen, nitrogen, and chlorine radicals in the lower stratosphere: Implications for changes in O₃ due to emission of NO(y) from supersonic aircraft
[HTN-95-70935] p 351 A95-78000

KELLEY, HENRY L.

Exploratory flow visualization investigation of mast-mounted sights in presence of a rotor
[NASA-TM-4634] p 330 N95-24566

KELLY, JOHN C., JR.

Dynamic behavior of a magnetic bearing supported jet engine rotor with auxiliary bearings
[NASA-CR-197860] p 338 N95-24213

KELLY, R. E.

Effect of density gradients in confined supersonic shear layers, part 1
[NASA-CR-198029] p 348 N95-24412

Effect of density gradients in confined supersonic shear layers. Part 2: 3-D modes
[NASA-CR-198030] p 349 N95-24413

KESSELI, J. B.

Small gas turbine component evaluation study
[PB95-147542] p 338 N95-24293

KHULIEF, Y. A.

Modal characteristics of rotors using a conical shaft finite element
[BTN-94-EIX94401359745] p 346 A95-77379

KILGORE, W. ALLEN

Development of a model protection and dynamic response monitoring system for the national transonic facility
[NASA-CR-195041] p 340 N95-24388

KLEFFMANN, J.

Nitrous oxide and methane emissions from aero engines
[HTN-95-21363] p 353 A95-78678

KO, MALCOLM K. W.

Effects on stratospheric ozone from high-speed civil transport: Sensitivity to stratospheric aerosol loading
[HTN-95-91842] p 354 A95-80830

KOKINI, K.

Thermal fracture mechanisms in ceramic thermal barrier coatings
p 346 N95-26138

KOLENSKI, J. D.

Viscoplastic response of structures for intense local heating
[HTN-95-41540] p 346 A95-77921

KOLVE, D. I.

Describing an attitude
p 342 A95-80409

KORTEING, J. E.

Partial camera automation in a simulated Unmanned Air Vehicle
[AD-A288786] p 337 N95-26190

KURTENBACH, R.

Nitrous oxide and methane emissions from aero engines
[HTN-95-21363] p 353 A95-78678

L

LAIT, L. R.

Fine-scale, poleward transport of tropical air during AASE 2
[HTN-95-70949] p 352 A95-78014

LAMB, MILTON

Internal performance characteristics of thrust-vectorable axisymmetric ejector nozzles
[NASA-TM-4610] p 331 N95-25338

LANEN, T. A. W. M.

Quantitative comparison between interferometric measurements and Euler computations for supersonic cone flows
[BTN-95-EIX95222650782] p 358 A95-79238

LAPUCHA, DARIUSZ

Real-time testing and demonstration of the US Army Corps of Engineers' Real-Time On-The-Fly positioning system
[AD-A288624] p 334 N95-25609

LATORELLA, KARA A.

A crew-centered flight deck design philosophy for High-Speed Civil Transport (HSCT) aircraft
[NASA-TM-109171] p 335 N95-24582

LAUBERTS, A.

Aspect estimation of an aircraft using library model silhouettes
[PB95-141834] p 360 N95-25894

LAZARUS, KENNETH B.

Fundamental mechanisms of aeroelastic control with control surface and strain actuation
[BTN-95-EIX95242670746] p 327 A95-81101

LEBOZEC, A.

Hypersonic model testing in a shock tunnel
[BTN-95-EIX95222650789] p 329 A95-79245

LEE, ABRAHAM P.

Impact, friction, and wear testing of microsamples of polycrystalline silicon
p 361 A95-79988

LEE, SOOGBAB

Dynamic stall control for advanced rotorcraft application
[BTN-95-EIX95222650793] p 334 A95-79249

LEE, W. Y.

Thermal Barrier Coating Workshop
[NASA-CP-10170] p 344 N95-26119
Thermal barrier coatings issues in advanced land-based gas turbines
p 344 N95-26122

LEONDES, CORNELIUS

Assessment of avionics technology in European aerospace organizations
[NASA-CR-189201] p 337 N95-24624

LI, WEI-LIN

Aeroservoelastic aspects of wing/control surface planform shape optimization
[BTN-95-EIX95222650795] p 340 A95-79251

LIEBECK, ROBERT H.

Advanced subsonic airplane design and economic studies
[NASA-CR-195443] p 338 N95-24304

LIM, MARTIN G.

Impact, friction, and wear testing of microsamples of polycrystalline silicon
p 361 A95-79988

LIN, CHARRISSA Y.

Fundamental mechanisms of aeroelastic control with control surface and strain actuation
[BTN-95-EIX95242670746] p 327 A95-81101

LIN, CHING-FANG

High-performance, robust, bank-to-turn missile autopilot design
[BTN-95-EIX95242670751] p 336 A95-81096

LISCINSKY, D. S.

Crossflow mixing of noncircular jets
[NASA-TM-106865] p 338 N95-24390

LIU, BAW-LIN

High frequency flow-structural interaction in dense subsonic fluids
[NASA-CR-4652] p 330 N95-24217

LIU, S. C.

An analysis of aircraft exhaust plumes from accidental encounters
[HTN-95-70943] p 351 A95-78008

LIVNE, ELI

Aeroservoelastic aspects of wing/control surface planform shape optimization
[BTN-95-EIX95222650795] p 340 A95-79251

LOEWENSTEIN, M.

Fine-scale, poleward transport of tropical air during AASE 2
[HTN-95-70949] p 352 A95-78014

LOEWENSTEIN, MAX

Vertical transport rates in the stratosphere in 1993 from observations of CO₂, N₂O, and CH₄
[HTN-95-70941] p 351 A95-78006

LOOSE, R. R.

Wind technology development: Large and small turbines
[DE95-000286] p 358 N95-26090

LOUISNARD, N.

Potential effects on ozone of future supersonic aircraft/2D simulation
[HTN-95-51282] p 356 A95-80867

LUTTGES, MARVIN W.

Application of neural networks to unsteady aerodynamic control
p 360 N95-25264

LYON, ROGER

Advanced subsonic airplane design and economic studies
[NASA-CR-195443] p 338 N95-24304

LYON, T. F.

Chemical composition and photochemical reactivity of exhaust from aircraft turbine engines
[HTN-95-51277] p 356 A95-80862

M

MACPHERSON, J. IAN

Comparison of wind profiler and aircraft wind measurements at Chebogue Point, Nova Scotia
[HTN-95-41833] p 353 A95-80559

MANKIN, W. G.

Comparison of column abundances from three infrared spectrometers during AASE 2
[HTN-95-70946] p 352 A95-78011

MARIOCCHI, A.

PVD TBC experience on GE aircraft engines
p 345 N95-26126

MARTINEC, D. A.

Assessment of avionics technology in European aerospace organizations
[NASA-CR-189201] p 337 N95-24624

MASUYA, GORO

Effect of film cooling/regenerative cooling on scramjet engine performances
[NAL-TR-1242] p 339 N95-24990

MAYER, DAVID W.

Prediction of supersonic inlet unstart caused by freestream disturbances
[BTN-95-EIX95222650790] p 329 A95-79246

MAYTON, MONICA

Assessment of avionics technology in European aerospace organizations
[NASA-CR-189201] p 337 N95-24624

MCALISTER, KENNETH W.

Dynamic stall control for advanced rotorcraft application
[BTN-95-EIX95222650793] p 334 A95-79249

MCCARTHY, THOMAS R.

Multilevel decomposition procedure for efficient design optimization of helicopter rotor blades
[BTN-95-EIX95222650784] p 334 A95-79240

MCELROY, MICHAEL B.

Vertical transport rates in the stratosphere in 1993 from observations of CO₂, N₂O, and CH₄
[HTN-95-70941] p 351 A95-78006

MCNEIL, WALTER E.

Aerodynamics model for a generic ASTOVL lift-lan aircraft
[NASA-TM-110347] p 332 N95-26302

MEE, D.

Shock tunnel studies of scramjet phenomena 1993
[NASA-CR-195038] p 350 N95-25394

Thrust measurements of a complete axisymmetric scramjet in an impulse facility
p 339 N95-25395

MEE, D. J.

Scramjet thrust measurement in a shock tunnel
p 339 N95-25396
Balances for the measurement of multiple components of force in flows of a millisecond duration
p 350 N95-25400

MEGIE, G.

Impact of present aircraft emissions of nitrogen oxides on tropospheric ozone and climate forcing
[HTN-95-21364] p 353 A95-78679

MEGUID, S. A.

Theoretical and experimental studies of fretting-initiated fatigue failure of aeroengine compressor discs
[BTN-94-EIX94421372285] p 343 A95-78467

MEI, RENWEI

Flow due to an oscillating sphere and an expression for unsteady drag on the sphere at finite Reynolds number
[BTN-94-EIX95011441142] p 347 A95-81012

MENDOZA, J.

Effects of cavity dimensions, boundary layer, and temperature on cavity noise with emphasis on benchmark data to validate computational aeroacoustic codes
[NASA-CR-4653] p 361 N95-24879

METZ, WERNER

North Atlantic air traffic within the lower stratosphere: Cruising times and corresponding emissions
[HTN-95-91841] p 354 A95-80829

MILLER, R. A.

Thermal barrier coatings for aircraft engines: History and directions
p 344 N95-26121

- MILLER, R. F.**
Residual Stress Measurements with Laser Speckle Correlation Interferometry and Local Heat Treating [DE95-060082] p 349 N95-24598
- MOHUDDIN, M. A.**
Modal characteristics of rotors using a conical shaft finite element [BTN-94-EIX94401359745] p 346 A95-77379
- MOLEZZI, MICHAEL J.**
Study of subsonic base cavity flowfield structure using particle image velocimetry [BTN-95-EIX95222650781] p 327 A95-79237
- MONTGOMERY, BRAD**
Parts washing alternatives study: United States Coast Guard. Project summary and report [PB95-166146] p 343 N95-26004
- MOORE, C. S.**
Thermal conductivity of zirconia thermal barrier coatings p 345 N95-26133
- MOORE, PATRICK D.**
Identification of aviation weather hazards based on the integration of radar and lightning data [HTN-95-51323] p 356 A95-80906
- MORAGA, CLAUDIO**
Fault detection in multiprocessor systems and array processors [BTN-95-EIX95242679097] p 359 A95-81253
- MORGAN, R. G.**
Shock tunnel studies of scramjet phenomena 1993 [NASA-CR-195038] p 350 N95-25394
The Supercritical Expansion Tube concept, experiment and analysis p 341 N95-25399
- MOSS, J. N.**
DSMC calculations for 70-deg blunted cone at 3.2 km/s in nitrogen [NASA-TM-109181] p 348 N95-24396
- MUROTA, KATSUCHI**
Measurements of longitudinal static aerodynamic coefficients by the cable mount system [NAL-TR-1226] p 331 N95-25761
- MUTASIM, Z. Z.**
Perspective on thermal barrier coatings for industrial gas turbine applications p 345 N95-26128
- MYOSE, ROY Y.**
On the role of the outer region in the turbulent-boundary-layer bursting process [BTN-94-EIX95011441078] p 348 A95-81056
- N**
- NAGARAJ, B. A.**
Thermal conductivity of zirconia thermal barrier coatings p 345 N95-26133
- NAKAMURA, MASARU**
Flight reference display for powered-lift STOL aircraft [NAL-TR-1251] p 337 N95-25005
- NAPOLITANO, MARCELLO R.**
On-line learning nonlinear direct neurocontrollers for restructurable control systems [BTN-95-EIX95242670768] p 359 A95-81079
- NAYLOR, STEVE**
On-line learning nonlinear direct neurocontrollers for restructurable control systems [BTN-95-EIX95242670768] p 359 A95-81079
- NEELY, A. J.**
The Supercritical Expansion Tube concept, experiment and analysis p 341 N95-25399
- NEPPACH, CHARLES**
On-line learning nonlinear direct neurocontrollers for restructurable control systems [BTN-95-EIX95242670768] p 359 A95-81079
- NEWMAN, P. A.**
Fine-scale, poleward transport of tropical air during AASE 2 [HTN-95-70949] p 352 A95-78014
- NISSLEY, D. M.**
Thermal barrier coating life modeling in aircraft gas turbine engines p 346 N95-26140
- NO, T. S.**
Dynamics and control of a tethered flight vehicle [BTN-95-EIX95242670754] p 342 A95-81093
- NODA, JUNICHI**
Aerodynamic characteristics of the orbital reentry vehicle experimental probe fins in a supersonic flow [NAL-TR-1232] p 342 N95-25664
- NOEL, BRUCE W.**
Turbine-engine applications of thermographic-phosphor temperature measurements [DE95-003625] p 358 N95-25110
- NOGUCHI, MASAYOSHI**
Numerical and experimental study of drag characteristics of two-dimensional HLFC airfoils in high subsonic, high Reynolds number flow [NAL-TR-1244T] p 331 N95-24998
- NOGUCHI, YOSHIO**
Study on tensile fatigue testing method of unidirectional fiber-resin matrix composites [NAL-TR-1241] p 343 N95-24989
- NORBERG, C.**
Experimental investigation of the flow around a circular cylinder: Influence of aspect ratio [BTN-94-EIX95011441120] p 347 A95-80044
- O**
- OFARRELL, J. M.**
High frequency flow-structural interaction in dense subsonic fluids [NASA-CR-4652] p 330 N95-24217
- OKISHI, THEODORE H.**
Study of compressible flow through a rectangular-to-semiannular transition duct [NASA-CR-4660] p 338 N95-24392
- OLIVIER, H.**
Hypersonic model testing in a shock tunnel [BTN-95-EIX95222650789] p 329 A95-79245
- OLSSON, H. A.**
Orientation determination of aircraft using visual 3D matching and radar. Case study 2 [PB95-165791] p 350 N95-25749
- ONO, FUMIEI**
Effect of film cooling/regenerative cooling on scramjet engine performances [NAL-TR-1242] p 339 N95-24990
- ONO, TAKATSUGU**
Flight reference display for powered-lift STOL aircraft [NAL-TR-1251] p 337 N95-25005
- P**
- PAGALDIPTI, NARAYANAN**
Multilevel decomposition procedure for efficient design optimization of helicopter rotor blades [BTN-95-EIX95222650784] p 334 A95-79240
- PALEPPI, S.**
Impact on ozone of high-speed stratospheric aircraft: Effects of the emission scenario [HTN-95-51283] p 356 A95-80868
- PALMER, MICHAEL T.**
A crew-centered flight deck design philosophy for High-Speed Civil Transport (HSCT) aircraft [NASA-TM-109171] p 335 N95-24582
- PAPANIKOS, P.**
Theoretical and experimental studies of fretting-initiated fatigue failure of aeroengine compressor discs [BTN-94-EIX94421372285] p 343 A95-78467
- PARKER, JAMES F., JR.**
Development of an intervention program to encourage shoulder harness use and aircraft retrofit in general aviation aircraft, phases 1 and 2 [DOT/FAA/AM-95/2] p 333 N95-24384
- PARKS, W. P.**
Thermal barrier coatings issues in advanced land-based gas turbines p 344 N95-26122
- PATEL, INDU**
Dynamic imaging and RCS measurements of aircraft [BTN-95-EIX95202637582] p 347 A95-78576
- PAULEY, H.**
Experimental study of the effects of Reynolds number on high angle of attack aerodynamic characteristics of forebodies during rotary motion [NASA-CR-195033] p 330 N95-24443
- PAULL, A.**
Shock tunnel studies of scramjet phenomena 1993 [NASA-CR-195038] p 350 N95-25394
Thrust measurements of a complete axisymmetric scramjet in an impulse facility p 339 N95-25395
Scramjet thrust measurement in a shock tunnel p 339 N95-25396
- PAXSON, DANIEL E.**
Recent improvements to and validation of the one dimensional NASA wave rotor model [NASA-TM-106913] p 332 N95-25862
- PAYNE, J. L.**
Verification of computational aerodynamic predictions for complex hypersonic vehicles using the INCA(trademark) code [DE95-004757] p 330 N95-24308
- PAYNTER, GERALD C.**
Prediction of supersonic inlet unstart caused by freestream disturbances [BTN-95-EIX95222650790] p 329 A95-79246
- PEAKE, N.**
Unsteady lift on a swept blade tip [BTN-94-EIX95011441154] p 329 A95-80030
- PEARSON, A. E.**
Aerodynamic parameter estimation via Fourier modulating function techniques [NASA-CR-4654] p 335 N95-24630
- PECHERSKY, M. J.**
Residual Stress Measurements with Laser Speckle Correlation Interferometry and Local Heat Treating [DE95-060082] p 349 N95-24598
- PEROOMIAN, OSHIN**
Effect of density gradients in confined supersonic shear layers, part 1 [NASA-CR-198029] p 348 N95-24412
Effect of density gradients in confined supersonic shear layers. Part 2: 3-D modes [NASA-CR-198030] p 349 N95-24413
- PHIPPS, GARY**
Emerging nondestructive inspection for aging aircraft [PB95-143053] p 328 N95-25401
- PISANO, ALBERT P.**
Impact, friction, and wear testing of microsamples of polycrystalline silicon p 361 A95-79988
- PITARI, G.**
High-speed civil transport impact: Role of sulfate, nitric acid trihydrate, and ice aerosols studied with a two-dimensional model including aerosol physics [HTN-95-91843] p 354 A95-80831
Impact on ozone of high-speed stratospheric aircraft: Effects of the emission scenario [HTN-95-51283] p 356 A95-80868
- PLUMB, R. A.**
Fine-scale, poleward transport of tropical air during AASE 2 [HTN-95-70949] p 352 A95-78014
- PODOLSKIE, J. R.**
Fine-scale, poleward transport of tropical air during AASE 2 [HTN-95-70949] p 352 A95-78014
- PODOLSKIE, JAMES R.**
Vertical transport rates in the stratosphere in 1993 from observations of CO₂, N₂O, and CH₄ [HTN-95-70941] p 351 A95-78006
- POELLOT, MICHAEL R.**
Preliminary analysis of University of North Dakota aircraft data from the FIRE Cirrus IFO-2 [NASA-CR-198038] p 357 N95-24219
- PORDON, R.**
A new guidance and flight control system for the DELTA 2 launch vehicle p 342 A95-80427
- PORTER, L.**
Shock tunnel studies of scramjet phenomena 1993 [NASA-CR-195038] p 350 N95-25394
- PRESS, HAYES N.**
A crew-centered flight deck design philosophy for High-Speed Civil Transport (HSCT) aircraft [NASA-TM-109171] p 335 N95-24582
- PRICE, J. M.**
DSMC calculations for 70-deg blunted cone at 3.2 km/s in nitrogen [NASA-TM-109181] p 348 N95-24396
- PURVIS, BRADLEY D.**
Visual contrast detection thresholds for aircraft contrails [AD-A288618] p 328 N95-25607
- PYLE, J. A.**
Sensitivity of supersonic aircraft modeling studies to HNO₃ photolysis rate [HTN-95-11475] p 353 A95-79453
- R**
- RAGSDALE, WILLIAM C.**
Supercooling in hypersonic nitrogen wind tunnels [BTN-94-EIX95011441134] p 340 A95-81020
- RAHEMATPURA, MANOJ**
Analysis of warping effects on the static and dynamic response of a seal-type structure [NIAR-94-12] p 348 N95-24211
- RALSTON, J.**
Experimental study of the effects of Reynolds number on high angle of attack aerodynamic characteristics of forebodies during rotary motion [NASA-CR-195033] p 330 N95-24443
- RAMAROSON, R.**
Potential effects on ozone of future supersonic aircraft/2D simulation [HTN-95-51282] p 356 A95-80867
- RAMER, DAVID P.**
Visual contrast detection thresholds for aircraft contrails [AD-A288618] p 328 N95-25607
- RAO, M.**
Dynamics of phase ordering of nematics in a pore [DE95-607662] p 362 N95-25978

RASMUSSEN, ROBERT D.

The Cassini spacecraft: Object oriented flight control software p 359 A95-80405

RAVISHANKARA, A. R.

The atmospheric effects of stratospheric aircraft: A fourth program report [NASA-RP-1359] p 357 N95-24274

RAWDON, BLAINE K.

Advanced subsonic airplane design and economic studies [NASA-CR-195443] p 338 N95-24304

REBBECCHI, B.

A portable transmission vibration analysis system for the S-70A-9 Black Hawk helicopter [DSTO-TR-0072] p 348 N95-24203

REICHERT, BRUCE A.

Study of compressible flow through a rectangular-to-semiannular transition duct [NASA-CR-4660] p 338 N95-24392

REINER, JACOB

Robust dynamic inversion for control of highly maneuverable aircraft [BTN-95-EIX95242670747] p 359 A95-81100

REINHARDT, MANFRED E.

North Atlantic air traffic within the lower stratosphere: Cruising times and corresponding emissions [HTN-95-91841] p 354 A95-80829

REMONDI, BENJAMIN W.

Real-time testing and demonstration of the US Army Corps of Engineers' Real-Time On-The-Fly positioning system [AD-A288624] p 334 N95-25609

REUTHER, JAMES

Aerodynamic shape optimization of wing and wing-body configurations using control theory [NASA-CR-198024] p 335 N95-25334

RICCIARDULLI, L.

High-speed civil transport impact: Role of sulfate, nitric acid trihydrate, and ice aerosols studied with a two-dimensional model including aerosol physics [HTN-95-91843] p 354 A95-80831

RICE, EDWARD J.

Jet mixer noise suppressor using acoustic feedback [NASA-CASE-LEW-15170-2] p 362 N95-26187

RICKLEY, JUNE ELIZABETH

The effect of altitude conditions on the particle emissions of a J85-GE-5L turbojet engine [NASA-TM-106669] p 339 N95-24561

RIDLEY, B. A.

An analysis of aircraft exhaust plumes form accidental encounters [HTN-95-70943] p 351 A95-78008

Meridional distributions of NO(X), NO(Y), and other species in the lower stratosphere and upper troposphere during AASE 2 [HTN-95-70944] p 352 A95-78009

RIGGIN, R. M.

Chemical composition and photochemical reactivity of exhaust from aircraft turbine engines [HTN-95-51277] p 356 A95-80862

RIMBEY, P. R.

Consistent approach to describing aircraft HIRF protection [NASA-CR-195067] p 334 N95-25341

RINIOE, KENICHI

Low speed aerodynamic characteristics of delta wings with vortex flaps: 60 deg and 70 deg delta wings [NAL-TR-1245] p 331 N95-25105

RIZI, V.

High-speed civil transport impact: Role of sulfate, nitric acid trihydrate, and ice aerosols studied with a two-dimensional model including aerosol physics [HTN-95-91843] p 354 A95-80831

ROACH, DENNIS

Emerging nondestructive inspection for aging aircraft [PB95-143053] p 328 N95-25401

RODRIGUEZ, JOSE M.

Effects on stratospheric ozone from high-speed civil transport: Sensitivity to stratospheric aerosol loading [HTN-95-91842] p 354 A95-80830

The atmospheric effects of stratospheric aircraft: A fourth program report [NASA-RP-1359] p 357 N95-24274

ROGERS, WILLIAM H.

A crew-centered flight deck design philosophy for High-Speed Civil Transport (HSCT) aircraft [NASA-TM-109171] p 335 N95-24582

ROIVAINEN, P.

Orientation determination of aircraft using visual 3D matching and radar. Case study 2 [PB95-165791] p 350 N95-25749

ROOD, RICHARD B.

Tracer transport for realistic aircraft emission scenarios calculated using a three-dimensional model [HTN-95-41799] p 353 A95-80525

ROSENBERGER, TODD E.

Workshop report: Measurement techniques in highly transient, spectrally rich combustion environments [AD-A288395] p 350 N95-25606

ROWLAND, F. S.

Meridional distributions of NO(X), NO(Y), and other species in the lower stratosphere and upper troposphere during AASE 2 [HTN-95-70944] p 352 A95-78009

ROZINER, TATYANA D.

Fault detection in multiprocessor systems and array processors [BTN-95-EIX95242670907] p 359 A95-81253

S
SACHSE, G. W.

An analysis of aircraft exhaust plumes form accidental encounters [HTN-95-70943] p 351 A95-78008

Meridional distributions of NO(X), NO(Y), and other species in the lower stratosphere and upper troposphere during AASE 2 [HTN-95-70944] p 352 A95-78009

SAITO, TOSHIHITO

Effect of film cooling/regenerative cooling on scramjet engine performances [NAL-TR-1242] p 339 N95-24990

SALAWITCH, R. J.

The distribution of hydrogen, nitrogen, and chlorine radicals in the lower stratosphere: Implications for changes in O3 due to emission of NO(y) from supersonic aircraft [HTN-95-70935] p 351 A95-78000

SALTZMAN, ERIC S.

An intercomparison of aircraft instrumentation for tropospheric measurements of carbonyl sulfide, hydrogen sulfide, and carbon disulfide [HTN-95-91856] p 355 A95-80844

An intercomparison of instrumentation for tropospheric measurements of dimethyl sulfide: Aircraft results for concentrations at the parts-per-trillion level [HTN-95-91857] p 355 A95-80845

SANANDRES, LUIS

Thermohydrodynamic analysis of cryogenic liquid turbulent flow fluid film bearings, phase 2 [NASA-CR-197412] p 349 N95-24461

SATO, MAMORU

Numerical and experimental study of drag characteristics of two-dimensional HLFC airfoils in high subsonic, high Reynolds number flow [NAL-TR-1244T] p 331 N95-24998

SCALLION, W. I.

Performance of an aerodynamic yaw controller mounted on the space shuttle orbiter body flap at Mach 10 [NASA-TM-109179] p 330 N95-24397

SCHAEFER, J.

Empirical corrections of the rigid rotor interaction potential of H2-H2 in the attractive region: Dimer features in the FIR absorption spectra [HTN-95-41943] p 361 A95-81690

SCHMIDT, DAVID K.

Integrated development of the equations of motion for elastic hypersonic flight vehicles [BTN-95-EIX95242670755] p 327 A95-81092

SCHNEIDER, STEVEN P.

Supersonic quiet-tunnel development for laminar-turbulent transition research [NASA-CR-198040] p 340 N95-24302

SCHOEERL, M. R.

Fine-scale, poleward transport of tropical air during AASE 2 [HTN-95-70949] p 352 A95-78014

SCHRECK, SCOTT J.

Application of neural networks to unsteady aerodynamic control p 360 N95-25264

SCHREIER, F.

Modeling of aircraft exhaust emissions and infrared spectra for remote measurement of nitrogen oxides [HTN-95-51276] p 355 A95-80861

SCHROEDER, JEFFERY A.

Identification and simulation evaluation of a combat helicopter in hover [BTN-95-EIX95242670749] p 335 A95-81098

SCHWIND, JOSEPH

Assessment of avionics technology in European aerospace organizations [NASA-CR-189201] p 337 N95-24624

SCOTT, PAUL W.

Advanced subsonic airplane design and economic studies [NASA-CR-195443] p 338 N95-24304

SCOTT, WILLIAM B.

SR-71 may launch targets for missile defense tests [HTN-95-91872] p 335 A95-81974

SCULLY, JOHN R.

NASA-UVA light aerospace alloy and structures technology program (LA2ST) [NASA-CR-198041] p 343 N95-24220

SEEGMILLER, H. LEE B.

Angular displacement measuring device [NASA-CASE-ARC-11937-1] p 362 N95-26015

SEKINE, HIDEO

Aerodynamic characteristics of the orbital reentry vehicle experimental probe fins in a supersonic flow [NAL-TR-1232] p 342 N95-25664

SEYWALD, HANS

Load alleviation maneuvers for a launch vehicle p 342 A95-81360

SHAGAM, RICH

Emerging nondestructive inspection for aging aircraft [PB95-143053] p 328 N95-25401

SHANG, J. S.

Structure of a double-fin turbulent interaction at high speed [BTN-95-EIX95222650780] p 347 A95-79236

SHEKARRIZ, A.

Flow structure in the lee of an inclined 6:1 prolate spheroid [BTN-94-EIX95011441127] p 348 A95-81027

SHEPARD, WILLIAM T.

Development of an intervention program to encourage shoulder harness use and aircraft retrofit in general aviation aircraft, phases 1 and 2 [DOT/FAA/AM-95/2] p 333 N95-24384

SHIFLET, GARY J.

NASA-UVA light aerospace alloy and structures technology program (LA2ST) [NASA-CR-198041] p 343 N95-24220

SHIRES, A.

A theoretical and experimental investigation of the flow over supersonic leading edge wing/body configurations [DRA-TM-AERO-PROP-41] p 331 N95-25649

SIMMONS, J. M.

Shock tunnel studies of scramjet phenomena 1993 [NASA-CR-195038] p 350 N95-25394

Balances for the measurement of multiple components of force in flows of a millisecond duration p 350 N95-25400

SINGH, SAHJENDRA N.

Direct adaptive and neural control of wing-rock motion of slender delta wings [BTN-95-EIX95242670748] p 327 A95-81099

SINHA, S. C.

Dynamic behavior of a magnetic bearing supported jet engine rotor with auxiliary bearings [NASA-CR-197860] p 338 N95-24213

SKINNER, K.

Shock tunnel studies of scramjet phenomena 1993 [NASA-CR-195038] p 350 N95-25394

SLATER, JOHN W.

A combined geometric approach for solving the Navier-Stokes equations on dynamic grids [NASA-TM-106919] p 332 N95-26075

SOECHTING, F. O.

A design perspective on thermal barrier coatings p 344 N95-26120

SOMERS, D. M.

NREL airfoil families for HAWTs [DE95-000267] p 357 N95-24882

SOTOMAYOR, JORGE

The 1994 Fiber Optic Sensors for Aerospace Technology (FOSAT) Workshop [NASA-CP-10166] p 337 N95-24207

SOTOZAKI, TOKUO

Fundamental wind tunnel experiments on low-speed flutter of a tip-fin configuration wing [NAL-TR-1228] p 332 N95-25762

SPICER, C. W.

Chemical composition and photochemical reactivity of exhaust from aircraft turbine engines [HTN-95-51277] p 356 A95-80862

SPIVEY, KATHY H.

Quantity-distance requirements for earth-bermed aircraft shelters [AD-A279692] p 341 N95-24424

SQUIRE, L. C.

Three-dimensional interaction of wake/boundary-layer and vortex/boundary-layer data report [CUED/A-AERO/TR-23] p 329 N95-24210

STALKER, R. J.

Shock tunnel studies of scramjet phenomena 1993 [NASA-CR-195038] p 350 N95-25394

Thrust measurements of a complete axisymmetric scramjet in an impulse facility p 339 N95-25395

Scramjet thrust measurement in a shock tunnel p 339 N95-25396

STARKE, E. A., JR.

NASA-UVA light aerospace alloy and structures technology program supplement: Aluminum-based materials for high speed aircraft
[NASA-CR-4645] p 343 N95-24878

STARKE, EDGAR A., JR.

NASA-UVA light aerospace alloy and structures technology program (LA2ST)
[NASA-CR-198041] p 343 N95-24220

STENGEL, ROBERTS

Real-time decision aiding: Aircraft guidance for wind shear avoidance
[BTN-95-EIX95202637575] p 332 A95-78583

STERN, ANDREW D.

Identification of aviation weather hazards based on the integration of radar and lightning data
[HTN-95-51323] p 356 A95-80908

STIMPLE, R. M.

The distribution of hydrogen, nitrogen, and chlorine radicals in the lower stratosphere: Implications for changes in O₃ due to emission of NO(y) from supersonic aircraft
[HTN-95-70935] p 351 A95-78000

STOLARSKI, RICHARD S.

The atmospheric effects of stratospheric aircraft: A fourth program report
[NASA-RP-1359] p 357 N95-24274

STONER, GLENN E.

NASA-UVA light aerospace alloy and structures technology program (LA2ST)
[NASA-CR-198041] p 343 N95-24220

STRATTON, D. ALEXANDER

Real-time decision aiding: Aircraft guidance for wind shear avoidance
[BTN-95-EIX95202637575] p 332 A95-78583

STRATTON, MICHAEL D.

Visual contrast detection thresholds for aircraft contrails
[AD-A288618] p 328 N95-25607

SUZUKI, HIROKAZU

Reentry guidance for hypersonic Flight Experiment (HYFLEX) vehicle
[NAL-TR-1235] p 334 N95-25764

SZE, NIEN-DAK

Effects on stratospheric ozone from high-speed civil transport: Sensitivity to stratospheric aerosol loading
[HTN-95-91842] p 354 A95-80830

SZETO, J. T.

Latitude variations of stratospheric trace gases
[HTN-95-70948] p 352 A95-78013

T

TABAZADEH, A.

Analysis of the physical state of one Arctic polar stratospheric cloud based on observations
[HTN-95-70917] p 351 A95-77982

TAKEUCHI, Y. R.

Thermal fracture mechanisms in ceramic thermal barrier coatings
p 346 N95-26138

TANAKA, KEIJI

Flight reference display for powered-lift STOL aircraft
[NAL-TR-1251] p 337 N95-25005

TANGLER, J. L.

NREL airfoil families for HAWTs
[DE95-000267] p 357 N95-24882

TATE, ATSUSHI

Aerodynamic characteristics of the orbital reentry vehicle experimental probe fins in a supersonic flow
[NAL-TR-1232] p 342 N95-25664

TERUI, YUSHI

Flight reference display for powered-lift STOL aircraft
[NAL-TR-1251] p 337 N95-25005

THOMPSON, KYLE

Emerging nondestructive inspection for aging aircraft
[PB95-143053] p 328 N95-25401

THORNTON, DONALD C.

An intercomparison of aircraft instrumentation for tropospheric measurements of sulfur dioxide
[HTN-95-91855] p 354 A95-80843

An intercomparison of aircraft instrumentation for tropospheric measurements of carbonyl sulfide, hydrogen sulfide, and carbon disulfide
[HTN-95-91856] p 355 A95-80844

THORNTON, EARL A.

Viscoplastic response of structures for intense local heating
[HTN-95-41540] p 346 A95-77921

THRESHER, R. W.

Wind technology development: Large and small turbines
[DE95-000286] p 358 N95-26090

TISCHLER, MARK B.

Identification and simulation evaluation of a combat helicopter in hover
[BTN-95-EIX95242670749] p 335 A95-81098

TOMPETRINI, K.

A new guidance and flight control system for the DELTA 2 launch vehicle
p 342 A95-80427

TOON, G. C.

Comparison of column abundances from three infrared spectrometers during AASE 2
[HTN-95-70946] p 352 A95-78011

Latitude variations of stratospheric trace gases
[HTN-95-70948] p 352 A95-78013

TORRES, FRANCISCO J.

Geometric analysis of wing sections
[NASA-TM-110346] p 335 N95-24629

TRAUB, W. A.

Comparison of column abundances from three infrared spectrometers during AASE 2
[HTN-95-70946] p 352 A95-78011

TRAUB, WESLEY A.

Chemical change in the arctic vortex during AASE 2
[HTN-95-70947] p 352 A95-78012

TRAYBAR, JOSEPH

Assessment of avionics technology in European aerospace organizations
[NASA-CR-189201] p 337 N95-24624

TRUE, B.

Crossflow mixing of noncircular jets
[NASA-TM-106865] p 338 N95-24390

TSUKANO, YUKICHI

Flight reference display for powered-lift STOL aircraft
[NAL-TR-1251] p 337 N95-25005

TUMA, MEG

The 1994 Fiber Optic Sensors for Aerospace Technology (FOSAT) Workshop
[NASA-CP-10166] p 337 N95-24207

TUNG, CHEE

Dynamic stall control for advanced rotorcraft application
[BTN-95-EIX95222650793] p 334 A95-79249

Geometric analysis of wing sections
[NASA-TM-110346] p 335 N95-24629

TURCO, R. P.

Analysis of the physical state of one Arctic polar stratospheric cloud based on observations
[HTN-95-70917] p 351 A95-77982

TURLEY, W. DALE

Turbine-engine applications of thermographic-phosphor temperature measurements
[DE95-003625] p 358 N95-25110

TUTTLE, S.

Shock tunnel studies of scramjet phenomena 1993
[NASA-CR-195038] p 350 N95-25394

TUTTLE, S. L.

Balances for the measurement of multiple components of force in flows of a millisecond duration
p 350 N95-25400

TUTTLE, SEAN

Thrust measurement in a 2-D scramjet nozzle
p 339 N95-25397

TWOHY, C.

Analysis of the physical state of one Arctic polar stratospheric cloud based on observations
[HTN-95-70917] p 351 A95-77982

U

UEDA, TETSUHIKO

Fundamental wind tunnel experiments on low-speed flutter of a tip-fin configuration wing
[NAL-TR-1228] p 332 N95-25762

V

VANDERBORG, W.

Partial camera automation in a simulated Unmanned Air Vehicle
[AD-A288786] p 337 N95-26190

VAUGHAN, K. W.

A portable transmission vibration analysis system for the S-70A-9 Black Hawk helicopter
[DSTO-TR-0072] p 348 N95-24203

VIKRAM, C. S.

Residual Stress Measurements with Laser Speckle Correlation Interferometry and Local Heat Treating
[DE95-000082] p 349 N95-24598

VISBAL, MIGUEL

Structure of a double-fin turbulent interaction at high speed
[BTN-95-EIX95222650780] p 347 A95-79236

VISCINTI, G.

High-speed civil transport impact: Role of sulfate, nitric acid trihydrate, and ice aerosols studied with a two-dimensional model including aerosol physics
[HTN-95-91843] p 354 A95-80831

Impact on ozone of high-speed stratospheric aircraft: Effects of the emission scenario
[HTN-95-51283] p 356 A95-80868

W

WAKAIRO, KAORU

Preliminary experiments of an optical fiber display
[NAL-TR-1257] p 362 N95-25004

WAKAMATSU, YOSHIO

Effect of film cooling/regenerative cooling on scramjet engine performances
[NAL-TR-1242] p 339 N95-24990

WALEGA, J. G.

Mendional distributions of NO(X), NO(Y), and other species in the lower stratosphere and upper troposphere during AASE 2
[HTN-95-70944] p 352 A95-78009

WALEN, D. B.

Consistent approach to describing aircraft HIRF protection
[NASA-CR-195067] p 334 N95-25341

WALKER, M. A.

Verification of computational aerodynamic predictions for complex hypersonic vehicles using the INCA(trademark) code
[DE95-004757] p 330 N95-24308

WANG, CLIN M.

Dynamic stall control for advanced rotorcraft application
[BTN-95-EIX95222650793] p 334 A95-79249

WARDWELL, DOUGLAS A.

Aerodynamics model for a generic ASTOVL lift-fan aircraft
[NASA-TM-110347] p 332 N95-26302

WARREN, LINDA S.

An intercomparison of instrumentation for tropospheric measurements of dimethyl sulfide: Aircraft results for concentrations at the parts-per-trillion level
[HTN-95-91857] p 355 A95-80845

WATANABE, AKIRA

Preliminary experiments of an optical fiber display
[NAL-TR-1257] p 362 N95-25004

WATANABE, MITSUNORI

Aerodynamic characteristics of the orbital reentry vehicle experimental probe fins in a supersonic flow
[NAL-TR-1232] p 342 N95-25664

WATSON, DOUGLAS C.

Identification and simulation evaluation of a combat helicopter in hover
[BTN-95-EIX95242670749] p 335 A95-81098

WAUGH, D. W.

Fine-scale, poleward transport of tropical air during AASE 2
[HTN-95-70949] p 352 A95-78014

WEINBERG, P. O.

The distribution of hydrogen, nitrogen, and chlorine radicals in the lower stratosphere: Implications for changes in O₃ due to emission of NO(y) from supersonic aircraft
[HTN-95-70935] p 351 A95-78000

WEAVER, CLARK J.

Tracer transport for realistic aircraft emission scenarios calculated using a three-dimensional model
[HTN-95-41799] p 353 A95-80525

WENHEIMER, A. J.

An analysis of aircraft exhaust plumes form accidental encounters
[HTN-95-70943] p 351 A95-78008

Mendional distributions of NO(X), NO(Y), and other species in the lower stratosphere and upper troposphere during AASE 2
[HTN-95-70944] p 352 A95-78009

WEINSTEIN, S.

A new guidance and flight control system for the DELTA 2 launch vehicle
p 342 A95-80427

WEISENSTEIN, DEBRA K.

Effects on stratospheric ozone from high-speed civil transport: Sensitivity to stratospheric aerosol loading
[HTN-95-91842] p 354 A95-80830

WELLS, WILLIAM R.

Direct adaptive and neural control of wing-rock motion of slender delta wings
[BTN-95-EIX95242670748] p 327 A95-81099

WENDT, BRUCE J.

Study of compressible flow through a rectangular-to-semicircular transition duct
[NASA-CR-4660] p 338 N95-24392

WENDT, M.

Shock tunnel studies of scramjet phenomena 1993
[NASA-CR-195038] p 350 N95-25394

WENHAN, QIN

Aerodynamic parameters of crop canopies estimated with a center-of-pressure technique
[HTN-95-41901] p 356 A95-81648

WERT, JOHN A.

WERT, JOHN A.

NASA-UVA light aerospace alloy and structures
technology program (LA2ST)
[NASA-CR-198041] p 343 N95-24220

WESOKY, HOWARD L.

The atmospheric effects of stratospheric aircraft: A
fourth program report
[NASA-RP-1359] p 357 N95-24274

WHITNEY, MARK G.

Quantity-distance requirements for earth-bermed aircraft
shelters
[AD-A279692] p 341 N95-24424

WIESEN, P.

Nitrous oxide and methane emissions from aero
engines
[HTN-95-21363] p 353 A95-78678

WILSON, JACK

Recent improvements to and validation of the one
dimensional NASA wave rotor model
[NASA-TM-106913] p 332 N95-25962

WOFSY, S. C.

The distribution of hydrogen, nitrogen, and chlorine
radicals in the lower stratosphere: Implications for changes
in O₃ due to emission of NO(y) from supersonic aircraft
[HTN-95-70935] p 351 A95-78000

WOFSY, STEVEN C.

Vertical transport rates in the stratosphere in 1993 from
observations of CO₂, N₂O, and CH₄
[HTN-95-70941] p 351 A95-78006

The atmospheric effects of stratospheric aircraft: A
fourth program report
[NASA-RP-1359] p 357 N95-24274

WOODBRIIDGE, E. L.

The distribution of hydrogen, nitrogen, and chlorine
radicals in the lower stratosphere: Implications for changes
in O₃ due to emission of NO(y) from supersonic aircraft
[HTN-95-70935] p 351 A95-78000

WORTMAN, D. J.

PVD TBC experience on GE aircraft engines
p 345 N95-26126

WRIGHT, I. G.

Thermal barrier coatings issues in advanced land-based
gas turbines p 344 N95-26122

WRIGHT, ROBERT A.

Advanced subsonic airplane design and economic
studies
[NASA-CR-195443] p 338 N95-24304

X

XIE, H.

Dynamic behavior of a magnetic bearing supported jet
engine rotor with auxiliary bearings
[NASA-CR-197860] p 338 N95-24213

Y

YAKOVLEV, V. A.

Laser device for measuring a vessel's speed
[HTN-95-60992] p 361 A95-80633

YANAGIHARA, MASAOKI

Measurements of longitudinal static aerodynamic
coefficients by the cable mount system
[NAL-TR-1226] p 331 N95-25761

YANTA, WILLIAM J.

Supercooling in hypersonic nitrogen wind tunnels
[BTN-94-EIX95011441134] p 340 A95-81020

YEUNG, C. P.

Three-dimensional interaction of wake/boundary-layer
and vortex/boundary-layer data report
[CUED/A-AEREO/TR-23] p 329 N95-24210

YIM, WOOSOOK

Direct adaptive and neural control of wing-rock motion
of slender delta wings
[BTN-95-EIX95242670748] p 327 A95-81099

YOUNG, CLARENCE P., JR.

Development of a model protection and dynamic
response monitoring system for the national transonic
facility
[NASA-CR-195041] p 340 N95-24388

YOUNG, HARRY J.

Preload release mechanism
[NASA-CASE-MS-C-22327-1] p 350 N95-25592

YOUNG, TERESA

Using digital filtering techniques as an aid in wind turbine
data analysis
[DE94-011862] p 357 N95-24853

YU, YUNG H.

Dynamic stall control for advanced rotorcraft
application
[BTN-95-EIX95222650793] p 334 A95-79249

YUAN, PIN-JAR

Ideal proportional navigation p 342 A95-81374

Z

ZHENG, J.

An analysis of aircraft exhaust plumes form accidental
encounters
[HTN-95-70943] p 351 A95-78008

ZURABYAN, A. Z.

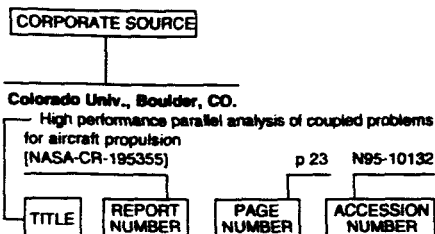
Laser device for measuring a vessel's speed
[HTN-95-60992] p 361 A95-80633

CORPORATE SOURCE INDEX

AERONAUTICAL ENGINEERING / A Continuing Bibliography (Supplement 320)

August 1995

Typical Corporate Source Index Listing



Listings in this index are arranged alphabetically by corporate source. The title of the document is used to provide a brief description of the subject matter. The page number and the accession number are included in each entry to assist the user in locating the abstract in the abstract section. If applicable, a report number is also included as an aid in identifying the document.

A

- Aeronautical Research Labs., Melbourne (Australia).**
Configuration and other differences between Black Hawk and Seahawk helicopters in military service in the USA and Australia
[AR-008-386] p 336 N95-25935
- Assessment of overhaul surge margin tests applied to the T53 engines in ADF Iroquois helicopters
[AR-008-389] p 339 N95-25936
- Air Force Academy, CO.**
Application of neural networks to unsteady aerodynamic control
p 360 N95-25264
- Army Aviation Systems Command, Hampton, VA.**
Exploratory flow visualization investigation of mast-mounted sights in presence of a rotor
[NASA-TM-4634] p 330 N95-24566
- Army Engineer Waterways Experiment Station, Vicksburg, MS.**
Real-time testing and demonstration of the US Army Corps of Engineers' Real-Time On-The-Fly positioning system
[AD-A288624] p 334 N95-25609
- Army Research Lab., Aberdeen Proving Ground, MD.**
Workshop report: Measurement techniques in highly transient, spectrally rich combustion environments
[AD-A288395] p 350 N95-25606
- Auburn Univ., AL.**
Dynamic behavior of a magnetic bearing supported jet engine rotor with auxiliary bearings
[NASA-CR-197860] p 338 N95-24213

B

- Baker (Wilfred) Engineering, Inc., San Antonio, TX.**
Quantity-distance requirements for earth-bermed aircraft shelters
[AD-A279692] p 341 N95-24424

- Bihrie Applied Research, Inc., Hampton, VA.**
Experimental study of the effects of Reynolds number on high angle of attack aerodynamic characteristics of forebodies during rotary motion
[NASA-CR-195033] p 330 N95-24443
- Boeing Commercial Airplane Co., Seattle, WA.**
Consistent approach to describing aircraft HIRF protection
[NASA-CR-195067] p 334 N95-25341
- Brown Univ., Providence, RI.**
Aerodynamic parameter estimation via Fourier modulating function techniques
[NASA-CR-4654] p 335 N95-24630

C

- California Univ., Los Angeles, CA.**
Effect of density gradients in confined supersonic shear layers, part 1
[NASA-CR-198029] p 348 N95-24412
- Effect of density gradients in confined supersonic shear layers, Part 2: 3-D modes
[NASA-CR-198030] p 349 N95-24413
- Cambridge Univ., Cambridge (England).**
Three-dimensional interaction of wake/boundary-layer and vortex/boundary-layer data report
[CUED/A-AEREO/TR-23] p 329 N95-24210
- Civil Aeromedical Inst., Oklahoma City, OK.**
Development of an intervention program to encourage shoulder harness use and aircraft retrofit in general aviation aircraft, phases 1 and 2
[DOT/FAA/AM-95/2] p 333 N95-24384
- Clemson Univ., SC.**
Characterizing the wake vortex signature for an active line of sight remote sensor
[NASA-CR-197697] p 333 N95-24391

D

- Defence Research Agency, Farnborough, Hampshire (England).**
A theoretical and experimental investigation of the flow over supersonic leading edge wing/body configurations
[DRA-TM-AERO-PROP-41] p 331 N95-25649
- Defence Science and Technology Organisation, Melbourne (Australia).**
An overview of Health and Usage Monitoring Systems (HUMS) for military helicopters
[DSTO-TR-0061] p 327 N95-24200
- Helicopter life substantiation: Review of some USA and UK initiatives
[DSTO-TR-0062] p 328 N95-24201
- A portable transmission vibration analysis system for the S-70A-9 Black Hawk helicopter
[DSTO-TR-0072] p 348 N95-24203
- Department of Energy, Washington, DC.**
Thermal barrier coatings issues in advanced land-based gas turbines
p 344 N95-26122
- Thermal barrier coatings application in diesel engines
p 345 N95-26124

E

- EG and G Energy Measurements, Inc., Goleta, CA.**
Turbine-engine applications of thermographic-phosphor temperature measurements
[DE95-003625] p 358 N95-25110
- Energy and Environmental Research Corp., Durham, NC.**
Nitrogen oxide emissions and their control from uninstalled aircraft engines in enclosed test cells: Joint report to Congress on the Environmental Protection Agency - Department of Transportation study
[PB95-166237] p 358 N95-26005

F

- Federal Aviation Administration, Atlantic City, NJ.**
Bird ingestion into large turbofan engines
[DOT/FAA/CT-93/14] p 333 N95-24631
- Federal Aviation Administration, Cambridge, MA.**
Estimate of probability of crack detection from service difficulty report data
[PB95-149381] p 328 N95-24295
- Federal Aviation Administration, Washington, DC.**
Federal Aviation Administration plan for research, engineering and development, 1995
p 363 N95-24202

G

- General Accounting Office, Washington, DC.**
Report to Congressional Committees. Tactical Aircraft: Concurrency in development and production of F-22 aircraft should be reduced
[GAO/NSIAD-95-59] p 336 N95-26338
- General Electric Co., Cincinnati, OH.**
PVD TBC experience on GE aircraft engines
p 345 N95-26126
- Georgia Tech Research Inst., Atlanta, GA.**
Effects of cavity dimensions, boundary layer, and temperature on cavity noise with emphasis on benchmark data to validate computational aeroacoustic codes
[NASA-CR-4653] p 361 N95-24879

I

- Institute for Computer Applications in Science and Engineering, Hampton, VA.**
Cumulative reports and publications through December 31, 1994
[NASA-CR-195043] p 361 N95-26085
- International Centre for Theoretical Physics, Trieste (Italy).**
Dynamics of phase ordering of nematics in a pore
[DE95-607662] p 362 N95-25978
- Iowa State Univ. of Science and Technology, Ames, IA.**
Study of compressible flow through a rectangular-to-semiannular transition duct
[NASA-CR-4660] p 338 N95-24392

J

- Jet Propulsion Lab., California Inst. of Tech., Pasadena, CA.**
Meridional distributions of NO(X), NO(Y), and other species in the lower stratosphere and upper troposphere during AASE 2
[HTN-95-70944] p 352 A95-78009
- Comparison of column abundances from three infrared spectrometers during AASE 2
[HTN-95-70946] p 352 A95-78011
- Latitude variations of stratospheric trace gases
[HTN-95-70948] p 352 A95-78013
- Guidance and control, 1993: Annual Rocky Mountain Guidance and Control Conference, 16th, Keystone, CO, Feb. 6-10, 1993
[ISBN-0-87703-365-X] p 341 A95-80389
- The Cassini spacecraft: Object oriented flight control software
p 359 A95-80405
- Joint Publications Research Service, Arlington, VA.**
JPRS report: Science and technology. Central Eurasia
[JPRS-UST-95-011] p 335 N95-24541
- Joint Publications Research Service, Washington, DC.**
JPRS report: Science and technology. Central Eurasia
[JPRS-UST-94-027] p 349 N95-24470
- JPRS report: Science and technology. Central Eurasia
[JPRS-UST-94-018] p 349 N95-24472
- JPRS Report: Science and technology. Central Eurasia
[JPRS-UST-94-032] p 350 N95-24759

L

Linköping Univ. (Sweden).

Aspect estimation of an aircraft using library model silhouettes
[PB95-141834] p 360 N95-25894

Lockheed Environmental Systems and Technologies Co., Las Vegas, NV.

Parts washing alternatives study: United States Coast Guard. Project summary and report
[PB95-166146] p 343 N95-26004

M

McDonnell-Douglas Aerospace, Long Beach, CA.

Advanced subsonic airplane design and economic studies
[NASA-CR-195443] p 338 N95-24304
Noise impact of advanced high lift systems
[NASA-CR-195028] p 362 N95-26160

Mechanical Engineering Lab., Sakura (Japan).

Long endurance stratospheric solar powered airship
[PB95-178729] p 336 N95-26009

N

National Aeronautics and Space Administration, Washington, DC.

Analysis of the physical state of one Arctic polar stratospheric cloud based on observations
[HTN-95-70917] p 351 A95-77982

The distribution of hydrogen, nitrogen, and chlorine radicals in the lower stratosphere: Implications for changes in O₃ due to emission of NO(y) from supersonic aircraft
[HTN-95-70935] p 351 A95-78000

An analysis of aircraft exhaust plumes form accidental encounters
[HTN-95-70943] p 351 A95-78008

Fine-scale, poleward transport of tropical air during AASE 2
[HTN-95-70949] p 352 A95-78014

Guidance and control, 1993; Annual Rocky Mountain Guidance and Control Conference, 16th, Keystone, CO, Feb. 6-10, 1993
[ISBN-0-87703-365-X] p 341 A95-80389

NASA video catalog
[NASA-SP-7109(01)] p 363 N95-24238

The atmospheric effects of stratospheric aircraft: A fourth program report
[NASA-RP-1359] p 357 N95-24274

Aeronautical engineering: A continuing bibliography with indexes (supplement 316)
[NASA-SP-7037(316)] p 328 N95-24465

Aeronautical engineering: A continuing bibliography with indexes (supplement 317)
[NASA-SP-7037(317)] p 328 N95-25798

National Aeronautics and Space Administration, Ames Research Center, Moffett Field, CA.

Analysis of the physical state of one Arctic polar stratospheric cloud based on observations
[HTN-95-70917] p 351 A95-77982

The distribution of hydrogen, nitrogen, and chlorine radicals in the lower stratosphere: Implications for changes in O₃ due to emission of NO(y) from supersonic aircraft
[HTN-95-70935] p 351 A95-78000

Vertical transport rates in the stratosphere in 1993 from observations of CO₂, N₂O, and CH₄
[HTN-95-70941] p 351 A95-78006

Fine-scale, poleward transport of tropical air during AASE 2
[HTN-95-70949] p 352 A95-78014

Identification and simulation evaluation of a combat helicopter in hover
[BTN-95-EIX95242670749] p 335 A95-81098

SOFIA: Stratospheric Observatory for Infrared Astronomy
[NASA-TM-110347] p 332 N95-26302

Geometric analysis of wing sections
[NASA-TM-110346] p 335 N95-24629

Aerodynamic shape optimization of wing and wing-body configurations using control theory
[NASA-CR-198024] p 335 N95-25334

Angular displacement measuring device
[NASA-CASE-ARC-11937-1] p 362 N95-26015

Aerodynamics model for a generic ASTOVL lift-fan aircraft
[NASA-TM-110347] p 332 N95-26302

National Aeronautics and Space Administration, Goddard Space Flight Center, Greenbelt, MD.

The distribution of hydrogen, nitrogen, and chlorine radicals in the lower stratosphere: Implications for changes in O₃ due to emission of NO(y) from supersonic aircraft
[HTN-95-70935] p 351 A95-78000

Comparison of column abundances from three infrared spectrometers during AASE 2
[HTN-95-70946] p 352 A95-78011

Chemical change in the arctic vortex during AASE 2
[HTN-95-70947] p 352 A95-78012

Fine-scale, poleward transport of tropical air during AASE 2
[HTN-95-70949] p 352 A95-78014

Guidance and control, 1993; Annual Rocky Mountain Guidance and Control Conference, 16th, Keystone, CO, Feb. 6-10, 1993
[ISBN-0-87703-365-X] p 341 A95-80389

National Aeronautics and Space Administration, Lyndon B. Johnson Space Center, Houston, TX.

Guidance and control, 1993; Annual Rocky Mountain Guidance and Control Conference, 16th, Keystone, CO, Feb. 6-10, 1993
[ISBN-0-87703-365-X] p 341 A95-80389

Preload release mechanism
[NASA-CASE-MS-22327-1] p 350 N95-25592

National Aeronautics and Space Administration, Langley Research Center, Hampton, VA.

Viscoplastic response of structures for intense local heating
[HTN-95-41540] p 346 A95-77921

The distribution of hydrogen, nitrogen, and chlorine radicals in the lower stratosphere: Implications for changes in O₃ due to emission of NO(y) from supersonic aircraft
[HTN-95-70935] p 351 A95-78000

An analysis of aircraft exhaust plumes form accidental encounters
[HTN-95-70943] p 351 A95-78008

Meridional distributions of NO(X), NO(Y), and other species in the lower stratosphere and upper troposphere during AASE 2
[HTN-95-70944] p 352 A95-78009

Guidance and control, 1993; Annual Rocky Mountain Guidance and Control Conference, 16th, Keystone, CO, Feb. 6-10, 1993
[ISBN-0-87703-365-X] p 341 A95-80389

Effects on stratospheric ozone from high-speed civil transport: Sensitivity to stratospheric aerosol loading
[HTN-95-91842] p 354 A95-80830

An intercomparison of aircraft instrumentation for tropospheric measurements of sulfur dioxide
[HTN-95-91855] p 354 A95-80843

An intercomparison of aircraft instrumentation for tropospheric measurements of carbonyl sulfide, hydrogen sulfide, and carbon disulfide
[HTN-95-91856] p 355 A95-80844

An intercomparison of instrumentation for tropospheric measurements of dimethyl sulfide: Aircraft results for concentrations at the parts-per-trillion level
[HTN-95-91857] p 355 A95-80845

Load alleviation maneuvers for a launch vehicle
[HTN-95-91860] p 342 A95-81360

DSMC calculations for 70-deg blunted cone at 3.2 km/s in nitrogen
[NASA-TM-109181] p 348 N95-24396

Performance of an aerodynamic yaw controller mounted on the space shuttle orbiter body flap at Mach 10
[NASA-TM-109179] p 330 N95-24397

A crew-centered flight deck design philosophy for High-Speed Civil Transport (HSCT) aircraft
[NASA-TM-109171] p 335 N95-24582

Aviation system capacity improvements through technology
[NASA-TM-109165] p 333 N95-24633

Internal performance characteristics of thrust-vectoring axisymmetric ejector nozzles
[NASA-TM-4610] p 331 N95-25338

Design and evaluation of a foam-filled hat-stiffened panel concept for aircraft primary structural applications
[NASA-TM-109175] p 346 N95-26251

National Aeronautics and Space Administration, Lewis Research Center, Cleveland, OH.

The 1994 Fiber Optic Sensors for Aerospace Technology (FOSAT) Workshop
[NASA-CP-10166] p 337 N95-24207

Crossflow mixing of noncircular jets
[NASA-TM-106865] p 338 N95-24390

The effect of altitude conditions on the particle emissions of a J85-GE-5L turbojet engine
[NASA-TM-106669] p 339 N95-24561

Assessment of avionics technology in European aerospace organizations
[NASA-CR-189201] p 337 N95-24624

Recent improvements to and validation of the one dimensional NASA wave rotor model
[NASA-TM-106913] p 332 N95-25962

A combined geometric approach for solving the Navier-Stokes equations on dynamic grids
[NASA-TM-106919] p 332 N95-26075

Thermal Barrier Coating Workshop
[NASA-CP-10170] p 344 N95-26119

Thermal barrier coatings for aircraft engines: History and directions
[NASA-CASE-LEW-15170-2] p 362 N95-26187

National Aeronautics and Space Administration, Marshall Space Flight Center, Huntsville, AL.

Guidance and control, 1993; Annual Rocky Mountain Guidance and Control Conference, 16th, Keystone, CO, Feb. 6-10, 1993
[ISBN-0-87703-365-X] p 341 A95-80389

National Aerospace Lab., Tokyo (Japan).

Study on tensile fatigue testing method of unidirectional fiber-resin matrix composites
[NAL-TR-1241] p 343 N95-24989

Effect of film cooling/regenerative cooling on scramjet engine performances
[NAL-TR-1242] p 339 N95-24990

Numerical and experimental study of drag characteristics of two-dimensional HLFC airfoils in high subsonic, high Reynolds number flow
[NAL-TR-1244T] p 331 N95-24998

Preliminary experiments of an optical fiber display
[NAL-TR-1257] p 362 N95-25004

Flight reference display for powered-lift STOL aircraft
[NAL-TR-1251] p 337 N95-25005

Low speed aerodynamic characteristics of delta wings with vortex flaps: 60 deg and 70 deg delta wings
[NAL-TR-1245] p 331 N95-25105

Aerodynamic characteristics of the orbital reentry vehicle experimental probe fins in a supersonic flow
[NAL-TR-1232] p 342 N95-25664

Measurements of longitudinal static aerodynamic coefficients by the cable mount system
[NAL-TR-1226] p 331 N95-25761

Fundamental wind tunnel experiments on low-speed flutter of a tip-fin configuration wing
[NAL-TR-1228] p 332 N95-25762

Reentry guidance for hypersonic Flight Experiment (HYFLEX) vehicle
[NAL-TR-1235] p 334 N95-25764

A quiet STOL Research Aircraft Development program
[NAL-TR-1223] p 336 N95-25862

National Defence Research Establishment, Linköping (Sweden).

Interfacing a digital compass to a remote-controlled helicopter
[PB95-164927] p 340 N95-24260

National Inst. of Standards and Technology, Gaithersburg, MD.

Measurement methods and standards for processing and application of thermal barrier coatings
[DE95-000267] p 344 N95-26123

National Renewable Energy Lab., Golden, CO.

Using digital filtering techniques as an aid in wind turbine data analysis
[DE94-011862] p 357 N95-24853

NREL airfoil families for HAWTs
[DE95-000267] p 357 N95-24882

Wind technology development: Large and small turbines
[DE95-000286] p 358 N95-26090

National Transportation Safety Board, Washington, DC.

Aircraft accident report: Impact with blast fence upon landing rollout Action Air Charters flight 990 Piper PA-31-350, N990RA, Stratford, Connecticut, 27 April 1994
[PB94-910410] p 333 N95-24206

Native American Services, Huntsville, AL.

NLS Flight Simulation Laboratory (FSL) documentation
[NASA-CR-196564] p 363 N95-24439

North Carolina State Univ., Raleigh, NC.

Development of a model protection and dynamic response monitoring system for the national transonic facility
[NASA-CR-195041] p 340 N95-24388

North Dakota Univ., Grand Forks, ND.

Preliminary analysis of University of North Dakota aircraft data from the FIRE Cirrus IFO-2
[NASA-CR-198038] p 357 N95-24219

Northern Research and Engineering Corp., Woburn, MA.

Small gas turbine component evaluation study
[PB95-147542] p 338 N95-24293

O

Oak Ridge National Lab., TN.

Thermal conductivity of zirconia thermal barrier coatings
[AD-A288217] p 345 N95-26133

Oklahoma City Air Logistics Center, Tinker AFB, OK.

Proceedings of the 2d USAF Aging Aircraft Conference
[AD-A288217] p 336 N95-25576

Organisatie voor Toegepast Natuurwetenschappelijk Onderzoek, Delft (Netherlands).

Partial camera automation in a simulated Unmanned Air Vehicle
[AD-A288786] p 337 N95-26190

Overset Methods, Inc., Los Altos, CA.

Aerodynamic optimization studies on advanced architecture computers
[NASA-CR-198045] p 330 N95-24379

The coupling of fluids, dynamics, and controls on advanced architecture computers
[NASA-CR-197727] p 360 N95-25797

P**Polish Academy of Sciences, Warsaw (Poland).**

Actuating signals in adaptive control systems
[IFTR-13/1994] p 361 N95-26330

Pratt and Whitney Aircraft, East Hartford, CT.

Thermal barrier coating experience in the gas turbine engine
p 345 N95-26125

Thermal barrier coating life modeling in aircraft gas turbine engines
p 346 N95-26140

Pratt and Whitney Aircraft, West Palm Beach, FL.

A design perspective on thermal barrier coatings
p 344 N95-26120

Jet engine applications for materials with nanometer-scale dimensions
p 345 N95-26131

Purdue Univ., West Lafayette, IN.

Supersonic quiet-tunnel development for laminar-turbulent transition research
[NASA-CR-198040] p 340 N95-24302

Thermal fracture mechanisms in ceramic thermal barrier coatings
p 346 N95-26138

Q**Queensland Univ., Saint Lucia (Australia).**

Shock tunnel studies of scramjet phenomena 1993
[NASA-CR-195038] p 350 N95-25394

Thrust measurements of a complete axisymmetric scramjet in an impulse facility
p 339 N95-25395

Scramjet thrust measurement in a shock tunnel
p 339 N95-25396

Thrust measurement in a 2-D scramjet nozzle
p 339 N95-25397

The Superorbital Expansion Tube concept, experiment and analysis
p 341 N95-25399

Balances for the measurement of multiple components of force in flows of a millisecond duration
p 350 N95-25400

R**Radian Corp., Research Triangle Park, NC.**

Nitrogen oxide emissions and their control from uninstalled aircraft engines in enclosed test cells: Joint report to Congress on the Environmental Protection Agency - Department of Transportation study
[PB95-166237] p 358 N95-26005

Research Inst. of National Defence, Linköping (Sweden).

Orientation determination of aircraft using visual 3D matching and radar. Case study 2
[PB95-165791] p 350 N95-25749

Rockwell International Corp., Huntsville, AL.

High frequency flow-structural interaction in dense subsonic fluids
[NASA-CR-4652] p 330 N95-24217

S**Sandia National Labs., Albuquerque, NM.**

Verification of computational aerodynamic predictions for complex hypersonic vehicles using the INCA(trademark) code
[DE95-004757] p 330 N95-24308

Emerging nondestructive inspection for aging aircraft
[PB95-143053] p 328 N95-25401

Science Applications International Corp., Dayton, OH.

Visual contrast detection thresholds for aircraft contrails
[AD-A288618] p 328 N95-25607

Solar Turbines, Inc. San Diego, CA.

Perspective on thermal barrier coatings for industrial gas turbine applications
p 345 N95-26128

T**Texas A&M Univ., College Station, TX.**

Thermohydrodynamic analysis of cryogenic liquid turbulent flow fluid film bearings, phase 2
[NASA-CR-197412] p 349 N95-24461

Texas Technological Univ., Lubbock, TX.

A brief survey of constrained mechanics and variational problems in terms of differential forms
p 360 N95-25803

How to fly an aircraft with control theory and splines
p 360 N95-25805

V**Virginia Univ., Charlottesville, VA.**

NASA-UVA light aerospace alloy and structures technology program (LA2ST)
[NASA-CR-198041] p 343 N95-24220

Virginia Univ. Hospital, Charlottesville, VA.

NASA-UVA light aerospace alloy and structures technology program supplement: Aluminum-based materials for high speed aircraft
[NASA-CR-4645] p 343 N95-24878

W**Westinghouse Savannah River Co., Aiken, SC.**

Residual Stress Measurements with Laser Speckle Correlation Interferometry and Local Heat Treating
[DE95-060082] p 349 N95-24598

Wichita State Univ., Wichita, KS.

Analysis of warping effects on the static and dynamic response of a seat-type structure
[NIAR-94-12] p 348 N95-24211

Wright Lab., Wright-Patterson AFB, OH.

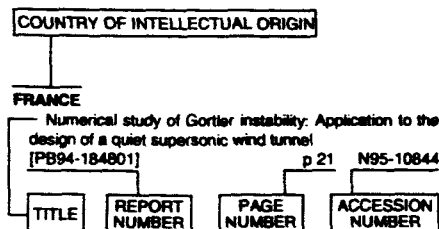
Heat transfer measurements in small scale wind tunnels
[AD-A288689] p 341 N95-26053

FOREIGN TECHNOLOGY INDEX

AERONAUTICAL ENGINEERING / A Continuing Bibliography (Supplement 320)

August 1995

Typical Foreign Technology Index Listing



Listings in this index are arranged alphabetically by country of intellectual origin. The title of the document is used to provide a brief description of the subject matter. The page number and accession number are included in each entry to assist the user in locating the abstract in the abstract section. If applicable, a report number is also included as an aid in identifying the document.

A

AUSTRALIA

- An overview of Health and Usage Monitoring Systems (HUMS) for military helicopters
[DSTO-TR-0061] p 327 N95-24200
- Helicopter life substantiation: Review of some USA and UK initiatives
[DSTO-TR-0062] p 328 N95-24201
- A portable transmission vibration analysis system for the S-70A-9 Black Hawk helicopter
[DSTO-TR-0072] p 348 N95-24203
- Shock tunnel studies of scramjet phenomena 1993
[NASA-CR-195038] p 350 N95-25394
- Thrust measurements of a complete axisymmetric scramjet in an impulse facility p 339 N95-25395
- Scramjet thrust measurement in a shock tunnel p 339 N95-25396
- Thrust measurement in a 2-D scramjet nozzle p 339 N95-25397
- The Supersonic Expansion Tube concept, experiment and analysis p 341 N95-25399
- Balances for the measurement of multiple components of force in flows of a millisecond duration p 350 N95-25400
- Configuration and other differences between Black Hawk and Seahawk helicopters in military service in the USA and Australia
[AR-008-386] p 336 N95-25935
- Assessment of overhaul surge margin tests applied to the T53 engines in ADF Iroquois helicopters
[AR-008-389] p 339 N95-25936

C

CANADA

- Theoretical and experimental studies of fretting-initiated fatigue failure of aeroengine compressor discs
[BTN-94-EIX94421372285] p 343 A95-78467

CHINA

- Aerodynamic parameters of crop canopies estimated with a center-of-pressure technique
[HTN-95-41901] p 356 A95-81648

F

FRANCE

- Impact of present aircraft emissions of nitrogen oxides on tropospheric ozone and climate forcing
[HTN-95-21364] p 353 A95-78679
- Potential effects on ozone of future supersonic aircraft/2D simulation
[HTN-95-51282] p 356 A95-80867

G

GERMANY

- Nitrous oxide and methane emissions from aero engines
[HTN-95-21363] p 353 A95-78678
- North Atlantic air traffic within the lower stratosphere: Cruising times and corresponding emissions
[HTN-95-91841] p 354 A95-80829
- Dynamics of aircraft exhaust plumes in the jet-regime
[HTN-95-51275] p 355 A95-80860
- Modeling of aircraft exhaust emissions and infrared spectra for remote measurement of nitrogen oxides
[HTN-95-51276] p 355 A95-80861
- Empirical corrections of the rigid rotor interaction potential of H₂-H₂ in the attractive region: Dimer features in the FIR absorption spectra
[HTN-95-41943] p 361 A95-81690

I

ITALY

- High-speed civil transport impact: Role of sulfate, nitric acid trihydrate, and ice aerosols studied with a two-dimensional model including aerosol physics
[HTN-95-91843] p 354 A95-80831
- Impact on ozone of high-speed stratospheric aircraft: Effects of the emission scenario
[HTN-95-51283] p 356 A95-80868
- Dynamics of phase ordering of nematics in a pore
[DE95-607662] p 362 N95-25978

J

JAPAN

- Similarity rule for jet-temperature effects on transonic base pressure
[BTN-95-EIX95222650791] p 329 A95-79247
- Determination of piloting feedback structures for an altitude tracking task
[BTN-95-EIX95242670770] p 327 A95-81077
- Study on tensile fatigue testing method of unidirectional fiber-resin matrix composites
[NAL-TR-1241] p 343 N95-24989
- Effect of film cooling/regenerative cooling on scramjet engine performances
[NAL-TR-1242] p 339 N95-24990
- Numerical and experimental study of drag characteristics of two-dimensional HLFC airfoils in high subsonic, high Reynolds number flow
[NAL-TR-1244T] p 331 N95-24988
- Preliminary experiments of an optical fiber display
[NAL-TR-1257] p 362 N95-25004
- Flight reference display for powered-lift STOL aircraft
[NAL-TR-1251] p 337 N95-25005
- Low speed aerodynamic characteristics of delta wings with vortex flaps: 60 deg and 70 deg delta wings
[NAL-TR-1245] p 331 N95-25105
- Aerodynamic characteristics of the orbital reentry vehicle experimental probe fins in a supersonic flow
[NAL-TR-1232] p 342 N95-25664
- Measurements of longitudinal static aerodynamic coefficients by the cable mount system
[NAL-TR-1226] p 331 N95-25761

- Fundamental wind tunnel experiments on low-speed flutter of a tip-fin configuration wing
[NAL-TR-1228] p 332 N95-25762
- Reentry guidance for hypersonic Flight Experiment (HYFLEX) vehicle
[NAL-TR-1235] p 334 N95-25764
- A quiet STOL Research Aircraft Development program
[NAL-TR-1223] p 336 N95-25862
- Long endurance stratospheric solar powered airship
[PB95-178729] p 336 N95-26009

N

NETHERLANDS

- Quantitative comparison between interferometric measurements and Euler computations for supersonic cone flows
[BTN-95-EIX95222650782] p 358 A95-79238
- Partial camera automation in a simulated Unmanned Air Vehicle
[AD-A288786] p 337 N95-26190

P

POLAND

- Actuating signals in adaptive control systems
[IFTR-13/1994] p 361 N95-26330

R

RUSSIA

- Laser device for measuring a vessel's speed
[HTN-95-60992] p 361 A95-80633
- JPRS report: Science and technology. Central Eurasia
[JPRS-UST-94-027] p 349 N95-24470
- JPRS report: Science and technology. Central Eurasia
[JPRS-UST-94-018] p 349 N95-24472
- JPRS report: Science and technology. Central Eurasia
[JPRS-UST-95-011] p 335 N95-24541
- JPRS Report: Science and technology. Central Eurasia
[JPRS-UST-94-032] p 350 N95-24759

S

SAUDI ARABIA

- Modal characteristics of rotors using a conical shaft finite element
[BTN-94-EIX94401359745] p 346 A95-77379

SWEDEN

- Experimental investigation of the flow around a circular cylinder: Influence of aspect ratio
[BTN-94-EIX95011441120] p 347 A95-80044
- Interfacing a digital compass to a remote-controlled helicopter
[PB95-164927] p 340 N95-24260
- Orientation determination of aircraft using visual 3D matching and radar. Case study 2
[PB95-165791] p 350 N95-25749
- Aspect estimation of an aircraft using library model silhouettes
[PB95-141834] p 360 N95-25894

T

TAIWAN, PROVINCE OF CHINA

- Impingement cooling of an isothermally heated surface with a confined slot jet
[BTN-94-EIX94421348950] p 347 A95-78494
- Ideal proportional navigation
[PB95-141834] p 342 A95-81374

U

UNITED KINGDOM

- Sensitivity of supersonic aircraft modelling studies to HNO₃ photolysis rate
[HTN-95-11475] p 353 A95-79453

FOREIGN

UNKNOWN

FOREIGN TECHNOLOGY INDEX

Unsteady lift on a swept blade tip
[BTN-94-EIX95011441154] p 329 A95-80030
Three-dimensional interaction of wake/boundary-layer
and vortex/boundary-layer data report
[CUED/A-AEREO/TR-23] p 329 N95-24210
A theoretical and experimental investigation of the flow
over supersonic leading edge wing/body configurations
[DRA-TM-AERO-PROP-41] p 331 N95-25649

UNKNOWN

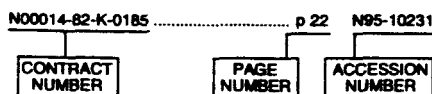
Hypersonic model testing in a shock tunnel
[BTN-95-EIX95222650789] p 329 A95-79245
SR-71 may launch targets for missile defense tests
[HTN-95-91872] p 335 A95-81974

CONTRACT NUMBER INDEX

AERONAUTICAL ENGINEERING / A Continuing Bibliography (Supplement 320)

August 1995

Typical Contract Number Index Listing



Listings in this index are arranged alphanumerically by contract number. Under each contract number the accession numbers denoting documents that have been produced as a result of research done under the contract are shown. The accession number denotes the number by which the citation is identified in the abstract section. Preceding the accession number is the page number on which the citation may be found.

AF PROJ. 2404 p 341 N95-26053
 DE-AC04-94AL-85000 p 330 N95-24308
 DE-AC08-93NV-11265 p 358 N95-25110
 DE-AC09-89SR-18035 p 349 N95-24598
 DE-AC36-83CH-10093 p 357 N95-24853
 p 357 N95-24882
 p 358 N95-26090
 DOT-FA4H2/A4044 p 328 N95-24295
 DTF A03-91-A-00018 p 328 N95-25401
 EPA-68-C4-0020 p 343 N95-26004
 EPA-68-D1-0177 p 358 N95-26005
 F08635-82-C-0131 p 356 A95-80862
 F08635-91-C-0189 p 341 N95-24424
 F33615-92-D-2293 p 328 N95-25607
 GRI-5089-291-2077 p 338 N95-24293
 NAGW-1230 p 351 A95-78000
 NAGW-1727 p 352 A95-78014
 NAGW-2183 p 351 A95-77982
 NAGW-674 p 350 N95-25394
 NAG1-1065 p 335 N95-24630
 NAG1-1351 p 357 N95-24219
 NAG1-1607 p 340 N95-24302
 NAG1-745 p 343 N95-24220
 p 343 N95-24878
 NAG2-731 p 351 A95-78000
 NAG3-1434 p 349 N95-24461
 NAG3-1507 p 338 N95-24213
 NAG3-1561 p 338 N95-24392
 NAS1-14101 p 361 N95-26085
 NAS1-14472 p 361 N95-26085
 NAS1-15810 p 361 N95-26085
 NAS1-16394 p 361 N95-26085
 NAS1-17070 p 361 N95-26085
 NAS1-17130 p 361 N95-26085
 NAS1-18605 p 361 N95-26085
 NAS1-18935 p 342 A95-81360
 NAS1-19000 p 342 A95-81360
 NAS1-19061 p 361 N95-24879
 NAS1-19192 p 354 A95-80830
 NAS1-19360 p 334 N95-25341
 NAS1-19480 p 361 N95-26085
 NAS1-19955 p 351 A95-78000
 NAS1-20103 p 362 N95-26180
 NAS1-20228 p 330 N95-24443
 NAS2-13721 p 335 N95-25334
 NAS3-25286 p 332 N95-25962
 NAS3-25954 p 338 N95-24390
 NAS3-25965 p 338 N95-24304
 NAS3-88622 p 337 N95-24624
 NAS8-37925 p 363 N95-24439
 NAS8-38187 p 330 N95-24217

NCC1-141 p 340 N95-24388
 NCC2-374 p 348 N95-24412
 p 349 N95-24413
 NCC2-694 p 351 A95-78006
 NCC2-799 p 360 N95-25797
 NCC2-806 p 330 N95-24379
 NGT-50975 p 333 N95-24391
 NSF ATM-89-21119 p 351 A95-78000
 NSG5-175 p 352 A95-78011
 p 352 A95-78012
 RTOP 242-80-01-01 p 348 N95-24396
 p 330 N95-24397
 RTOP 282-10-01-01 p 330 N95-24566
 RTOP 505-10-11 p 335 N95-24629
 RTOP 505-59-30-04 p 331 N95-25338
 RTOP 505-59-36-01 p 330 N95-24566
 RTOP 505-59-52-01 p 361 N95-24879
 RTOP 505-59-85-01 p 340 N95-24388
 RTOP 505-60-00 p 337 N95-24207
 RTOP 505-62-00 p 339 N95-24561
 RTOP 505-62-50 p 332 N95-25962
 RTOP 505-62-52 p 332 N95-26075
 RTOP 505-63-50-08 p 346 N95-26251
 RTOP 505-63-52 p 344 N95-26119
 RTOP 505-64-52-01 p 335 N95-24630
 RTOP 505-68-30-01 p 330 N95-24443
 RTOP 505-68-32 p 332 N95-26302
 RTOP 505-68-20-01 p 333 N95-24633
 RTOP 505-70-62-04 p 350 N95-25394
 RTOP 505-90-52-01 p 361 N95-26085
 RTOP 537-06-20-06 p 343 N95-24878
 RTOP 537-06-21-01 p 335 N95-24582
 RTOP 538-01-13-01 p 334 N95-25341
 RTOP 538-03-15-01 p 362 N95-26160
 RTOP 538-08-11 p 338 N95-24304

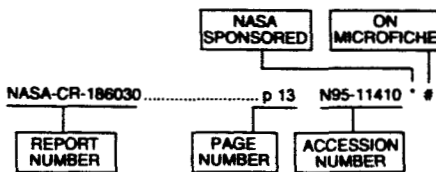
CONTRACT

REPORT NUMBER INDEX

AERONAUTICAL ENGINEERING / A Continuing Bibliography (Supplement 320)

August 1995

Typical Report Number Index Listing



Listings in this index are arranged alphabetically by report number. The page number indicates the page on which the citation is located. The accession number denotes the number by which the citation is identified. An asterisk (*) indicates that the item is a NASA report. A pound sign (#) indicates that the item is available on microfiche.

A-950049	p 335	N95-24629 *	#
A-950051	p 332	N95-26302 *	#
AD-A279692	p 341	N95-24424	
AD-A288217	p 336	N95-25578	
AD-A288395	p 350	N95-25606	
AD-A288618	p 328	N95-25607	
AD-A288624	p 334	N95-25609	
AD-A288689	p 341	N95-26053	
AD-A288786	p 337	N95-26190	
AFCEA/ESL-TR-92-25	p 341	N95-24424	
AFOSR-94-0756TR	p 336	N95-25578	
AIAA PAPER 95-0732	p 338	N95-24390 *	#
AL-TR-1994-0116	p 328	N95-25607	
AR-008-386	p 336	N95-25935	
AR-008-389	p 339	N95-25936	
AR-008-923	p 327	N95-24200	
AR-008-924	p 328	N95-24201	
AR-008-938	p 348	N95-24203	
ARL-GD-43	p 336	N95-25935	
ARL-SR-18	p 350	N95-25806	
ARL-TN-48	p 339	N95-25836	
ATCOM-TR-95-A-001	p 330	N95-24566 *	#
B-259204	p 336	N95-26338	#
BTN-94-EIX94401359745	p 346	A95-77379	
BTN-94-EIX94421348950	p 347	A95-78494	
BTN-94-EIX94421372265	p 343	A95-78467	
BTN-94-EIX95011441078	p 348	A95-81056	
BTN-94-EIX95011441120	p 347	A95-80044	
BTN-94-EIX95011441127	p 348	A95-81027	
BTN-94-EIX95011441134	p 340	A95-81020	
BTN-94-EIX95011441142	p 347	A95-81012	
BTN-94-EIX95011441154	p 329	A95-80030	
BTN-95-EIX95202637575	p 332	A95-78583	
BTN-95-EIX95202637582	p 347	A95-78576	
BTN-95-EIX95222650780	p 347	A95-79236	
BTN-95-EIX95222650781	p 327	A95-79237	
BTN-95-EIX95222650782	p 358	A95-79238	
BTN-95-EIX95222650784	p 334	A95-79240	
BTN-95-EIX95222650789	p 329	A95-79245	
BTN-95-EIX95222650790	p 329	A95-79246	
BTN-95-EIX95222650791	p 329	A95-79247	
BTN-95-EIX95222650792	p 329	A95-79248	
BTN-95-EIX95222650793	p 334	A95-79249	

BTN-95-EIX95222650795	p 340	A95-79251	
BTN-95-EIX95242670746	p 327	A95-81101	
BTN-95-EIX95242670747	p 359	A95-81100	
BTN-95-EIX95242670748	p 327	A95-81099	
BTN-95-EIX95242670749	p 335	A95-81098 *	
BTN-95-EIX95242670750	p 334	A95-81097	
BTN-95-EIX95242670751	p 336	A95-81096	
BTN-95-EIX95242670754	p 342	A95-81093	
BTN-95-EIX95242670755	p 327	A95-81092	
BTN-95-EIX95242670759	p 359	A95-81088	
BTN-95-EIX95242670766	p 359	A95-81081	
BTN-95-EIX95242670768	p 359	A95-81079	
BTN-95-EIX95242670770	p 327	A95-81077	
BTN-95-EIX95242679087	p 359	A95-81253	
CONF-9304280-1	p 357	N95-24853	#
CONF-9410259-1	p 358	N95-25110	
CONF-941210-2	p 358	N95-26090	#
CONF-950130-3	p 330	N95-24308	#
CONF-950226-3	p 349	N95-24598	#
CRAD-9310-TR-0127	p 362	N95-26160 *	#
CUED/A-AERO/TR-23	p 329	N95-24210	#
DE94-011862	p 357	N95-24853	#
DE95-000267	p 357	N95-24882	#
DE95-000286	p 358	N95-26080	#
DE95-003625	p 358	N95-25110	
DE95-004757	p 330	N95-24308	#
DE95-060082	p 349	N95-24598	#
DE95-607662	p 362	N95-25978	#
DOT-VNTSC-FAA-94-4	p 328	N95-24295	#
DOT/FAA/AM-95/2	p 333	N95-24384	#
DOT/FAA/CT-93/14	p 333	N95-24631	#
DOT/FAA/CT-94/11	p 328	N95-25401	
DOT/FAA/CT-94/90	p 328	N95-24295	#
DRA-TM-AERO-PROP-41	p 331	N95-25649	#
DRA/AP/TM9341/1.0	p 331	N95-25649	#
DSTO-TR-0061	p 327	N95-24200	
DSTO-TR-0062	p 328	N95-24201	
DSTO-TR-0072	p 348	N95-24203	
E-9143	p 339	N95-24561 *	#
E-9426	p 337	N95-24207 *	#
E-9477	p 338	N95-24390 *	#
E-9488	p 338	N95-24304 *	#
E-9509	p 344	N95-26119 *	#
E-9582	p 338	N95-24392 *	#
E-9582	p 337	N95-24624 *	#
E-9621	p 332	N95-25862 *	#
E-9630	p 332	N95-26075 *	#
EGG-11265-3011	p 358	N95-25110	
EPA/453/R-94/068	p 358	N95-26005	#
EPA/600/R-95/006	p 343	N95-26004	#
FOA-C-30763-8.4.3.4	p 360	N95-25894	#
FOA-C-30768-3.6	p 340	N95-24260	
GAO/NSIAD-95-59	p 336	N95-26338	#
GRI-94/0350	p 338	N95-24293	
HTN-95-A0314	p 341	A95-80389 *	
HTN-95-11475	p 353	A95-79453	
HTN-95-21363	p 353	A95-78678	
HTN-95-21364	p 353	A95-78679	
HTN-95-41540	p 348	A95-77821 *	
HTN-95-41799	p 353	A95-80525 *	
HTN-95-41833	p 353	A95-80559	
HTN-95-41901	p 356	A95-81648	
HTN-95-41943	p 361	A95-81680	
HTN-95-51275	p 355	A95-80860	
HTN-95-51276	p 355	A95-80861	
HTN-95-51277	p 356	A95-80862	

HTN-95-51282	p 356	A95-80867	
HTN-95-51283	p 356	A95-80868	
HTN-95-51323	p 356	A95-80908	
HTN-95-60992	p 361	A95-80633	
HTN-95-70917	p 351	A95-77982 *	
HTN-95-70935	p 351	A95-78000 *	
HTN-95-70941	p 351	A95-78006 *	
HTN-95-70943	p 351	A95-78008 *	
HTN-95-70944	p 352	A95-78009 *	
HTN-95-70946	p 352	A95-78011 *	
HTN-95-70947	p 352	A95-78012 *	
HTN-95-70948	p 352	A95-78013 *	
HTN-95-70949	p 352	A95-78014 *	
HTN-95-91841	p 354	A95-80829	
HTN-95-91842	p 354	A95-80830 *	
HTN-95-91843	p 354	A95-80831 *	
HTN-95-91855	p 354	A95-80843 *	
HTN-95-91856	p 355	A95-80844 *	
HTN-95-91857	p 355	A95-80845 *	
HTN-95-91872	p 335	A95-81974	
IC-94/138	p 362	N95-25978	#
IFTR-13/1994	p 361	N95-26330	
INT-PATENT-CLASS-F02C-7/00	p 362	N95-26187 *	
INT-PATENT-CLASS-G01B-11/16	p 362	N95-26015 *	
INT-PATENT-CLASS-H01R-13/629	p 350	N95-25592 *	
ISBN-0-87703-365-X	p 341	A95-80389 *	
JPRS-UST-94-018	p 349	N95-24472	#
JPRS-UST-94-027	p 349	N95-24470	#
JPRS-UST-94-032	p 350	N95-24759	#
JPRS-UST-95-011	p 335	N95-24541	#
L-17386	p 331	N95-25338 *	#
L-17409	p 330	N95-24566 *	#
M-773	p 330	N95-24217 *	#
NAL-TR-1223	p 336	N95-25862	#
NAL-TR-1226	p 331	N95-25761	#
NAL-TR-1228	p 332	N95-25762	#
NAL-TR-1232	p 342	N95-25664	#
NAL-TR-1235	p 334	N95-25764	#
NAL-TR-1241	p 343	N95-24989	#
NAL-TR-1242	p 339	N95-24990	#
NAL-TR-1244T	p 331	N95-24998	#
NAL-TR-1245	p 331	N95-25105	#
NAL-TR-1251	p 337	N95-25005	#
NAL-TR-1257	p 362	N95-25004	#
NAS 1.15:106669	p 339	N95-24561 *	#
NAS 1.15:106865	p 338	N95-24390 *	#
NAS 1.15:106913	p 332	N95-25862 *	#
NAS 1.15:106919	p 332	N95-26075 *	#
NAS 1.15:109165	p 333	N95-24633 *	#
NAS 1.15:109171	p 335	N95-24582 *	#
NAS 1.15:109175	p 346	N95-26251 *	#
NAS 1.15:109179	p 330	N95-24397 *	#
NAS 1.15:109181	p 348	N95-24396 *	#
NAS 1.15:110346	p 335	N95-24629 *	#
NAS 1.15:110347	p 332	N95-26302 *	#
NAS 1.15:4610	p 331	N95-25338 *	#
NAS 1.15:4634	p 330	N95-24566 *	#
NAS 1.21:7037(316)	p 328	N95-24465 *	#
NAS 1.21:7037(317)	p 328	N95-25798 *	#
NAS 1.21:7109(01)	p 363	N95-24238 *	#
NAS 1.26:188201	p 337	N95-24624 *	#
NAS 1.26:195028	p 362	N95-26160 *	#
NAS 1.26:195033	p 330	N95-24443 *	#
NAS 1.26:195038	p 350	N95-25394 *	#
NAS 1.26:195041	p 340	N95-24388 *	#
NAS 1.26:195043	p 361	N95-26085 *	#
NAS 1.26:195443	p 338	N95-24304 *	#
NAS 1.26:196564	p 363	N95-24439 *	#
NAS 1.26:197412	p 349	N95-24461 *	#
NAS 1.26:197697	p 333	N95-24391 *	#
NAS 1.26:197727	p 360	N95-25797 *	#
NAS 1.26:197860	p 338	N95-24213 *	#

REPORT

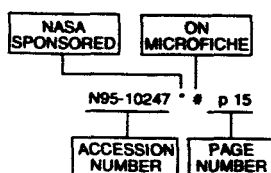
NAS 1.26:198024	p 335	N95-25334 * #	RIACS-TR-95-01	p 335	N95-25334 * #
NAS 1.26:198029	p 348	N95-24412 * #			
NAS 1.26:198030	p 349	N95-24413 * #	SAND-94-3190C	p 330	N95-24308 #
NAS 1.26:198038	p 357	N95-24219 * #			
NAS 1.26:198040	p 340	N95-24302 * #	TDCK-94-2179	p 337	N95-26190
NAS 1.26:198041	p 343	N95-24220 * #			
NAS 1.26:198045	p 330	N95-24379 * #	TNO-TM-1994-B-16	p 337	N95-26190
NAS 1.26:4645	p 343	N95-24878 * #			
NAS 1.26:4652	p 330	N95-24217 * #	TR-080594-4871F	p 333	N95-24391 * #
NAS 1.26:4653	p 361	N95-24879 * #			
NAS 1.26:4654	p 335	N95-24630 * #	UC-706	p 358	N95-25110
NAS 1.26:4660	p 338	N95-24392 * #			
NAS 1.55:10166	p 337	N95-24207 * #	US-PATENT-APPL-SN-046256	p 362	N95-26187 *
NAS 1.55:10170	p 344	N95-26119 * #	US-PATENT-APPL-SN-194654	p 362	N95-26187 *
NAS 1.61:1359	p 357	N95-24274 * #	US-PATENT-APPL-SN-230571	p 350	N95-25592 *
			US-PATENT-APPL-SN-774490	p 362	N95-26015 *
NASA-CASE-ARC-11937-1	p 362	N95-26015 *			
NASA-CASE-LEW-15170-2	p 362	N95-26187 *	US-PATENT-CLASS-250-225	p 362	N95-26015 *
			US-PATENT-CLASS-356-152	p 362	N95-26015 *
NASA-CASE-MS-22327-1	p 350	N95-25592 *	US-PATENT-CLASS-356-34	p 362	N95-26015 *
			US-PATENT-CLASS-439-248	p 350	N95-25592 *
NASA-CP-10166	p 337	N95-24207 * #	US-PATENT-CLASS-60-204	p 362	N95-26187 *
NASA-CP-10170	p 344	N95-26119 * #	US-PATENT-CLASS-60-271	p 362	N95-26187 *
NASA-CR-189201	p 337	N95-24624 * #	US-PATENT-5,137,353	p 362	N95-26015 *
NASA-CR-195028	p 362	N95-26160 * #	US-PATENT-5,392,597	p 362	N95-26187 *
NASA-CR-195033	p 330	N95-24443 * #	US-PATENT-5,397,244	p 350	N95-25592 *
NASA-CR-195038	p 350	N95-25394 * #			
NASA-CR-195041	p 340	N95-24388 * #	UVA/528266/MSE94/117	p 343	N95-24220 * #
NASA-CR-195043	p 361	N95-26085 * #			
NASA-CR-195067	p 334	N95-25341 * #	WBE-228-001	p 341	N95-24424
NASA-CR-195443	p 338	N95-24304 * #			
NASA-CR-196564	p 363	N95-24439 * #	WES/TN/DRP-4-10	p 334	N95-25609
NASA-CR-197412	p 349	N95-24461 * #			
NASA-CR-197697	p 333	N95-24391 * #	WL-TR-94-3097	p 341	N95-26053
NASA-CR-197727	p 360	N95-25797 * #			
NASA-CR-197860	p 338	N95-24213 * #	WSRC-MS-94-0632	p 349	N95-24598 #
NASA-CR-198024	p 335	N95-25334 * #			
NASA-CR-198029	p 348	N95-24412 * #			
NASA-CR-198030	p 349	N95-24413 * #			
NASA-CR-198038	p 357	N95-24219 * #			
NASA-CR-198040	p 340	N95-24302 * #			
NASA-CR-198041	p 343	N95-24220 * #			
NASA-CR-198045	p 330	N95-24379 * #			
NASA-CR-4645	p 343	N95-24878 * #			
NASA-CR-4652	p 330	N95-24217 * #			
NASA-CR-4653	p 361	N95-24879 * #			
NASA-CR-4654	p 335	N95-24630 * #			
NASA-CR-4660	p 338	N95-24392 * #			
NASA-RP-1359	p 357	N95-24274 * #			
NASA-SP-7037(316)	p 328	N95-24465 *			
NASA-SP-7037(317)	p 328	N95-25798 *			
NASA-SP-7109(01)	p 363	N95-24238 * #			
NASA-TM-106669	p 339	N95-24561 * #			
NASA-TM-106865	p 338	N95-24390 * #			
NASA-TM-106913	p 332	N95-25962 * #			
NASA-TM-106919	p 332	N95-26075 * #			
NASA-TM-109165	p 333	N95-24633 * #			
NASA-TM-109171	p 335	N95-24582 * #			
NASA-TM-109175	p 346	N95-26251 * #			
NASA-TM-109179	p 330	N95-24397 * #			
NASA-TM-109181	p 348	N95-24396 * #			
NASA-TM-110346	p 335	N95-24629 * #			
NASA-TM-110347	p 332	N95-26302 * #			
NASA-TM-4610	p 331	N95-25338 * #			
NASA-TM-4634	p 330	N95-24566 * #			
NIAR-94-12	p 348	N95-24211 #			
NREC-1762	p 338	N95-24293			
NREL/TP-440-7224	p 358	N95-26090 #			
NREL/TP-441-7077	p 357	N95-24853 #			
NREL/TP-442-7109	p 357	N95-24882 #			
NTSB/AAR-94/08	p 333	N95-24206 #			
OMI-02-93	p 330	N95-24379 * #			
PB94-910410	p 333	N95-24206 #			
PB95-141834	p 360	N95-25894 #			
PB95-143053	p 328	N95-25401 #			
PB95-147542	p 338	N95-24293 #			
PB95-149381	p 328	N95-24295 #			
PB95-164927	p 340	N95-24260			
PB95-165791	p 350	N95-25749			
PB95-166146	p 343	N95-26004 #			
PB95-166237	p 358	N95-26005 #			
PB95-178729	p 336	N95-26009			
REPT-94-4	p 330	N95-24443 * #			

ACCESSION NUMBER INDEX

AERONAUTICAL ENGINEERING / A Continuing Bibliography (Supplement 320)

August 1995

Typical Accession Number Index Listing



Listings in this index are arranged alphanumerically by accession number. The page number indicates the page on which the citation is located. The accession number denotes the number by which the citation is identified. An asterisk (*) indicates that the item is a NASA report. A pound sign (#) indicates that the item is available on microfiche.

A95-77379	p 346	A95-81077	p 327
A95-77921 *	p 346	A95-81079	p 359
A95-77982 *	p 351	A95-81081	p 359
A95-78000 *	p 351	A95-81088	p 359
A95-78006 *	p 351	A95-81092	p 327
A95-78008 *	p 351	A95-81093	p 342
A95-78009 *	p 352	A95-81096	p 336
A95-78011 *	p 352	A95-81097	p 334
A95-78012 *	p 352	A95-81098 *	p 335
A95-78013 *	p 352	A95-81099	p 327
A95-78014 *	p 352	A95-81100	p 359
A95-78467	p 343	A95-81101	p 327
A95-78494	p 347	A95-81253	p 359
A95-78576	p 347	A95-81360 *	p 342
A95-78583	p 332	A95-81374	p 342
A95-78678	p 353	A95-81583 *	p 363
A95-78679	p 353	A95-81648	p 356
A95-79236	p 347	A95-81690	p 361
A95-79237	p 327	A95-81974	p 335
A95-79238	p 358		
A95-79240	p 334	N95-24200	p 327
A95-79245	p 329	N95-24201	p 328
A95-79246	p 329	N95-24202 #	p 363
A95-79247	p 329	N95-24203	p 348
A95-79248	p 329	N95-24206 #	p 333
A95-79249	p 334	N95-24207 *	p 337
A95-79251	p 340	N95-24210 #	p 329
A95-79453	p 353	N95-24211 #	p 348
A95-79988	p 361	N95-24213 *	p 338
A95-80030	p 329	N95-24217 *	p 330
A95-80044	p 347	N95-24219 *	p 357
A95-80389 *	p 341	N95-24220 *	p 343
A95-80390	p 341	N95-24238 *	p 363
A95-80405 *	p 359	N95-24260	p 340
A95-80409	p 342	N95-24274 *	p 357
A95-80427	p 342	N95-24293	p 338
A95-80525 *	p 353	N95-24295 #	p 328
A95-80559	p 353	N95-24302 *	p 340
A95-80633	p 361	N95-24304 *	p 338
A95-80829	p 354	N95-24308 #	p 330
A95-80830 *	p 354	N95-24379 *	p 330
A95-80831	p 354	N95-24384 #	p 333
A95-80843 *	p 354	N95-24388 *	p 340
A95-80844 *	p 355	N95-24390 *	p 338
A95-80845 *	p 355	N95-24391 *	p 333
A95-80860	p 355	N95-24392 *	p 338
A95-80861	p 355	N95-24396 *	p 348
A95-80862	p 356	N95-24397 *	p 330
A95-80867	p 356	N95-24412 *	p 348
A95-80868	p 356	N95-24413 *	p 349
A95-80908	p 356	N95-24424	p 341
A95-81012	p 347	N95-24439 *	p 363
A95-81020	p 340	N95-24443 *	p 330
A95-81027	p 348	N95-24461 *	p 349
A95-81056	p 348	N95-24465 *	p 328

N95-24470 #	p 349	N95-26338 #	p 336
N95-24472 #	p 349		
N95-24541 #	p 335		
N95-24561 *	p 339		
N95-24566 *	p 330		
N95-24582 *	p 335		
N95-24598 #	p 349		
N95-24624 *	p 337		
N95-24629 *	p 335		
N95-24630 *	p 335		
N95-24631 #	p 333		
N95-24633 *	p 333		
N95-24759 #	p 350		
N95-24853 #	p 357		
N95-24878 *	p 343		
N95-24879 *	p 361		
N95-24882 #	p 357		
N95-24989 #	p 343		
N95-24990 #	p 339		
N95-24998 #	p 331		
N95-25004 #	p 362		
N95-25005 #	p 337		
N95-25105 #	p 331		
N95-25110	p 358		
N95-25264 *	p 360		
N95-25334 *	p 335		
N95-25338 *	p 331		
N95-25341 *	p 334		
N95-25394 *	p 350		
N95-25395 *	p 339		
N95-25396 *	p 339		
N95-25397 *	p 339		
N95-25399 *	p 341		
N95-25400 *	p 350		
N95-25401	p 328		
N95-25578	p 336		
N95-25592 *	p 350		
N95-25606	p 350		
N95-25607	p 328		
N95-25609	p 334		
N95-25649 #	p 331		
N95-25664 #	p 342		
N95-25749	p 350		
N95-25761 #	p 331		
N95-25762 #	p 332		
N95-25764 #	p 334		
N95-25797 *	p 360		
N95-25798 *	p 328		
N95-25803 *	p 360		
N95-25805 *	p 360		
N95-25862 #	p 336		
N95-25894 #	p 360		
N95-25935	p 336		
N95-25936	p 339		
N95-25962 *	p 332		
N95-25978 #	p 362		
N95-26004 #	p 343		
N95-26005 #	p 358		
N95-26009	p 336		
N95-26015 *	p 362		
N95-26053	p 341		
N95-26075 *	p 332		
N95-26085 *	p 361		
N95-26090 #	p 358		
N95-26119 *	p 344		
N95-26120 *	p 344		
N95-26121 *	p 344		
N95-26122 *	p 344		
N95-26123 *	p 344		
N95-26124 *	p 345		
N95-26125 *	p 345		
N95-26126 *	p 345		
N95-26128 *	p 345		
N95-26131 *	p 345		
N95-26133 *	p 345		
N95-26138 *	p 346		
N95-26140 *	p 346		
N95-26160 *	p 362		
N95-26187 *	p 362		
N95-26190	p 337		
N95-26251 *	p 346		
N95-26302 *	p 332		
N95-26330	p 361		

ACCESSION

AVAILABILITY OF CITED PUBLICATIONS

OPEN LITERATURE ENTRIES (A95-60000 Series)

Inquiries and requests should be addressed to NASA Center for AeroSpace Information, 800 Elkridge Landing Road, Linthicum Heights, MD 21090-2934. Orders are also taken by telephone, (301) 621-0390, e-mail, help@sti.nasa.gov, and fax, (301) 621-0134. Please refer to the accession number when requesting publications.

STAR ENTRIES (N95-10000 Series)

One or more sources from which a document announced in *STAR* is available to the public is ordinarily given on the last line of the citation. The most commonly indicated sources and their acronyms or abbreviations are listed below, and their addresses are listed on page APP-3. If the publication is available from a source other than those listed, the publisher and his address will be displayed on the availability line or in combination with the corporate source line.

Avail: CASI. Sold by the NASA Center for AeroSpace Information. Prices for hard copy (HC) and microfiche (MF) are indicated by a price code following the letters HC or MF in the *STAR* citation. Current values for the price codes are given in the tables on page APP-5.

NOTE ON ORDERING DOCUMENTS: When ordering publications from NASA CASI, use the N accession number or other report number. It is also advisable to cite the title and other bibliographic identification.

Avail: SOD (or GPO). Sold by the Superintendent of Documents, U.S. Government Printing Office, in hard copy.

Avail: BLL (formerly NLL): British Library Lending Division, Boston Spa, Wetherby, Yorkshire, England. Photocopies available from this organization at the price shown. (If none is given, inquiry should be addressed to the BLL.)

Avail: DOE Depository Libraries. Organizations in U.S. cities and abroad that maintain collections of Department of Energy reports, usually in microfiche form, are listed in *Energy Research Abstracts*. Services available from the DOE and its depositories are described in a booklet, *DOE Technical Information Center - Its Functions and Services* (TID-4660), which may be obtained without charge from the DOE Technical Information Center.

Avail: ESDU. Pricing information on specific data, computer programs, and details on Engineering Sciences Data Unit (ESDU) topic categories can be obtained from ESDU International Ltd. Requesters in North America should use the Virginia address while all other requesters should use the London address, both of which are on page APP-3.

Avail: Fachinformationszentrum Karlsruhe. Gesellschaft für wissenschaftlich-technische Information mbH 76344 Eggenstein-Leopoldshafen, Germany.

Avail: HMSO. Publications of Her Majesty's Stationery Office are sold in the U.S. by Pendragon House, Inc. (PHI), Redwood City, CA. The U.S. price (including a service and mailing charge) is given, or a conversion table may be obtained from PHI.

Avail: Issuing Activity, or Corporate Author, or no indication of availability. Inquiries as to the availability of these documents should be addressed to the organization shown in the citation as the corporate author of the document.

Avail: NASA Public Document Rooms. Documents so indicated may be examined at or purchased from the National Aeronautics and Space Administration (JBD-4), Public Documents Room (Room 1H23), Washington, DC 20546-0001, or public document rooms located at NASA installations, and the NASA Pasadena Office at the Jet Propulsion Laboratory.

Avail: NTIS. Sold by the National Technical Information Service. Initially distributed microfiche under the NTIS SRIM (Selected Research in Microfiche) are available. For information concerning this service, consult the NTIS Subscription Section, Springfield, VA 22161.

Avail: Univ. Microfilms. Documents so indicated are dissertations selected from *Dissertation Abstracts* and are sold by University Microfilms as xerographic copy (HC) and microfilm. All requests should cite the author and the Order Number as they appear in the citation.

Avail: US Patent and Trademark Office. Sold by Commissioner of Patents and Trademarks, U.S. Patent and Trademark Office, at the standard price of \$1.50 each, postage free.

Avail: (US Sales Only). These foreign documents are available to users within the United States from the National Technical Information Service (NTIS). They are available to users outside the United States through the International Nuclear Information Service (INIS) representative in their country, or by applying directly to the issuing organization.

Avail: USGS. Originals of many reports from the U.S. Geological Survey, which may contain color illustrations, or otherwise may not have the quality of illustrations preserved in the microfiche or facsimile reproduction, may be examined by the public at the libraries of the USGS field offices whose addresses are listed on page APP-3. The libraries may be queried concerning the availability of specific documents and the possible utilization of local copying services, such as color reproduction.

FEDERAL DEPOSITORY LIBRARY PROGRAM

In order to provide the general public with greater access to U.S. Government publications, Congress established the Federal Depository Library Program under the Government Printing Office (GPO), with 53 regional depositories responsible for permanent retention of material, inter-library loan, and reference services. At least one copy of nearly every NASA and NASA-sponsored publication, either in printed or microfiche format, is received and retained by the 53 regional depositories. A list of the regional GPO libraries, arranged alphabetically by state, appears on the inside back cover of this issue. These libraries are *not* sales outlets. A local library can contact a regional depository to help locate specific reports, or direct contact may be made by an individual.

PUBLIC COLLECTION OF NASA DOCUMENTS

An extensive collection of NASA and NASA-sponsored publications is maintained by the British Library Lending Division, Boston Spa, Wetherby, Yorkshire, England for public access. The British Library Lending Division also has available many of the non-NASA publications cited in *STAR*. European requesters may purchase facsimile copy or microfiche of NASA and NASA-sponsored documents, those identified by both the symbols # and * from ESA — Information Retrieval Service European Space Agency, 8-10 rue Mario-Nikis, 75738 CEDEX 15, France.

STANDING ORDER SUBSCRIPTIONS

NASA SP-7037 supplements and annual index are available from the NASA Center for Aerospace Information (CASI) on standing order subscription. Standing order subscriptions do not terminate at the end of a year, as do regular subscriptions, but continue indefinitely unless specifically terminated by the subscriber.

ADDRESSES OF ORGANIZATIONS

British Library Lending Division
Boston Spa, Wetherby, Yorkshire
England

National Technical Information Service
5285 Port Royal Road
Springfield, VA 22161

Commissioner of Patents and Trademarks
U.S. Patent and Trademark Office
Washington, DC 20231

Pendragon House, Inc.
899 Broadway Avenue
Redwood City, CA 94063

Department of Energy
Technical Information Center
P.O. Box 62
Oak Ridge, TN 37830

Superintendent of Documents
U.S. Government Printing Office
Washington, DC 20402

European Space Agency-
Information Retrieval Service ESRIN
Via Galileo Galilei
00044 Frascati (Rome) Italy

University Microfilms
A Xerox Company
300 North Zeeb Road
Ann Arbor, MI 48106

Engineering Sciences Data Unit International
P.O. Box 1633
Manassas, VA 22110

University Microfilms, Ltd.
Tylers Green
London, England

Engineering Sciences Data Unit
International, Ltd.
251-259 Regent Street
London, W1R 7AD, England

U.S. Geological Survey Library National Center
MS 950
12201 Sunrise Valley Drive
Reston, VA 22092

Fachinformationszentrum Karlsruhe
Gesellschaft für wissenschaftlich-technische
Information mbH
76344 Eggenstein-Leopoldshafen, Germany

U.S. Geological Survey Library
2255 North Gemini Drive
Flagstaff, AZ 86001

Her Majesty's Stationery Office
P.O. Box 569, S.E. 1
London, England

U.S. Geological Survey
345 Middlefield Road
Menlo Park, CA 94025

NASA Center for AeroSpace Information
800 Elkridge Landing Road
Linthicum Heights, MD 21090-2934

U.S. Geological Survey Library
Box 25046
Denver Federal Center, MS914
Denver, CO 80225

National Aeronautics and Space Administration
Scientific and Technical Information Office
(JT)
Washington, DC 20546-0001

NASA CASI PRICE CODE TABLE

(Effective January 1, 1995)

CASI PRICE CODE	NORTH AMERICAN PRICE	FOREIGN PRICE
A01	\$ 6.00	\$ 12.00
A02	9.00	18.00
A03	17.50	35.00
A04-A05	19.50	39.00
A06-A09	27.00	54.00
A10-A13	36.50	73.00
A14-A17	44.50	89.00
A18-A21	52.00	104.00
A22-A25	61.00	122.00
A99	Call For Price	Call For Price

IMPORTANT NOTICE

For users not registered at the NASA CASI, prepayment is required. Additionally, a shipping and handling fee of \$1.00 per document for delivery within the United States and \$9.00 per document for delivery outside the United States is charged.

For users registered at the NASA CASI, document orders may be invoiced at the end of the month, charged against a deposit account, or paid by check or credit card. NASA CASI accepts American Express, Diners' Club, MasterCard, and VISA credit cards. There are no shipping and handling charges. To register at the NASA CASI, please request a registration form through the NASA Access Help Desk at the numbers or addresses below.

RETURN POLICY

Effective June 1, 1995, the NASA Center for AeroSpace Information will gladly replace or make full refund on items you have requested if we have made an error in your order, if the item is defective, or if it was received in damaged condition and you contact us within 30 days of your original request. Just contact our NASA Access Help Desk at the numbers or addresses listed below.

NASA Center for AeroSpace Information
800 Elkridge Landing Road
Linthicum Heights, MD 21090-2934
Telephone: (301) 621-0390
E-mail: help@sti.nasa.gov
Fax: (301) 621-0134

REPORT DOCUMENT PAGE

1. Report No. NASA SP-7037 (320)	2. Government Accession No.	3. Recipient's Catalog No.	
4. Title and Subtitle Aeronautical Engineering A Continuing Bibliography (Supplement 320)		5. Report Date August 1995	
		6. Performing Organization Code JT	
7. Author(s)		8. Performing Organization Report No.	
		10. Work Unit No.	
9. Performing Organization Name and Address NASA Scientific and Technical Information Office		11. Contract or Grant No.	
		13. Type of Report and Period Covered Special Publication	
12. Sponsoring Agency Name and Address National Aeronautics and Space Administration Washington, DC 20546-0001		14. Sponsoring Agency Code	
		15. Supplementary Notes	
16. Abstract This report lists 193 reports, articles and other documents recently announced in the NASA STI Database.			
17. Key Words (Suggested by Author(s)) Aeronautical Engineering Aeronautics Bibliographies		18. Distribution Statement Unclassified - Unlimited Subject Category - 01	
19. Security Classif. (of this report) Unclassified	20. Security Classif. (of this page) Unclassified	21. No. of Pages 90	22. Price A05/HC

FEDERAL REGIONAL DEPOSITORY LIBRARIES

ALABAMA

AUBURN UNIV. AT MONTGOMERY LIBRARY
Documents Dept.
7300 University Dr.
Montgomery, AL 36117-3596
(205) 244-3650 Fax: (205) 244-0678

UNIV. OF ALABAMA

Amelia Gayle Gorgas Library
Govt. Documents
P.O. Box 870266
Tuscaloosa, AL 35487-0266
(205) 348-6046 Fax: (205) 348-0760

ARIZONA

DEPT. OF LIBRARY, ARCHIVES, AND PUBLIC RECORDS
Research Division
Third Floor, State Capitol
1700 West Washington
Phoenix, AZ 85007
(602) 542-3701 Fax: (602) 542-4400

ARKANSAS

ARKANSAS STATE LIBRARY
State Library Service Section
Documents Service Section
One Capitol Mall
Little Rock, AR 72201-1014
(501) 682-2053 Fax: (501) 682-1529

CALIFORNIA

CALIFORNIA STATE LIBRARY
Govt. Publications Section
P.O. Box 942837 - 914 Capitol Mall
Sacramento, CA 94337-0091
(916) 654-0069 Fax: (916) 654-0241

COLORADO

UNIV. OF COLORADO - BOULDER
Libraries - Govt. Publications
Campus Box 184
Boulder, CO 80309-0184
(303) 492-8834 Fax: (303) 492-1881

DENVER PUBLIC LIBRARY

Govt. Publications Dept. BSG
1357 Broadway
Denver, CO 80203-2165
(303) 640-8846 Fax: (303) 640-8817

CONNECTICUT

CONNECTICUT STATE LIBRARY
231 Capitol Avenue
Hartford, CT 06106
(203) 566-4971 Fax: (203) 566-3322

FLORIDA

UNIV. OF FLORIDA LIBRARIES
Documents Dept.
240 Library West
Gainesville, FL 32611-2048
(904) 392-0366 Fax: (904) 392-7251

GEORGIA

UNIV. OF GEORGIA LIBRARIES
Govt. Documents Dept.
Jackson Street
Athens, GA 30602-1645
(706) 542-8949 Fax: (706) 542-4144

HAWAII

UNIV. OF HAWAII
Hamilton Library
Govt. Documents Collection
2550 The Mall
Honolulu, HI 96822
(808) 948-8230 Fax: (808) 956-5968

IDAHO

UNIV. OF IDAHO LIBRARY
Documents Section
Rayburn Street
Moscow, ID 83844-2353
(208) 885-6344 Fax: (208) 885-6817

ILLINOIS

ILLINOIS STATE LIBRARY
Federal Documents Dept.
300 South Second Street
Springfield, IL 62701-1796
(217) 782-7596 Fax: (217) 782-6437

INDIANA

INDIANA STATE LIBRARY
Serials/Documents Section
140 North Senate Avenue
Indianapolis, IN 46204-2296
(317) 232-3679 Fax: (317) 232-3728

IOWA

UNIV. OF IOWA LIBRARIES
Govt. Publications
Washington & Madison Streets
Iowa City, IA 52242-1166
(319) 335-5926 Fax: (319) 335-5900

KANSAS

UNIV. OF KANSAS
Govt. Documents & Maps Library
6001 Malott Hall
Lawrence, KS 66045-2800
(913) 864-4660 Fax: (913) 864-3855

KENTUCKY

UNIV. OF KENTUCKY
King Library South
Govt. Publications/Maps Dept.
Patterson Drive
Lexington, KY 40506-0039
(606) 257-3139 Fax: (606) 257-3139

LOUISIANA

LOUISIANA STATE UNIV.
Middleton Library
Govt. Documents Dept.
Baton Rouge, LA 70803-3312
(504) 388-2570 Fax: (504) 388-6992

LOUISIANA TECHNICAL UNIV.

Prescott Memorial Library
Govt. Documents Dept.
Ruston, LA 71272-0046
(318) 257-4962 Fax: (318) 257-2447

MAINE

UNIV. OF MAINE
Raymond H. Fogler Library
Govt. Documents Dept.
Orono, ME 04469-5729
(207) 581-1673 Fax: (207) 581-1653

MARYLAND

UNIV. OF MARYLAND - COLLEGE PARK
McKeldin Library
Govt. Documents/Maps Unit
College Park, MD 20742
(301) 405-9165 Fax: (301) 314-9416

MASSACHUSETTS

BOSTON PUBLIC LIBRARY
Govt. Documents
666 Boylston Street
Boston, MA 02117-0286
(617) 536-5400, ext. 226
Fax: (617) 536-7758

MICHIGAN

DETROIT PUBLIC LIBRARY
5201 Woodward Avenue
Detroit, MI 48202-4093
(313) 833-1025 Fax: (313) 833-0156

LIBRARY OF MICHIGAN

Govt. Documents Unit
P.O. Box 30007
717 West Allegan Street
Lansing, MI 48909
(517) 373-1300 Fax: (517) 373-3381

MINNESOTA

UNIV. OF MINNESOTA
Govt. Publications
409 Wilson Library
309 19th Avenue South
Minneapolis, MN 55455
(612) 624-5073 Fax: (612) 626-9353

MISSISSIPPI

UNIV. OF MISSISSIPPI
J.D. Williams Library
106 Old Gym Bldg.
University, MS 38677
(601) 232-5857 Fax: (601) 232-7465

MISSOURI

UNIV. OF MISSOURI - COLUMBIA
106B Ellis Library
Govt. Documents Sect.
Columbia, MO 65201-5149
(314) 882-6733 Fax: (314) 882-8044

MONTANA

UNIV. OF MONTANA
Mansfield Library
Documents Division
Missoula, MT 59812-1195
(406) 243-6700 Fax: (406) 243-2060

NEBRASKA

UNIV. OF NEBRASKA - LINCOLN
D.L. Love Memorial Library
Lincoln, NE 68588-0410
(402) 472-2562 Fax: (402) 472-5131

NEVADA

THE UNIV. OF NEVADA LIBRARIES
Business and Govt. Information Center
Reno, NV 89557-0044
(702) 784-6579 Fax: (702) 784-1751

NEW JERSEY

NEWARK PUBLIC LIBRARY
Science Div. - Public Access
P.O. Box 630
Five Washington Street
Newark, NJ 07101-7812
(201) 733-7782 Fax: (201) 733-5648

NEW MEXICO

UNIV. OF NEW MEXICO
General Library
Govt. Information Dept.
Albuquerque, NM 87131-1466
(505) 277-5441 Fax: (505) 277-6019

NEW MEXICO STATE LIBRARY

325 Don Gaspar Avenue
Santa Fe, NM 87503
(505) 827-3824 Fax: (505) 827-3888

NEW YORK

NEW YORK STATE LIBRARY
Cultural Education Center
Documents/Gift & Exchange Section
Empire State Plaza
Albany, NY 12230-0001
(518) 474-5355 Fax: (518) 474-5786

NORTH CAROLINA

UNIV. OF NORTH CAROLINA - CHAPEL HILL
Walter Royal Davis Library
CB 3912, Reference Dept.
Chapel Hill, NC 27514-8890
(919) 962-1151 Fax: (919) 962-4451

NORTH DAKOTA

NORTH DAKOTA STATE UNIV. LIB.
Documents
P.O. Box 5599
Fargo, ND 58105-5599
(701) 237-8886 Fax: (701) 237-7138

UNIV. OF NORTH DAKOTA

Chester Fritz Library
University Station
P.O. Box 9000 - Centennial and
University Avenue
Grand Forks, ND 58202-9000
(701) 777-4632 Fax: (701) 777-3319

OHIO

STATE LIBRARY OF OHIO
Documents Dept.
65 South Front Street
Columbus, OH 43215-4163
(614) 644-7051 Fax: (614) 752-9178

OKLAHOMA

OKLAHOMA DEPT. OF LIBRARIES
U.S. Govt. Information Division
200 Northeast 18th Street
Oklahoma City, OK 73105-3298
(405) 521-2502, ext. 253
Fax: (405) 525-7804

OKLAHOMA STATE UNIV.

Edmon Low Library
Stillwater, OK 74078-0375
(405) 744-6546 Fax: (405) 744-5183

OREGON

PORTLAND STATE UNIV.
Branford P. Millar Library
934 Southwest Harrison
Portland, OR 97207-1151
(503) 725-4123 Fax: (503) 725-4524

PENNSYLVANIA

STATE LIBRARY OF PENN.
Govt. Publications Section
116 Walnut & Commonwealth Ave.
Harrisburg, PA 17105-1601
(717) 787-3752 Fax: (717) 783-2070

SOUTH CAROLINA

CLEMSON UNIV.
Robert Muldrow Cooper Library
Public Documents Unit
P.O. Box 343001
Clemson, SC 29634-3001
(803) 656-5174 Fax: (803) 656-3025

UNIV. OF SOUTH CAROLINA

Thomas Cooper Library
Green and Sumter Streets
Columbia, SC 29208
(803) 777-4841 Fax: (803) 777-9503

TENNESSEE

UNIV. OF MEMPHIS LIBRARIES
Govt. Publications Dept.
Memphis, TN 38152-0001
(901) 678-2206 Fax: (901) 678-2511

TEXAS

TEXAS STATE LIBRARY
United States Documents
P.O. Box 12927 - 1201 Brazos
Austin, TX 78701-0001
(512) 463-5455 Fax: (512) 463-5436

TEXAS TECH. UNIV. LIBRARIES

Documents Dept.
Lubbock, TX 79409-0002
(806) 742-2282 Fax: (806) 742-1920

UTAH

UTAH STATE UNIV.
Merrill Library Documents Dept.
Logan, UT 84322-3000
(801) 797-2678 Fax: (801) 797-2677

VIRGINIA

UNIV. OF VIRGINIA
Alderman Library
Govt. Documents
University Ave. & McCormick Rd.
Charlottesville, VA 22903-2498
(804) 824-3133 Fax: (804) 924-4337

WASHINGTON

WASHINGTON STATE LIBRARY
Govt. Publications
P.O. Box 42478
16th and Water Streets
Olympia, WA 98504-2478
(206) 753-4027 Fax: (206) 586-7575

WEST VIRGINIA

UNIV. OF WEST VIRGINIA LIBRARY
Govt. Documents Section
P.O. Box 6069 - 1549 University Ave.
Morgantown, WV 26506-6069
(304) 293-3051 Fax: (304) 293-6638

WISCONSIN

ST. HIST. SOC. OF WISCONSIN LIBRARY
Govt. Publication Section
816 State Street
Madison, WI 53706
(608) 264-6525 Fax: (608) 264-6520

MILWAUKEE PUBLIC LIBRARY

Documents Division
814 West Wisconsin Avenue
Milwaukee, WI 53233
(414) 286-3073 Fax: (414) 286-8074

National Aeronautics and
Space Administration
Code JT
Washington, DC 20546-0001

Official Business
Penalty for Private Use \$300